Regulation of Interleukin-6 Receptor Cell-surface Levels by Internalization and Proteolysis

Dissertation

Zur Erlangung des Doktorgrades
der Mathematisch-Naturwissenschaftlichen Fakultät
der Christian-Albrechts-Universität zu Kiel

vorgelegt von

Charlotte Flynn

Kiel, Oktober 2018

Referent: Prof. Dr. Stefan Rose-John

Korreferent: Prof. Dr. Thomas Roeder

Tag der mündlichen Prüfung: 22.02.2019

Zum Druck genehmigt: 22.02.2019

Table of Contents

Summary

Receptor cell-surface levels can be regulated by different mechanisms, namely internalization, proteolytic cleavage of the membrane-bound receptor or synthesis of new receptors that are transported to the cell-surface. Following internalization, the receptors are either transported back to the cell-surface (recycling) or to lysosomes where they are degraded. IL-6 belongs to the IL-6 cytokine family and plays an important role in pro- and anti-inflammatory processes. IL-6-mediated signal transduction can occur via the membrane bound IL-6R, which is named classic signaling, as well as via a soluble form of the IL-6R (sIL-6R), called trans-signaling. In both cases intracellular signaling cascades are activated via a homodimer of glycoprotein 130 (gp130). The majority of the sIL-6R is generated by proteolytic cleavage of the membrane-bound IL-6R by the metalloproteases A disintegrin and metalloproteinase (ADAM) 10 and 17.

Internalization was already observed for the IL-6R and gp130, but it was unclear whether both are degraded or recycled afterwards. Furthermore, it was unclear how IL-6 influences both processes. Within this thesis, I could show that the IL-6R and gp130 are internalized in a clathrin- and dynamin-dependent manner which was not influenced by IL-6. Furthermore, the intracellular domain (ICD) of the IL-6R is dispensable for IL-6R internalization. Further experiments revealed that on the one hand gp130 influences IL-6R internalization, but IL-6R is also internalized independently of gp130. Furthermore, it could be shown that both receptors are recycled back to the cell surface via Rab11-positive recycling endosomes but are also degraded in the lysosome. Stimulation with IL-6 led to an increase in recycling of both receptors, but only degradation of gp130 in the lysosome was enhanced.

Additionally, it was revealed that STAT3 signaling was only activated upon internalization of the IL-6/IL-6R/gp130 signaling complex, indicating that signaling is initiated at endosomes.

Only little is known about endogenous stimuli leading to the release of sIL-6R *in vivo*. In experiments with mice it could be shown that activation of the Toll-like receptor (TLR) 4 with lipopolysaccharide leads to the release of sIL-6R. In contrast to mice, not the activation of TLR4, but rather activation of TLR2, resulted in an increase in sIL-6R release in humans. As a source of sIL-6R upon TLR2 activation, monocytes could be identified, and the underlying mechanism was shown to be proteolytic cleavage of the membrane-bound IL-6R mediated by the metalloproteases ADAM10 and ADAM17. Furthermore, TLR2 activation led to the activation of the ERK signaling pathway. Inhibition of ERK signaling resulted in an increase in sIL-6R release, whereas IL-6 secretion was reduced, indicating opposing functions of the ERK signaling pathway in the regulation of classic and trans-signaling.

The sIL-6R is also released constitutively but the responsible protease has not been clearly identified so far. Using a screening procedure, cathepsin S was identified as a new protease that

can proteolytically cleave the IL-6R. Further experiments revealed, however, that cathepsin S uses a different cleavage site in the IL-6R *in vitro* as has been determined for the sIL-6R *in vivo*, indicating that it is rather not involved in the generation of the constitutively released sIL-6R.

Zusammenfassung

Die Oberflächenexpression von Rezeptoren wird durch verschiedene Mechanismen reguliert. Dazu zählen Internalisierung der Rezeptoren, proteolytische Spaltung der membrangebundenen Rezeptoren sowie die Generierung neuer Rezeptoren, welche an die Oberfläche transportiert werden. Nach der Internalisierung von Rezeptoren können diese entweder an die Zelloberfläche zurück transportiert werden (*Recycling*) oder im Lysosom abgebaut werden. Interleukin-6 gehört zur Familie der IL-6 Zytokine und spielt eine wichtige Rolle in pro- und anti-inflammatorischen Prozessen. IL-6-vermittelte Signaltransduktion kann sowohl durch einen membranständigen Rezeptor (IL-6R) als auch durch lösliche Rezeptoren (sIL-6R) aktiviert werden, wobei Signaltransduktion über den membrangebundenen Rezeptor als *classic signaling* bezeichnet wird und Signaltransduktion über einen löslichen Rezeptor als *trans-signaling*. In beiden Fällen erfolgt die Aktivierung intrazellulärer Signalkaskaden durch ein Homodimer von Glykoprotein 130 (gp130). Der Großteil des sIL-6R wird durch proteolytische Spaltung des membrangebundenen IL-6R durch die Metalloproteasen *A disintegrin and metalloproteinase* (ADAM) 10 und 17 generiert. Für den IL-6R und gp130 konnte bereits gezeigt werden, dass sie internalisiert werden. Es war jedoch unklar, ob sie anschließend abgebaut oder *recycled* werden. Ebenso war unklar, welchen Einfluss IL-6 in diesem Zusammenhang hat. Im Rahmen dieser Arbeit konnte ich zeigen, dass beide Rezeptoren über einen Clathrin- und Dynamin-abhängigen Mechanismus internalisiert werden, wobei IL-6 die Internalisierung nicht beeinflusste. Der intrazelluläre Teil des IL-6R wird dabei für die IL-6R Internalisierung nicht benötigt. Weitere Untersuchungen belegten sowohl einen Einfluss von gp130 auf die Internalisierung des IL-6R, zeigten jedoch auch IL-6R-Internalisierung unabhängig von gp130. Weiterhin konnte gezeigt werden, dass IL-6R und gp130 sowohl über Rab11-positive *Recycling* Endosomen an die Zelloberfläche zurück transportiert werden, als auch im Lysosom abgebaut werden. Stimulation mit IL-6 führte zu einem erhöhten *Recycling* beider Rezeptoren, jedoch wurde nur gp130 vermehrt im Lysosom abgebaut.

Des Weiteren zeigte sich, dass die STAT3-Signaltransduktion erst nach Internalisierung des IL-6/IL-6R/gp130-Komplexes aktiviert wird, was darauf schließen lässt, dass diese an Endosomen stattfindet.

Bislang ist wenig über endogene Aktivatoren der sIL-6R Generierung *in vivo* bekannt. In Experimenten mit Mäusen konnte gezeigt werden, dass Aktivierung des Toll-like Rezeptors (TLR) 4 durch Lipopolysaccharide zur Generierung des sIL-6R führt. Im Gegensatz zu Mäusen führte im Menschen nicht die Aktivierung von TLR4, sondern die von TLR2, zur Generierung des sIL-6R. Als Quelle des sIL-6R nach TLR2 Aktivierung konnten Monozyten identifiziert werden und als verantwortlicher Mechanismus die proteolytische Spaltung des membrangebundenen IL-6R durch die Metalloproteasen ADAM10 und ADAM17. TLR2-Aktivierung resultierte außerdem in

der Aktivierung des ERK-Signalweges. Inhibition des ERK-Signalweges führte entgegen aller Erwartungen zu vermehrter Freisetzung des sIL-6R, verminderte jedoch die Sekretion von IL-6, was auf eine gegensätzliche Funktion des ERK-Signalwegs in der Steuerung von *classic* und *trans-signaling* hindeutet.

Der sIL-6R wird auch konstitutiv gebildet, jedoch ist die hierfür verantwortliche Protease noch nicht eindeutig nachgewiesen. Durch ein Screeningverfahren wurde Cathepsin S als eine neue Protease identifiziert, die den IL-6R proteolytisch spalten kann. Weitere Experimente zeigten jedoch, dass Cathepsin S *in vitro* eine andere Schnittstelle im IL-6R verwendet als *in vivo* für den sIL-6R nachgewiesen wurde und daher vermutlich keine Rolle in der Generierung des konstitutiv gebildeten sIL-6R spielt.

1 Introduction

The human body has to cope with pathogens that try to enter the organism every day. Different mechanisms have evolved that enable the body to fight these intruders. The first line of defense is hereby the skin, which functions as a barrier and prevents that pathogens enter the body. In case of damage of the skin, however, pathogens can invade the organism. To cope with these nevertheless, the immune system is activated. To efficiently fight pathogens the immune system uses two different mechanisms, the innate and the adaptive immune system [4]. The innate immune system is the first defense mechanism activated by intruders which are phagocytosed by macrophages. Subsequently, macrophages secrete special factors, especially cytokines and chemokines, which attract neutrophils, monocytes or lymphocytes, facilitated by an increased blood flow and increased permeability of the blood vessels [5]. Additionally to macrophages, also dendritic cells engulf pathogens. The activated dendritic cells present bacterial or viral particles to lymphocytes thereby inducing the adaptive immune system. The activated T cells, which express specific receptors at the cell-surface, bind and help clear the pathogens, and the activated B cells secrete antibodies marking the pathogens for destruction [6]. Orchestration of all the cells belonging to the innate and adaptive immune system, finally, leads to the resolution of the infection.

Cytokines released by macrophages upon phagocytosis of pathogens can be divided into five groups, namely chemokines, interleukins, interferons, colony stimulating factors and tumor necrosis factors, which attract different cells, activate cells and lead to proliferation of the different cell types involved in fighting pathogens [4].

1.1 The Interleukin-6 (IL-6) cytokine family

The cytokines belonging to the IL-6 cytokine family play different roles in pro- as well as anti-inflammatory conditions. Members of the IL-6 cytokine family include Interleukin-6 (IL-6), Interleukin-11 (IL-11), Interleukin-27 (IL-27), Interleukin-30 (IL-30), Interleukin-31 (IL-31), oncostatin M (OSM), cardiotrophin-1 (CT-1), leukemia inhibitory factor (LIF), cardiotrophin-like cytokine (CLC) and ciliary neurotrophic factor (CNTF) (Fig. 1.1) [7]. These cytokines have in common that they display a four α-helix bundle structure [8] and that they bind to at least one molecule of the β-receptor glycoprotein 130 (gp130). IL-6 and IL-11 bind to their α-receptor, Interleukin-6 receptor (IL-6R) and Interleukin-11 receptor (IL-11R) respectively, before recruiting a homodimer of gp130 [9, 10]. LIF, CT-1, CLC and CNTF bind to a heterodimer of gp130 and leukemia inhibitory factor receptor (LIFR), but CLC and CNTF first require binding to their α-receptor CNTF receptor (CNTFR) [11, 12]. OSM can also activate a heterodimer consisting of gp130 and LIFR but can additionally signal via a gp130/oncostatin M receptor (OSMR)

heterodimer [13, 14]. IL-27 was shown to bind to a gp130 heterodimer consisting of gp130 and WSX-1 [15]. Among the cytokines of the IL-6 cytokine family IL-31 is special as complex formation does not involve the β-receptor gp130 but GPL, the gp130-like receptor that forms a heterodimer with OSMR upon IL-31 binding [16, 17].

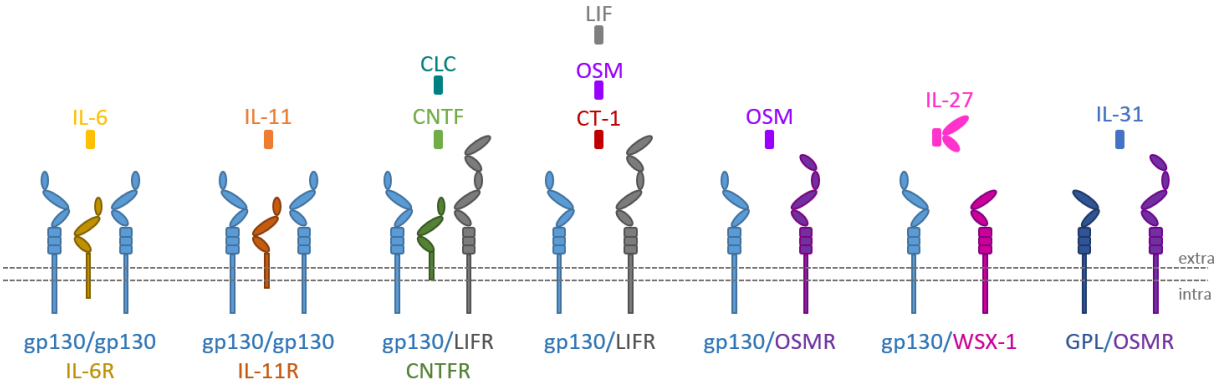

Figure 1.1: Schematic overview of the IL-6 cytokine family. The cytokines IL-6 and IL-11 signal via a homodimer of gp130 and their α-receptors IL-6R and IL-11R, respectively. CLC and CNTF bind to the α-receptor CNTFR and signal via a heterodimer consisting of gp130 and LIFR. All the other cytokines do not bind to an α-receptor but directly interact with a gp130 heterodimer. OSM interacts with a gp130/OSMR heterodimer but also with a gp130/LIFR heterodimer which also binds LIF and CT-1. IL-27 can signal via a gp130/WSX-1 heterodimer. The only cytokine that does not bind to gp130 is IL-31 which interacts with a heterodimer of GPL and OSMR. Extra: Extracellular space; Intra: Intracellular space.

The different cytokines of the IL-6 cytokine family display a variety of functions in the human body and contribute e.g. to lymphocyte differentiation and activation [18-20], bone metabolism [21], fertility [22], hematopoiesis [23, 24], liver regeneration [25] or neuroprotection [26, 27].

1.1.1 The cytokine Interleukin-6

Interleukin-6 is a pleiotropic cytokine with a plethora of functions, e.g. the activation of the acute-phase response in the liver [28, 29], T and B cell differentiation [30-32], secretion of immunoglobulins [33], activation of oxidative burst response by monocytes and neutrophils [34], proliferation of thymocytes [35, 36] or the regulation of hematopoiesis [37].

The cytokine is secreted mainly from monocytes/macrophages, endothelial cells or fibroblasts [38-40]triggered either by bacterial proteins like lipopolysaccharide (LPS), or other cytokines like Interleukin-1 (IL-1) or tumor necrosis factor alpha (TNF-α) [41, 42]. In sera from healthy individuals IL-6 is detected only in very low amounts (1-10 pg/ml) and often even below the detection limit. However, concentrations are increased in almost every inflammatory condition with levels in the lower ng/ml region. During sepsis, a severe inflammatory condition, levels can even range between 100-1000 ng/ml [43].

The human *IL6* gene is located on chromosome 7 p15-p21 [44] and transcription gives rise to an mRNA encoding a 212 amino-acid residue precursor protein. Removal of the signal peptide results in the 184 amino-acid residue mature protein which is further post-translationally modified by addition of N- and O-linked glycans [45, 46]. As post-translationally unmodified IL-6 is still

biologically active it is believed that these modifications are not directly necessary for binding to the receptors but could rather influence the plasma half-life of the IL-6. Analysis of the *IL6* gene revealed three transcription initiation sites [47] where the transcription machinery binds to which is activated by the help of different transcription factors. The most prominent transcription factor identified is the nuclear factor kappa B (NF-κB) [41, 48] but also AP-1, CCAAT/enhancer binding protein (C/EBP) and cAMP response element-binding protein (CREB) activated by cAMP contribute to IL-6 gene expression [49]. IL-6 gene expression is not only regulated at the transcriptional level but also post-transcriptionally by the RNA-binding proteins (RBP) Arid5a and Regnase-1 which differentially control IL-6 mRNA stability. Regnase-1 is an RNAse and was shown to degrade IL-6 mRNA [50] whereas Arid5a has stabilizing functions on the IL-6 mRNA [51].

IL-6 was found to be associated with many diseases like inflammatory bowel disease [52], multiple sclerosis [53], Parkinson [54, 55], Alzheimer's disease [56] or Castleman's disease [57, 58]. The probably best-studied disease in which IL-6 is involved in the pathogenesis is rheumatoid arthritis (RA), a chronic inflammatory disorder characterized by chronic joint inflammation and bone and cartilage destruction. Increased infiltration of lymphocytes and monocytes into the synovium of joints is observed during RA, resulting in increased levels of IL-6 [59] which contributes to the pathological conditions during RA. Recruitment of neutrophils which release proteolytic enzymes that lead to tissue destruction and joint inflammation [60] and activation of osteoclasts in the inflamed joint resulting in bone destruction [61] are some of the main effects induced by IL-6. Additionally, IL-6 induces the pro-matrix-metalloprotease (MMP) expression, proteins targeting the extracellular matrix leading to cartilage destruction in RA [62-64]. A number of different treatment options for RA are available that function by inhibiting human IL-6 or human IL-6R. Tofacitinib, an inhibitor of JAK1 and JAK3 thereby blocking IL-6 functions, has been approved for the treatment of RA in the US, Japan and Switzerland. The monoclonal antibodies tocilizumab and sarilumab, both targeting the IL-6R, have been also approved for the treatment of RA [65, 66]. With the generation of sgp130Fc, a fusion protein consisting of the extracellular part of gp130 and the Fc-part of a human IgG antibody, it became clear that the pro-inflammatory effects of IL-6, leading to RA, are mediated by IL-6 trans-signaling via the sIL-6R, whereas the regenerative, anti-inflammatory effects are mediated by classic signaling using the membrane-bound IL-6R [67, 68]. Therefore, a specific blockade of IL-6 trans-signaling could be sufficient for the treatment of RA. Currently, sgp130Fc is tested in phase II clinical trials [69].

1.2 Receptors of the cytokine Interleukin-6

In order to exert its functions, IL-6 needs to bind to its receptors to induce signal transduction. Receptors used by IL-6 are the non-signaling α-receptor Interleukin-6 receptor (IL-6R) and the

signaling β-receptor glycoprotein 130 (gp130). Both receptors are also present in the human blood as soluble receptors, sIL-6R and sgp130.

1.2.1 The β-receptor glycoprotein 130 (gp130)

Glycoprotein 130 is a ubiquitously expressed receptor used for signal transduction by cytokines of the IL-6 cytokine family. The human *IL6ST* gene is located on chromosome 7p21-p14 coding for a 918 amino-acid residue gp130 precursor protein. Removal of a 22 amino-acid long signaling peptide results in a 896 amino-acid residue mature protein [70] consisting of an extracellular part, a transmembrane part and an intracellular part. The extracellular part consists of one Ig-like domain and five fibronectin type-III domains (Fig. 1.2). Gp130 is further post-transcriptionally modified which results in a heavily N-glycosylated receptor with glycans being added at 9 asparagine residues in the extracellular part of the receptor. Deeper analysis of gp130 glycosylation revealed its importance for protein stability and localization to the plasma membrane but glycosylation seemed to be dispensable for ligand binding and subsequent signaling [71, 72]. Cell-surface expression is additionally regulated by the phosphorylation of S782 which leads to a down-regulation of the receptor at the cell-surface [73].

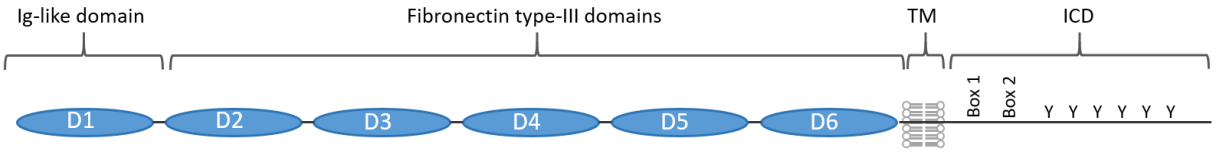

Figure 1.2: Schematic overview of the domain structure of glycoprotein 130. Gp130 consists of an extracellular part, a transmembrane region (TM) and an intracellular part (ICD) which carries the box 1 and box 2 motifs and five tyrosins. The extracellular part is furthermore built up by one Ig-like domain (D1) and five fibronectin type-III domains (D2-D6).

Three conserved motifs are present in the gp130 receptor. A WSXWS motif in the extracellular part was identified to be part of the arginine-tryptophan zipper thus being important for proper protein folding, protein stability and subsequent efficient intracellular transport [74]. The box 1 and box 2 motifs in the intracellular part are associated with proper signaling activation. Box 1 is important for Janus kinase (JAK) association with the intracellular domain of gp130 whereas box 2 is essential for JAK activation [75, 76].

As mentioned before, gp130 is present in human body fluids as soluble gp130 (sgp130) with concentrations of about 400 ng/ml in the blood. Different forms of sgp130 can be found in the human circulation [77]. One form of sgp130 has a molecular weight of approximately 100 kDa and consists of the five extracellular domains of gp130 [78]. Another smaller version of sgp130 called sgp130-RAPS has a molecular weight of about 50 kDa and comprises only the domains 1-3 of full-length gp130 [79]. The soluble forms of gp130 are mostly generated by differential splicing of the gp130 mRNA, but a minor fraction is also generated through proteolytic cleavage of the membrane-bound gp130 by the metalloproteases a disintegrin and metalloprotease (ADAM) 10

and ADAM17 [80]. Sgp130 functions as a natural inhibitor of IL-6-induced trans-signaling, a pathway involved in chronic pro-inflammatory conditions like e.g. rheumatoid arthritis [67, 81].

1.2.2 The α-receptor Interleukin-6 receptor (IL-6R)

Unlike gp130, which is expressed ubiquitously, the expression of the IL-6R is restricted to certain cell-types like hepatocytes and different subsets of immune cells, namely neutrophils, monocytes, macrophages, T cells, dendritic cells and megakaryocytes [82-85].

The human *IL6R* gene is located on chromosome 1 coding for a 468 amino-acid residue precursor protein. Removal of the first 19 amino-acid residues, which form the signal peptide, results in the 449 amino-acid residue mature protein (80 kDa) consisting of an extracellular part (346 aa), a transmembrane part (21 aa) and an intracellular part (82 aa). The extracellular part is, furthermore, made up by three domains, one Ig-like domain and two fibronectin type-III domains that form the cytokine binding module (CBM), and a 55 amino-acid residue long flexible stalk region (Fig. 1.3). Analysis of the intracellular part revealed that it lacks a tyrosine/kinase domain that is found in other growth factor receptors and therefore does not contribute to signaling activation [86, 87].

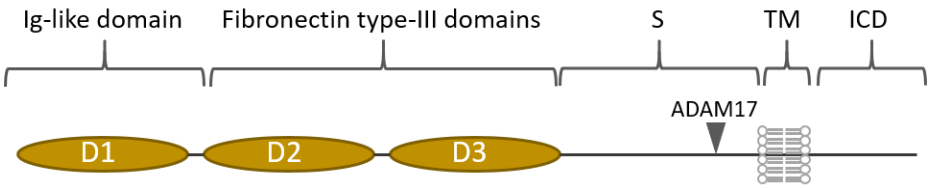

Figure 1.3: Schematic overview of the domain structure of the Interleukin-6 receptor. The IL-6R consists of an extracellular part, a transmembrane region (TM) and an intracellular part (ICD). The extracellular part is furthermore built up by one Ig-like domain (D1), two fibronectin type-III domains (D2-D3) and a stalk region (S) which carries the ADAM17 cleavage site.

IL-6R expression can be regulated by several factors, which seem to differ in various cell types. The first analysis of IL-6R expression regulation showed that it is influenced by steroid hormones or its synthetic derivatives as treatment of the hepatoma cell line HepG2 with dexamethasone or glucocorticoids led to an increase in IL-6R expression [88, 89]. Furthermore, IL-6R expression could be induced by EGF stimulation in MCF7 cells, HepG2 cells and primary murine hepatocytes which was found to be mTOR-dependent [90].

Hirata et al. identified the IL-6R as a glycoprotein as the predicted molecular weight for the IL-6R from 50 kDa differed from the experimentally obtained molecular weight of the IL-6R of 80 kDa. Treatment of the mature IL-6R with 0- and N-glycanase and neuraminidase reduced the molecular weight to 50 kDa indicating IL-6R glycosylation [91]. Further experiments revealed five N-linked glycosylation sites (N55, N93, N221, N245, N350) and one O-linked glycosylation site (T352) [92, 93] which are dispensable for protein transport, signaling and cell-surface turnover. However,

N55 was found to play a crucial regulatory role in the proteolysis of the membrane-bound IL-6R [93].

The IL-6R is not only present as a membrane-bound form but also as soluble forms (sIL-6R) which can be found in human body fluids like blood or urine [94]. Concentrations in the serum of healthy humans range between 30-80 ng/ml, mainly influenced by the single nucleotide polymorphism (SNP) rs2228145, which is a non-synonymous SNP that results in the exchange of the aspartic acid residue at position 358 to an alanine residue. This SNP leads to higher levels of sIL-6R in the serum, most likely due to an increase in proteolytic cleavage of the membrane-bound IL-6R [95] by the proteases ADAM10 and ADAM17, which are the major proteases involved in the proteolytic cleavage of the murine and human IL-6R [96, 97]. However, it seems that ADAM17 does not contribute to endogenous steady-state sIL-6R levels but is rather responsible for induced sIL-6R generation, e.g. during inflammatory events. This assumption comes from experiments in hypomorphic ADAM17$^{ex/ex}$ mice, which display only about 5% of normal ADAM17 activity [98] but show normal endogenous sIL-6R levels [97]. Also ADAM10 and Cathepsin G, a neutrophil-derived protease which is also able to cleave the IL-6R [99], seem not to be involved in the generation of endogenous sIL-6R levels. It is therefore likely that either a yet unidentified protease is responsible for the generation of endogenous sIL-6R levels [100] or that different proteases can compensate for one another.

Using sIL-6R released from COS-7 cells the cleavage site in the IL-6R used by ADAM17 could be identified to be between Q357 and N358 [101] which was, however, found to be disfavored by ADAM17 [102]. A recent study revealed a different cleavage site between P355 and V356 [93], which is also on good agreement with the cleavage site profile for ADAM17. This study also showed that ADAM10 and ADAM17 seem to use the same cleavage site in the IL-6R stalk as detected by LC-MS analysis. The sIL-6R is not only generated by proteolysis but also differential splicing contributes to sIL-6R serum levels in humans which results in a sIL-6R form containing a unique 10 amino-acid C-terminal residue [103]. Although differential splicing was the first mechanism identified in sIL-6R generation in humans it contributes only to about 15% of overall sIL-6R levels. The remaining 85% must therefore arise from proteolysis of the membrane-bound full-length IL-6R [93, 95]. Recently, the IL-6R was also found to be present on microvesicles isolated from murine serum [100]. Thus, IL-6R on microvesicles might also contribute to the remaining sIL-6R measured in human sera.

1.3 IL-6 mediated signal transduction

1.3.1 The IL-6/IL-6R/gp130 signaling complex

IL-6-dependent signal transduction relies on the binding to and dimerization of the signal transducing β-receptor gp130. IL-6, though, cannot bind to gp130 alone, but must bind to its α-

receptor IL-6R first. The IL-6/IL-6R complex can then induce gp130 homodimerization and, subsequently, IL-6 is able to interact with gp130 [9]. IL-6 interaction with the IL-6R and gp130 is mediated by three distinct binding sites in the cytokine. *Site I* binds to the α-receptor (domains D2 and D3), *site II* binds to the CBM of gp130 located in domains D2 and D3, and *site III* binds to the Ig-like domain of the other gp130 molecule [104-107]. This leads to the formation of a tetrameric complex consisting of one molecule IL-6, one molecule IL-6R and two molecules gp130. The exact complex structure, though, is still under debate, as also a hexameric complex consisting of two molecules each was proposed. Grötzinger et al. were the first to speculate that a tetrameric complex for IL-6-induced signal transduction forms whereas the hexameric structure would only form upon cytokine excess as a regulatory mechanism [108]. Different structural studies, however, also identified the hexameric structure as the IL-6 signaling complex which could be confirmed partially *in vitro* [104, 109-111].

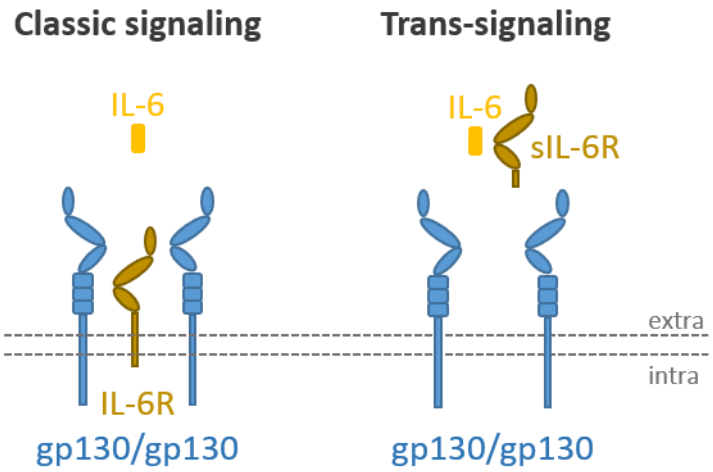

Figure 1.4: Overview of IL-6 classic and trans-signaling. IL-6 can induce signaling by binding to the membrane-bound form of IL-6R which induces homodimerization of gp130 and recruitment to the IL-6/IL-6R complex. This pathway is termed "classic signaling". IL-6 can also bind to a soluble version of the IL-6R (sIL-6R). This IL-6/sIL-6R complex can interact then with a gp130 homodimer thereby inducing signal transduction. This signaling pathway is termed "trans-signaling".

Signaling via IL-6 can be induced in two different ways (Fig. 1.4). Binding of IL-6 to the membrane-bound form of the IL-6R induces homodimerization of gp130 and recruitment to the IL-6/IL-6R complex where IL-6 interacts with the gp130 homodimer. This pathway is termed "classic signaling". Additionally, signaling can be induced by binding of the cytokine to the soluble form of the IL-6R, sIL-6R, and subsequent interaction with a homodimer of gp130 at the cell-surface. This signaling pathway is termed "trans-signaling" [112]. As IL-6R expression is restricted only to some cell-types, "trans-signaling" via the sIL-6R broadens the spectrum of cells that can be activated by IL-6 through binding to the ubiquitously expressed β-receptor gp130. These two pathways do not only differ in their mode of activation, but they are also thought to exert different functions. Whereas classic signaling is associated with anti-inflammatory properties, trans-signaling is found to play a role in pro-inflammatory conditions [68].

1.3.2 Signaling pathways activated by Interleukin-6

Binding of IL-6 to the IL-6R results in the dimerization of gp130 which is necessary for signaling initiation. Dimerization of gp130 leads to autophosphorylation of the Janus kinases 1 (JAK1), 2 (JAK2) and tyrosine kinase 2 (Tyk2) which are constitutively associated with the box 1 motif located in the intracellular part of gp130 [76, 113]. Further analysis of JAK involvement in IL-6 signaling revealed that JAK1 plays a non-redundant role in signal transducer and activator of transcription (STAT) activation as deletion of JAK1 abrogated signaling while deletion of the other two did not alter signaling [114]. Activated JAKs phosphorylate five distinct tyrosine residues in the intracellular domain of gp130 that are important for signal transduction [115, 116]. STAT proteins bind to the four phosphorylated distal tyrosines Y767, Y814, Y905, and Y915, resulting in phosphorylation of the STATs and their subsequent homo- or heterodimerization. The dimers then translocate into the nucleus where they function as transcription factors. The main STATs activated by IL-6 are STAT1 and STAT3 but also STAT5 activation can take place [116-119]. Although the JAK1/STAT3 pathway is the main pathway induced by IL-6 binding, other pathways are also activated like the mitogen-activated protein kinase/extracellular signal regulated kinase (MAPK/ERK) pathway or the phosphoinositide-3-kinase (PI3K) pathway. Both are influenced by the adaptor protein Src homology-2 domain containing phosphatase 2 (SHP-2) which binds to the phosphorylated tyrosine Y759 [120]. SHP-2 binding is dependent of JAK1 and interacts with growth factor receptor-bound protein 2 (Grb2) which results in the recruitment of SOS (son of sevenless) and subsequently activation of Ras (rat sarcoma) and the MAPK/ERK-cascade. SHP-2 can also interact with Grb2-associated binding protein 1 (Gab1) which leads to activation of the PI3K pathway (Fig. 1.5) [121]. Additionally, YAP (yes-associated protein) was found to be phosphorylated by Src family kinases bound to gp130 [122].

To prevent overstimulation by cytokine-induced signaling, different ways for signaling inhibition are present. The most prominent inhibitor of signaling is SOCS3 (suppressor of cytokine signaling 3) whose expression is absent in unstimulated cells but is rapidly induced by STAT3. It binds to the phosphorylated tyrosine Y759 in gp130 and exerts its inhibitory function by different mechanisms [123-125]. On the one hand, signaling is terminated via SOCS3 by inhibiting the kinase activity of the JAKs bound to gp130 [126]. On the other hand, it leads to an increase in proteasomal degradation of gp130 and the associated JAKs by recruiting an E3-ubiquitin ligase which marks the proteins for proteasomal degradation [127]. In addition to inhibition by SOCS3, IL-6 induced signaling can also be negatively regulated on the transcriptional level by PIAS (protein inhibitor of activated STAT). It binds phosphorylated STATs that enter the nucleus thus preventing STAT interaction with the DNA and transcription of IL-6 target genes [128, 129]. A further mechanism regulating IL-6-mediated signaling is endocytosis of the receptor complex and

subsequent degradation in the lysosome thereby removing IL-6 binding sites from the cell-surface and blocking signaling [130].

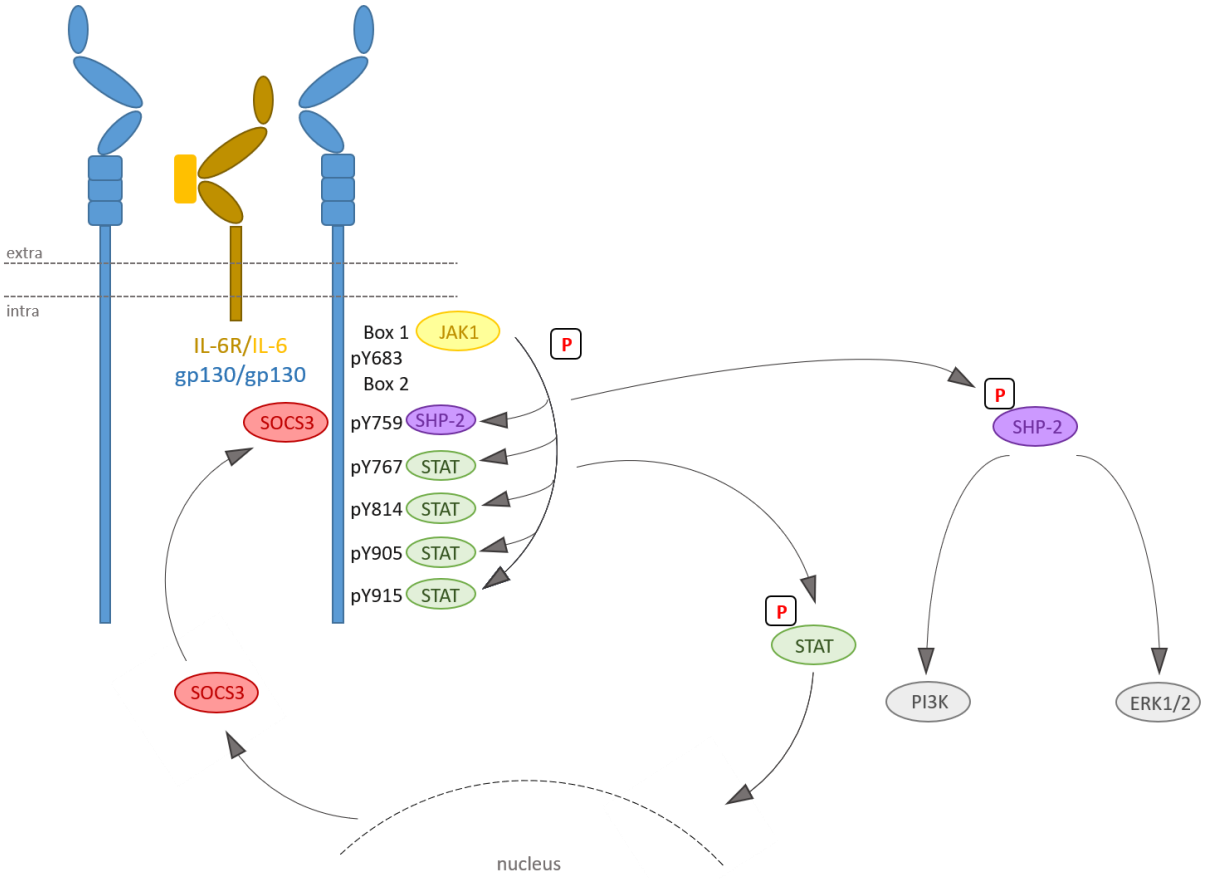

Figure 1.5: Schematic overview of the IL-6-induced signaling pathways. Upon IL-6/IL-6R/gp130 complex formation, JAK1 which is constitutively associated with the box 1 motif, is autophosphorylated. The phosphorylated JAK1, in turn, phosphorylates four tyrosine residues in the gp130 ICD where STAT proteins bind to (Y767, Y814, Y905, and Y915), resulting in phosphorylation of the STAT3 proteins and their subsequent homo- or heterodimerization. The dimers then translocate to the nucleus where they function as transcription factors for the transcription of e.g. SOCS3, an inhibitor of IL-6-induced signaling. Additionally, JAK1 phosphorylates the tyrosine residue Y759 where SHP-2 binds to. This leads to the phosphorylation of SHP-2 and, subsequently, to the activation of the PI3K and MAPK/Erk pathways. SOCS3 can also bind to the tyrosine residue Y759 thereby inhibiting IL-6-induced signaling. The red "P" indicates phosphorylation.

1.4 The fate of cell-surface proteins

Internalization and degradation of proteins is important for cell-surface protein level regulation and signal termination as constitutive signaling could lead to the generation of severe diseases like e.g. tumors. Once receptors are activated, they are internalized and fuse with early endosomes. From there, the proteins are sorted either for recycling to the cell surface or for degradation in the lysosome.

1.4.1 Internalization of cell-surface proteins

Several different ways of receptor internalization are known that can be mainly divided into clathrin-dependent and clathrin-independent pathways. The clathrin-independent pathways that use dynamin for vesicle detachment are the caveolae or the IL-2R pathways. The uptake of GPI-

anchored proteins occurs dynamin- and clathrin-independently via the CLIC/GEEC pathway (clathrin-independent carriers/GPI-enriched endocytic compartment), via flotillins or via Arf6 (ADP-ribosylation factor 6) [131]. The most abundant pathway of receptor internalization, though, occurs clathrin- and dynamin-dependently.

The process of endocytosis was first described in protein uptake experiments into the oocyte of the mosquito *Aedes Aegypti* where it was shown that coated invaginations formed that protruded into the cell which were released as vesicles into the cytoplasm where they lost their coat [132]. These coat proteins were later identified as clathrin which formed network structures around the observed invaginations [133]. Further experiments revealed that several accessory molecules and adaptors are necessary for binding of clathrin to the cell membrane, bud formation and subsequently pinching off the vesicle from the membrane (Fig. 1.6). The first step of endocytosis, the nucleation, depends on the formation of a nucleation module consisting of FCH domain only proteins (FCHO), EGFR pathway substrate 15 (EPSIN15) and intersectins around phosphatidylinositol-4,5-bisphosphate (PIP2) leading to slight bending of the plasma membrane [134]. This module recruits the heterotetrameric adaptor protein 2 (AP-2) complex which is composed of α, β2, μ2 and σ2 subunits. Recruitment of the AP-2 complex is mediated through binding of the subunits α, β2 and μ2 to PIP2 [135]. Afterwards, clathrin is recruited and interacts with the β2 subunit [136] which results in the phosphorylation of T156 in the μ2 subunit by the adaptor-associated kinase 1 (AAK1) [137, 138]. This phosphorylation leads to a conformational change of the μ2 subunit opening the binding site which binds specifically to cargo proteins containing tyrosine-based motifs Yxxϕ (Y:tyrosine; x: any amino-acid; ϕ: bulky hydrophobic amino-acid) [135, 139]. The AP-2 complex can not only bind to Yxxϕ-based motifs via the μ2 subunit but also to dileucine-like motifs via its σ2 subunit [140]. Bud formation at the plasma membrane is further regulated by the endocytic accessory clathrin assembly lymphoid myeloid leukemia protein (CALM), a homolog of the neuron-specific protein AP180 (adaptor protein 180). It can bind to PIP2 at the plasma membrane by its AP180 N-terminal homology (ANTH)-domain, but it also interacts with clathrin and AP-2. Depletion of CALM results in irregular shaped buds indicating an important role of CALM in the regulation and proper progression of bud formation [141]. The N-BAR-domain containing proteins amphiphysin, endophilin or SNX9 recruit the mechanoenzymatic protein dynamin to the clathrin-coated buds at the plasma membrane [142, 143]. The involvement of dynamin in the process of endocytosis was discovered after it was identified as the homologue of the shibire protein in Drosophila which was already known to be involved in endocytosis [144]. After polymerization around the neck of the clathrin-coated buds, dynamin constricts upon GTP hydrolysis, which leads to fission of the vesicle and release into the cytoplasm [145, 146]. There, the vesicle is uncoated after binding of the cyclin-G associated kinase (GAK) and recruitment of the ATPase heat shock cognate 70 (HSC70) [147, 148]. The vesicle can

then fuse with the early endosome from where internalized proteins are either sorted to late endosomes, to recycling endosomes, or directly back to the cell surface.

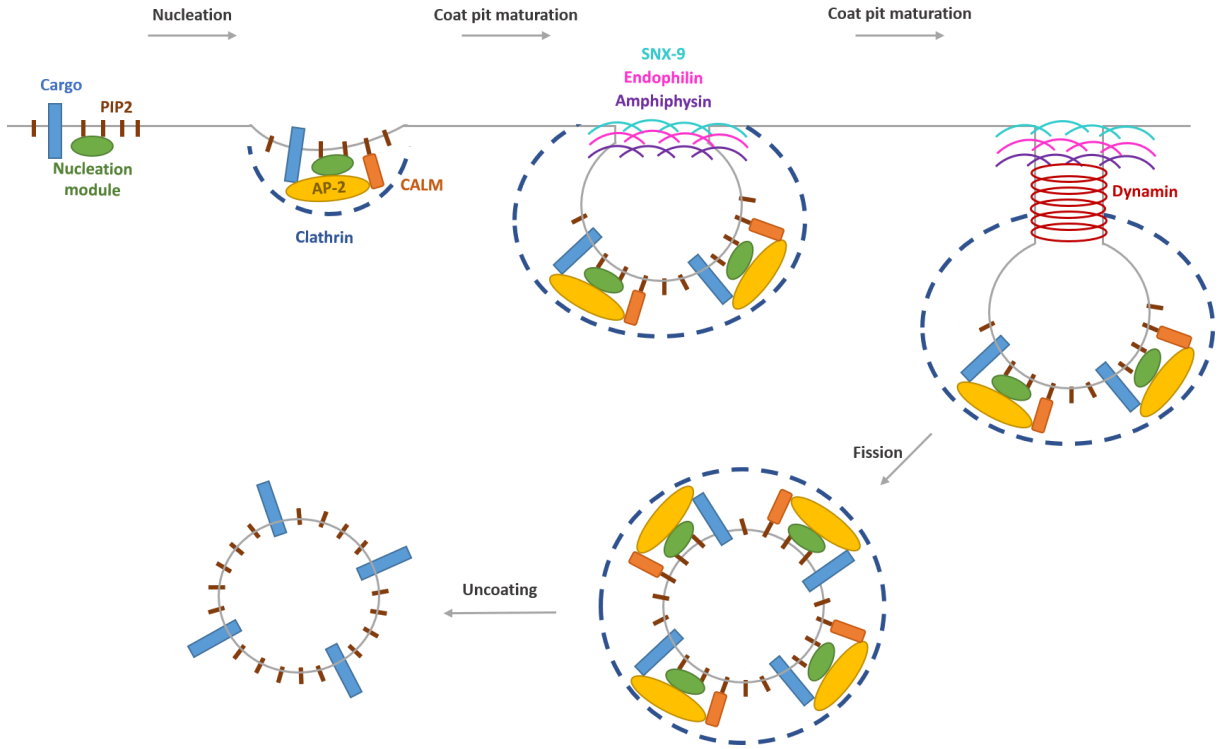

Figure 1.6: Schematic overview of clathrin- and dynamin-dependent internalization. The nucleation module consisting of FCH domain only proteins (FCHO), EGFR pathway substrate 15 (EPSIN15) and intersectins binds to phosphatidylinositol-4,5-bisphosphate (PIP2) which is located in the plasma membrane thereby inducing slight bending of the membrane. Following nucleation, the module recruits the heterotetrameric adaptor protein 2 (AP-2) complex which, in turn, recruits clathrin. Additionally, CALM is recruited which also binds to PIP2 but also interacts with AP-2 and clathrin and stabilizes the formed complex. Amphiphysin, endophilin and SNX-9 bind to the base of the forming bud and recruit dynamin to the neck of the bud. Dynamin polymerizes around the neck and upon constriction of the dynamin molecules induced by GTP-hydrolysis, the clathrin-coated vesicle is released into the cytoplasm. Finally, the vesicle is uncoated mediated by cyclin-G associated kinase (GAK) and ATPase heat shock cognate 70 (HSC70) (adapted from Takei and Haucke, 2001 [2]).

Analysis of IL-6R internalization in MDCK cells or hepatocytes revealed that it occurs constitutively and independently of its cytokine IL-6. Accordingly, IL-6 stimulation did not lead to an increase in internalization of the IL-6R [149-151]. Constitutive internalization was also found to be true for gp130 [149, 150]. Fujimoto et al. further analyzed the pathway of IL-6R and gp130 internalization and found that the IL-6R is internalized in a clathrin- and dynamin-dependent way, whereas gp130 seems to be internalized independently of clathrin as inhibition of AP-2 showed only little effect on endocytosis [152]. Thiel et al., however, stated that gp130 is also internalized via clathrin and dynamin as it interacts with AP-2 [150]. The involvement of clathrin/AP-2 in IL-6R and gp130 internalization is further supported by the identification of internalization motifs that are recognized by AP-2. Dittrich et al. identified the amino-acid sequence STQPLLD in the gp130 cytoplasmic portion to be essential for receptor internalization. Specifically, the di-leucine motif and the upstream serine were crucial for this process because mutations of both disrupted gp130 internalization [153]. Such motifs were also identified in the short cytoplasmic part of the IL-6R, namely the tyrosine-based motif YSLG and a di-leucine-like motif LI. The importance in IL-

6R internalization was revealed by analysis of internalization of a truncated version of the receptor where both motifs were deleted which resulted in little to no internalization [152].
The function of receptor internalization was long believed to be solely that of signaling termination. However, several studies showed that internalization can have a fundamental different purpose and is often a prerequisite for signal transduction at endosomes as it was shown for ERK or Akt signaling via APPL1 or TGFβ signaling via SMAD2-SMAD4 [154, 155]. Similar effects have also been described for IL-6-induced signaling. STAT3 and ERK1/2 phosphorylation was abolished in HepG2 cells after inhibition of internalization with chlorpromazine which led to the conclusion that activation of these signaling pathways indeed takes place at vesicular structures or endosomes [156]. These findings could be partially confirmed in gp130 overexpressing cells that were treated with the dynamin-inhibitor dynasore. Here, inhibition of internalization also led to abrogated STAT3 phosphorylation whereas ERK1/2 phosphorylation was even increased [157]. Different studies revealed that the process of signaling termination after IL-6 stimulation was regulated by *de novo* synthesized proteins that were identified as SOCS3 and PIAS [158, 159].
The fate of the IL-6R and gp130 after internalization is currently unclear, and published results in this regard are contradictory. Zohlnhöfer et al. stated that the IL-6R is probably degraded and not recycled back to the cellular membrane as it took more than 8 hours to fully restore the IL-6 binding sites at the cell surface [151]. Fujimoto et al., however, stated that, although the IL-6R is found to be transported to the lysosome and degraded there, a fraction of the IL-6R is also recycled back to the cell surface [152]. Analysis of gp130 revealed that the receptor is probably degraded after internalization and is not recycled as inhibition of protein synthesis after IL-6 treatment led to diminished gp130 surface levels [160]. This was confirmed by Tanaka et al. who even found differences in receptor degradation after IL-6 stimulation. They showed that gp130 is degraded through the proteasome in the absence of IL-6 stimulation but is transported to the lysosome after IL-6 stimulation by binding of SHP2 to gp130, recruitment of and monoubiquitination by c-Cbl and transport from early to late endosomes by Hrs [161].

1.4.2 Recycling of internalized proteins

Once a protein is internalized, it is targeted to early endosomes, also called sorting endosomes, from where it is transported either to recycling endosomes or to late endosomes/lysosomes.
The first hint for the process of recycling came from the analysis of endocytosis of transferrin (Tf) and the transferrin receptor (TfR), where it was shown that endocytosed TfR and Tf were found in vesicular endosomes that were distinct of lysosomes. These vesicular endosomes were able to fuse with the plasma membrane and release their content into the extracellular space [162]. Further analysis of Tf and TfR recycling revealed the existence of two separate ways of recycling, which were termed fast and slow. Pulse-chase experiments showed that the rapidly recycling proteins reappeared at the cell surface with a half-life of 7.5 min, but also 60 min later proteins

were still recycled to the plasma membrane [163]. “Fast recycling” involves the transport from early endosomes directly back to the cell surface whereas in “slow recycling” internalized proteins are transported from the early endosomes to recycling endosomes and from there to the cell surface.

Over the years, several studies focused on recycling and identified Rab GTPases and different effectors and adaptors of these to be important, especially Rab4 and Rab11 were found to be involved in “fast” and “slow recycling”, respectively (Fig. 1.7) [164, 165]. Sorting of proteins for recycling occurs through tubulation of early endosomal membranes leading to a Rab5-positive cisternal region and Rab4-positive tubules that undergo fission [166]. “Fast” recycling was shown to be mediated by binding of the γ-subunit of AP-1 to Rab4 and formation of clathrin-coated vesicles and was regulated by the effectors rabaptin-5a/rabex-5, which inhibit recycling through interaction with AP-1γ [167, 168]. Subsequently, D’Souza et al. presented a small GTPase cascade which is mediated by Rab4 and that is responsible for the recruitment of adaptor proteins to early endosomes and the formation of recycling vesicles. They showed that Rab4 recruits the Arf-like protein Arl1 to Rab4 positive endosomal tubules and that it in turn recruits the Arf GEFs BIG1 and BIG2. These induce the assembly of the adaptors AP-1, AP-3 and GGA-3 to the tubular structures by activation of Arf1 and Arf3. The adaptors select their cargo and induce vesicle formation and fission [169]. The released vesicles localize to the plasma-membrane and most probably interact there with SNARE proteins thereby inducing fusion of the vesicle with the plasma membrane. Another Rab GTPase found to be involved in fast recycling is Rab35, as inhibition of Rab35 led to an accumulation of proteins at early endosomes [170].

Rab11, a protein involved in “slow” recycling, was found to function in the release of recycling vesicles from recycling endosomes which is facilitated by the interaction of Bin1 and amphiphysin 2 [171]. Following, the released Rab11-positive vesicles are transported along microtubules to the cell surface by binding Rab11-FIP2 (Rab11-family interacting protein 2) which interacts with Myosin Vb (MyoVb), a motor protein involved in the transport of vesicles along actin [172, 173]. Finally, Rab11 induces tethering of the recycling vesicle to the plasma membrane by binding Sec15, a component of the exocyst tethering complex, which in turn binds Exo70, another component of the exocyst tethering complex. Exo70 then interacts with PIP2 present at the cell surface thereby bringing the recycling vesicle in close contact with the plasma membrane which results in the fusion of the vesicle with the plasma membrane [174]. In neutrophils, another protein involved in vesicle trafficking and docking to the plasma membrane was found, namely Munc 13-4, which is able to interact with Rab11 [175].

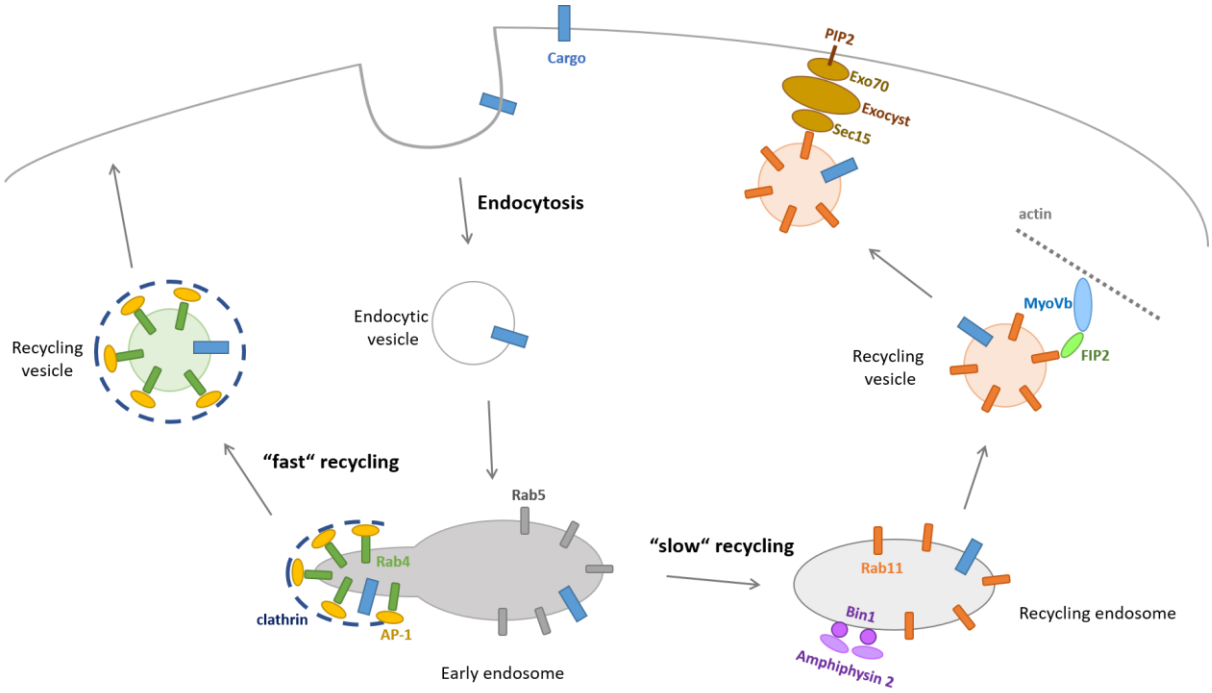

Figure 1.7: Schematic overview of "fast" and "slow" recycling. Upon endocytosis, the cargo is transported to the early endosome from where it can be recycled to the plasma membrane either via "slow" or "fast" recycling. Sorting of proteins for recycling occurs through tubulation of early endosomal membranes leading to a Rab5-positive cisternal region and Rab4-positive tubules that undergo fission. For "fast" recycling, the cargo is transported to the Rab4-positive tubules in the early endosome. There, Rab4 interacts with AP-1 to which clathrin binds. The Rab4-positive clathrin-coated recycling vesicles are released from the early endosome, lose their coat and are transported to the plasma membrane. There, the recycling vesicle fuses with the plasma membrane thereby recycling the cargo. During "slow" recycling, the cargo is sorted to Rab11-positive recycling endosomes. Recycling vesicles are released from recycling endosomes by interaction of Bin1 and amphiphysin 2 which results in the fission of the recycling vesicle. Following, the recycling vesicles are transported to the plasma membrane along actin microtubules via Myosin Vb (MyoVb) which interacts with Rab11-family interacting protein 2 (FIP2) bound to Rab11 present on the recycling vesicles. Once the recycling vesicle is close enough to the plasma membrane, Rab11 can bind Sec15, a component of the exocyst tethering complex associated with the plasma membrane by interaction of Exo70 with PIP2. This brings the vesicle into close contact with the plasma membrane thereby facilitating fusion of the vesicle with the plasma membrane and recycling of the cargo (adapted from Guichard et al., 2014 [3]).

1.4.3 Lysosomal degradation of internalized proteins

Degradation of extracellular and membrane proteins takes place in the lysosome after these have been internalized and sorted from the early endosome to the late endosomal compartment. The presence of lysosomes was first identified after analysis of enzymatic activities in different tissue fractions in which high levels of acid phosphatases, ribonucleases, deoxyribonucleases, cathepsins, β-glucuronidase and uricase were identified [176]. Electron-microscopy studies of fractions with high acid phosphatase activity revealed structures that were named "dense bodies" and later renamed lysosomes [177].

Lysosomes are generated by the fusion of late endosomes (also called multivesicular bodies) with transport vesicles that originate from the trans-Golgi network. These transport vesicles contain the lysosomal enzymes, which are produced in the ER and transported to the Golgi. Packaging of acid hydrolases into the transport vesicles is facilitated by mannose-6-phosphate (M6P) and is bound by M6P-receptors located in the trans-Golgi network. Subsequently, this complex is

packaged into clathrin-coated vesicles. Once the vesicle has fused with the late endosome the acid hydrolases are released into the late endosome which will gradually develop into a mature lysosome [178]. Lysosomal enzymes can not only be transported in a M6P-dependent manner but also independently of M6P by e.g. sortilin or the lysosomal integral membrane protein type 2 (LIMP-2) [179, 180].

A prerequisite for protein degradation in the lysosomal compartment is a low pH of about 5, which is required for the activation of the lysosomal enzymes. This low pH is achieved by influx of H^+ by a vacuolar-type H^+-ATPase (V-ATPase) and by efflux of the counterion Cl^- by the Cl^-/H^+ antiporter ClC-7 [181, 182]. The acidic pH is not only responsible for the activation of the acid hydrolases but also for the dissociation of the enzymes from the M6P receptors.

In order to protect the cell from lysosomal enzymes, the lysosomes are surrounded by a limiting membrane that is lined on the inside by a thick glycocalyx which is composed of lysosomal integral membrane proteins (LIMPs) and lysosomal-associated membrane proteins (LAMPs) [183, 184]. These compounds make the membrane impermeable for proteins to leave the lysosome. As the enzymes are only active at acidic pH lysosomal enzymes would also not be harmful to the cell but be inactivated in the cytoplasm.

Up to now, about 50 acid hydrolases are known that serve as phosphatases, nucleases, glucosidases, proteases, peptidases or lipases. The most prominent members of lysosomal enzymes are the cathepsins [185].

1.4.3.1 The family of cathepsins

The first member of the cathepsin family, papain, was isolated from the papaya fruit [186]. Over the years a total of 15 cathepsins were identified and grouped according to their active site catalytic residue. Cathepsin A and G belong to the serine cathepsins and Cathepsin D and E belong to the aspartate cathepsins. The largest group with 11 members (Cathepsins B, C, F, H, K, L, O, S, V, W and X) are called cysteine cathepsins. All the cysteine cathepsins display endopeptidase activity with cathepsins B, H, X and C also showing exopeptidase activity [185].

Cysteine cathepsins are generated as inactive pre-proenzymes consisting of a signal peptide, a propeptide and the active enzyme. Directing of the pre-proenzyme to the endoplasmic reticulum (ER) occurs via the signal peptide, which is then cleaved off, and N-linked glycosylation with high-mannose glycans takes place. The proenzyme is then transported to the Golgi where the mannose is phosphorylated to generate M6P, which is necessary for the trafficking to the endosome. Following acidification of the endosome, the propeptide, which facilitates proper folding and functions as an inhibitor of the enzyme, is cleaved off leading to the formation of the mature and fully active enzyme [187, 188].

Enzyme activity of mature cysteine cathepsins can be regulated by the endogenous inhibitors of the cystatin superfamily consisting of stefins (cystatins A and B), cystatins (cystatins C and D) and

kininogens. They function as regulatory inhibitors but also as emergency inhibitors, binding to cathepsins that accidentally were released into the cytoplasm of the cell [189]. Cathepsin K activity was shown to be inhibited by cystatin C [190], whereas Cathepsin H is inhibited by cystatin A [191]. The inhibitors cystatin C and B are involved in the regulation of Cathepsin B and S [192].

Cathepsins have diverse functions e.g. in thymocyte and T cell apoptosis (Cathepsin B), bone remodeling (Cathepsin K), protein degradation or antigen presentation (Cathepsin S) [192, 193].

1.4.3.2 The cysteine Cathepsin S

The endopeptidase Cathepsin S (CTSS) was first identified in calf lymph nodes by Turnsek et al. in 1975 [194], but CTSS expression was later also found in heart, lung and spleen [195]. Further analysis of CTSS expression revealed that it is restricted to macrophages [195], B cells or antigen-presenting cells (APCs) like dendritic cells (DCs) [196, 197], which makes CTSS unique among the other cysteine cathepsins that are expressed ubiquitously.

By Fluorescence in Situ Hybridization the human *CTSS* gene was found to be localized at chromosome position 1q21 [195]. CTSS is synthesized as a 331 aa long inactive pre-proenzyme which consists of a signaling peptide (16aa), a propeptide (98aa) and the mature CTSS enzyme (217aa; 28kDa) [198]. The mature CTSS is a monomer which consists of two domains. Situated at the interface of these two domains, the substrate-binding cleft with the catalytic triade (C25, H164, N184) is responsible for binding and cleavage of the substrate [199, 200]. Rückrich et al. (2006) could demonstrate that the substrate's P2 position determines specificity of CTSS favoring valine, leucine, methionine, cysteine or phenylalanine at this position [201].

CTSS is not only unique among the other cysteine cathepsins due to its restricted expression but also due to its stability at neutral pH. Whereas all the other cysteine cathepsins are only active at acidic pH (pH ~5), CTSS retains its activity at neutral or even slightly alkaline pH [202, 203]. This feature makes it possible for CTSS not only to cleave and degrade proteins in the lysosome where it is localized primarily but it can e.g. also cleave extracellular matrix proteins like laminin, fibronectin or elastin after CTSS has been transported to the cell-surface and has been secreted into the extracellular space [204-207]. The first important function of CTSS discovered was the involvement in MHC class II antigen presentation. Studies in B cells showed that CTSS was responsible for the removal of the invariant chain (Ii, CD74) from MHC class II molecules rendering it open for binding and presentation of peptide fragments [208]. This finding was supported by analyses of B cells and dendritic cells of CTSS-deficient mice which displayed diminished MHC class II antigen presentation produced by a lack of invariant chain processing [196].

Several studies link CTSS to different diseases. In a murine antigen-induced arthritis model it was shown that CTSS was upregulated and disease progression could be reduced when CTSS was

absent [196, 209]. Furthermore, CTSS was linked to Multiple Sclerosis (MS) as the protease can cleave myelin basic protein (MBP), a protein found in the myelin sheet of neurons important for neuron protection. Degradation of MBP was found to be the key process in demyelination during MS disease progression. Analysis of serum samples from MS patients revealed significantly elevated levels of CTSS [192, 210]. CTSS is also involved in many types of cancer mainly through its effects on angiogenesis and microvessel growth. Knockout of CTSS revealed not only reduced angiogenesis but also delayed tumor growth and progression. Inhibition of CTSS led to reduced cell invasion in colorectal, hepatocellular, breast and prostate cancer cell lines and *in vivo* inhibition could also reduce tumor growth in colorectal cancer [206, 211, 212].

1.5 Toll-like Receptors

Innate immune responses depend on the recognition of pathogen-associated microbial peptides (PAMPs) by pattern-recognition receptors (PRRs) like the Toll-like receptors (TLRs). Extensive work was done by Watson et al. on the identification of the first TLR, a lipopolysaccharide (LPS) responsive receptor, by analyzing different mouse strains being low-responders to LPS from gram-negative bacteria. He could link the unresponsiveness of these mice strains to a gene locus on the murine chromosome 4, which he named the *Lps* gene [213-215]. This gene was later analyzed more closely and found to be a homologue of a gene located on the human chromosome 9 (resembles murine chromosome 4) which encodes the Toll-like receptor 4 (TLR4) [216], that was shortly before identified together with TLR1, 2, 3 and 5 as homologs of the Toll receptor from *Drosophila melanogaster* [217]. Over the years a total of 10 functional TLRs were identified in humans that can be classified by their localization: TLR1, 2, 4, 5, 6 and 10 are found on the cell surface where they recognize mainly lipids and proteins from bacteria and fungi. In contrast, TLR3, 7 and 9 are located on intracellular structures like the endoplasmic reticulum, endosomes or lysosomes, where they bind nucleic acids from different viruses and bacteria [218]. TLRs are expressed by different cell types like macrophages, neutrophils, DCs and NK cells but also by T and B cells or even epithelial cells [219], making these immune cells susceptible for the binding of viral or bacterial factors.

TLRs are type-I trans-membrane receptors that consist of a N-terminal horseshoe-shaped extracellular part (ECD) with leucine-rich repeats (LRRs) which binds ligands, a trans-membrane region and a C-terminal intracellular domain, the TIR (Toll IL-1 receptor) domain, which is important for signaling [220]. Once the ligand binds to the ECD, different signaling pathways are activated, mostly via the TIR domain-containing adaptor molecules MyD88 (Myeloid differentiation primary response 88) or TRIF (TIR-domain-containing adapter-inducing interferon-β). MyD88, an adaptor molecule for all TLRs except TLR3, binds to the adaptor TIRAP (TIR domain containing adaptor protein) which leads to the activation of NF-κB or MAPK signaling pathways resulting in the induction of inflammatory cytokines. The adaptor molecule for TLR3

signaling is TRIF which binds to the adaptor TRAM (TRIF-related adaptor molecule) and activates IRF3 and NF-κB. This leads to the induction of type I interferon and inflammatory cytokines. TLR4 can use both adaptors, TRIF or MyD88, depending on its cellular localization. At the cell surface it binds MyD88, but recruits TRIF after internalization [221]. Some of the TLRs rely on coreceptors for binding of ligands and signal initiation like for example MD2 for TLR4, CD14 for TLR2, 3 and 4 or TLR1 and 6 for TLR2 [222].

Analysis in mice revealed a link between TLR4 activation and the release of sIL-6R. After injecting mice with LPS, thereby activating TLR4, an increase in murine sIL-6R serum levels could be observed, the release of which was mediated by ADAM17 [223]. Whether there is also a link between sIL-6R release and the other TLRs in mice is unclear. In humans, endogenous stimuli that lead to sIL-6R release are only poorly understood and the involvement of TLR4 or other TLRs in sIL-6R release has not been investigated so far.

1.5.1 Toll-like Receptor 2

Toll-like receptor 2 (TLR2) is expressed by different cell types like dendritic cells, monocytes, B cells, activated T cells, microglia, astrocytes or even epithelial cells [224, 225]. TLR-2 was found to mainly form heterodimers with TLR1 or TLR6 [226-229] which bind lipoproteins or lipopeptides of different pathogens, like bacteria, viruses, fungi or even protozoans. These dimers differ though in their specificity for different lipoproteins/lipopetides as TLR2/TLR1 only recognizes triacetylated proteins whereas TLR2/TLR6 binds diacetylated proteins [227, 228]. Toll-like receptors cannot only bind pathogenic ligands but also endogenous ligands that are secreted as a result of cell death and injury or by tumor cells. These endogenous ligands are mainly degradation products of the extracellular matrix (ECM), heat-shock proteins or high-mobility group box 1 (HMGB1) proteins. Especially ECM components were identified to activate TLR2, namely biglycan [230], hyaluronic acid [231] or versican [232].

Loading of ligands onto the TLR2 dimers depends on different co-receptors. CD36 was shown to interact with diacetylated lipoproteins loading these ligands onto TLR2/TLR6 dimers with the help of CD14 [233-235]. Loading of triacetylated lipoproteins onto TLR2/TLR1 dimers is facilitated by the co-receptor CD14 alone [236]. Integrin-β3 was identified as a further co-receptor which helps to induce TLR2 functions via vitronectin [237]. Another co-receptor of TLR2 was found to be Dectin-1 as blockade of Dectin-1 led to a reduced TLR2-dependent cytokine release from bone-marrow derived macrophages [238]. Once the ligand is bound to the TLR2 heterodimers the intracellular TIR domain is phosphorylated at Y616 and Y761 by Rac-1[239], which leads to binding of TIRAP and MyD88. MyD88 phosphorylation by Brutons tyrosine kinase (Btk) recruits IRAK1 (interleukin-1 receptor associated kinase 1) and IRAK4 proteins which interact with TRAF6 resulting in K63-linked ubiquitination of IRAK1, leading to the activation of different signaling pathways, namely the MAPK pathway (ERK and p38 dependent) or the NF-κB

pathway [240, 241]. This induces the release of inflammatory cytokines like IL-6. Signaling is negatively regulated by conjugation of K48-linked polyubiquitination residues to TIRAP by Triad3A or SOCS1 (suppressor of cytokine signaling 1) which marks the TLR associated protein for proteasomal degradation (Fig. 1.8) [242, 243].

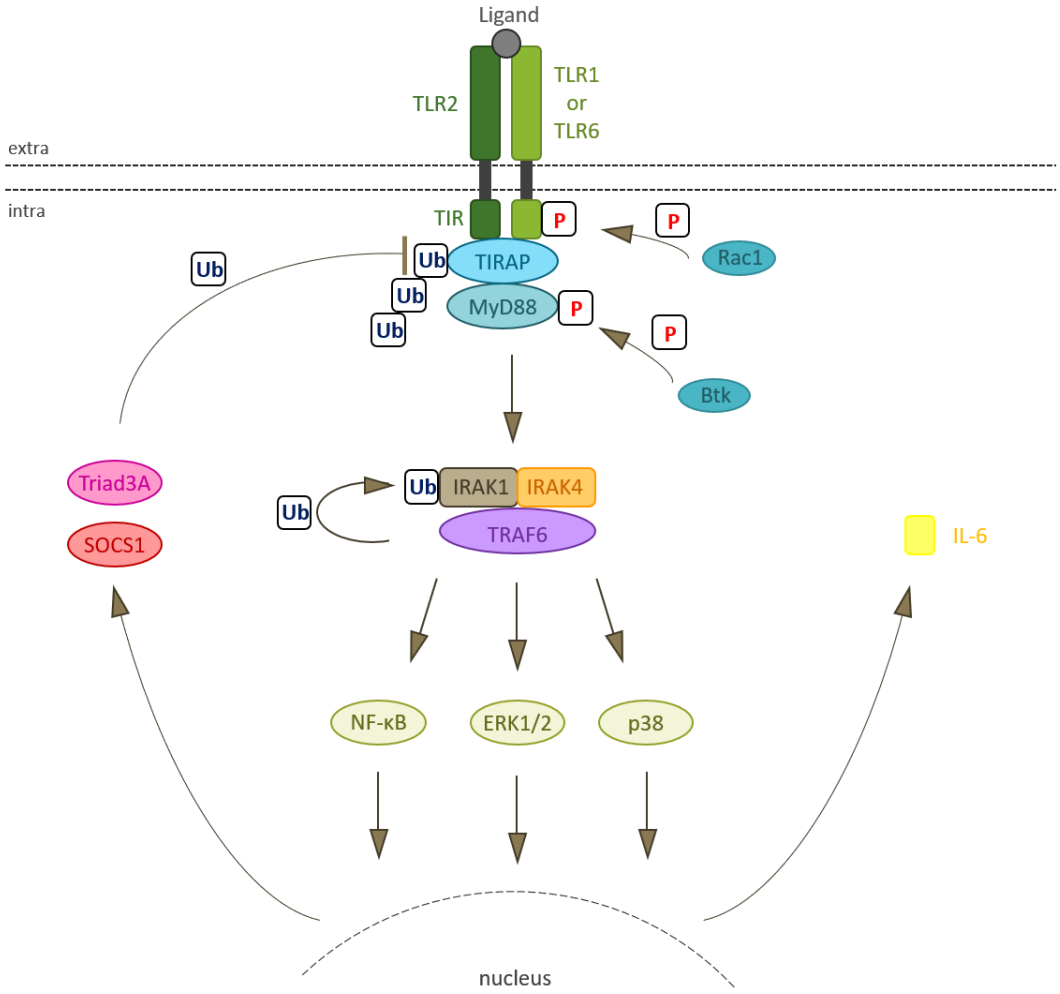

Figure 1.8: Schematic overview of TLR2 signaling. TLR2 signaling is induced by ligand binding either onto TLR2/TLR1 dimers or onto TLR2/TLR6 dimers. Upon ligand binding, the TIR domains of the receptors are phosphorylated by Rac-1, which leads to binding of TIRAP and MyD88. Brutons tyrosine kinase phosphorylates MyD88 thereby inducing complex formation of IRKA1, IRAK4 and TRAF6. Ubiquitination of IRAK1 by TRAF6 leads to the activation of MAPK/p38, MAPK/ERK and NF-κB signaling pathways. This induces the release of pro-inflammmatory cytokines like e.g. IL-6. TLR2 signaling is negatively regulated by SOCS1 and Triad3A which polyubiquitinate TIRAP thereby marking it for proteasomal degradation (adapted from Takeda and Akira, 2004 [1]).

TLR2 activation is further regulated by the soluble Toll-like receptor 2 (sTLR2), which is released from monocytes due to proteolysis of the membrane-bound TLR2 by metalloproteinases [244] and can be detected in the blood plasma, human milk, saliva or amniotic fluid [245-247].

2 Aims of this thesis

Different mechanisms are known that contribute to the regulation of cell-surface levels of receptors. Cell-surface levels are reduced upon internalization or proteolytic cleavage of the receptors. To maintain receptor levels at the cell-surface, new receptors are constantly synthesized and transported to the plasma membrane. Upon internalization receptors are either recycled back to the cell surface or are degraded in the lysosome. How exactly gp130 and IL-6R cell-surface levels are regulated is still unclear. However, it would be important to elucidate the regulation of both receptors as IL-6-mediated signaling is involved in many different inflammatory conditions like e.g. rheumatoid arthritis. These diseases are treated e.g. with tocilizumab, a monoclonal antibody directed against the IL-6R. Deciphering the regulatory mechanisms involved in maintaining the receptors' cell-surface levels would help to improve the treatment of inflammatory diseases.

Despite previous investigations it is still unclear whether IL-6R and gp130 undergo recycling, degradation or a combination of both following internalization. Furthermore, the influence of IL-6 on internalization, recycling and degradation has not been elucidated so far.

IL-6-mediated signaling cannot only be induced by binding of IL-6 to the membrane-bound form of the IL-6R, but also by complex formation of IL-6 and a soluble form of the IL-6R (sIL-6R). The sIL-6R can be generated by differential splicing or by proteolytic cleavage of the membrane-bound IL-6R by the metalloproteases A disintegrin and metalloproteinase (ADAM) 10 and 17. In mice, it was shown that activation of the Toll-like receptor (TLR) 4 induced ADAM17-mediated release of sIL-6R, but the involvement of TLRs and endogenous stimuli in the release of sIL-6R have not been identified in humans so far.

In humans, sIL-6R is present in the blood serum at concentrations ranging from 30-80 ng/ml which are slightly increased upon stimulation. While ADAM17 is involved in sIL-6R cleavage upon stimulation, its role in the generation of the constitutively released sIL-6R is still unclear. Therefore, it is important to identify additional proteases that are able to cleave the membrane-bound IL-6R and might therefore be involved in the generation of the constitutively released sIL-6R.

Thus, the aims of this thesis cover several aspects of IL-6 biology: the elucidation of the intracellular fate of the IL-6R following internalization of the receptor complex, the identification of endogenous stimuli leading to sIL-6R generation, and the discovery of novel proteases of the IL-6R and their potential role in IL-6 signaling *in vivo*.

3 Materials and methods

3.1 Materials

3.1.1 Antibiotics

Antibiotics	Supplier	Working concentration
Ampicillin	Carl Roth GmbH, Karlsruhe, Germany	100 µg/ml
Kanamycin	Carl Roth GmbH, Karlsruhe, Germany	25 µg/ml
Puromycin	Carl Roth GmbH, Karlsruhe, Germany	1,5 µg/ml

3.1.2 Antibodies

3.1.2.1 Primary antibodies

Antibody	Supplier
anti-IL-6R (4-11)	Produced in house as described in Chalaris, 2007 [248]
anti-IL-6R (BAF227)	R&D Systems, Minneapolis, USA
anti-gp130 (B-P4)	abcam, Cambridge, UK
anti-phospho-STAT3 (Y^{705}; D3A7)	Cell Signaling Technology, Frankfurt/Main, Germany
anti-phospho-ERK (T^{202}/Y^{204}; D13.14.4E)	Cell Signaling Technology, Frankfurt/Main, Germany
anti-phospho-p65 (S^{536})	biorbyt, Cambridge, UK
anti-phospho-p38 (T^{180}/Y^{182})	Cell Signaling Technology, Frankfurt/Main, Germany
anti-STAT3 (124H6)	Cell Signaling Technology, Frankfurt/Main, Germany
anti-ERK (L34F12)	Cell Signaling Technology, Frankfurt/Main, Germany
anti-p65 (D14E12)	Cell Signaling Technology, Frankfurt/Main, Germany

Antibody	Supplier
anti-p38	Cell Signaling Technology, Frankfurt/Main, Germany
anti-GAPDH (14C10)	Cell Signaling Technology, Frankfurt/Main, Germany
anti-Actinin (D6F6)	Cell Signaling Technology, Frankfurt/Main, Germany
anti-LAMP2 (H4B4)	DSHB, Iowa, USA
anti-LAMP2 (PA1-655)	Thermo Fisher Scientific, Life Technologies GmbH, Darmstadt, Germany
anti-Rab11 (65200)	abcam, Cambridge, UK
anti-IL-6R-APC	BioLegend, San Diego, USA
anti-TLR2-BV421	BioLegend, San Diego, USA
anti-CD45-BV510	BioLegend, San Diego, USA
anti-CD14-APC/Cy7	BioLegend, San Diego, USA
anti-B220-PE	BioLegend, San Diego, USA
anti-CD3-AlexaFlour488	BioLegend, San Diego, USA
anti-CD56-PE/Cy7	BioLegend, San Diego, USA

3.1.2.2 Secondary antibodies

Antibody	Supplier
Anti-mouse-HRP	Dianova, Hamburg, Germany
Anti-rabbit-HRP	Dianova, Hamburg, Germany
Anti-mouse-APC	Dianova, Hamburg, Germany
Anti-mouse-AlexaFlour488	Thermo Fisher Scientific, Life Technologies GmbH, Darmstadt, Germany
Anti-goat-AlexaFlour488	Thermo Fisher Scientific, Life Technologies GmbH, Darmstadt, Germany
Anti-rabbit-AlexaFlour594	Thermo Fisher Scientific, Life Technologies GmbH, Darmstadt, Germany
Anti-mouse-AlexFlour594	Thermo Fisher Scientific, Life Technologies GmbH, Darmstadt, Germany

3.1.3 Enzymes

3.1.3.1 Restriction enzymes

Enzyme	Restriction site	Supplier
Bsu36I (Eco18I)	5'-CC/TNAGG-3'	Thermo Fisher Scientific, Life Technologies GmbH, Darmstadt, Germany
NotI	5'-GC/GGCCGC-3'	Thermo Fisher Scientific, Life Technologies GmbH, Darmstadt, Germany
BshTI (AgeI)	5'-A/CCGGT-3'	Thermo Fisher Scientific, Life Technologies GmbH, Darmstadt, Germany
PmlI (Eco72I)	5'-CAC/GTG-3'	Thermo Fisher Scientific, Life Technologies GmbH, Darmstadt, Germany

3.1.3.2 Other enzymes

Enzyme	Supplier
Phusion-Polymerase	Thermo Fisher Scientific, Life Technologies GmbH, Darmstadt, Germany
FastAP	Thermo Fisher Scientific, Life Technologies GmbH, Darmstadt, Germany
T4-Ligase	Thermo Fisher Scientific, Life Technologies GmbH, Darmstadt, Germany

3.1.4 Oligonucleotides

All used oligonucleotides were obtained from Sigma-Aldrich, Steinheim, Germany.

Name	Sequence
Y408A-Fwd	5'-TGCATCCGCCGGCCTCTTTGGGGCAGCTGG-3'
Y408A-Rev	5'-CCAGCTGCCCCAAAGAGGCCGGCGGATGCA-3'
LI427/28AA-Fwd	5'-AGTGC TTGTTCCTGCCGCCTCCCCACCGGT-3'
LI427/28AA-Rev	5'-ACCGGTGGGGAGGCGGCAGGAACAAGCACT-3'
Bsu36I-Fwd	5'-CTGGAGCGGCCTGAGGCACGTGGTGCAGCT-3'
NotI-Rev	5'-CTAGACTCGAGCGGCCGCTTATCTGGGGAA-3'

3.1.5 Plasmids

3.1.5.1 Existing plasmids

Plasmid	Resistance	Description
pcDNA3.1-IL-6R	Ampicillin	Expression plasmid encoding for wildtype human IL-6R
p409-myc-gp130	Ampicillin	Expression plasmid encoding for wildtype human gp130
pN1-eGFP	Kanamycin	Expression plasmid encoding for enhanced green fluorescent protein
pcDNA3.1-DN-AP180_BFP2	Ampicillin	Expression plasmid encoding for a dominant-negative form of AP-180 together with blue fluorescent protein. Kindly provided by Dr. Stefan Düsterhöft
pEGFP-endophilinA1	Ampicillin	Expression plasmid encoding for endophilin variant A1 and enhanced green fluorescent protein. Kindly provided by Dr. Stefan Düsterhöft
pEGFP-endophilin-A2	Ampicillin	Expression plasmid encoding for endophilin variant A2 and enhanced green fluorescent protein. Kindly provided by Dr. Stefan Düsterhöft
pEGFP-endophilin-A3	Ampicillin	Expression plasmid encoding for endophilin variant A3 and enhanced green fluorescent protein. Kindly provided by Dr. Stefan Düsterhöft
pcDNA3.1-mCTSS	Ampicillin, Hygromycin	Expression plasmid encoding for murine cathepsin S. Kindly provided by Dr. Bernd Schröder
pMOWS-puro-IL-6R	Puromycin	Expression plasmid used for retroviral transduction and coding for human wild-type IL-6R [249]

3.1.5.2 Generated plasmids

Plasmid	Resistance	Description
pcDNA3.1-IL-6R-Y/A	Ampicillin	Expression plasmid encoding for human IL-6R carrying a mutation at Y408A
pcDNA3.1-IL-6R-LI/AA	Ampicillin	Expression plasmid encoding for human IL-6R carrying a mutation at LI427/428AA

Plasmid	Resistance	Description
pMOWS-puro-IL-6R-Y/A	Puromycin	Expression plasmid used for retroviral transduction and coding for human IL-6R carrying a mutation at Y408A
pMOWS-puro-IL-6R-LI/AA	Puromycin	Expression plasmid used for retroviral transduction and coding for human carrying a mutation at LI427/428AA

3.1.6 Synthetic inhibitors

Name	Target	Supplier
Pit-Stop2	Clathrin inhibitor	abcam, Cambridge, UK
Dyngo-4a	Dynamin inhibitor	abcam, Cambridge, UK
Marimastat	matrix metalloprotease inhibitor and ADAM17 inhibitor	Sigma-Aldrich, St. Louis, USA
GI254023X	ADAM10 inhibitor	Iris Biotech, Marktredwitz, Germany
GW280264X	ADAM10/17 inhibitor	Iris Biotech, Marktredwitz, Germany
Src-I	Scr inhibitor	Sigma-Aldrich, St. Louis, USA
Ly294	PI3K inhibitor	Sigma-Aldrich, St. Louis, USA
Tofacitinib	JAK1/2 inhibitor	Sigma-Aldrich, St. Louis, USA
U0126 monoethanolate	ERK inhibitor	Sigma-Aldrich, St. Louis, USA
Rapamycin	mTOR inhibitor	Sigma-Aldrich, St. Louis, USA
SB203580	P38/MAPK inhibitor	Sigma-Aldrich, St. Louis, USA
BisI	PKC inhibitor	Calbiochem GmbH, Frankfurt, Germany

3.1.7 Recombinant cytokines and proteins

3.1.7.1 Recombinant cytokines

Cytokine	
Interleukin-6 (IL-6)	Produced in house as described in van Dam et al., 2013 [250]
Hyper-IL-6	Produced in house as described in Fischer et al., 1997 [251] and Schroers et al., 2005 [252]

3.1.7.2 Recombinant proteins

Protein/protease	Supplier
PRCP	R&D Systems, Minneapolis, USA
CD26	R&D Systems, Minneapolis, USA
Cathepsin S	R&D Systems, Minneapolis, USA
DPP8	abcam, Cambridge, UK
CPA6	abcam, Cambridge, UK
MMP-2	R&D Systems, Minneapolis, USA
MMP-3	R&D Systems, Minneapolis, USA
MMP-7	R&D Systems, Minneapolis, USA
MMP-9	R&D Systems, Minneapolis, USA
MMP-12	R&D Systems, Minneapolis, USA
MMP-13	R&D Systems, Minneapolis, USA
MMP-14	R&D Systems, Minneapolis, USA
ADAM10	R&D Systems, Minneapolis, USA
ADAM17	R&D Systems, Minneapolis, USA

3.1.8 Toll-like receptor agonists

Agonist	Working concentration	Supplier
Pam3CSK4 (TLR1/2)	1 µg/ml	Invivogen, San Diego, USA
HKLM (TLR2)	10^8 cells/ml	Invivogen, San Diego, USA
Poly(I:C) (TLR3)	25 µg/ml	Invivogen, San Diego, USA
Poly(I:C) LMW (TLR3)	25 µg/ml	Invivogen, San Diego, USA
LPS K12 (TLR4)	5 µg/ml	Invivogen, San Diego, USA
Flagellin (TLR5)	1 µg/ml	Invivogen, San Diego, USA
FSL-1 (TLR6/2)	1 µg/ml	Invivogen, San Diego, USA
Imiquimod (TLR7)	5 µg/ml	Invivogen, San Diego, USA
ssRNA40 (TLR8)	5 µg/ml	Invivogen, San Diego, USA

3.1.9 Cell culture media and reagents

Product	Description
DMEM (-/-)	Dulbecco's modified Eagle's Medium (DMEM), high Glucose (4,5 g/l); Thermo Fisher Scientific, Life Technologies GmbH, Darmstadt, Germany
DMEM (+/+)	Dulbecco's modified Eagle's Medium (DMEM), high Glucose (4,5 g/l), with 10% FCS and 1% Penicillin/Streptomycin
RPMI 1640 (-/-)	Roswell Park Memorial Institute (RPMI), 2 g/l glucose; Sigma-Aldrich, St. Louis, USA
FCS	Fetal calf serum; Thermo Fisher Scientific, Life Technologies GmbH, Darmstadt, Germany
Pen/Strep	Penicillin/Streptomycin; Sigma-Aldrich, St. Louis, USA
TurboFect	Transfection Reagent; Thermo Fisher Scientific, Life Technologies GmbH, Darmstadt, Germany
Polybren	PAA laboratories, Pasching Austria

3.1.10 Cell lines

3.1.10.1 Existing cell lines

Cell line	Description
THP-1	Human monocytic cell line derived from acute monocytic leukemia of a 1-year-old male patient (ATCC number: TIB-202)
HeLa	Human epithelial cell line derived from cervical adenocarcinoma of a 31-year-old female (ATCC number: CCL-2)
HEK293	Human epithelial cell line derived from embryonic kidney (ATCC number: CRL-1573)
HEK293 A10/17$^{-/-}$	Human epithelial cell line derived from embryonic kidney. Deficient for the metalloproteases ADAM10 and ADAM17 generated by the CRISPR/Cas9 system as described in Riethmueller et al., 2016 [253]
Phoenix-Eco	HEK293T derived packaging cell line stably transfected with a cDNA encoding for antigen, polymerase and envelope protein of ecotropic murine retroviruses [249]
Ba/F3	Murine pro-B cell line which grows IL-3 dependently

Cell line	Description
Ba/F3-gp130	Murine pro-B cell line transduced with cDNA encoding for human glycoprotein 130 (gp130) which grows IL-3 or Hyper-IL-6 dependently [251]
Ba/F3-IL-6R	Murine pro-B cell line transduced with cDNA encoding for human Interleukin-6 receptor (IL-6R) which grows IL-3 dependently.
Ba/F3-gp130-IL-6R	Murine pro-B cell line transduced with cDNA encoding for human gp130 and human IL-6R which grows IL-3, IL-6 or Hyper-IL-6 dependently [254]
Ba/F3-IL-6R-delta-ICD	Murine pro-B cell line transduced with cDNA encoding for human IL-6R lacking the intracellular domain (ICD) which grows IL-3 dependently.
Ba/F3-gp130-IL-6R-delta-ICD	Murine pro-B cell line transduced with cDNA encoding for human gp130 and IL-6R lacking the intracellular domain (ICD) which grows IL-3 or Hyper-IL-6 dependently

3.1.10.2 Generated cell lines

Cell line	Description
Ba/F3-IL-6R-Y/A	Murine pro-B cell line transduced with cDNA encoding for human IL-6R containing a Y408A mutation which grows IL-3 dependently
Ba/F3-IL-6R-LI/AA	Murine pro-B cell line transduced with cDNA encoding for human IL-6R containing a LI427/428AA mutation which grows IL-3 dependently
Ba/F3-gp130-IL-6R-Y/A	Murine pro-B cell line transduced with cDNA encoding for human gp130 and IL-6R containing a Y408A mutation which grows IL-3 or Hyper-IL-6 dependently
Ba/F3-gp130-IL-6R-LI/AA	Murine pro-B cell line transduced with cDNA encoding for human gp130 and IL-6R containing a LI427/428AA mutation which grows IL-3 or Hyper-IL-6 dependently

3.1.11 Kits

Kit name	Description	Supplier
BCA Protein Assay	Determination of protein concentrations in cell lysates	Thermo Fisher Scientific, Life Technologies GmbH, Darmstadt, Germany
GeneJet Gel Extraction Kit	Plasmid DNA extraction from agarose gels	Thermo Fisher Scientific, Life Technologies GmbH, Darmstadt, Germany

Kit name	Description	Supplier
GeneJet Plasmid Miniprep Kit	Plasmid DNA extraction from bacteria	Thermo Fisher Scientific, Life Technologies GmbH, Darmstadt, Germany
NucleoBond Xtra Midi	Plasmid DNA extraction from bacteria	Macherey-Nagel GmbH & Co.KG, Düren, Germany
CellTiter-Blue Cell Viability Assay	Determination of cell viability	Promega GmbH, Mannheim, Germany
DuoSet ELISA Human IL-6Rα	Detection of sIL-6R in sera and cell culture supernatants	R&D Systems, Minneapolis, USA
Human Interleukin-6 ELISA	Detection of IL-6 in sera and cell culture supernatants	ImmunoTools, Friesoythe, Germany

3.1.12 Chemicals

All chemicals that were used were obtained from Carl Roth GmbH (Karlsruhe, Germany), Sigma-Aldrich (St. Louis, USA) or Roche (Mannheim, Germany).

3.1.13 Buffers and solutions

Buffer name	Composition
Stacking gel buffer (SDS gel)	0.5 M Tris 0.4% SDS pH 6.8
Running gel buffer (SDS gel)	1.5 M Tris 0.4% SDS pH 8.8
10x SDS running buffer	25 mM Tris-HCl 192 mM Glycin 0.1% SDS
Blocking buffer	5% milk powder in TBS-T
10x transfer buffer	250 mM Tris 2 M Glycin pH 8.5

Buffer name	Composition
Mild lysis buffer	50 mM Tris pH 7.5 150 mM NaCl 1% Triton-X-100 One tablet of Complete protease inhibitor cocktail (Roche, Mannheim, Germany) per 50ml buffer
pSTAT3 lysis buffer	50 mM Tris-HCl pH 7.5 150 mM NaCl 2 mM EDTA 1 mM NaF 1 mM Na_3VO_4 1% IGEPAL (NP-40) 1% Triton-X-100 One tablet of Complete protease inhibitor cocktail (Roche, Mannheim, Germany) per 50ml buffer
5x Laemmli buffer	67 mM Tris-HCl pH 6.8 10% Glycerol 2% SDS 5% β-mercaptoethanol One spatula tip bromophenol blue
6x DNA loading buffer	30% glycerol 10% EDTA (pH 8.0) One spatula tip bromophenol blue One spatula tip xylencyanol
TBS	10 mM Tris-HCl pH 8.0 150 mM NaCl
TBS-T	10x TBS 0.05% Tween
PBS	150 mM NaCl 8 mM Na_2HPO_4 pH 7.4 1.7 mM NaH_2PO_4 pH 7.4
PBS-T	PBS 0.05% Tween

Buffer name	Composition
Lysis buffer for biotinylation	20 mM Tris pH 7.4 150 mM NaCl 2 mM EDTA 0.5% Triton-X-100 0.01% SDS One tablet of Complete protease inhibitor cocktail (Roche, Mannheim, Germany) per 50ml buffer
Stripping buffer for biotinylation	50 mM l-Glutathione reduced 75 mM NaCl 75 mM NaOH 1% bovine serum albumin (BSA) 10 mM EDTA
Wash buffer for biotinylation	20 mM Tris pH 7.4 500 mM NaCl 2 mM EDTA 0.5% Triton-X-100
LB medium	1% NaCl 1% pepton 0.5% yeast extract
Freezing medium for cryoconservation of cells	10% DMSO in FCS
FACS-buffer	1% BSA in PBS

3.2 Methods

3.2.1 Molecular biology methods

3.2.1.1 Polymerase chain reaction (PCR)

The polymerase chain reaction was performed to amplify specific DNA sequences. For this, the following pipetting scheme was used:

Template	100 ng
5'-primer	0.2 mM
3'-primer	0.2 mM
dNTPs	0.2 mM
PCR buffer (10x)	5 µl
Phusion polymerase	1 U
ddH2O	ad 50 µl

For the PCR the following program was run:

95°C	10 min	
95°C	1 min	32x
60°C	1 min	
72°C	500 bp/min	
72°C	5 min	

3.2.1.1.1 SOE-PCR

To introduce specific mutations into DNA sequences a splicing by overlap extension PCR was used (scheme see Fig. 4.9). For this, four different primers are needed, from which two primers, one forward primer and one reverse primer, enclose the region that should be amplified, and contain restrictions sites for enzymatic digestion. The two other primers are complementary to one another and carry the mutation that should be introduced. Two PCRs are run which use each one of the forward primers together with one of the reverse primers. The thereby generated PCR fragments are used together in the SOE-PCR as template which leads to the introduction of the mutation into the designated DNA sequence. The generated PCR fragment was then digested and cloned into the vector.

3.2.1.2 Enzymatic digestion

Digestion of plasmid DNA or PCR fragments was performed using restriction endonucleases. For digestion of plasmid DNA used for cloning, 10 µg plasmid DNA was mixed with 10 U of the enzyme

and corresponding buffer in a total volume of 50 µl. For the digestion of PCR fragments, the whole PCR reaction (30 µl) was used, mixed with enzyme and buffer and filled up with water to a total volume of 50 µl. For analytical digestion of plasmid DNA 2.5 µl of the mini-preparation was mixed with enzyme and corresponding buffer in a total volume of 20 µl.
When digestion was performed with two different enzymes the buffer was used that showed the highest activity for both enzymes.
Plasmid DNA and PCR fragments were digested at 37°C for 3 h and, following, the enzymes were inactivated as stated in the datasheets. Finally, the generated fragments were separated by agarose gel electrophoresis.

3.2.1.3 Dephosphorylation of DNA fragments

To avoid re-ligation of the plasmid backbone following enzymatic digestion, 2 µl FastAP (Thermo Fisher Scientific, Life Technologies GmbH, Darmstadt, Germany) were added to the sample and incubated together for 2 h at 37°C. Following, the sample was loaded onto an agarose gel.

3.2.1.4 Agarose gel electrophoresis

For the separation of DNA fragments according to their size an agarose gel electrophoresis was performed using the horizontal electrophoresis system from Bio-Rad Laboratories GmbH (Munich, Germany). Therefore, a 1% agarose gel was poured by melting agarose in 0.5x TBE buffer and adding 0.05% ethidium bromide. The DNA fragment samples were mixed with 6x loading dye, loaded onto the gel and separated at a constant voltage of 100 V in 0.5x TBE buffer. Additionally, the GeneRuler 1 kb DNA ladder (Thermo Fisher Scientific, Life Technologies GmbH, Darmstadt, Germany) was loaded onto to the gel as size standard. Finally, the bands of the separated DNA fragments were documented using the BioDocAnalyze system (Biometra GmbH, Göttingen, Germany).

3.2.1.5 Isolation of DNA fragments from agarose gels

For the isolation of DNA fragments from agarose gels upon agarose gel electrophoresis, the gel was transferred onto a UV table to visualize the separated bands. The corresponding fragment was cut out of the gel with the help of a scalpel and transferred into a 1.5 ml reaction tube. The DNA fragment was isolated using the GeneJet Gel Extraction Kit (Thermo Fisher Scientific, Life Technologies GmbH, Darmstadt, Germany). The isolation was performed according to the datasheet, but the DNA fragment was finally eluted in 30 µl H_2O instead of elution buffer.

3.2.1.6 Ligation of DNA fragments

For the ligation of digested and dephosphorylated vector with digested insert the T4 ligase (Thermo Fisher Scientific, Life Technologies GmbH, Darmstadt, Germany) was used. As control, a second sample was incubated without insert to exclude re-ligation of the used vector. Both

samples were pipetted according to the scheme below and incubated for 1 h at room temperature before transformation into *E. coli* bacteria.

Ligation	**Control**
14 µl H_2O	16 µl H_2O
2 µl insert	-- insert
1 µl vector	1 µl vector
2 µl ligation buffer	2 µl ligation buffer
1 µl T4-ligase	1 µl T4-ligase

3.2.1.7 Transformation of plasmid DNA into *E. coli*

For the transformation of chemically competent *E.coli* XL-1 blue bacteria with plasmid DNA, a 25 µl aliquot of the bacteria was thawed on ice and 1 µl plasmid DNA or 10 µl of a ligation was added. The bacteria and the plasmid DNA were mixed carefully, incubated for 5 min on ice and transferred to 42°C for 30 sec. Following, the cells were cooled down on ice for 5 min, 500 µl LB medium was added and the cells were incubated in a shaker for 1 h at 37°C and 100 g. Finally, 100 µl of the transformed bacteria were spread onto a LB agar plate containing the corresponding antibiotic and were incubated at 37°C overnight.

3.2.1.8 Plasmid preparation by Mini-preparation

For the isolation of plasmid DNA from bacteria, single bacterial colonies were isolated from LB agar plates and each colony was transferred into a 2.0 ml reaction tube containing 2 ml LB medium with the corresponding antibiotic. The LB culture was incubated at 37°C under constant agitation at 100 g overnight. The next day, the suspension was centrifuged for 10 min at 5000 g and 4°C, the supernatant was discarded, and the cell pellet was used for plasmid DNA preparation with the GeneJet Plasmid Miniprep Kit (Thermo Fisher Scientific, Life Technologies GmbH, Darmstadt, Germany). The isolation was performed according to the datasheet, but the plasmid DNA was finally eluted in 30 µl H_2O instead of elution buffer.

3.2.1.9 Plasmid preparation by Midi-preparation

To generate higher amounts of plasmid DNA a single bacterial colony was isolated from an LB agar plate and transferred into 100 ml LB medium containing the corresponding antibiotic. The LB culture was incubated at 37°C under constant agitation at 160 rpm overnight. The next day the bacteria suspension was transferred into 50 ml collection tubes, centrifuged at 10,000 g and 4°C for 15 min and the bacterial pellet was used for plasmid-DNA preparation with the NucleoBond Xtra Midi kit (Macherey-Nagel GmbH & Co.KG, Düren, Germany). Isolation was performed according to the datasheet. To obtain higher purity of the eluted plasmid DNA, the eluted plasmid

DNA was distributed in four 2.0 ml reaction tubes and 700 µl isopropanol was added to every tube and mixed well. The tubes were centrifuged for 30 min at 4°C and 15,000 g, the supernatant was discarded and 500 µl of 70% ethanol was added to the pellet. The tubes were centrifuged for 5 min at 13000 g at room temperature and the supernatant was discarded. The pellet was dried completely, and every pellet was resuspended in 30 µl H_2O by incubation overnight at room temperature. The following day, the four tubes were combined, and the plasmid DNA concentration was determined (see 3.2.1.10).

3.2.1.10 Determination of plasmid DNA concentration

The concentration of plasmid DNA was measured using the NanoDrop® ND-1000 (Peqlab Biotechnologie GmbH, Erlangen,). The purity of the plasmid DNA was determined by the ratio of absorption at 260 nm to absorption at 280 nm which should be greater than 1.8.

3.2.1.11 Sequencing of plasmid DNA

For sequencing, plasmid DNA was diluted in water to a concentration between 30-100 ng/ml. 20 µl of the diluted plasmid DNA was transferred into a 1.5 ml reaction tube and sent for sequencing. The primers for the sequencing reaction were diluted to 10 µM and 20 µl were also transferred into a 1.5 ml reaction tube and sent for sequencing. The sequencing was performed by GATC Biotech AG (Köln, Germany).

3.2.2 Cell biology methods

3.2.2.1 Cultivation of cells

All cell lines were cultivated in DMEM high glucose medium with 10% FCS and 1% penicillin/streptomycin. For cultivation of HeLa cells, the medium was removed from the cells, the cells were washed with 10 ml PBS and detached from the cell culture dish using 1 ml Trypsin/EDTA. The cells were incubated at 37°C and 5% CO_2 until they were detached, mixed with 9 ml DMEM+/+, transferred into a 15 ml reaction tube and centrifuged for 5 min at 1,500 g. The cell pellet was resuspended in fresh DMEM+/+ and diluted 1:10 twice a week for sub-cultivation. HEK293 cells were removed from the cell culture dish after a careful wash with PBS using 5 ml DMEM+/+. The cells were mixed thoroughly and diluted 1:20 in fresh DMEM+/+ twice a week for sub-cultivation.

The suspension cell line THP-1 was mixed in the medium and diluted 1:10 in fresh DMEM+/+ twice a week for sub-cultivation.

Ba/F3 cells, Ba/F3-gp130 cells and the cell lines derived therefrom were resuspended in the medium they were cultivated in to receive a single-cell suspension, and 50 µl of the cell suspension was transferred into 10 ml fresh DMEM+/+ for sub-cultivation. For the proliferation of the cells, the corresponding cytokine (see 4.1.10) was added to a final concentration of 10 ng/ml.

3.2.2.2 Cryo-conservation of cells

To freeze cells for long-time storage, adherent cells were detached from confluent 10 cm cell culture dishes using Trypsin/EDTA and transferred into 15 ml collection tubes. Suspension cells were directly transferred into 15 ml collection tubes. The cells were centrifuged for 5 min at 1500 g, the supernatant discarded, and the cell pellet washed in PBS. The cells were centrifuged a second time and the cell pellet was resuspended in 3 ml 10% DMSO in FCS. The cell suspension was distributed onto three cryotubes, and the tubes were put into a cryobox filled with isopropanol and were frozen at -80°C.

3.2.2.3 Transient transfection of cells

For transient transfection of HEK293 cells and HeLa cells, $2x10^6$ cells per transfection were seeded onto 10 cm cell culture dishes and incubated overnight at 37°C and 5% CO_2 allowing the cells to adhere to the culture dish. The next day, the medium was removed from the cells and 5 ml fresh DMEM+/+ was added carefully. 5 µg plasmid DNA were mixed well with 1 ml DMEM-/- in a 1.5 ml reaction tube, 10 µl TurboFect Transfection Reagent (Thermo Fisher Scientific, Life Technologies GmbH, Darmstadt, Germany) was added, mixed well and incubated for 15 min at room temperature. The transfection mix was pipetted carefully onto the cells and the cells were incubated for 48 h at 37°C and 5% CO_2 before they were used for further experiments.
For transient transfection of the retroviral packaging cell line Phoenix-Eco, $5x10^5$ cells in 2 ml DMEM+/+ per transfection were seeded onto 6-well plates and incubated overnight at 37°C and 5% CO_2. For the transfection 1 µg plasmid DNA was mixed first with 200 µl DMEM-/- and then with 2 µl TurboFect Transfection Reagent (Thermo Fisher Scientific, Life Technologies GmbH, Darmstadt, Germany). The transfection mix was incubated for 15 min at room temperature and then pipetted carefully onto the cells. The cells were incubated for 24 h at 37°C and 5% CO_2 before the supernatant was used for retroviral transduction.

3.2.2.4 Retroviral transduction of Ba/F3 and Ba/F3-gp130 cells

For the retroviral transduction of Ba/F3 and Ba/F3-gp130 cells, Phoenix-Eco cells were transfected as described above (3.2.2.3). The following day, supernatant was collected from the transfected cells, transferred into 1.5 ml reaction tubes and centrifuged at 15,000 g and 4°C for 5 min. Ba/F3 and Ba/F3-gp130 cells were collected, centrifuged for 5 min at 1,500 g, washed in PBS, centrifuged again and resuspended in DMEM+/+. The cell suspension was adjusted to $2x10^6$ cells/ml and 50 µl per transfection was transferred into 1.5 ml reaction tubes. 250 µl of the centrifuged Phoenix-Eco supernatant per transfection was mixed with 3 µl polybrene and transferred to the cell suspension. Everything was mixed well, and the cell suspension was centrifuged for 2 h at 350 g and 21°C. Following, the supernatant was discarded carefully, and the cell pellet was resuspended in 50 µl DMEM+/+ and transferred into 6-well plates with 5 ml

DMEM+/+ containing either 10 ng/ml IL-3 (for transduced Ba/F3 cells) or 10 ng/ml Hyper-IL-6 (for transduced Ba/F3-gp130 cells). The cells were incubated 48 h at 37°C and 5% CO_2 before 1.5 mg/ml puromycin was added for selection of successfully transduced cells. The cells were cultivated in the presence of puromycin at 37°C and 5% CO_2 for at least two weeks.

3.2.2.5 Ba/F3-gp130 cell viability assay (proliferation assay)

To analyze whether generated sIL-6R is biologically active, a cell viability assay was performed. Therefore, Ba/F3-gp130 cells were used, which are only able to grow in the presence of IL-6 and sIL-6R or Hyper-IL-6, a designer protein consisting of sIL-6R linked to IL-6 via a flexible linker.
Ba/F3-gp130 cells were transferred into 50 ml collection tubes, centrifuged at 1200 g for 5 min and resuspended in PBS. The cells were centrifuged again and resuspended in DMEM+/+. The cells were counted, and the cell number adjusted to $1x10^5$ cell/ml. 50 µl of the adjusted cell suspension (≙ 5000 cells) was transferred into a well of a 96-well plate and 50 µl of conditioned medium or fresh DMEM+/+ was added to the cells. The cells were mixed with IL-6 to a final concentration of 25 ng/ml or, as positive control, with Hyper-IL-6 (10 ng/ml) or without cytokine as negative control and were incubated for 48 h at 37°C and 5% CO_2. After addition of 20 µl Cell Titer Blue Viability Assay (Promega, Madison, USA) to each well, fluorescence was measured at λem = 590 nm for one hour every 20 min using the Synergy HTX multimode reader (BioTek, Winooski, VT, USA). Fluorescence at time-point 120 min was normalized by subtracting the fluorescence measured at time point 0 min. An increase in fluorescence indicates cell proliferation mediated by sIL-6R present in the conditioned medium.

3.2.2.6 Flow cytometry

3.2.2.6.1 Analysis of IL-6R shedding upon PMA stimulation

THP-1 cells were centrifuged at 600 g for 8 min, the supernatant was discarded, and the cell pellet resuspended in PBS. The cells were centrifuged again, $1x10^6$ cells per stimulation were resuspended in 250 µl FACS buffer (1% BSA in PBS) containing primary antibody (anti-IL-6R antibody 4-11, 1:100) and were incubated on ice for 1 h to stain cell-surface IL-6R. Following, the cells were centrifuged as before, washed twice in PBS, resuspended in 2 ml serum-free DMEM and were transferred into 6-well plates. To induce shedding, the cells were stimulated with PMA (2 µM) or DMSO as negative control for 2 h at 37°C and 5% CO_2. Following, the cells were collected, transferred into 1.5 ml reaction tubes and were centrifuged as before. The cells were washed twice in FACS buffer and were resuspended in 30 µl FACS buffer containing the fluorescently-labelled secondary antibody anti-mouse-APC (1:100). The cells were incubated for 1 h on ice in the dark, washed three times in FACS buffer and resuspended in 150 µl FACS buffer. Finally, fluorescence was measured by flow cytometry using the BD Biosciences FACS Canto II (Becton-

Dickinson, Heidelberg, Germany) and IL-6R shedding was determined by analysis of the FACS data using the FCS Express software (De Novo Software, Glendale, USA).

3.2.2.6.2 Internalization assay of gp130 and IL-6R

THP-1 cells were centrifuged at 600 g for 8 min, the supernatant was discarded and the cell pellet resuspended in PBS. The cells were centrifuged again, resuspended in serum-free DMEM and $1x10^7$ cells per stimulation were transferred into 10 cm cell culture dishes in a total volume of 10 ml serum-free DMEM. The cells were incubated for 40 min at 37°C and 5% CO_2 with or without the addition of 10 µM Marimastat. Following, the cells were transferred into 15 ml collection tubes, centrifuged at 600 g for 8 min at 4°C, resuspended in PBS and transferred into 1.5 ml reaction tubes. The cells were centrifuged again, resuspended in 250 µl FACS buffer (1% BSA in PBS) containing primary antibody (anti-IL-6R antibody 4-11, 1:100 or anti-gp130 antibody B-P4, 1:100) and were incubated on ice for 1 h with or without the addition of Marimastat (10 µM) to stain cell-surface IL-6R or gp130. Following, the cells were centrifuged as before, washed twice in PBS, resuspended in 10 ml serum-free DMEM containing Marimastat (2 µM) or not and were transferred into 10 cm cell culture dishes. The cells were stimulated with or without 10 ng/ml IL-6 and incubated for different points (0, 15, 30, 60, 90, 120, 150 and 180 min) at 37°C and 5% CO_2. For every time point 1 ml cell suspension was collected, transferred into 1.5 ml reaction tubes and kept on ice until all samples were collected. The cells were centrifuged as before, resuspended in 100 µl FACS buffer and transferred onto a 96-well plate. The plate was centrifuged at 300 g and 4°C for 3 min, the supernatant was removed, and the cells were washed once in FACS buffer. The cells were resuspended in 30 µl FACS buffer containing the fluorescently-labelled secondary antibody anti-mouse-APC (1:100) and were incubated for 1 h on ice in the dark. Following, the cells were washed three times in FACS buffer and resuspended in 150 µl FACS buffer. Finally, fluorescence was measured by flow cytometry using the BD Biosciences FACS Canto II with HTS loader (Becton-Dickinson, Heidelberg, Germany) and IL-6R or gp130 internalization was determined by analysis of the obtained FACS data using the FCS Express software (De Novo Software, Glendale, USA).

To analyze the involvement of clathrin or dynamin on IL-6R and gp130 internalization the experiment was performed as stated above but the cells were pre-incubated not only with Marimastat but also with the inhibitors Pit-Stop2 (clathrin inhibitor; 25 µM) and Dyngo-4a (dynamin inhibitor; 50 µM) or DMSO as control for 40 min at 37°C and 5% CO_2. The inhibitors were also added during the time-course of internalization.

Analysis of internalization using the different Ba/F3 or Ba/F3-gp130 cell lines was performed as described for the THP-1 cells, but the cells were incubated in serum-free DMEM for 3 h at 37°C at the beginning to reduce effects caused by the cytokines that were added to the cells for cultivation.

3.2.2.6.3 Cell-surface staining of PBMCs to determine different PBMC subsets

To determine the different cell types in PBMCs, four samples with each $1x10^6$ PBMCs in 1.5 ml reaction tubes were centrifuged at 300 g for 10 min at 4°C, resuspended in FACS buffer, centrifuged again, and the cell pellets were resuspended in 50 µl blocking solution (50 µl FACS buffer, 0.5 µl Fc-Block, 0.5 µl human serum). After incubation for 15 min at 4°C, the cells were washed once in FACS buffer and the cell pellets were resuspended in 50µl FACS buffer containing different fluorescently-labeled antibodies (IL-6R-APC, TLR2-BV421, CD45-BV510, CD14-APC/Cy7, B220-PE, CD3-AlexaFlour488 and CD56-PE/Cy7). The different antibodies were diluted 1:100 and combined as noted below:

Staining 1	IL-6R-APC TLR2-BV421 CD45-BV510 CD3-AlexaFluor488 CD56-PE/Cy7 CD123-PE	**Isotype 1**	IgG1-APC IgG1-BV421 CD45-BV510 CD3-AlexaFluor488 CD56-PE/Cy7 CD123-PE
Staining 2	IL-6R-APC TLR2-BV421 CD45-BV510 B220-PE CD14-APC/Cy7	**Isotype 2**	IgG1-APC IgG1-BV421 CD45-BV510 B220-PE CD14-APC/Cy7

The cells were incubated with the antibodies for 1 h at 4°C on ice in the dark, centrifuged as before, washed twice in FACS buffer, centrifuged again and the cell pellet was resuspended in 50 µl 1x RBC Lysis/Fixation Solution (BioLegend San Diego, USA) diluted in water to lyse remaining erythrocytes. After incubation in the dark at room temperature for 15 min, the cells were centrifuged as before, resuspended in FACS buffer, centrifuged again and resuspended again in 200 µl FACS buffer. Finally, fluorescence was measured by flow cytometry using the BD Biosciences FACS Canto II (Becton-Dickinson, Heidelberg, Germany) and the different PBMCs subsets were determined by analysis of the obtained FACS data using the FCS Express software (De Novo Software, Glendale, USA).

3.2.2.6.4 Analysis of IL-6R shedding

For the analysis of IL-6R cleavage by proteases using flow cytometry, THP-1 cells were centrifuged at 600 g for 8 min, the supernatant was discarded, and the cell pellet was resuspended in PBS to wash the cells. The cells were centrifuged as before, the supernatant was removed, and the cell pellet was resuspended in serum-free DMEM. $1x10^6$ cells in 1 ml serum-free DMEM per sample were transferred onto a 24-well plate before different protease inhibitors (GI (ADAM10

inhibition; 3 µM), GW (ADAM17 inhibition; 3 µM), Marimastat (matrix-metalloprotease inhibitor; 2 µM)) or DMSO as control were added to two wells each. The cells together with the inhibitors or DMSO were pre-incubated at 37°C and 5% CO_2 for 30 min. Following, the cells were transferred into 1.5 ml reaction tubes, centrifuged at 600 g and 4°C for 8 min, the supernatants were discarded, and the cells were resuspended and washed in PBS. After another centrifugation step the cell pellets were resuspended in 50 µl FACS buffer (1% BSA in PBS) with anti-IL-6R antibody (4-11; 1:100) to stain surface IL-6R. The cells were incubated with primary antibody for 1 h on ice, centrifuged at 600 g and 4°C for 8 min, the cell pellet was washed in PBS and centrifuged again. The cell pellet was resuspended in 1 ml serum-free DMEM and transferred onto a 24-well plate. GI, GW, Marimastat or DMSO were added again to the cells and the cells were additionally stimulated with the TLR2 agonist HKLM (10^8 cells/ml). The cells were incubated for 24 h at 37°C and 5% CO_2, transferred into 1.5 ml reaction tubes, centrifuged at 600 g and 4°C for 8 min, the cell pellet was washed in PBS, centrifuged again before the cell pellets were resuspended in 50 µl FACS buffer with secondary anti-mouse-APC antibody (1:100). The cells were incubated for 1 h on ice in the dark to stain remaining surface IL-6R. Following, the cells were centrifuged, the cell pellet was resuspended in FACS buffer, centrifuged again and washed a second time in FACS buffer. Finally, the cell pellets were resuspended in 150 µl FACS buffer and APC-fluorescence was measured by flow cytometry using the BD Biosciences FACS Canto II (Becton-Dickinson, Heidelberg, Germany). The obtained FACS data and remaining surface IL-6R were analyzed using the FCS Express software (De Novo Software, Glendale, USA).

3.2.2.7 Isolation of peripheral blood mononuclear cells (PBMCs) by density gradient centrifugation

PBMCs were isolated from plasma-free blood which was mixed with 100 ml PBS. 25 ml of the blood suspension was transferred into 50 ml collection tubes and 15 ml Histopaque® 1077 (Sigma-Aldrich, St. Louis, USA) was added carefully. The tubes were centrifuged at 900 g for 20 min without the brake turned on which results in four layers. The top layer was removed carefully and discarded to make the yellowish layer accessible that contains the PBMCs. The layer containing the PBMCs was isolated, transferred into a 50 ml collection tube and PBS was added to a total volume of 50 ml. The PBMC suspension was centrifuged for 5 min at 900 g with the brake turned on, the supernatant was discarded, and the cell pellet was resuspended in 50 ml PBS before being centrifuged for 10 min at 300 g. The supernatant was discarded again, the cell pellet resuspended in 50 ml PBS and centrifuged for 10 min at 300 g. Finally, the supernatant was discarded again, and the cell pellet was resuspended either in serum-free RPMI or in PBS and kept on ice until further usage.

3.2.2.8 Isolation of monocytes and dendritic cells from PBMCs by magnetic activated cell sorting (MACS)

Dendritic cells and monocytes were isolated from PBMCs using MACS. For efficient isolation, beads, LS columns, the magnetic separator (Miltenyi Biotec, Bergisch Gladbach, Germany) and all solutions were pre-cooled to 4°C. The procedure of isolation was performed as described in the datasheet of the beads that were used. Dendritic cells were isolated out of $4x10^8$ PBMCs using CD123-beads, monocytes were isolated out of $2x10^8$ PBMCs using CD14-beads. To improve the purity of the isolated dendritic cells or monocytes, the isolated cells were transferred onto fresh LS columns a second time and washed again two times with 3 ml MACS buffer before wash-out of the column. The cells were centrifuged at 300 g for 10 min at 4°C, the supernatant was discarded, the cell pellet was resuspended in cold PBS and centrifuged again. The supernatant was removed, and the cells were resuspended in cold PBS or serum-free RPMI and kept on ice until further usage.

3.2.2.9 Stimulation of cells

3.2.2.9.1 Stimulation with IL-6

To analyze how STAT3 activation is influenced by inhibition of internalization, $2x10^6$ THP-1 cells per time-point and inhibitor were washed in PBS, centrifuged for 10 min at 1200 g at room temperature and the pellet was resuspended in 2 ml serum-free DMEM. The cells were transferred into 6-well plates and incubated for 3 h at 37°C and 5% CO_2 to starve the cells thereby reducing signal transduction to basal levels. Following, the internalization inhibitors (Pit-Stop2 (25 µM) or Dyngo-4a (50µM)) or DMSO as control were added to the cells which were then pre-incubated for 40 min at 37°C and 5% CO_2 before 10 ng/ml IL-6 was added to each sample for different periods of time (0, 15, 30, 60, 90 and 120 min) to induce signal transduction. The cells were transferred into 2.0 ml reaction tubes, were centrifuged at 18,000 g for 5 min at 4°C to pellet the cells and the pellets were resuspended in 50 µl pSTAT3 lysis buffer and incubated on ice for at least 30 min to lyse the cells. The cells were centrifuged at 18,000 g for 15 min at 4°C, the supernatants were transferred into new 1.5 ml reaction tubes and stored at -20°C until further analysis.

To further analyze the effect of internalization inhibition on STAT3 signaling, $4x10^6$ HeLa cells were transfected either with pN1-eGFP as control or with pcDNA3.1-DN-AP180_BFP2 and were incubated at 37°C and 5% CO_2. The next day, the cells were detached from the cell culture dish using trypsin/EDTA, transferred into 15 ml collection tubes, centrifuged for 10 min at 1,200 g at room temperature, were resuspended in 12 ml fresh DMEM+/+ and distributed into 6 wells of a 6-well plate. The cells were incubated overnight at 37°C and 5% CO_2 so the cells can attach to the plate. The next day, the medium was removed from the cells, the cells were washed with PBS and 2 ml serum-free DMEM was added. The cells were incubated at 37°C and 5% CO_2 for 4 h to starve the cells before 10 ng/ml IL-6 was added to each sample for different time-points (0, 15, 30, 60,

90 and 120 min). The cells were put on ice, the cell culture medium was removed, and the cells were washed with cold PBS. The cells were scratched from the plate in 1 ml PBS, were transferred into 2.0 ml reaction tubes and centrifuged at 18,000 g for 5 min at 4°C. The pellets were resuspended in 50 µl pSTAT3 lysis buffer and incubated on ice for at least 30 min to lyse the cells. The cells were centrifuged at 18,000 g for 15 min at 4°C, the supernatants were transferred into new 1.5 ml reaction tubes and stored at -20°C until further analysis.

To analyze the effect of endophilin on internalization, $4x10^6$ HeLa cells were transfected either with pN1-eGFP or pEGFP-endophilinA1, pEGFP-endophilinA2 or pEGFP-endophilinA3. Following, the cells were treated as described before.

3.2.2.9.2 Stimulation with Toll-like receptor (TLR) agonists

To analyze which TLR activation is involved in the release of sIL-6R and IL-6, $5x10^5$ PBMCs per agonist were washed with cold PBS, centrifuged for 10 min at 1,200 g and 4°C and resuspended in 1 ml serum-free RPMI cell culture medium. The cells were transferred into 24-well plates and different Toll-like receptor agonists (Pam3CSK4 (1 µg/ml), HKLM (10^8 cells/ml), Poly(I:C) (25 µg/ml), Poly(I:C) LMW (25 µg/ml), LPS K12 (5 µg/ml), Flagellin (1 µg/ml), FSL-1 (1 µg/ml), Imiquimod (5 µg/ml), ssRNA40 (5 µg/ml)) were added in duplicates. The cells were incubated for 24 h at 37°C and 5% CO_2 and the supernatants were collected, transferred into 1.5 ml reaction tubes and centrifuged for 10 min at 1,200 g and 4°C to remove cells and cell debris. Finally, the supernatants were transferred into new 1.5 ml reaction tubes and stored at -20°C until further analysis.

To analyze signaling pathways activated by the TLR2 agonist HKLM, $2x10^6$ PBMCs per time-point were washed in PBS, resuspended in 1 ml serum-free RPMI, transferred into 24-well plates and incubated for 2 h at 37°C and 5% CO_2 to starve the cells. Following, the TLR2 agonist HKLM (10^8 cells/ml) was added to the cells for different periods of time (0, 15, 30 and 60 min), the cells were transferred into a 1.5 ml reaction tube and centrifuged at 18,000 g for 5 min at 4°C to pellet the cells. The supernatants were discarded, the pellets were resuspended in 50 µl pSTAT3 lysis buffer and incubated on ice for at least 30 min to lyse the cells. The cells were centrifuged at 18,000 g for 15 min at 4°C, the supernatants were transferred into new 1.5 ml reaction tubes and stored at -20°C until further analysis.

3.2.2.9.3 Stimulation with protease inhibitors

To analyze which protease is involved in the generation of sIL-6R upon TLR2 activation, $5x10^5$ PBMCs or THP-1 cells per sample were washed with cold PBS, centrifuged for 10 min at 1,200 g and 4°C and resuspended in 1 ml serum-free RPMI cell culture medium. The cells were transferred into 24-well plates and different protease inhibitors (GI (ADAM10 inhibition; 3 µM), GW (ADAM17

inhibition; 3 µM) or Marimastat (matrix-metalloprotease inhibitor; 2 µM)) were added in duplicates. After a 30 min pre-incubation with the inhibitors, the cells were stimulated with the TLR2 agonist HKLM (10^8 cells/ml) for 24 h at 37°C and 5% CO_2. The supernatants were collected, transferred into 1.5 ml reaction tubes and centrifuged for 10 min at 1,200 g and 4°C to remove cells and cell debris. Finally, the supernatants were transferred into new 1.5 ml reaction tubes and stored at -20°C until further analysis.

3.2.2.9.4 Stimulation with signaling pathway inhibitors

To analyze which pathway is involved in the release of sIL-6R and IL-6 upon TLR2 activation, $5x10^5$ PBMCs or monocytes per inhibitor were washed with cold PBS, centrifuged for 10 min at 1,200 g and 4°C and resuspended in 1 ml serum-free RPMI cell culture medium. The cells were transferred into 24-well plates and different signaling pathway inhibitors (SrcI (SrcI inhibitor, 10 µM), TBB (CK2 inhibitor, 100 µM), Ly294 (PI3K inhibitor, 4 µM), Tofacitinib (JAK1/2 inhibitor, 3 µM), U0126 monoethanolate (Erk inhibitor, 10 µM), Rapamycin (mTOR inhibitor, 500 ng/ml), SB203580 (p38/MAPK inhibitor, 10 µM) and BisI (PKC inhibitor, 500 nM)) were added in duplicates. After a 90 min pre-incubation time with the inhibitors, the cells were stimulated with the TLR2 agonist HKLM (10^8 cells/ml) for 24 h at 37°C and 5% CO_2. The supernatants were collected, transferred into 1.5 ml reaction tubes and centrifuged for 10 min at 1,200 g and 4°C to remove cells and cell debris. Finally, the supernatants were transferred into new 1.5 ml reaction tubes and stored at -20°C until further analysis.

3.2.2.9.5 Stimulation with phorbol-12-myristate-13-acetate (PMA)

To induce ADAM17-mediated shedding, $4x10^6$ HEK293 cells were transfected with pcDNA3.1-IL-6R and incubated at 37°C and 5% CO_2. 48 h after the transfection the cell culture medium was removed, the cells were carefully washed with PBS and 5 ml serum-free DMEM was added to the cells. The cells were stimulated with 2 µM PMA (Sigma-Aldrich, St. Louis, USA) for 2 h at 37°C and 5% CO_2 to induce ADAM17-mediated cleavage of the IL-6R. Following, the supernatant was transferred into 1.5 ml reaction tubes and centrifuged for 10 min at 1,200 g and 4°C to remove cells and cell debris. Finally, the supernatants were transferred into new 1.5 ml reaction tubes and stored at -20°C until further analysis.

3.2.2.10 Cell lysis

3.2.2.10.1 Lysis of adherent cells

The cell culture medium was removed from transfected cells and/or stimulated cells and 1 ml cold PBS was added to the cells. The cells were removed from the cell culture dish, transferred into a 1.5 ml reaction tube and centrifuged at 18,000 g for 5 min at 4°C to pellet the cells. The supernatant was removed, and the pellet was resuspended in 50 µl (6-well plate) or 150 µl (10 cm culture dish) of lysis buffer. Cells that were used for the analysis of phosphorylation were resuspended in

pSTAT3 lysis buffer, all other cells were resuspended in mild lysis buffer. The cells were incubated on ice for at least 30 min before being centrifuged at 18,000 g for 15 min at 4°C to remove cell debris. The supernatant containing the proteins was transferred into a new 1.5 ml reaction tube and was stored at -20°C.

3.2.2.10.2 Lysis of suspension cells

The (stimulated) cells were transferred into 1.5 ml reaction tubes, centrifuged at 18,000 g for 5 min at 4°C and the supernatant was discarded. The cell pellet was resuspended in cold PBS, centrifuged again at 18,000 g for 5 min and 4°C and the supernatant was discarded again. The cell pellet was resuspended in 50 µl lysis buffer, either pSTAT3 lysis buffer or mild lysis buffer, and incubated on ice for at least 30 min. Following, the lysed cells were centrifuged at 18,000 g for 15 min at 4°C to remove cell debris. The supernatant containing the proteins was transferred into a new 1.5 ml reaction tube and was stored at -20°C.

3.2.3 Protein biochemistry methods

3.2.3.1 Determination of protein concentrations by BCA

To determine protein concentrations in cell lysates the BCA protein Assay Kit (Thermo Fisher Scientific, Life Technologies GmbH, Darmstadt, Germany) was used according to the datasheet. The generated cell lysates were diluted 1:10 in water and 25 µl of this suspension was transferred onto a 96-well plate in duplicates. Additionally, the BSA-standard was diluted according to the datasheet with water and was also transferred onto the plate in duplicates. Reagent A and B were mixed in a ratio of 50:1 and 200 µl of this mixture was added to every well containing cell lysates or BSA standard. The plate was incubated for 15 min at 37°C and, finally, the absorption was measured at 562 nm using the Tecan Spectra Rainbow plate reader (Tecan, Crailsheim, Germany). The protein concentration in the lysates was determined with the help of the BSA samples of known concentrations.

3.2.3.2 Protein precipitation using trichloroacetic acid (TCA)

To analyze proteins that are present in cell culture supernatants via SDS-PAGE and Western Blot the proteins need to be precipitated using TCA. Therefore, 1 ml of the cell culture supernatant was centrifuged for 10 min at 4°C and 1200 g to remove cells and cell debris. The supernatant was transferred into a new reaction tube and centrifuged for another 20 min at 4°C and 18,000 g. Supernatants from which microvesicles should be removed were ultra-centrifuged for 60 min at 4°C and 300,000 g instead. Following, 900 µl of the supernatant was transferred into a 2 ml reaction tube, mixed with 900 µl 20% TCA and incubated for 20 min on ice. The suspension was centrifuged for 20 min at 4°C and 18,000 g, the supernatant was discarded, and the pellet was dried completely before 350 µl ice-cold acetone was added to the pellet and mixed. After

incubation on ice for 20 min the reaction tube was centrifuged for 20 min at 4°C and 18,000 g, the supernatant was discarded, and the pellet was dried again. The precipitated proteins were resuspended by addition of 25 µl 2,5x Laemmli buffer and incubation for 10 min at 95°C and 100 g. The samples were then analyzed further or stored at -20°C.

3.2.3.3 SDS polyacrylamide gel electrophoresis (SDS-PAGE)

In order to separate proteins from cell lysates or precipitated supernatants according to their size, a SDS-PAGE was performed using the Mini-Protean 3 Cell-System (Bio-Rad Laboratories GmbH, Munich, Germany). 10% SDS-gels were generated with a thickness of 1.5 mm and 10 or 15 pockets. Stacking gel and running gel were composed as follows:

	Running gel (1 gel)	**Stacking gel (2 gels)**
Water	4.0 ml	3.44 ml
Acrylamide (30%)	3.3 ml	1.0 ml
Running gel buffer	2.6 ml	-
Stacking gel buffer	-	1.5 ml
TEMED	4 µl	6 µl
APS	100 µl	60 µl

30 µg of the cell lysates were mixed with 5x Laemmli buffer and boiled for 10 min at 95°C before being loaded onto the gel. Precipitated supernatants were prepared as described above (4.2.3.2) and 10 µl of the samples were loaded. Additionally, 5 µl of the PageRuler Prestained Protein Ladder (Thermo Fisher Scientific, Life Technologies GmbH, Darmstadt, Germany) were loaded onto the gel. The gels were connected to a power supply and the proteins were separated at 90-120 V until the running front left the gel.

3.2.3.4 Western Blot

The transfer of the separated proteins onto a PVDF membrane (Merck Millipore, Darmstadt, Germany) was performed by semi-dry blotting using the Trans-Blot®-Turbo™ system (Bio-Rad, Hercules, CA, USA). The PVDF membrane was activated for one minute in methanol and laid onto five Whatman paper that were soaked with transfer buffer before. The SDS gel was washed in transfer buffer and put on top of the PVDF membrane followed by another five Whatman paper also soaked with transfer buffer. Air bubbles were removed, and the proteins were transferred onto the membrane at 1 A and constant 25 V for 40 min. The membrane with the transferred proteins was incubated in blocking buffer (5% milk powder in TBS-T) for 1 h at room temperature, washed in TBS-T and incubated with primary antibody overnight at 4°C. Antibodies

were diluted 1:1000 in either 5% milk powder in TBS-T (STAT3, ERK, p38, p65) or 5% BSA in TBS-T (phospho-STAT3, phospho-ERK, phospho-p38, phospho-p65, Actinin, GAPDH). The following day, the membrane was washed in TBS-T and incubated with HRP-conjugated secondary antibody (anti-mouse-HRP or anti-rabbit-HRP) diluted 1:20,000 in 5% BSA in TBS-T for 1 h at room temperature in the dark. The membrane was washed again in TBS-T and proteins were detected with the ECL Chemocam Imager (Intas Science Imaging, Göttingen, Gemany) using the EMD Millipore™ Immobilon™ Western Chemiluminescent HRP Substrate (Merck Millipore, Darmstadt, Germany). To detect more than one protein on one membrane, the bound antibodies were stripped of the membrane by incubating the membrane for 40 min at room temperature in the dark in 10 ml Restore Western Blot Stripping Buffer (Thermo Fisher Scientific, Life Technologies GmbH, Darmstadt, Germany). The membrane was washed with TBS-T and incubated in 5% milk powder in TBS-T for 1 h at room temperature. After that the membrane was washed again in TBS-T and incubated with antibodies as described above and stained proteins were detected.

3.2.3.5 Enzyme-linked immunosorbent assay (ELISA)

Two different ELISA were used to detect either IL-6 or sIL-6R and to determine their amount in serum samples or cell culture supernatants. The human IL-6 ELISA kit from Immunotools (Friesoythe, Germany) was used for the detection of IL-6 and was performed according to the datasheet. Serum samples and cell culture supernatants were used undiluted. The *DuoSet Human IL-6Rα ELISA kit* from R&D systems (Minneapolis, USA) was used to measure sIL-6R and was also performed according to the datasheet although the used volumes were slightly adapted. Only 50 µl of capture antibody, detection antibody and samples were used, and 75 µl of substrate solution and stop solution. Serum samples were diluted 1:100 in blocking buffer, cell culture supernatants were used undiluted. Streptavidin-horseradish peroxidase (R&D Systems, Minneapolis, USA) and the peroxidase substrate BM blue POD (Roche, Mannheim, Germany) were used for the enzymatic reaction which was stopped by addition of 1.8 M sulfuric acid. The absorbance was read at 450 nm on a Tecan Spectra Rainbow plate reader (Tecan, Crailsheim, Germany).

3.2.3.6 Peptide cleavage assay

A peptide cleavage assay was performed to identify proteases capable of cleaving IL-6R peptides. For this three different quenched fluorogenic IL-6R peptides were used (synthesized by Genosphere Biotechnologies, Paris, France): [mca]-ATSLPVQDSS[K-dnp] (IL-6R_PVQD) containing the P355/V356 cleavage site, [mca]-ATSLPVQASS[K-dnp] (IL-6R_PVQA) containing a mutated form of the cleavage site preferentially cleaved by ADAM17, and [mca]-ATSLPGQDSS[K-dnp] (IL-6R_PGQD) containing the normal cleavage site with an additional mutation disrupting

cleavage of the IL-6R. Additionally, a TNFα peptide (Mca-PLAQAV-Dpa-RSSSR-NH2; R&D Systems, Minneapolis, USA) was used as positive control for ADAM17 cleavage.
10 µM of the quenched fluorogenic peptides were incubated together with 10 ng or 100 ng of the different proteases in PBS in a total volume of 100 µl. Duplicates were prepared and transferred onto a 96-well plate. Peptides and proteases were mixed just before fluorescent measurement at a Tecan spectrophotometer (Tecan, Crailsheim, Germany) at λem = 405 nm and λex = 320 nm at 37°C every 30 sec for 120 min. Fluorescence indicated cleavage of the quenched fluorogenic peptides. The increase in relative fluorescence units (RFUs) after 120 min was normalized to fluorescence at 0 sec.

3.2.3.7 Immunofluorescence staining

3.2.3.7.1 Co-localization assay of gp130 and IL-6R with Rab11 or LAMP-2

$4x10^6$ HeLa cells were transfected with either pcDNA3.1-IL-6R or p409-gp130wt plasmid (see 4.2.2.3) and incubated overnight at 37°C and 5% CO_2. The next day, the cells were detached from the cell culture dish and $5x10^6$ cells were seeded onto 16 coverslips. The following day, the cells were washed three times in PBS, incubated for 10 min at room temperature in 0.12% (w/v) glycine in PBS and washed again three times in PBS before being blocked in 10% FCS/PBS for 30 min at room temperature. Following, two cover slips each were transferred into small cell culture dishes and the cells were stained with either anti-IL-6R antibody (BAF227; 1:100 in 10% FCS/PBS) or anti-gp130 antibody (B-P4; 1:100 in 10% FCS/PBS) for one hour at 4°C. Afterwards, the cells were washed three times in PBS and were stained with secondary antibody anti-goat-AlexaFlour488 (IL-6R; 1:300 in 10% FCS/PBS) or anti-mouse-AlexaFlour488 (gp130; 1:300 in 10% FCS/PBS) for one hour at 4°C. The cells were washed three times in PBS and incubated in serum-free DMEM in the presence or absence of 10 ng/ml IL-6 for different time points (15, 30 and 60 min) before being washed again in PBS and fixed with 4% PFA/PBS for 10 min at room temperature. Following, the cells were washed again three times in PBS, incubated in 0.12% glycine in PBS for 10 min at room temperature and blocked and permeabilized in 10% FCS/0.2% saponin in PBS for 30 min at room temperature. The cells were stained either with anti-Rab11 antibody (1:100 in 10% FCS/0.2% saponin/PBS) or anti-LAMP-2 antibody (H4B4 1:300 in 10% FCS/0.2% saponin/PBS or Thermo antibody 1:100 in 10% FCS/0.2% saponin/PBS) for one hour at room temperature, washed five times with 0.2% saponin/PBS and stained with secondary antibody anti-mouse-AlexaFlour594 (for LAMP-2 H4B4 1:300 in 10% FCS/0.2% saponin/PBS) or anti-rabbit-AlexaFlour594 (for LAMP-2 Thermo or Rab11 1:300 in 10% FCS/0.2% saponin/PBS) for one hour at room temperature. Finally, the cells were washed five times in 0.2% saponin/PBS and once in ddH_2O, and the cover slips were mounted onto microscopy slides using ProLong™ Gold Antifade Mountant with DAPI (Thermo Fisher Scientific, Waltham, MA, USA) thereby also staining nuclei. Co-localization was analyzed using the Olympus FV1000 confocal laser scanning

microscope (Olympus, Hamburg, Germany) and ImageJ together with the JACoP plugin (NIH, Bethesda, USA).

3.2.3.7.2 Recycling assay of gp130 and IL-6R

This assay used to determine recycling of gp130 and the IL-6R was performed similarly as described in Stautz et al. [255]. Therefore, $4x10^6$ HeLa cells were transfected either with the pcDNA3.1-IL-6R plasmid or the p409-myc-gp130wt plasmid (see 4.2.2.3) and the cells were incubated at 37°C and 5% CO_2. The next day, the transfected cells were detached from the culture dish and $5x10^6$ cells were seeded into a new culture dish containing 16 cover slips. The following day, the cells were washed three times with PBS pH 7.4, incubated for 10 min with 0.12% (w/v) glycine in PBS pH 7.4 at room temperature, washed once in PBS pH 7.4 and blocked with 10% FCS in PBS for one hour at room temperature. Following, the cells were stained with either anti-IL-6R antibody (4-11; 1:100 in 10% FCS/PBS) or anti-gp130 antibody (B-P4; 1:100 in 10% FCS/PBS) for one hour at 37°C in the presence or absence of 10 ng/ml hIL-6 to allow internalization. Cells for the strip control and the surface staining control were incubated with primary antibody at 4°C to disrupt internalization. The cells were washed three times with PBS and remaining antibody bound to the cell surface was removed by incubation in serum-free DMEM pH 2.0 for 30 min at 4°C. Cells for the surface staining control was incubated in serum-free DMEM pH 7.4 whereas the cells for the strip control were incubated with serum-free DMEM pH 2.0. After a three-time wash in PBS, the secondary antibody anti-mouse-AlexFlour488 (1:300 in 10% FCS/PBS) was added to the cells for one hour at 37°C to allow recycling and staining. The cells for surface staining control and strip control were incubated with secondary antibody at 4°C. Following, the cells were washed three times with PBS, fixed in 4% PFA/PBS for 10min at room temperature, washed again three times in PBS and once in ddH_2O. Finally, the cover slips were mounted onto microscopy slides using ProLong™ Gold Antifade Mountant with DAPI (Thermo Fisher Scientific, Waltham, MA, USA) thereby also staining nuclei. The cells were analyzed for recycled gp130 and IL-6R using the Olympus FV1000 confocal laser scanning microscope (Olympus, Hamburg, Germany) and ImageJ (NIH, Bethesda, USA).

3.2.3.8 Cell-surface biotinylation to analyze recycling of gp130 and IL-6R

The cell-surface biotinylation assay used to determine recycling of gp130 and the IL-6R was performed according to Basagiannis and Christoforidis [256] with slight adaptations.

$4x10^6$ HeLa cells were transiently transfected either with the pcDNA3.1-IL-6R plasmid or with the p409-myc-gp130wt plasmid (see 3.2.2.3) and were incubated for two days at 37°C and 5% CO_2. The cells were washed trice in PBS pH 7.4 and once in PBS pH 8.0 and were labelled with 5 ml 0.25 mg/ml cell-impermeable EZ-Link Sulfo-NHS-SS-Biotin (Perbio Science, Bonn, Germany) in PBS pH 8.0 for 45 min at 4°C. Following, the cells were washed three times in cold PBS pH 8.0

supplemented with 100 mM glycine and were incubated in 5 ml serum-free DMEM for 90 min at 37°C to allow internalization of cell-surface proteins. The cells were washed with PBS pH 7.4 and were incubated three times for 10 min at 4°C in 5 ml stripping buffer before being washed again three times in PBS pH 7.4. To allow recycling of proteins 5 ml serum-free DMEM was added to the cells and the cells were kept at 37°C for different time-points (0, 30, 60, 90 and 120 min). Following, the cells were washed once in PBS pH 7.4, incubated again three times in 5 ml stripping buffer for 10 min at 4°C and washed again three times in PBS pH 7.4. The cells were lysed in 250 µl biotinylation lysis buffer (described in 3.2.2.10), protein concentrations were determined, and equal protein amounts of every sample were incubated with 40 µl Streptavidin Sepharose™ High Performance beads (GE Healthcare Bio-Sciences, Uppsala, Sweden) overnight at 4°C on a rotator for the pull-down of biotinylated proteins. The following day, the beads were washed three times each at 250 g and 4°C for 2 min in 100 µl lysis buffer or wash buffer before being boiled at 95°C for 10 min in 70 µl 2,5x Laemmli buffer. Finally, recycling was analyzed by SDS-PAGE and Western Blot.

As a reduction in biotinylated proteins was a sign for recycling, biotinylated proteins were excluded from the second round of incubation in stripping buffer to make sure that the observed reduction was not due to degradation of the biotinylated proteins. For the biotinylation control, HeLa cells were incubated with biotin and washed as described above. The cells were collected and kept on ice. For the strip control, the cells were biotinylated, washed, incubated in stripping buffer and washed as described above. The cells were collected and kept on ice.

4 Results

4.1 Cell-surface levels of the Interleukin-6 receptor (IL-6R) and glycoprotein 130 (gp130) are controlled by proteolysis, internalization and recycling

Internalization and degradation of membrane-anchored proteins is important for cell-surface protein level regulation. Internalized proteins can be recycled and transported back to the cell-surface or they are degraded in the lysosome. Gp130 and the IL-6R were shown to be internalized [149-151] but the fate of both receptors was unclear. IL-6R was initially thought to be exclusively degraded in the lysosome but further analysis additionally demonstrated recycling of the IL-6R [1, 2]. Recycling of gp130 was not demonstrated so far, and in which compartment gp130 is degraded is still under debate [3, 4]. Although it is clear that IL-6 induces signaling by IL-6R and a gp130 homodimer [5], it is still unclear whether gp130 and IL-6R internalization, recycling and degradation are influenced by their ligand.

4.1.1 IL-6R cell-surface expression is regulated by proteolytic cleavage and internalization

Generally, two mechanisms are possible that can control IL-6R cell-surface levels, namely proteolytic cleavage or internalization. It is already known that the metalloprotease ADAM17 is able to cleave the cell-surface IL-6R by a process called shedding [96, 97]. In order to verify the involvement of proteolytic cleavage by ADAM17 in the regulation of IL-6R cell-surface expression in the monocytic cell-line THP-1, surface-IL-6R was stained with primary antibody. Following, the cells were incubated with or without PMA (2 µM), a phorbol ester that activates IL-6R cleavage by ADAM17, for two hours at 37 °C. Remaining surface IL-6R bound with primary antibody was stained with fluorescently-labelled secondary antibody α-mouse-APC and, finally, IL-6R cell-surface expression was analyzed via flow cytometry. As seen in Fig. 4.1, the cells treated with PMA showed lower levels of surface-IL-6R after two hours of incubation indicated by a decrease in the fluorescence compared to the sample treated with the PMA-solvent DMSO. This confirms that ADAM17 activation by PMA leads to reduced IL-6R cell-surface levels as compared to untreated THP-1 cells, indicating that indeed ADAM17-dependent shedding is involved in the regulation of IL-6R cell-surface levels.

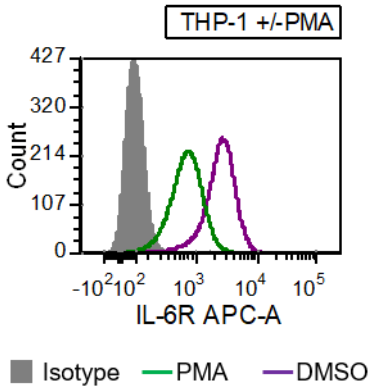

Figure 4.1: IL-6R surface expression after treatment with or without PMA. THP-1 cells were stained with the α-IL-6R antibody 4-11 for one hour one ice and were incubated with PMA (2 µM) or without (DMSO) for two hours at 37 °C. Following, remaining surface IL-6R bound with primary antibody was stained with fluorescently-labelled secondary antibody α-mouse-APC for one hour on ice in the dark and surface-IL-6R levels were finally analyzed by flow cytometry. As isotype control, THP-1 cells were only incubated with secondary antibody. The results from one experiment out of three independently performed experiments is shown.

As proteolytic cleavage of the IL-6R by ADAM17 was confirmed to regulate IL-6R cell-surface levels the involvement of internalization was additionally analyzed. Therefore, surface-IL-6R on THP-1 cells was stained with primary antibody and, following, the cells were incubated for different time points (0, 15, 30, 60, 90, 120 min) at 37°C with IL-6 to allow internalization, and with or without Marimastat (MM) (10 µM), a broad-spectrum metalloprotease inhibitor, to inhibit IL-6R proteolysis mediated by ADAM10 or ADAM17. Staining with secondary antibody and flow-cytometry measurement was performed as described above. The results are shown in Fig. 4.2.

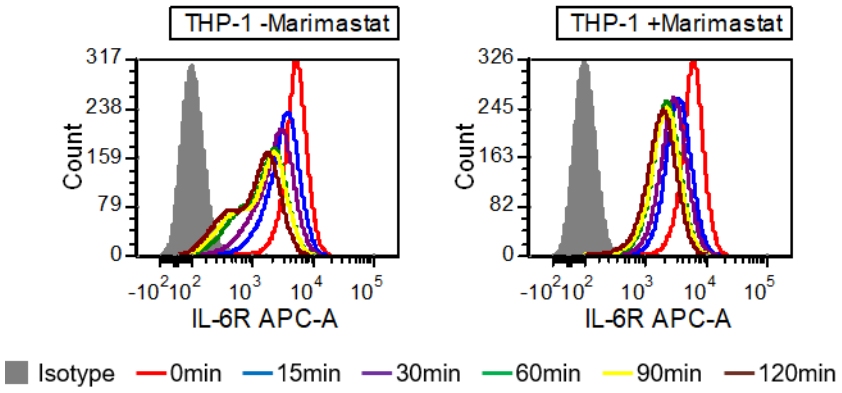

Figure 4.2: Internalization assay of the IL-6R in the presence or absence of Marimastat: THP-1 cells were stained with α-IL-6R antibody 4-11 for one hour on ice and transferred into cell culture medium without supplements. The cells were incubated for different time points (0, 15, 30, 60, 90, 120 min) at 37°C with IL-6 and with or without Marimastat (10 µM). Following, the remaining surface IL-6R was stained with the fluorescently-labelled secondary antibody α-mouse-APC and, finally, IL-6R cell-surface expression was analyzed via flow cytometry. As isotype control, cells were stained with the secondary antibody only. The results from one experiment out of three independently performed experiments is shown.

A reduction of cell-surface IL-6R over time could be observed in both conditions, i.e. with and without MM, as indicated by a decrease in APC-fluorescence. As a reduction in cell-surface IL-6R levels occurred also in the samples treated with MM, which induces inhibition of IL-6R proteolysis by metalloproteases, a process other than proteolysis by metalloproteases must be additionally involved in the regulation of IL-6R cell-surface levels. Most likely internalization contributes to IL-

6R cell-surface regulation in this experiment, but also a process that cannot be blocked by MM might play a role. In absence of MM the FACS plots showed a second peak indicating that proteolysis of the IL-6R by metalloproteases in addition to internalization contributes to the down-regulation of IL-6R cell-surface levels. From this it was concluded that both processes, shedding and internalization, are involved in the regulation of IL-6R cell-surface levels.

Basagiannis et al. reported previously that shedding of the VEGFR was increased once internalization was blocked [256]. Therefore, a possible compensatory effect of shedding for defective internalization in the context of IL-6R cell-surface level regulation was analyzed. To do so, $1x10^6$ IL-6R-overexpressing HeLa cells were incubated with DMSO as negative control, PMA (2 µM) as positive control, Pit-Stop2 (25 µM), an inhibitor of clathrin-dependent internalization, and Pit-Stop2 (25 µM) together with MM (10 µM) for 0 min or 60 min at 37°C. The supernatants were collected and centrifuged to remove remaining cells and other debris. Finally, sIL-6R released into the supernatants was analyzed by ELISA.

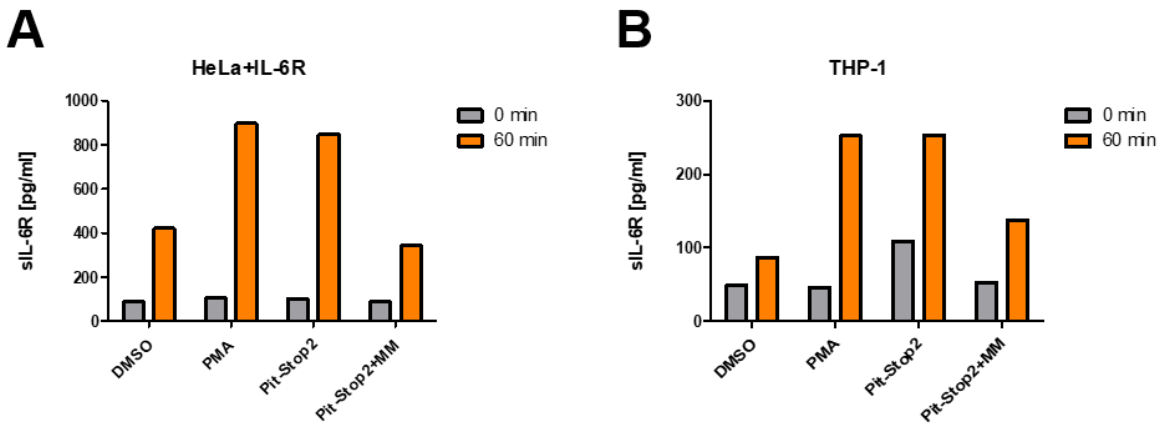

Figure 4.3: sIL-6R ELISA of cell culture supernatants after stimulation of cells with DMSO, PMA, Pit-Stop2 or Pit-Stop2 together with Marimastat. **(A)** $1x10^6$ IL-6R-overexpressing HeLa cells were incubated with either DMSO, PMA (2 µM), Pit-Stop2 (25 µM) or Pit-Stop2 together with Marimastat (MM; 10 µM) for 0 min or 60 min at 37°C before the supernatants were collected and centrifuged. The supernatants were analyzed for soluble IL-6R (sIL-6R) by ELISA. **(B)** The experiment was repeated using THP-1 cells that express the IL-6R endogenously. The results from one experiment out of two independently performed experiments is shown.

As shown in Fig. 4.3 (A), all samples showed an increase in sIL-6R levels after 60 min of incubation at 37°C compared to 0 min of incubation. The highest increase could be seen in the samples treated with PMA in which shedding of the receptor by ADAM17 was induced. A comparable increase could be achieved when clathrin-dependent internalization was blocked by treatment with the inhibitor Pit-Stop2 indicating that proteolytic cleavage of the IL-6R is increased in order to regulate cell-surface levels when internalization cannot take place. To exclude the contribution of dead cells to the increase in sIL-6R levels in the Pit-Stop2-treated samples and to verify the involvement of shedding, MM was added together with Pit-Stop2 to the cells. Analysis of these supernatants also revealed an increase after 60 min of incubation, but this increase was

comparable to the increase in the DMSO-treated, negative control samples which is most likely generated by constitutive shedding induced by ADAM10 as described before [96, 97].

To analyze a possible effect on endogenous IL-6R cell-surface expression, the experiment was also performed using THP-1 cells. The supernatants were also analyzed for soluble IL-6R (sIL-6R) by ELISA (Fig. 4.3 (B)). As seen in HeLa cells, incubation of THP-1 cells with PMA also led to an increase in sIL-6R after 60 min upon PMA stimulation in comparison to the DMSO-treated sample. The same increase could be seen when THP-1 cells were incubated together with Pit-Stop2 indicating that proteolytic cleavage of the IL-6R is increased in order to regulate cell-surface levels also in cells endogenously expressing the IL-6R. As incubation with Pit-Stop2 together with MM led to a decrease in sIL-6R it was confirmed that the increase in sIL-6R upon inhibition of internalization was due to proteolysis also in THP-1 cells.

These results indicate that shedding of the IL-6R was increased when internalization was blocked, hinting for a possible compensatory effect by shedding in the regulation of IL-6R cell-surface levels when internalization cannot take place.

As it was found that shedding could compensate for the loss of IL-6R internalization it was of further interest whether internalization or another process could also compensate for the loss of metalloprotease-mediated proteolysis by e.g. ADAM10 or ADAM17. To analyze this, cell-surface IL-6R on THP-1 cells was stained before the cells were incubated for 0 min or 120 min at 37°C in the presence of IL-6 and with or without MM (10 µM) to block proteolytic cleavage by metalloproteases like ADAM10 or ADAM17. Remaining surface IL-6R bound with primary antibody was stained with fluorescently-labelled secondary antibody α-mouse-APC and, finally, IL-6R cell-surface expression was analyzed via flow cytometry.

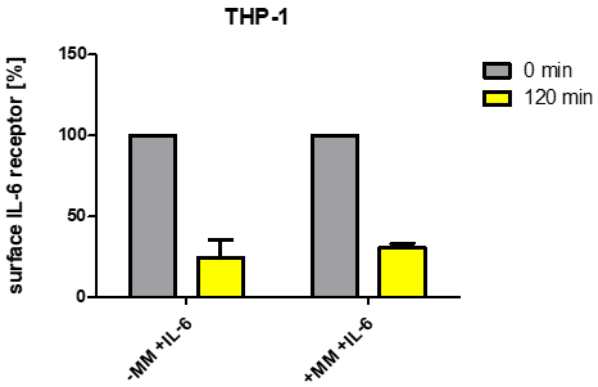

Figure 4.4: Quantification of the FACS analysis of THP-1 cells incubated with or without Marimastat. Cell-surface IL-6R on THP-1 cells was stained with the primary antibody 4-11 before the cells were incubated for 0 min or 120 min at 37°C in the presence of IL-6 and with or without MM (10 µM). Remaining surface IL-6R bound with primary antibody was stained with fluorescently-labelled secondary antibody α-mouse-APC for one hour on ice in the dark and, finally, IL-6R cell-surface expression was analyzed via flow cytometry. Mean fluorescent intensity of timepoint 0 min was set to 100% and the percentages for time-point 120 min was calculated therefrom.

Fig. 4.4 shows the quantification of the FACS analyses. A reduction in cell-surface IL-6R could be observed at 120 min compared to 0 min no matter whether the cells have been incubated with MM or not indicating that internalization takes place. Comparison of the remaining cell-surface

IL-6R after 120 min between the both conditions (± MM) revealed no statistically significant difference. This indicates that, indeed, internalization (or another process different from proteolysis by metalloproteases) can compensate for the loss of proteolytic cleavage, thereby regulating IL-6R cell-surface levels. If internalization (or another process) could not compensate for reduced shedding by ADAM10 or ADAM17, an increase in cell-surface IL-6R after 120 min would have been expected in the sample incubated with MM in comparison to the sample incubated without MM.

Therefore, not only shedding can compensate for the loss of internalization but also a loss of proteolytic cleavage by metalloproteases can be compensated for by internalization or another process. This indicates that IL-6R cell-surface levels are tightly regulated and a defect in a process contributing to the regulation of IL-6R cell-surface levels can be replaced by another one.

4.1.2 IL-6R and gp130 are internalized in a clathrin- and dynamin-dependent manner and independently of the cytokine Interleukin-6 (IL-6)

As we found that most likely IL-6R internalization was important for the regulation of IL-6R cell-surface levels next to proteolytic cleavage, we focused on the process of internalization of IL-6R and also gp130 in the following experiments.

IL-6R and gp130 internalization was analyzed before by other groups before but only contradictory results were obtained regarding the involvement of its ligand IL-6 and the pathway by which both receptors are internalized [149-151]. Therefore, IL-6R and also gp130 internalization was analyzed on THP-1 cells in more detail by a flow cytometry-based approach. In order to answer the question whether both receptors are internalized constitutively, independently of stimulation with the cytokine IL-6, cell-surface IL-6R or gp130 on THP-1 cells were stained with primary antibody 4-11 or B-P4, respectively. Subsequently, the cells were resuspended in 10 ml cell culture medium without supplements and MM (10 µM) was added to block shedding. The cells were incubated with or without IL-6 (10 ng/ml) for different time points (0, 15, 30, 60, 90, 120, 150, 180 min) at 37°C to allow internalization and remaining surface IL-6R and surface gp130 were stained with the fluorescently-labelled secondary antibody α-mouse-APC. Finally, IL-6R and gp130 cell-surface expression was analyzed via flow cytometry. A shown in Fig. 4.5, surface expression of both receptors was reduced in a time-dependent matter indicated by a reduction in APC-fluorescence for the different timepoints. Additionally, IL-6 did not seem to influence internalization of the IL-6R or gp130 as no apparent differences between the samples treated with and without IL-6 stimulation could be observed. As shedding was inhibited by addition of MM, a metalloprotease inhibitor, this decrease was most likely due to internalization but another process different from proteolysis by metalloproteases could also be involved.

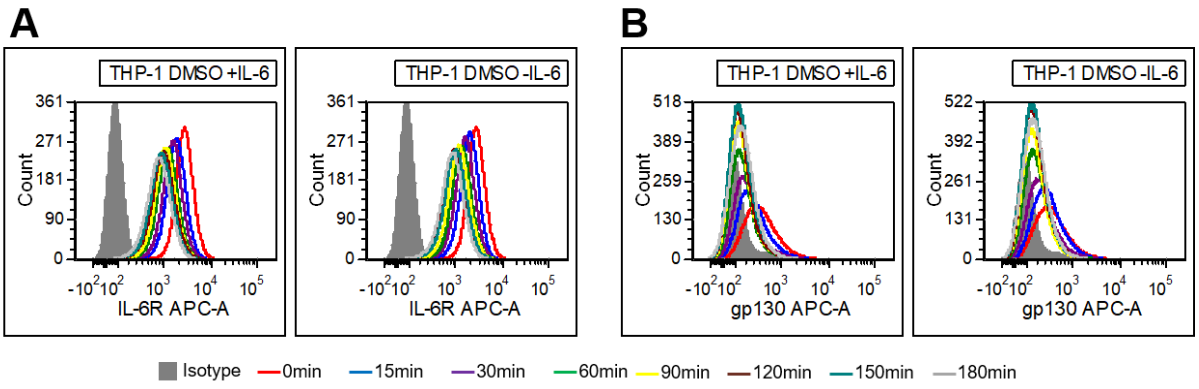

Figure 4.5 Internalization assay of the IL-6R and gp130 using THP-1 cells in the presence or absence of IL-6. (A) Cell-surface IL-6R on THP-1 cells was stained with the primary antibody 4-11. The cells were resuspended in 10 ml cell culture medium without supplements and with addition of Marimastat (MM; 10 µM) and with or without IL-6 (10 ng/ml). The cells were incubated at 37°C for different time points (0, 15, 30, 60, 90, 120, 150, 180 min), stained with the fluorescently-labelled secondary antibody α-mouse-APC and, finally, IL-6R cell-surface expression was analyzed by flow-cytometry. As isotype control THP-1 cells were incubated with the secondary antibody only. **(B)** The experiment was performed as described above but cell-surface gp130 was stained and analyzed. As isotype control THP-1 cells were incubated with the secondary antibody only. The results from one experiment out of six independently performed experiments is shown.

To better analyze the effect of IL-6 on IL-6R and gp130 internalization, a quantification was generated using the mean fluorescent intensities (MFI) of all time-points and calculating the percentages of remaining cell-surface IL-6R and gp130 therefrom. When comparing the half-lives of surface IL-6R of cytokine-stimulated and -unstimulated samples no significant differences between both conditions could be detected as each displayed half-lives of about 60 min (Fig. 4.6 (A)). In contrast, gp130 showed a slight increase in internalization upon IL-6 stimulation as it showed half-lives of 15 min for the stimulated and 30 min for the unstimulated conditions. After 180 min, though, the amount of internalized gp130 was the same for both conditions (Fig. 4.6 (B)). Therefore, it was concluded that internalization of both receptors occurred constitutively, i.e. independently of the cytokine IL-6.

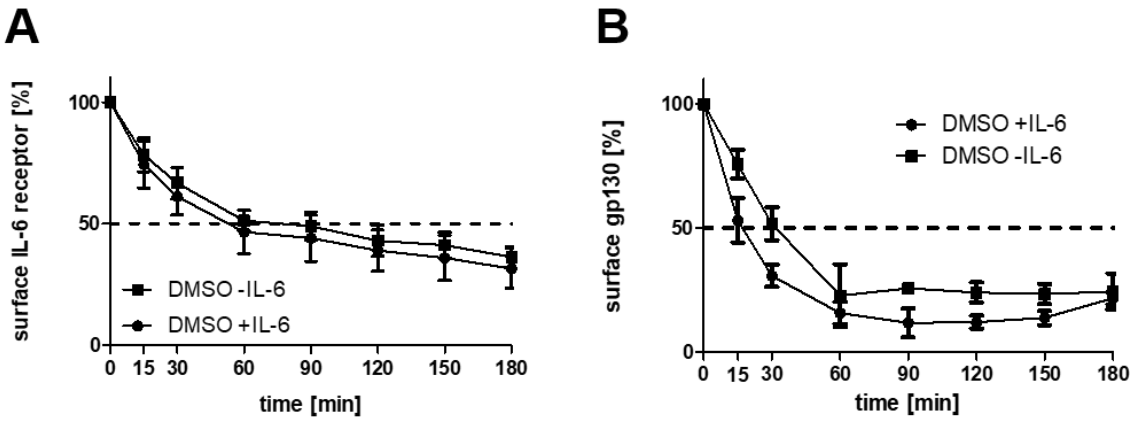

Figure 4.6: Quantification of the IL-6R and gp130 internalization assay. Quantification of the experiment shown in Figure 6.1.2a. The mean fluorescent intensity (MFI) of time-point 0 min was set to 100% of surface IL-6R **(A)** or surface gp130 **(B)**. The percentages for the other time-points were calculated therefrom using the corresponding MFIs. Data from six independent experiments are shown.

As we could show that the IL-6R and gp130 are internalized constitutively, i.e. independently of the cytokine IL-6, we focused on the pathway(s) by which both receptors are internalized.
Different pathways are known by which surface receptors can be internalized [131]. The most prominent pathway depends on the intracellular proteins clathrin and dynamin. The involvement of these two proteins in IL-6R and gp130 internalization was analyzed by flow cytometry using two different inhibitors, Pit-Stop2 and Dyngo-4a. Pit-Stop2 is a clathrin-specific inhibitor which interacts with the clathrin terminal domain (TD) thereby inhibiting its binding to the adaptor molecule amphiphysin which recruits clathrin molecules to the cell membrane in order to form clathrin-coated pits [257]. Dyngo-4a on the other hand is a specific inhibitor of dynamin action, preventing the formation of dynamin helical structures which are necessary for the GTP-dependent constriction and vesicle fission [258].
To identify the pathway by which the IL-6R and gp130 are internalized, a similar experimental set-up as before was used. THP-1 cells were washed, pre-incubated with the inhibitors Pit-Stop2 (25 µM), Dyngo-4a (50 µM) or DMSO as control for 40 min at 37°C and, afterwards, were stained with the primary antibody directed against the D1-domain of the IL-6R or with the primary antibody directed against the extracellular part of gp130. Following, the cells were resuspended in serum-free DMEM with addition of MM (10 µM) to avoid shedding, and Pit-Stop2, Dyngo-4a and DMSO were again added to the same cells as before. Additionally, the cells were stimulated with or without IL-6. Incubation, sampling and staining of the cells with secondary antibody was performed as described above. Finally, remaining surface IL-6R and gp130 were analyzed via flow cytometry. The samples treated with DMSO showed the same picture as before, meaning a reduction over time of surface IL-6R and gp130 which occurred independently of IL-6 indicating that DMSO, in which both inhibitors were dissolved, had no impact on internalization (Fig. 4.6). Analysis of the effect of both inhibitors on IL-6R or gp130 internalization revealed that internalization of the IL-6R and gp130 was reduced when clathrin-or dynamin was inhibited. After 3 h of incubation with IL-6 at 37°C, only 31% ± 8% of IL-6R and 22% ± 3% of gp130 surface receptors remained at the cell-surface in the DMSO control samples whereas 69% ± 20% of surface IL-6R (Fig. 4.7 (A)) and 53% ± 9% of surface gp130 (Fig. 4.7 (C)) were still present at the cell-surface when treated with Pit-Stop2. Inhibition with Dyngo-4a resulted in even higher levels of remaining surface receptors (79% ± 12% for IL-6R (Fig. 4.7 (B)), 68% ± 15% for gp130 (Fig. 4.7 (D)) after 3 h at 37°C. However, internalization of gp130 and IL-6R could not be inhibited by 100% after incubation with both inhibitors. Maybe another pathway different from clathrin and dynamin is also used to internalize both receptors or the inhibitors are not potent enough to block all clathrin and dynamin proteins.

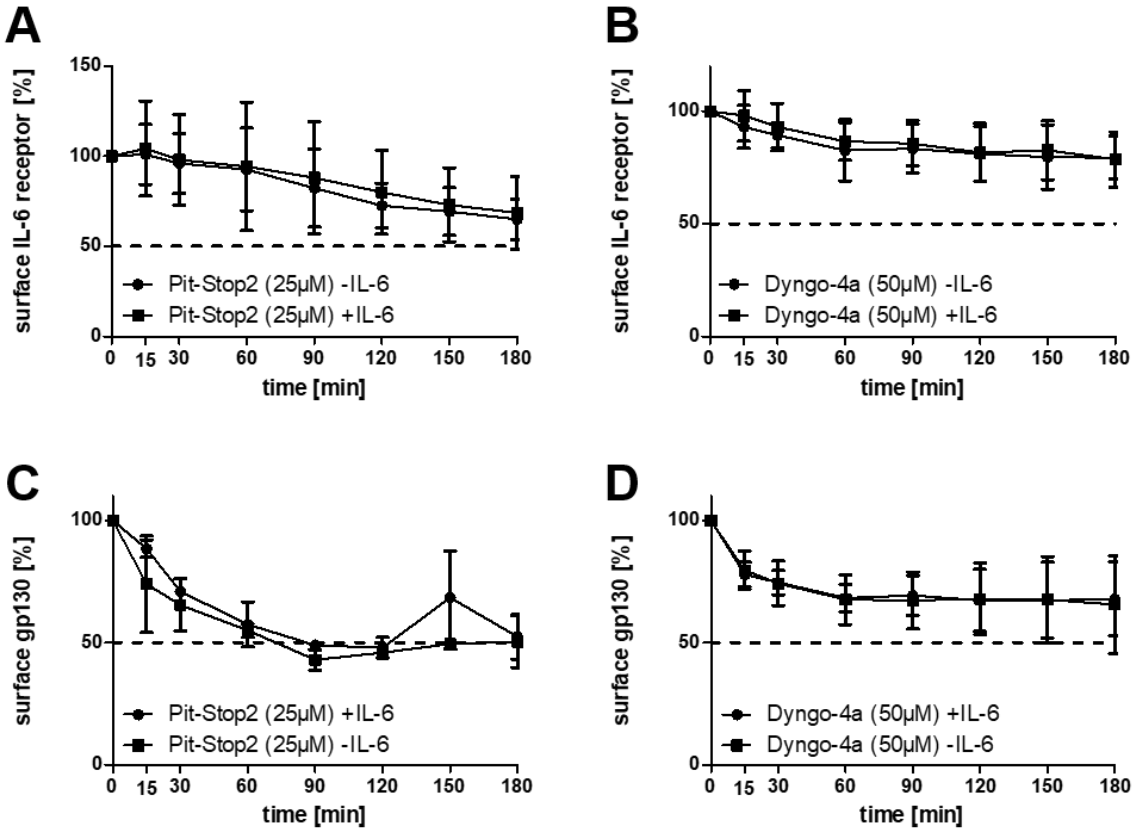

Figure 4.7 Quantification of the IL-6R and gp130 internalization assays in the presence of internalization inhibitors Dyngo-4a or Pit-Stop2. The quantification of the experiment described above is shown. The mean fluorescent intensity (MFI) of time-point 0 min was set to 100% of surface IL-6R. The percentages of remaining cell-surface IL-6R or gp130 were calculated therefrom using the corresponding MFIs. Data from three independent experiments are shown. **(A-D)** THP-1 cells were pre-incubated with Dyngo-4a (50 µM) or Pit-Stop2 (25 µM) for 40 min at 37 °C before being stained for one hour on ice with the α-IL-6R antibody 4-11 or the α-gp130 antibody B-P4. The cells were resuspended in cell culture medium without supplements and incubated with Marimastat (MM; 2 µM) and either Pit-Stop2 (25 µM; **A, C**) or Dyngo-4a (50 µM; **B, D**) or) Additionally, the cells were stimulated with or without IL-6 (10 ng/ml). The cells were incubated at 37°C and samples were collected at different time points (0, 15, 30, 60, 90, 120, 150, 180 min). The cells were stained with the fluorescently-labelled secondary antibody α-mouse-APC and remaining surface IL-6R or gp130 were analyzed via flow cytometry. As isotype control THP-1 cells were incubated with the secondary antibody only.

These results lead to the conclusion that IL-6R and gp130 are internalized in a clathrin- and dynamin-dependent manner. As the obtained results were the same for cells stimulated with IL-6 and unstimulated cells, this indicates that the receptors are internalized equally well in both conditions.

Recently, the involvement of endophilin in G-protein coupled receptor (GPCR) and IL-2R internalization was described [259]. Therefore, it was further analyzed whether endophilin also plays a role in IL-6/IL-6R/gp130 internalization additionally to clathrin and dynamin. As specific inhibitors for endophilin are still missing the involvement of this pathway was investigated using an indirect approach. Work by Schmidt-Arras et al. [157] suggested that STAT3 activation was reduced upon inhibition of internalization. Therefore, changes in STAT3 activation were used as a readout for the involvement of endophilin in internalization. HeLa cells were transiently co-transfected with IL-6R together with the different endophilin variants known so far (A1 (Fig. 4.8

(A)), A2 (B), A3 (C)) and as control with GFP. Two days later, the cells were starved for 4 hours in serum-free DMEM and stimulated with IL-6 for different time-points (0, 15, 30, 60, 90 and 120 min). Immunoblotting of the lysates generated from HeLa cells transfected with GFP showed normal activation of STAT3 that peaked at 30 min of IL-6 stimulation and decreased over time again. Transfection with the different endophilin variants did not influence STAT3 phosphorylation as it still peaked at 30 min and decreased over time (Fig. 4.8).

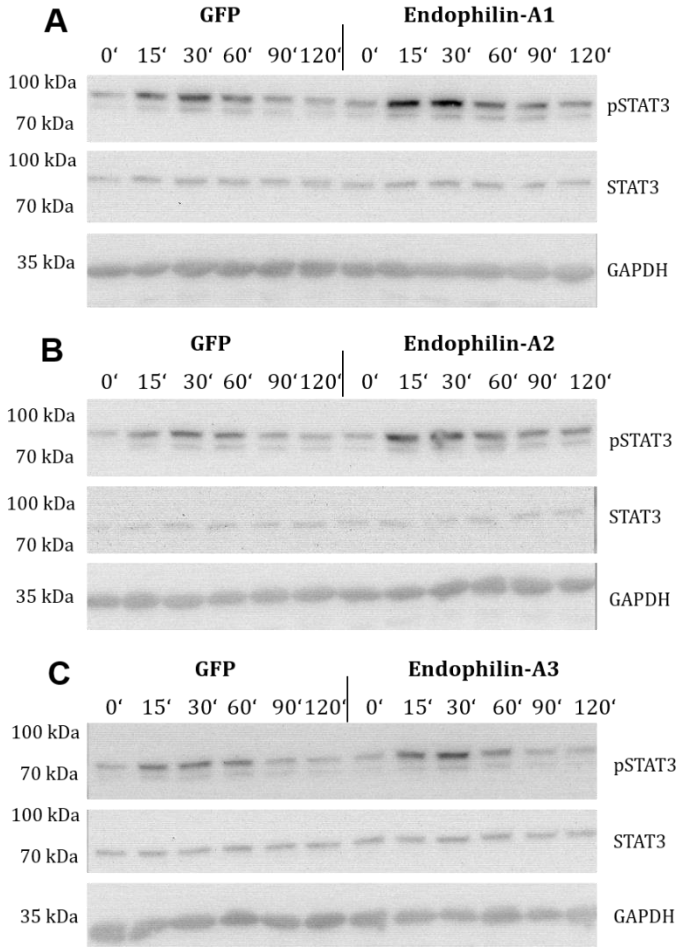

Figure 4.8: Analysis of STAT3 activation by Western Blot of HeLa cells transfected with different endophilin variants. HeLa cells were transiently transfected with the different endophilin variants (A1 **(A)**, A2 **(B)**, A3 **(C)**) together with IL-6R. As positive control, HeLa cells were co-transfected with IL-6R and GFP. The cells were starved for 4 hours in serum-free DMEM and stimulated with IL-6 for different time-points (0, 15, 30, 60, 90, 120 min). STAT3 activation in the different samples was analyzed by immunoblotting using antibodies directed against phosphorylated STAT3, total STAT3 and GAPDH and their corresponding HRP-coupled secondary antibodies.

These results indicate that endophilin does not play a major role in IL-6R/IL-6/gp130 internalization which is rather regulated by clathrin and dynamin.

4.1.3 The internalization motifs identified in the IL-6R cytoplasmic domain are dispensable for internalization

We found that the IL-6R and gp130 are internalized constitutively in a clathrin- and dynamin-dependent manner. As different internalization motifs are associated with clathrin and dynamin-dependent internalization, namely tyrosin-based motifs or di-leucine motifs, we wanted to analyze whether the motifs that have been identified in the cytoplasmic region of the IL-6R, namely 408-YSLG and 427-LI [152] also play a role in IL-6R internalization.

In order to analyze their involvement in IL-6R internalization these motifs were mutated by site-directed mutagenesis using SOE-PCR. Thereby, the YSLG motif was mutated to ASLG and the LI motif to AA.

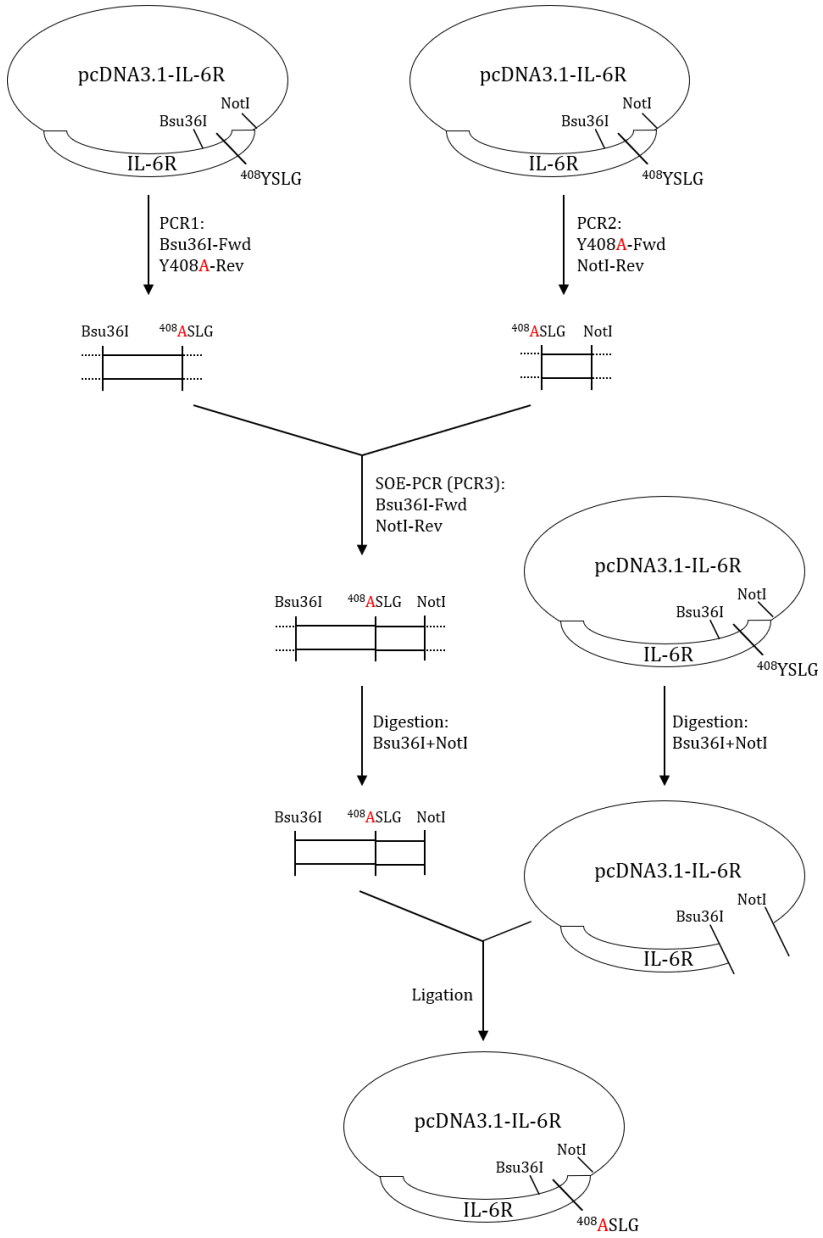

Figure 4.9: Cloning scheme of the pcDNA3.1-IL-6R-Y/A plasmid. After PCR1, PCR2 and PCR3 a fragment containing the Y/A-mutation was generated. Enzymatic digestion of the fragment and the pcDNA3.1-IL-6R plasmid using the enzymes Bsu36I and NotI was performed. Finally, the PCR fragment and the plasmid backbone were ligated resulting in the pcDNA3.1-IL-6R-Y/A plasmid. Red letters indicate the mutated amino-acid residue. Cloning was performed by Tina Daunke.

Figure 4.9 shows the cloning strategy for the 408-Y/A-mutation. The 427-LI/AA mutation was generated accordingly using different internal primers (described below). For the 408-Y/A-mutation, PCR1 was performed using the expression plasmid pcDNA3.1-IL-6R as a template, the 5'-primer Bsu36I-Fwd and the 3'-primer Y408A-Rev. For PCR2 the same template was used, the 5'-primer Y408-Fwd and the 3'-primer NotI-Rev. The fragments of both PCR reactions were isolated and used as templates for the PCR3 reaction together with the 5'-primer Bsu36I-Fwd and the 3'-primer NotI-Rev. The generated fragment and the pcDNA3.1-IL-6R plasmid were digested using the restriction enzymes Bsu36I and NotI. The fragment and the plasmid backbone were isolated and ligated resulting in the generation of the pcDNA3.1-IL-6R-Y/A plasmid. The LI/AA mutation was generated accordingly but the primers carrying the mutations were exchanged by the 3'-primer LI427/28AA-Rev and the 5'-primer LI427/28AA-Fwd.

As Ba/F3 and Ba/F3-gp130 cells were supposed to be transduced with plasmids carrying the mutations in the IL-6R cytoplasmic domain so these cells can be used to analyze the involvement of the internalization motifs, the mutated IL-6R was cloned into the pMOWS-puro-IL-6R plasmid by enzymatic digestion of the pcDNA3.1-IL-6R plasmids containing the mutations in the internalization motifs and the pMOWS-puro-IL-6R plasmid using the restriction enzymes AgeI and PmlI. For retroviral transduction, Phoenix cells (packaging cell line) were transfected with pMOWS-puro-IL-6R-Y/A or pMOWS-puro-IL-6R-LI/AA and the supernatants were incubated with Ba/F3 or Ba/F3-gp130 cells to introduce the YA- or the LIAA-mutations.

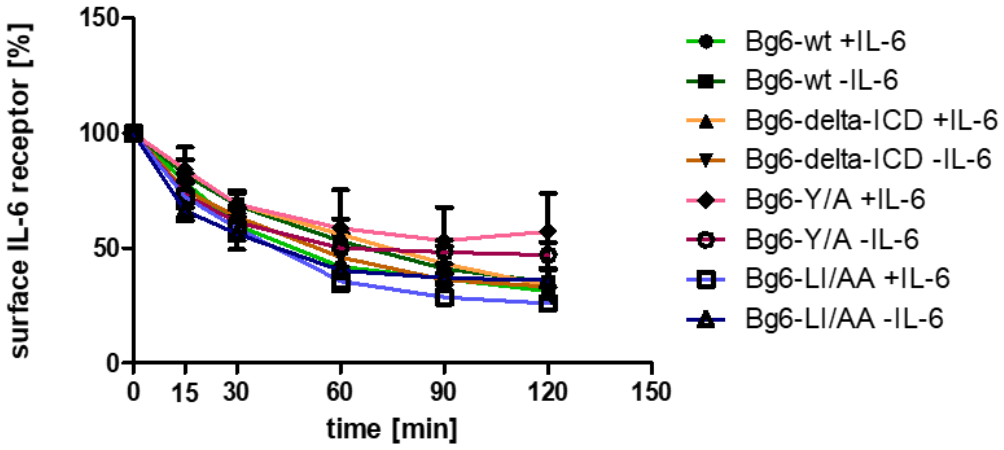

Figure 4.10: Internalization assay to test the involvement of the YSLG and LI internalization motifs on IL-6R internalization in the presence of gp130. The internalization assay was performed using Ba/F3-gp130-IL-6Rwt (Bg6-wt) cells, Ba/F3-gp130-IL-6R-delta-ICD (Bg6-delta-ICD) cells, Ba/F3-gp130-IL-6R-Y/A (Bg6-Y/A) cells and Ba/F3-gp130-IL-6R-LI/AA (Bg6-LI/AA) cells as described in chapter 4.1.2. Data from three independently performed experiments are shown. The experiment was performed together with Tina Daunke.

As transduction was successful, the involvement of the YSLG and LI motifs on IL-6R internalization could be analyzed. For this, the flow-cytometry based internalization assay described above was performed (see chapter 4.1.2). In addition to the newly generated cell lines, Ba/F3-gp130-IL-6Rwt cells and Ba/F3-gp130-IL-6R-delta-ICD cells, in which the intracellular part of the IL-6R is deleted,

were used. Internalization was quantified by setting the mean fluorescent intensity (MFI) of time-point 0 min to 100% surface IL-6R and calculating the percentages of surface IL-6R for the other time-points therefrom. Fig. 4.10 shows the results obtained with the help of the different Ba/F3-gp130-IL-6R (Bg6) cell lines. Analysis of IL-6R internalization using the Ba/F3-gp130-IL-6Rwt cells showed a reduction of cell-surface IL-6R over time which occurred constitutively and was not increased after stimulation with IL-6 which supports the results obtained from THP-1 cells. Surprisingly, all other cell lines expressing an IL-6R with mutations in one of the designated internalization motifs revealed internalization of the IL-6R comparable to internalization of the wild-type IL-6R. Maybe the loss of one internalization motif can be compensated for by the other motif. However, IL-6R internalization was also not reduced when the complete cytoplasmic part of the IL-6R was deleted, although this led to deletion of both internalization motifs, indicating that the YSLG and the LI motifs do not compensate for one another but rather are not necessary for IL-6R internalization. It could well be, that gp130 is more important than the internalization motifs and as long as gp130 is present IL-6R internalization mediated by gp130 can take place.

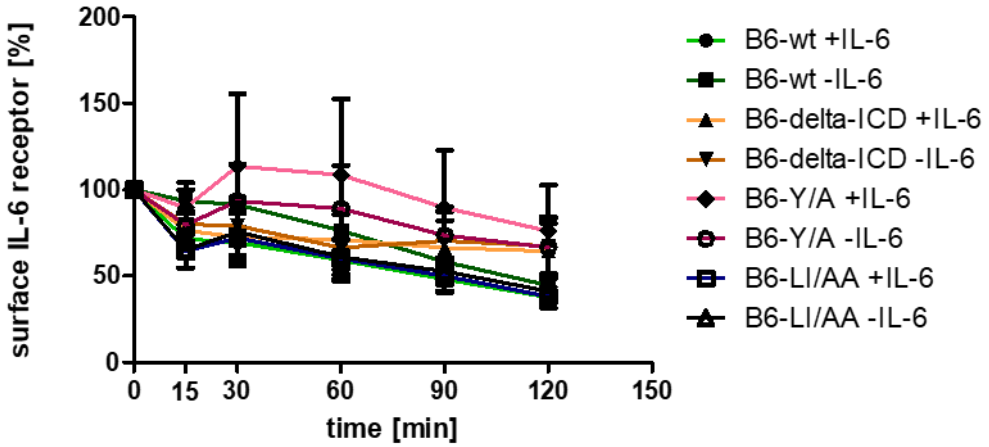

Figure 4.11: Internalization assay to test the involvement of the YSLG and LI internalization motifs on IL-6R internalization in the absence of gp130. The internalization assay was performed using Ba/F3-IL-6Rwt (B6-wt) cells, Ba/F3-IL-6R-delta-ICD (B6-delta-ICD) cells, Ba/F3-IL-6R-Y/A (B6-Y/A) cells and Ba/F3-IL-6R-LI/AA (B6-LI/AA) cells as described in chapter 4.1.2. Data from three independently performed experiments are shown. The experiment was performed together with Tina Daunke.

To test whether the presence of gp130 is more important for IL-6R internalization than the YSLG or LI internalization motifs, the internalization assay was also performed using the newly generated Ba/F3-IL-6R-Y/A and Ba/F3-IL-6R-LI/AA cells and, additionally, the Ba/F3-IL-6Rwt and the Ba/F3-IL-6R-delta-ICD cells. As Ba/F3 cells are the only cells that do not express gp130, also the generated cells are devoid of gp130 and are therefore perfect to analyze the involvement of gp130 on IL-6R internalization. The experiment was performed and quantified as before. Analysis of Ba/F3-IL-6Rwt cells showed IL-6R internalization over time which occurred constitutively and was not increased by IL-6. Additionally, all the other cell lines showed the same IL-6R internalization kinetics as in the Ba/F3-IL-6Rwt cells indicating again that the IL-6R

internalization motifs are not involved in IL-6R internalization (Fig. 4.11). As internalization took place in the Ba/F3-IL-6Rwt cells although gp130 was not present, it was concluded that IL-6R internalization also occurs independently of gp130, indicating that IL-6R/gp130 complex formation might be mainly necessary to induce signal transduction upon IL-6 stimulation. One should notice, though, that IL-6R internalization seems to be slower in the absence of gp130 indicating that gp130 is needed to some extent for IL-6R internalization.

4.1.4 Internalization of the IL-6/IL-6R/gp130 complex is necessary for STAT3 activation at endosomal structures and not for signaling termination

We found that, additionally to proteolysis, internalization is important for the regulation of IL-6R and gp130 cell-surface levels. Internalization was long believed to be solely important for signaling termination, but studies nowadays indicate that internalization can also be a prerequisite for signaling initiation [154-156]. In order to analyze the effect of internalization on IL-6-induced STAT3 signaling, THP-1 cells were starved for 3 hours at 37°C and were pre-incubated with the internalization inhibitors Pit-Stop2 or Dyngo-4a and DMSO as positive control for 40 min at 37°C. Following, 10 ng/ml IL-6 was added and the cells were harvested at different

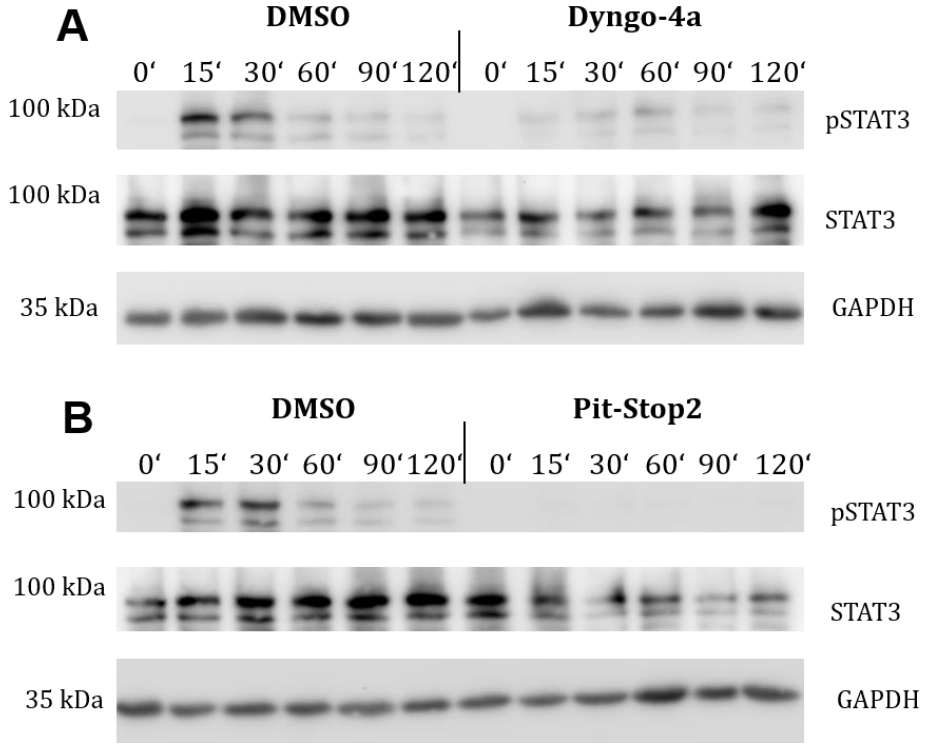

Figure 4.12: Analysis of STAT3 activation by Western Blot of THP-1 cells treated with DMSO, Dyngo-4a or Pit-Stop2. THP-1 cells were starved for 4 hours in serum-free DMEM, were pre-treated with DMSO, Dyngo-4a **(A)** or Pit-Stop2 **(B)** for 40 min at 37°C and stimulated with 10 ng/ml IL-6 for different time-points (0, 15, 30, 60, 90, 120 min). STAT3 activation in these cells was analyzed by Western Blot using antibodies directed against phosphorylated STAT3, total STAT3 and GAPDH and their corresponding HRP-coupled secondary antibodies.

time points (0, 15, 30, 60, 90, 120 min) and analyzed by immunoblotting. The results are shown in Fig. 4.12.

The samples in which the cells were treated with DMSO and stimulated with IL-6 revealed STAT3 phosphorylation with highest levels after 15min of IL-6 stimulation and a decrease thereafter over time indicating that IL-6 stimulation worked in THP-1 cells and led to STAT3 activation. In contrast, almost no STAT3 activation could be detected when cells were treated with Dyngo-4a (A) and even no phosphorylation at all was detected when treated with Pit-Stop2 (B). As the GAPDH loading control revealed equal loading between DMSO-treated cells and cells treated with one of the inhibitors, it was concluded that inhibition of internalization resulted in a decrease in STAT3 activation.

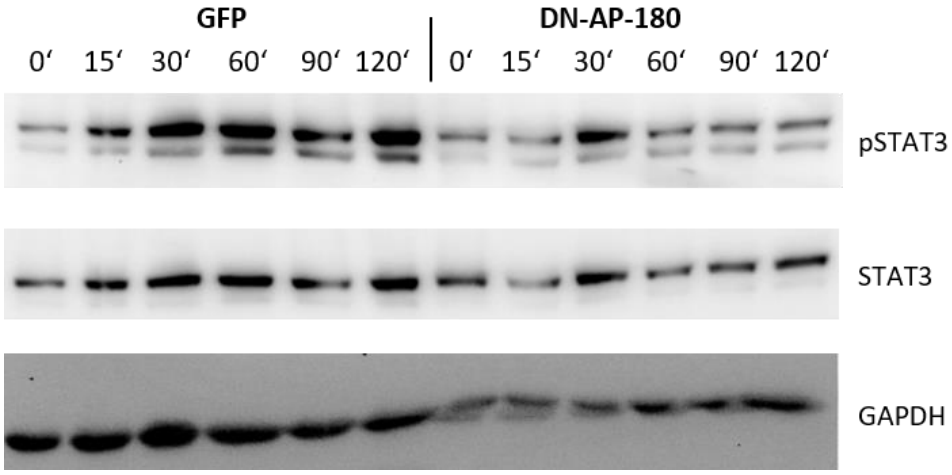

Figure 4.13: Analysis of STAT3 activation by Western Blot analysis of HeLa cells transfected with pN1-eGFP or pcDNA3.1-DN-AP-180-BFP2. HeLa cells transfected with pN1-eGFP or pcDNA3.1-DN-AP-180-BFP2 were starved for 4 hours in serum-free DMEM and stimulated with IL-6 (10 ng/ml) for different time-points (0, 15, 30, 60, 90, 120 min). STAT3 activation was analyzed in these cells by Western Blot using antibodies directed against phosphorylated STAT3, total STAT3 and GAPDH and their corresponding HRP-coupled secondary antibodies.

As the inhibitors can be toxic to the cells to some extent and the diminished STAT3 phosphorylation could be due to a decrease in living cells, a second experiment was conducted using HeLa cells that were transfected with plasmids encoding eGFP or dominant-negative AP-180 (DN-AP-180), an adaptor protein that recruits clathrin to the cell-surface. Loss of wild-type AP-180 at the cell-surface results in a decrease of clathrin recruitment and therefore also a reduction in internalization. The transfected cells were starved for 4 hours at 37°C in 2 ml serum-free DMEM before 10 ng/ml IL-6 was added and the cells were harvested at different time points (0, 15, 30, 60, 90, 120 min) before being analyzed by immunoblotting (Fig. 4.13). Cells that were transfected with GFP and stimulated with IL-6 showed STAT3 phosphorylation after 30min of incubation and a decrease thereafter over time although STAT3 signaling was not completely shut-down after 120 min as it used to be. This indicates that the IL-6 stimulation worked and that HeLa cells are responsive to IL-6 by activating STAT3. In the samples where the cells have been transfected with DN-AP-180 STAT3 phosphorylation was markedly reduced although the STAT3

loading control showed equal loading indicating that inhibition of clathrin recruitment disrupts efficient STAT3 activation.

Taken together, it seems that internalization is not only important for the regulation of IL-6R and gp130 cell-surface levels but is also necessary to initiate IL-6 dependent STAT3 signaling. As some phosphorylation could be detected in the samples treated with Dyngo-4a, it is likely that pit formation at the cell-surface might be even sufficient to induce signaling to some extent although the effects seen in the Dyngo-4a treated samples could also be a result of incomplete dynamin inhibition.

4.1.5 Recycling of the IL-6R and gp130 is influenced by IL-6

After identifying that the IL-6R and gp130 are internalized in a clathrin- and dynamin-dependent manner the intracellular fate of both receptors was of further interest. Therefore, recycling of both receptors was analyzed by co-localization of gp130 or IL-6R with Rab11, a protein found on recycling endosomes [165], via immunofluorescent staining.

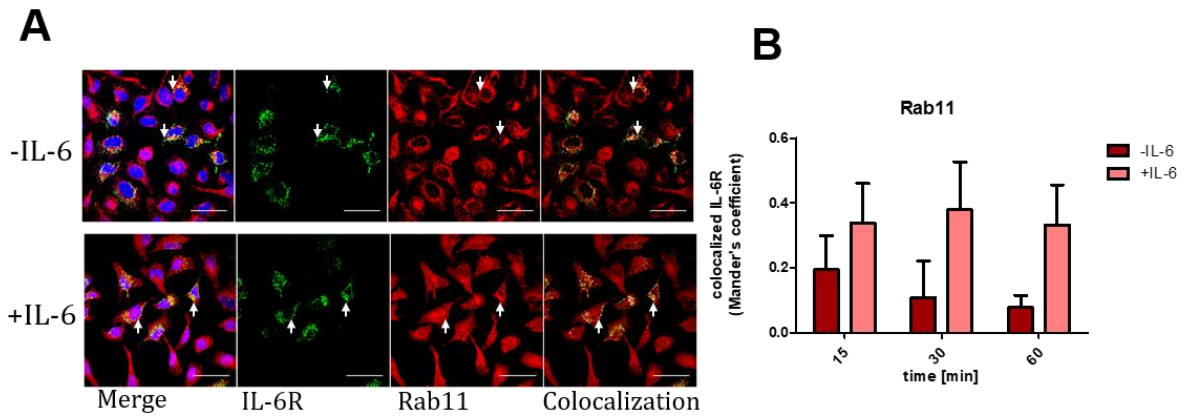

Figure 4.14: Immunofluorescent staining of IL-6R and Rab11 and analysis of co-localization. (A) HeLa cells were transfected with pcDNA3.1-IL-6R plasmid and surface IL-6R was stained for 1 h at 4°C using the BAF227 antibody following incubation with the fluorescently-labelled anti-goat-AlexaFlour488 antibody for 1 h at 4°C. The cells were incubated in serum-free DMEM for 15, 30 and 60 min at 37°C in the presence or absence of 10 ng/ml IL-6, fixed and permeabilized. Afterwards, the cells were incubated with primary antibody directed against the recycling endosome marker Rab11 following incubation with the fluorescently-labelled secondary antibody anti-rabbit-AlexaFlour594 for 1 h at room temperature. Finally, the cells were analyzed by confocal laser scanning microscopy. Arrows indicate co-localized IL-6R and Rab11. Scale bar: 50 µm **(B)** Co-localization between IL-6R and Rab11 was quantified using ImageJ and the JACoP plugin. Mander´s coefficient of 20 cells was calculated.

To analyze co-localization of internalized gp130 or IL-6R with Rab11, Hela cells were transfected with either pcDNA3.1-IL-6R or p409-gp130wt and cell-surface IL-6R and gp130 were stained with primary and fluorescently-labelled secondary antibody without prior permeabilization as only surface IL-6R and gp130 should be stained and not the intracellularly located IL-6R and gp130 to analyze only co-localization of Rab11 with internalized gp130 or IL-6R. Additionally, staining was performed at 4°C to inhibit internalization as these cells were used as a control for the cell-surface staining of the IL-6R and gp130. Following, stained surface-IL-6R and gp130 were shifted to 37°C for different time-points (15, 30 and 60 min) to induce internalization of both receptors. As the

involvement of IL-6 in the fate of internalized IL-6R and gp130 should be also analyzed the cells were incubated in the presence or absence of 10 ng/ml IL-6. To analyze co-localization with the intracellularly located Rab11 protein, the cells were fixed, permeabilized and stained with primary antibody directed against the recycling endosome marker Rab11 and afterwards with fluorescently-labelled secondary antibody anti-rabbit-AlexaFlour594 for one hour at room temperature. Finally, the cells were analyzed by confocal laser scanning microscopy and co-localization was quantified using ImageJ and the JACoP plugin. This plugin calculates the Mander´s coefficient, a factor representing the co-occurrence of pixels in each channel that should be analyzed for co-localization.

Figures 4.14 and 4.15 show successful staining of gp130, IL-6R and Rab11. The overlay of IL-6R and Rab11 revealed co-localization of both proteins (Fig. 4.14 (A)) which was also seen for gp130 and Rab11 (Fig. 4.15 (A)) revealing that both receptors are transported to Rab11-positive compartments, most likely to recycling endosomes, following internalization. The quantification of IL-6R and Rab11 co-localization of cells that were not stimulated with IL-6 showed the highest levels of co-localization after 15 min of internalization which decreased over time indicating that most of the internalized IL-6R was located at recycling endosomes after 15 min of incubation. When the cells were incubated with IL-6 no difference in the co-localization between the different time points could be seen but an increase in recycling was observed when stimulated with IL-6. These effects might lead to the conclusion that recycling of the IL-6R is enhanced upon stimulation with IL-6 (Fig. 4.14 (B)).

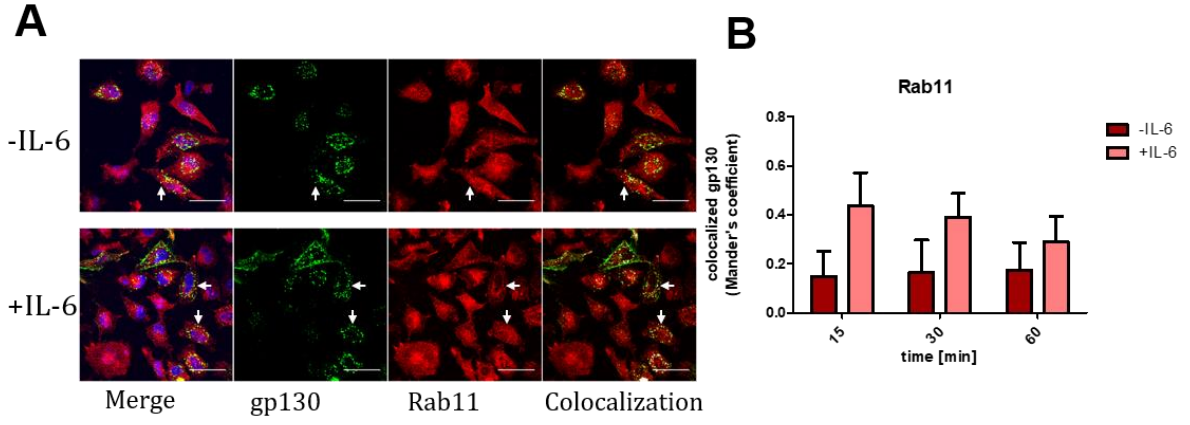

Figure 4.15: Immunofluorescent staining of gp130 and Rab11 and analysis of co-localization. (A) HeLa cells were transfected with p409-myc-gp130wt plasmid and surface gp130 was stained for 1 h at 4°C using the B-P4 antibody, following incubation with the fluorescently-labelled anti-mouse-AlexaFlour488 antibody for 1 h at 4°C. The cells were incubated in serum-free DMEM for 15, 30 and 60 min at 37°C in the presence or absence of 10 ng/ml IL-6, fixed and permeabilized. Afterwards, the cells were incubated with primary antibody directed against the recycling endosome marker Rab11 following incubation with the fluorescently-labelled secondary antibody anti-rabbit-AlexaFlour594 for 1 h at room temperature. Finally, the cells were analyzed by confocal laser scanning microscopy. Arrows indicate co-localized gp130 and Rab11. Scale bar: 50 µm **(B)** Co-localization between gp130 and Rab11 was quantified using ImageJ and the JACoP plugin. Mander´s coefficient of 20 cells from three individual experiments was calculated.

When analyzing co-localization of gp130 and Rab11 in cells that were not stimulated with IL-6 the same amount of co-localization was seen for the different time-points indicating that gp130 is

transported to recycling endosomes slower than the IL-6R as all time-points showed equal co-localization. IL-6 stimulation led to the highest co-localization at 15min of internalization and a decrease over time. Also for gp130 an increase in co localization with Rab11 was detected when the cells were stimulated with the cytokine IL-6 (Fig. 4.15 (B)). These results indicate that gp130 is faster recycled upon IL-6 stimulation and most of the receptor is recycled after 15 min of incubation.

Taken together, these experiments revealed that IL-6R and gp130 are transported to Rab11-positive recycling endosomes following constitutive internalization. Furthermore, the rate of co-localization was increased upon IL-6 stimulation.

As we could show that the IL-6R and gp130 co-localize with Rab11 most likely at recycling endosomes hinting to recycling of both receptors, we wanted to verify these results by visualizing recycling of both receptors at the cell-surface. Therefore a surface-biotinylation experiment was conducted that was slightly modified from Basagiannis and Christoforidis [256]. For the biotinylation experiment HeLa cells were transfected with pcDNA3.1-IL-6R or p409-gp130wt. Two days later, all proteins located at the cell-surface, including gp130 and the IL-6R, were labelled with 0.25 mg/ml cell-impermeable, cleavable EZ-Link Sulfo-NHS-SS-Biotin at 4°C for 45 min. To allow internalization of biotinylated surface receptors the cells were incubated in serum-free DMEM for 90 min at 37°C. As only internalized cell-surface receptors should be analyzed for recycling, remaining biotin at the cell surface was stripped off by incubation in stripping buffer that disrupts the SS-bond in the biotin. To allow possible recycling of the biotinylated internalized proteins, the cells were incubated in serum-free DMEM at 37°C for different time points (0, 30, 60, 90 and 120 min). At this point, biotinylated proteins are present inside the cell as well as at the cell-surface after they are recycled. Incubation of biotinylated proteins with streptavidin beads for pull-down would catch all the biotinylated proteins. As only recycling of internalized and biotinylated proteins should be analyzed and isolation of the cell-membrane for analysis is difficult, the cells were incubated a second time in the stripping buffer to remove the biotin from the recycled, cell-surface proteins leaving only the non-recycled proteins to be biotinylated. For the pull-down of the biotinylated proteins the cell lysates were incubated with Streptavidin beads over night at 4°C. The pulled-down biotinylated proteins were then analyzed by Western Blot. Recycling of biotinylated proteins is indicated by a reduction in protein levels as a result of reduced biotinylated intracellular proteins after recycling of some of the biotinylated surface proteins. To make sure this reduction is not due to degradation of biotinylated proteins but due to recycling control samples were treated as above but were excluded from the second round of incubation in stripping buffer. Incubation with streptavidin beads results in the pull-down of biotinylated, recycled proteins and intracellular-located, biotinylated proteins.

For both, IL-6R (Fig. 4.16 (A)) and gp130 (Fig. 4.16 (B)), surface-biotinylation and also strip off biotin from receptors was successful as indicated by the surface ctrl and the strip ctrl, respectively.

The surface ctrl revealed a distinct band for IL-6R or gp130 which hints to effective biotinylation as only proteins can be observed in the pull-down samples that have been biotinylated. In contrast, no band or only a faint band could be observed in the strip ctrl sample which proofs that strip of the biotin from biotinylated proteins worked. As the controls showed efficient biotinylation and strip of biotin, the other samples could be analyzed for recycling. Both receptors showed a decrease in protein levels over time indicating that IL-6R and gp130 were either recycled to the cell-surface or degraded. As described above, a reduction in biotinylated and pulled-down proteins is most likely due to recycling as biotin was stripped of from the recycled, biotinylated proteins, but also degradation would lead to a reduction in protein levels. To rule out the involvement of degradation, also the samples were analyzed that did not undergo the second strip round and thus contain recycled and intracellularly located biotinylated proteins. As in these samples protein levels stayed the same at all time-points it was proven that the reduction of protein levels over time was due to recycling and not due to degradation. Also, the protein levels in the cell lysates were the same in all samples indicating that over all protein levels were comparable in all samples.

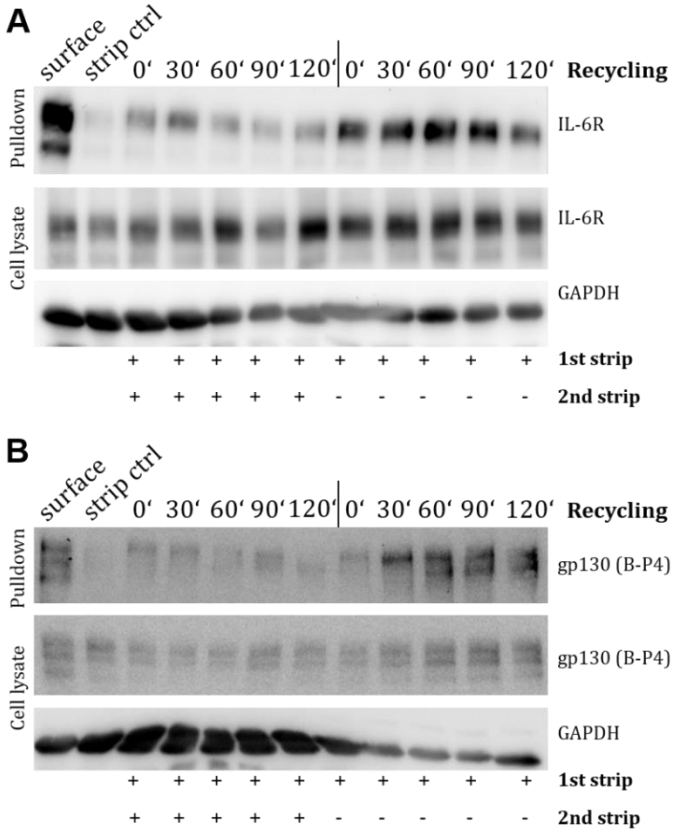

Figure 4.16: Western Blot analysis of IL-6R and gp130 recycling using surface-biotinylation. HeLa cells were transfected with pcDNA3.1-IL-6R **(A)** or p409-gp130wt **(B)**. Two days later the cells incubated with 0.25 mg/ml cell-impermeable EZ-Link Sulfo-NHS-SS-Biotin at 4°C for 45 min. Following, the cells were incubated in serum-free DMEM for 90 min at 37°C and remaining biotin at the cell surface was stripped of by incubation in stripping buffer. The cells were incubated again in serum-free DMEM at 37°C for different time points (0, 30, 60, 90, 120 min) and stripped again as described above. The cells were lysed, and biotinylated proteins were pulled down with streptavidin beads over night at 4°C. Recycling was analyzed via SDS-PAGE and Western Blot. Control samples were treated as above but were excluded from the second round of incubation in stripping buffer (- 2nd strip). For the biotinylation control (surface) the cells were only incubated with biotin and then kept on ice. For the strip ctrl cells were incubated with biotin, stripped and afterwards kept on ice. One from three individually performed experiments is shown.

This experiment supports the above finding that both, gp130 and the IL-6R, are transported to recycling endosomes and are recycled to the cell-surface from there.

Using the above experiment, it was difficult to analyze IL-6-induced differences in the rate of recycling that were observed in the co-localization experiment. To examine the effect of IL-6 on recycling and to validate the results of the surface-biotinylation, another experiment was conducted that was adapted from Stautz et al. [255] where recycling is detected via immuno-fluorescence microscopy. For this, HeLa cells were transfected again either with pcDNA3.1-IL-6R or p409-gp130wt plasmid and surface IL-6R and surface gp130 were stained with either 4-11 antibody (α-IL-6R) or B-P4 antibody (α-gp130) without fixation and permeabilization of the cells as the cells have to be alive to internalize and recycle proteins, and only cell-surface receptor should be analyzed. This staining was performed at 37°C to allow staining of surface receptors and internalization of the stained receptors at the same time. Cells for surface staining controls and strip controls were stained with primary antibodies for one hour at 4°C to block internalization whereas the cells for the isotype control where incubated without any antibody for one hour at 4°C. Staining with primary antibodies was performed either in presence or absence of the cytokine IL-6 to analyze the influence of IL-6 stimulation on receptor recycling. Subsequently, the cells used for the recycling experiment were incubated in serum-free DMEM pH 2.0 for 30 min at 4°C to remove the primary antibody bound to non-internalized surface IL-6R or surface gp130 as only internalized receptors should be analyzed. To be sure that this strip worked, cells, that were stained with primary antibody at 4°C, were also incubated in serum-free DMEM pH 2.0. The remaining controls were incubated in serum-free DMEM pH 7.4. Afterwards, the cells for the recycling experiment were stained with fluorescently-labelled secondary antibody α-mouse-AlexaFlour488 for one hour at 37°C. This allows recycling of the receptors that carry the primary antibody and subsequent binding of the secondary antibody that is only present in the buffer to the primary antibody once the receptor is recycled back to the cell-surface. Controls were also incubated with the secondary antibody but incubated at 4°C. Finally, the cells were fixed, mounted and recycling was analyzed by confocal laser scanning microscopy.

As shown in Fig. 4.17, surface staining of IL-6R (Fig. 4.17 (A)) and gp130 (Fig. 4.17 (C)) was successful and IL-6 stimulation had no influence on the staining. Stripping of non-internalized primary-antibody from the cell surface using DMEM pH 2.0 worked as no fluorescence could be detected in the strip controls. The cells of the actual recycling experiments showed a small number of fluorescent cells in the absence of IL-6 indicating that in the absence of IL-6 both receptors are recycled to cell-surface which could already be seen in the co-localization experiment. In contrast, when the cells were incubated together with the cytokine an increase in fluorescent cells could be detected for both receptors which hints to an IL-6-dependent increase in recycling of both, gp130 and IL-6R. This increase in recycling upon IL-6 stimulation was also observed in the co-localization experiment supporting the notion that IL-6 induces recycling of the IL-6R and gp130.

These differences between unstimulated and IL-6-stimulated conditions were also visible in the quantifications. About 12% of the IL-6R-overexpressing HeLa cells showed recycling in the absence of IL-6, which increased significantly to 22% when the cells were incubated together with IL-6 (Fig. 4.17 (B)). Quantification of gp130 recycling revealed that about 6% of the gp130-overexpressing cells showed recycling when not stimulated with IL-6 whereas IL-6 stimulation lead to a significant increase of recycling positive cells to about 10% (Fig. 4.17 (D)).

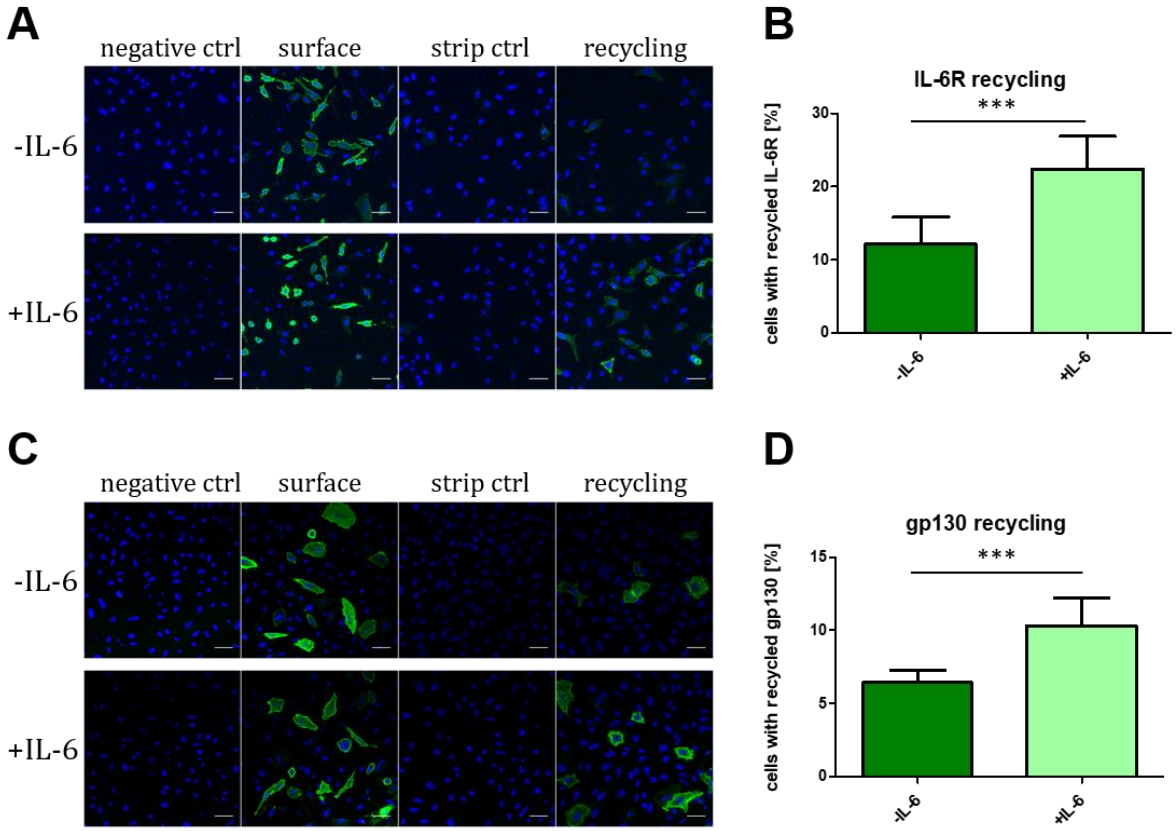

Figure 4.17: IL-6R and gp130 recycling assay using immunofluorescent microscopy. (A)+(C) HeLa cells were transfected with pcDNA3.1-IL-6R **(A)** or p409-myc-gp130 **(C)** before being stained with either 4-11 antibody (α-IL-6R) or B-P4 antibody (α-gp130) for 1 h at 37°C in the presence or absence of IL-6 (10 ng/ml). Cells for surface staining controls and strip controls were stained with primary antibodies for one hour at 4°C whereas the cells for the negative control where incubated without any antibody for one hour at 4°C. The cells were incubated in serum-free DMEM pH 2.0 for 30 min at 4°C or in serum-free DMEM pH 7.4 (surface and negative ctrls). Afterwards, the cells were stained with fluorescently-labelled secondary antibody α-mouse-AlexaFlour488 for one hour at 37°C. The control samples were incubated with secondary antibody at 4°C. Finally, the cells were fixed, mounted and recycling was analyzed by confocal laser scanning microscopy. Scale bar: 50 µm. **(B)+(D)** The quantification was done using ImageJ. All DAPI positive cells and green-fluorescent cells present in the pictures were counted and the percentage of green-fluorescent cells was calculated. 11 pictures taken from three individual experiments were analyzed.

Taken together, we could observe that the IL-6R and gp130 are transported to Rab11-positive recycling endosome which could be increased upon IL-6 stimulation. Additionally, we could show that both receptors are recycled to the cell-surface although only a small amount of both receptors is recycled constitutively. Recycling of both receptors, however, could be increased upon IL-6 stimulation indicating IL-6-dependent recycling of the IL-6R and gp130. In humans, the presence of IL-6 is a sign for inflammation which leads to the activation of different pro-inflammatory effects. To react to IL-6, IL-6R and gp130 are necessary to bind IL-6 which leads e.g. to the

activation of different immune cells. Thus, IL-6 might lead to an increase in the recycling of both receptors so more receptor is present at the cell-surface to react most efficiently to the circulating IL-6.

4.1.6 Lysosomal degradation of IL-6R and gp130 occurs independently of IL-6 but the presence of IL-6 leads to an increase in gp130 lysosomal degradation

Following internalization, surface receptors cannot only be recycled back to the cell-surface, but they can also be degraded in the lysosome. After we identified that the IL-6R and gp130 are recycled to the cell-surface following internalization we also wanted to analyze the involvement of lysosomal degradation in the regulation of IL-6R and gp130 protein levels. Therefore, a co-localization experiment was performed as described for the analysis of the transport of the IL-6R and gp130 to Rab11-positive recycling endosomes (see chapter 4.1.5). To analyze the transport of IL-6R and gp130 to lysosomes co-localization of both receptors with the lysosomal marker LAMP-2 was examined. HeLa cells were transfected with either pcDNA3.1-IL-6R or p409-gp130wt and cell-surface IL-6R and gp130 were stained as before and surface-IL-6R and gp130 were allowed to internalize for different time-points (15, 30 and 60 min) by shifting the cells to 37°C. To analyze the involvement of IL-6 in the fate of internalized IL-6R and gp130 the cells were incubated in the presence or absence of 10 ng/ml IL-6. To analyze co-localization with the lysosomal-located LAMP-2 proteins, the cells were fixed, permeabilized and stained with primary antibody directed against the lysosomal marker LAMP-2 and afterwards with fluorescently-labelled secondary antibody anti-mouse-AlexaFlour594 for 1 h at room temperature. Finally, the cells were analyzed by confocal laser scanning microscopy and co-localization was quantified using ImageJ and the JACoP plugin.

As shown in Figure 4.18, staining of IL-6R, gp130 and LAMP-2 was successful and could be visualized via fluorescence microscopy. The overlay of IL-6R and LAMP-2 revealed co-localization of both proteins (Fig. 4.18 (A)) which was also seen for gp130 and LAMP-2 (Fig. 4.18 (C)). The quantification of IL-6R and LAMP-2 co-localization revealed an increase over time no matter if stimulated with IL-6 or not which hints that most of the receptor destined for degradation is located at the lysosome after 60 min of incubation or even later, which is different from co-localization with Rab11 which peaked at 15 min of incubation. In contrast to the co-localization of Rab11 and the IL-6R where IL-6 induced an increase in recycling, IL-6 had no influence on the co-localization of LAMP-2 and the IL-6R (Fig. 4.18 (B)), indicating that lysosomal degradation of the IL-6R occurs constitutively and is not influenced by the presence of IL-6. In the quantification of LAMP-2 and gp130 co-localization an increase could be detected over time with and without IL-6 stimulation, which also peaked at 60 min of incubation or even later, which is different from co-localization with Rab11, which showed highest levels at 15 min, at least in the IL-6-stimulated

sample. In contrast to the IL-6R, though, an increase in gp130 co-localization with LAMP-2 could be observed when incubated with IL-6 (Fig. 4.18 (D)). This leads to the conclusion that gp130 is also constitutively degraded in the lysosome but upon IL-6 stimulation gp130 degradation via the lysosome is increased.

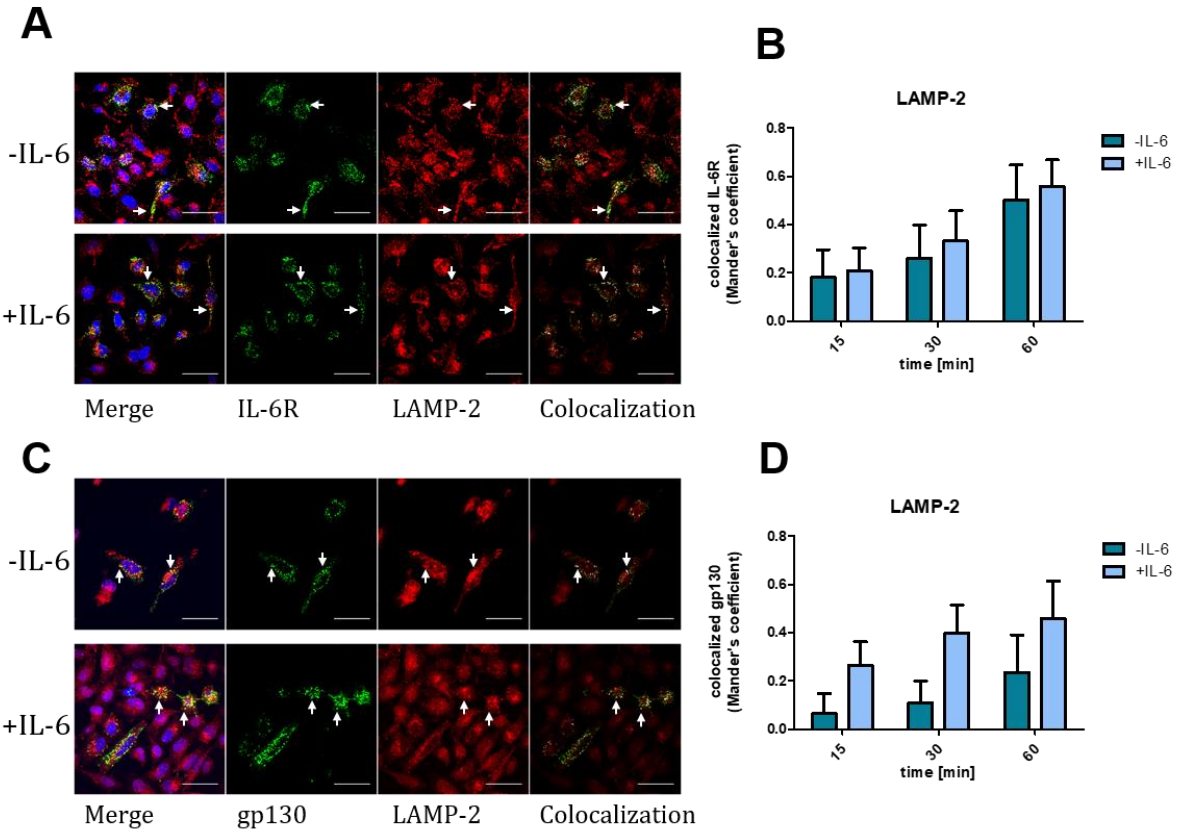

Figure 4.18: Immunofluorescent staining of IL-6R, gp130 and LAMP-2 and analysis of co-localization. (A)+(C) HeLa cells were transfected with pcDNA3.1-IL-6R **(A)** or p409-myc-gp130wt **(C)** and surface IL-6R or gp130 were stained with BAF227 or B-P4 antibody, respectively, for 1 h at 4°C and with fluorescently-labelled anti-goat-AlexaFlour488 (IL-6R) or anti-mouse-AlexaFlour488 (gp130) antibody for 1 h at 4°C. Following, the cells were incubated in serum-free DMEM for 15, 30 and 60 min at 37°C in the presence or absence of 10 ng/ml IL-6. The cells were fixed, permeabilited and stained with primary antibody directed against the lysosomal marker LAMP-2 for 1 h at room temperature. and with fluorescently-labelled secondary antibody for 1 h at room temperature. Finally, co-localization was analyzed by confocal laser scanning microscopy Arrows indicate co-localized IL-6R or gp130 with LAMP-2. Scale bar: 50 µm **(B)+(D)** Co-localization between IL-6R and LAMP-2 **(B)** and gp130 and LAMP-2 **(D)** was quantified using ImageJ and the JACoP plugin. Mander´s coefficient of 20 cells was calculated.

Taken together, analysis of IL-6R surface levels revealed that it is not only regulated by proteolytic cleavage but also by internalization and that both processes can compensate for one another in the process of IL-6R cell-surface regulation. In flow-cytometry based experiments it was shown that internalization of gp130 and IL-6R occurred constitutively in a clathrin- and dynamin-dependent manner. The fate of both receptors following internalization was analyzed and revealed constitutive recycling of gp130 and the IL-6R by Rab11-positive recycling endosomes and that recycling could be enhanced upon IL-6 stimulation. Gp130 and IL-6R were also found to co-localize with the lysosomal marker LAMP-2 indicating lysosomal degradation of both proteins

which occurred constitutively. IL-6R degradation could not be enhanced upon IL-6 stimulation, however, lysosomal degradation of gp130 was increased by IL-6 stimulation.

4.2 Activation of Toll-like Receptor 2 (TLR2) induces Interleukin-6 trans-signaling

After we focused on the membrane-bound IL-6R and examined internalization and the fate of this receptor, we now concentrate on the soluble IL-6R (sIL-6R) and try to identify endogenous stimuli and the involvement of different Toll-like receptors (TLRs) leading to the release of sIL-6R.
Recently it was shown that the sIL-6R is generated by alternative splicing and proteolysis *in vivo*, whereby alternative splicing accounts only for 15% of released sIL-6R [93]. Additionally, the cleavage site used for the generation of sIL-6R *in vivo* was identified to lie between proline355 and valine356, a site preferentially cleaved by ADAM10 and ADAM17, supporting findings that ADAM10 and ADAM17 are the main proteases involved in sIL-6R generation [96, 97, 253]. In mice, an increase in sIL-6R serum levels was mediated by ADAM17 after injection of LPS indicating an involvement of TLR4 activation [223]. In humans, endogenous stimuli that lead to sIL-6R release are only poorly understood and the involvement of TLR4 or other TLRs in sIL-6R release has not been investigated so far.

4.2.1 TLR4 activation does not induce sIL-6R release from human PBMCs or during sepsis

As it was found that LPS injection into mice thus activating TLR4 resulted in an increase in sIL-6R serum levels we wanted to analyze the involvement of TLR4 and LPS on sIL-6R generation by ADAM17 in humans. Therefore, PBMCs were isolated from plasma-free blood samples by density gradient centrifugation using Ficoll Histopaque 1077. $5x10^5$ PBMCs in 1 ml serum-free RPMI were incubated with or without 5 µg/ml LPS K12, an activator of TLR4, for 24 h at 37°C and 5% CO_2. The supernatants were collected, centrifuged to remove remaining cells and cell debris, and the amount of sIL-6R was analyzed via ELISA. As LPS is known to be a strong activator of IL-6 secretion, determination of IL-6 levels in the samples via ELISA was used as a positive control. A significant increase in IL-6 secretion could be observed after treatment with LPS (Fig. 4.19 (A)), which proved the functionality of the used LPS and that the isolated PBMCs were alive and reactive towards LPS. In contrast to IL-6 secretion, LPS did not alter the generation of sIL-6R from PBMCs (Fig. 4.19 (B)). This indicates that TLR4 activation via LPS leads to secretion of IL-6 but does not induce ADAM17-dependent proteolysis of the IL-6R in this *in vitro* setting.

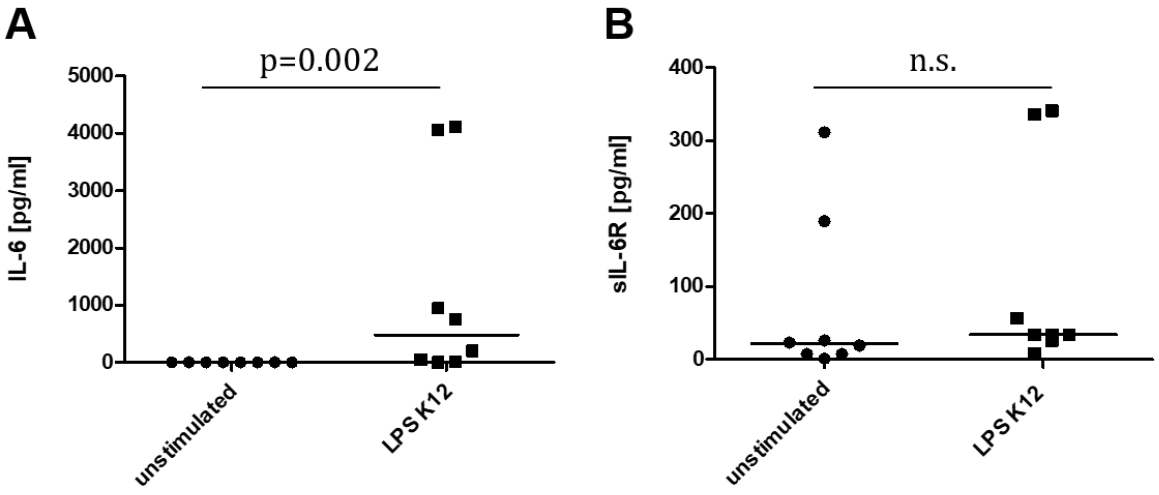

Figure 4.19: IL-6 and sIL-6R ELISA of supernatants collected from stimulated PBMCs. PBMCs were isolated from plasma-free blood by density gradient centrifugation using Ficoll Histopaque 1077. 5x10^5 cells in 1 ml serum-free RPMI were incubated with or without 5 µg/ml LPS K12 for 24 h at 37°C and 5% CO_2. The supernatants were collected, centrifuged and IL-6 **(A)** and sIL-6R **(B)** levels were measured by ELISA. Three independent experiments (n=8) were performed, which were analyzed by Mann-Whitney-U test.

We further investigated IL-6 and sIL-6R levels in serum samples of sepsis patients and sex- and age-matched healthy controls via ELISA. Sepsis is a severe inflammatory condition, which is characterized by a massive increase in IL-6 often caused by infection with gram-negative bacteria and therefore activation of TLR4. As expected, a significant increase of IL-6 could be detected in the samples of sepsis patients within 24 h after diagnosis (day 0) (0.84 ± 0.2 ng/ml) in comparison to healthy control samples (0.06 ± 0.04 ng/ml). Five days after diagnosis IL-6 levels decreased again (0.61 ± 0.2 ng/ml) (Fig. 4.20 (A)). Such an effect could not be observed for sIL-6R. Even during sepsis sIL-6R levels did not increase (Day 0: 61.1 ± 5.3 ng/ml; Day 5: 60.2 ± 3.7 ng/ml) in comparison to the healthy control samples (65.5 ± 3.8 ng/ml) (Fig. 4.20 (B))).

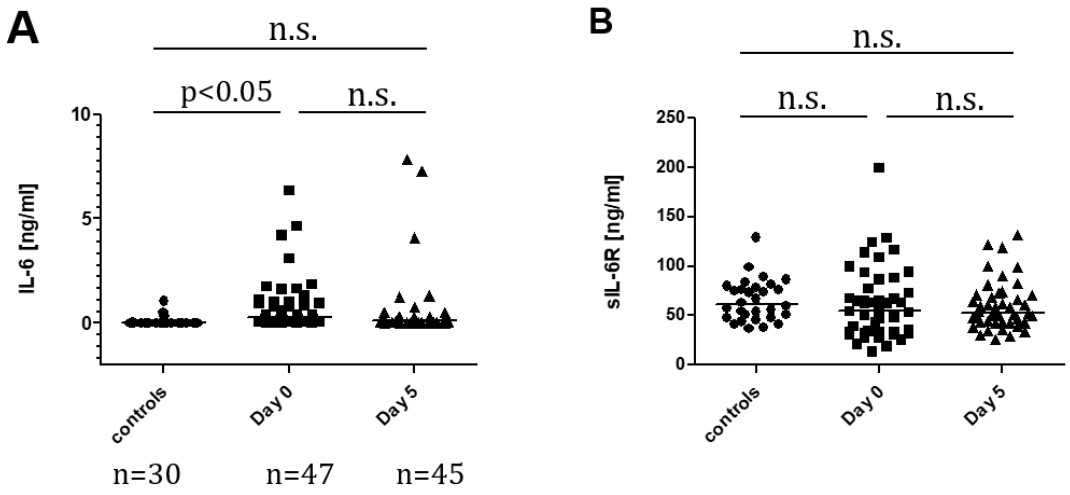

Figure 4.20: sIL-6R and IL-6 ELISA using serum samples from healthy controls and sepsis patients. Serum samples from sepsis patients at the day of sepsis diagnosis (day 0, n=47) and 5 days later (day 5, n=45) were used to determine IL-6 **(A)** or sIL-6R **(B)** levels via ELISA. Serum samples from healthy donors (n=30) were applied as control. Data were analyzed by one-way ANOVA followed by Bonferroni's Multiple Comparison test (n.s.: not significant).

These results show that LPS can induce the release of IL-6 *in vitro* and in sepsis patients *in viv*o most likely by activating TLR4, but LPS does not trigger the generation of sIL-6R. Therefore, the involvement of TLR4 in the release of sIL-6R was excluded.
As innate immune responses and the release of sIL-6R depend on the recognition of pathogen-associated microbial peptides (PAMPs) by pattern-recognition receptors (PRRs) like the Toll-like receptors (TLRs), the involvement of another TLR in the release of sIL-6R in humans seemed to be likely and was further analyzed.

4.2.2 sIL-6R generation and IL-6 release are increased after TLR2 activation on human PBMCs

The above results suggest that TLR4 does not play a major role in the generation of sIL-6R in humans, which is different compared to results obtained in mice [223]. However, the involvement of other TLRs in sIL-6R generation was likely, which was further supported by findings from Ullah et al. [260] who discovered that activation of TLR2 led to an increase in sIL-6R release. To further analyze the role of TLRs in sIL-6R generation, human PBMCs were isolated and $5x10^5$ cells in 1 ml serum-free RPMI were stimulated with agonists specific for the different TLRs: Pam3CSK4 (an activator of TLR1/2), HKLM (heat-killed *Listeria monocytogenes*; TLR2), Poly(I:C)/Poly(I:C) LMW (both TLR3), LPS K12 (TLR4), flagellin (TLR5), FSL-1 (TLR6/2), imiquimod (TLR7), ssRNA (TLR8) or the cells were left untreated. Supernatants were collected, centrifuged and amounts of sIL-6R and IL-6 were determined via specific ELISAs. As shown in Fig. 4.21 stimulation of PBMCs with the different agonists led to an increase of IL-6 levels in most of the samples except for cells treated with the TLR3 agonist Poly(I:C) LMW as compared to the untreated controls where no IL-6 could be detected. A significant increase in IL-6 release could be observed in the samples treated with the TLR2 agonists Pam3CSK4 (2.4 ± 0.88 ng/ml), HKLM (5.1 ± 0.82 ng/ml) or FSL-1 (2.7 ± 0.85 ng/ml) (Fig. 4.21 (A)). Analysis of sIL-6R generation after treatment with the different TLR agonists showed no statistically significant increase compared to the unstimulated control, but stimulation with the TLR2 agonist HKLM resulted in a three-fold increase of sIL-6R (208 ± 77 pg/ml) in comparison to the unstimulated control (73 ± 40 pg/ml) (Fig. 4.21 (B)).
Unstimulated cells did not release IL-6 whereas sIL-6R was released into the supernatant. This constitutive release of sIL-6R is most likely due to proteolytic cleavage of the membrane-bound IL-6R mediated by ADAM10 which was already described [96, 97].

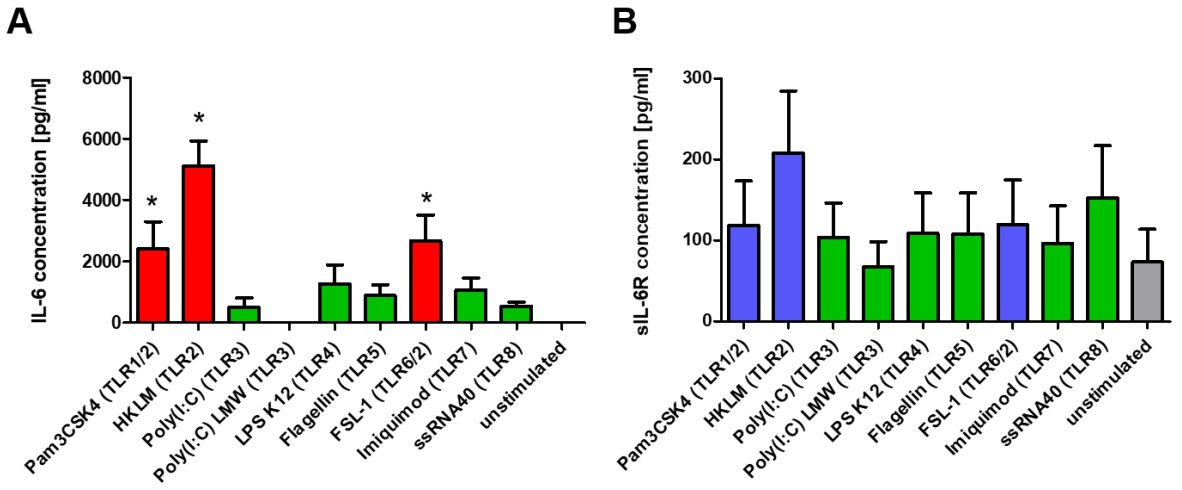

Figure 4.21: IL-6 and sIL-6R ELISA of supernatants collected from PBMCS stimulated with different TLR agonists. PBMCs were isolated from plasma-free whole blood by density gradient centrifugation using Histopaque. $5x10^5$ cells in 1 ml serum-free RPMI were stimulated with different TLR agonists (Pam3CSK4 (1 µg/ml), HKLM (10^8 cells/ml), Poly(I:C) (25 µg/ml), Poly(I:C) LMW (25 µg/ml), LPS K12 (5 µg/ml), Flagellin (1 µg/ml), FSL-1 (1 µg/ml), Imiquimod (5 µg/ml), ssRNA40 (5 µg/ml)) for 24 h at 37°C and 5% CO_2. Supernatants were collected, centrifuged and of IL-6 **(A)** and sIL-6R **(B)** levels were determined via ELISA. Data shown are the mean ± SEM from four independent experiments, which were analyzed by one-way ANOVA followed by Dunnett's Multiple Comparison test. Statistical significance compared to the unstimulated cells is indicated with an asterisk.

These results indicate that only activation of TLR2 on PBMCs simultaneously induces the release of IL-6 and sIL-6R. Therefore, the following experiments focus on TLR2 activation and the generation of sIL-6R. This connection was not described so far and could demonstrate that TLR2 might be involved in the recognition of endogenous stimuli which leads to the release of sIL-6R in humans.

4.2.3 sIL-6R and IL-6 are released from monocytes after TLR2 activation

We observed that TLR2 activation resulted in the release of sIL-6R, thus, it was of further interest which cell-type(s) generated sIL-6R in response to TLR2 activation. As PBMCs are a mixture of different cell types including monocytes, T cells, B cells, NK cells and immature dendritic cells, we used a flow-cytometry based approach to identify the cell-type(s) involved in sIL-6R release. Therefore, isolated PBMCs were stained with different cell surface markers for the individual subpopulations: CD45, a leukocyte marker, CD14 for monocytes, CD123 for dendritic cells, CD3 for T cells, B220 for B cells and CD56 for NK and T cells. Additionally, the cells were co-stained with antibodies directed against the IL-6R and TLR2. As the cell population(s) that express the IL-6R as well as TLR2 at the cell surface simultaneously are most likely to release sIL-6R upon HKLM stimulation we tried to identify such populations.

As shown in Fig. 4.22, monocytes, dendritic cells, T cells and to a lesser extent B cells and NK cells express the IL-6R at the cell-surface. From these, though, only monocytes and dendritic cells co-expressed TLR2 making these two cell-types the most likely sources for sIL-6R release after treatment with HKLM.

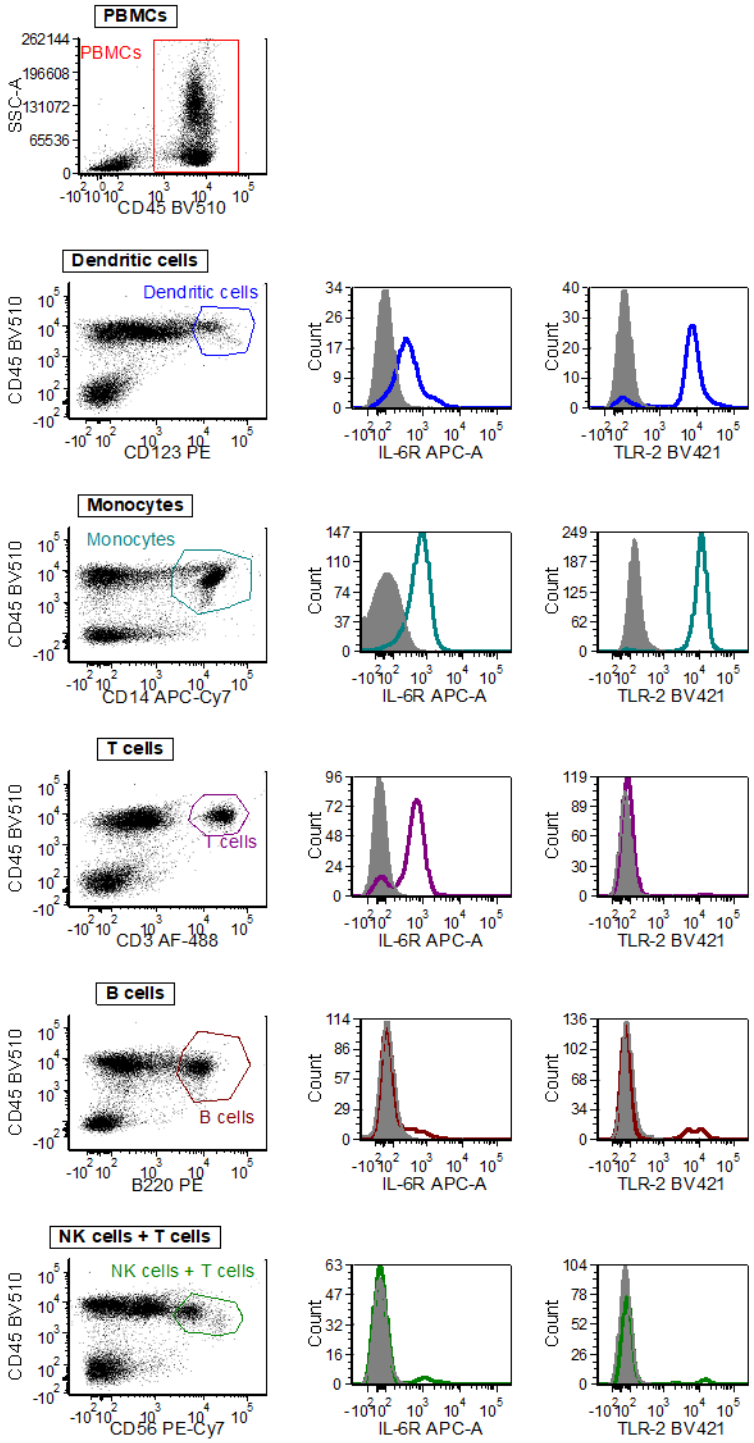

Figure 4.22: FACS staining of different cell-types in isolated PBMCs. PBMCs were isolated from plasma-free blood by density gradient centrifugation using Ficoll Histopaque. The cells were stained with specific antibodies against the different subsets, analyzed by flow cytometry and gated as follows: $CD45^+CD14^+$ monocytes, $CD45^+B220^+$ B cells, $CD45^+CD3^+$ T cells and $CD45^+CD56^+$ T cells or NKT cells. Additionally, surface IL-6R and surface TLR2 were stained and FACS plots are shown for each cell subset.

To further assess the involvement of monocytes and dendritic cells in the release of sIL-6R, both cell-types were isolated from PBMCs by antibody-based magnetic cell separation. $5x10^5$ cells in 1 ml serum-free RPMI were stimulated with the TLR2 agonist HKLM (10^8 cells/ml) or left untreated for 24 h at 37°C and 5% CO_2. The supernatants were isolated, centrifuged to remove remaining cells and cell debris and IL-6 and sIL-6R levels were determined via specific ELISAs. Unstimulated dendritic cells and monocytes released no IL-6 into the supernatant whereas stimulation with HKLM led to secretion of IL-6 indicating that stimulation of TLR2 was an effective IL-6-inducer in both cell-types (Fig. 4.23 (A)). Analysis of sIL-6R in the same supernatants revealed a release of sIL-6R already in unstimulated conditions, indicating constitutive shedding of the IL-6R, although higher sIL-6R levels could be detected in the supernatant of unstimulated monocytes compared to unstimulated dendritic cells. Stimulation with HKLM had no effect on sIL-6R release from dendritic cells making these cells an unlikely source of sIL-6R upon TLR2 activation. In contrast, supernatants from HKLM-stimulated monocytes displayed higher amounts of sIL-6R (98.9 ± 29.7 pg/ml) in comparison to supernatants from unstimulated monocytes (47.5 ± 12.7 pg/ml) although this increase was not statistically significant (Fig. 4.23 (B)).

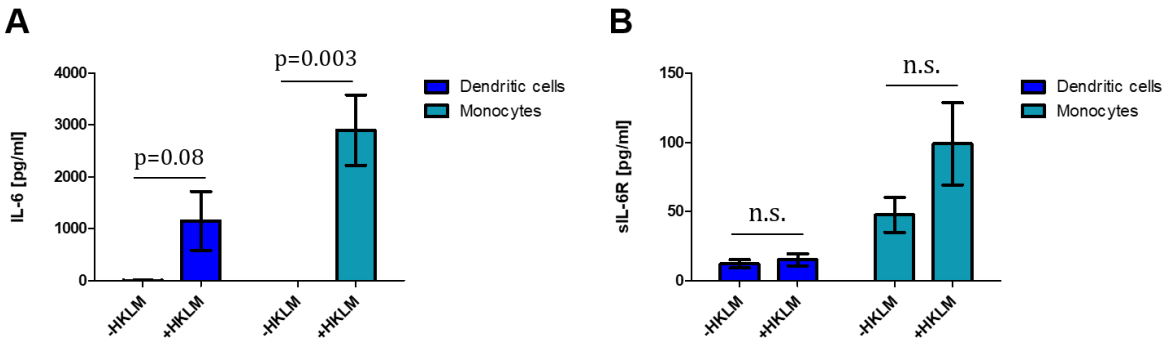

Figure 4.23: IL-6 and sIL-6R ELISA from supernatants collected from HKLM-stimulated dendritic cells or monocytes. Monocytes and dendritic cells were isolated from PBMCs by antibody-based magnetic cell separation. $5x10^5$ cells in 1 ml serum-free RPMI were stimulated with the TLR2 agonist HKLM (10^8 cells/ml) or left untreated for 24 h at 37°C and 5% CO_2. The supernatants were isolated, centrifuged and IL-6 **(A)** and sIL-6R **(B)** levels were determined via specific ELISAs. Data of three independent experiments (n=6) ± SEM are shown.

These findings lead to the conclusion that monocytes and to a lesser extent also dendritic cells are able to release IL-6, but only monocytes release sIL-6R upon HKLM-stimulation making these cells most likely the major source of sIL-6R after TLR2 activation upon HKLM-treatment.

4.2.4 Activation of TLR2 induces IL-6R proteolysis by ADAM10 and ADAM17

After we identified that monocytes are the major source of sIL-6R secretion after TLR2 activation, it was of further interest how this sIL-6R is generated. It is already known, that surface IL-6R can be cleaved by the metalloproteases ADAM10 and ADAM17 resulting in sIL-6R release, but also alternative splicing can contribute to sIL-6R levels [93, 96, 97] To determine whether proteases play a role in sIL-6R generation from PBMCs, PBMCs were again isolated from plasma-free blood.

$5x10^5$ cells in 1 ml serum-free RPMI were pre-incubated with the different metalloprotease inhibitors GI (ADAM10 inhibitor), GW (ADAM10 and ADAM17 inhibitor) or Marimastat (broad-spectrum metalloprotease inhibitor) or left untreated for 30 min at 37°C. Afterwards, HKLM (10^8 cells/ml) was added and the cells were stimulated for 24 h at 37°C and 5% CO_2. The supernatants were collected and centrifuged to remove remaining cells and cell debris.

Analysis of sIL-6R levels in the supernatants by ELISA revealed again low levels in the unstimulated sample but neither GI, nor GW or MM affected the basal sIL-6R levels. This hinted to alternative splicing as the responsible mechanism for the release of the basal sIL-6R from PBMCs. Treatment with HKLM resulted in an increase of sIL-6R, which was reduced again when PBMCs were incubated with HKLM together with one of the inhibitors. This pointed to ADAM10 as the responsible protease for sIL-6R proteolysis after TLR2 activation. As GI and MM treatment inhibited sIL-6R release even more effectively, ADAM17 seems to be involved here, too (Fig. 4.24 (A)). Therefore, it was concluded that sIL-6R is released from PBMCs by ADAM10 and ADAM17 upon TLR2-activation and that alternative splicing is rather not involved.

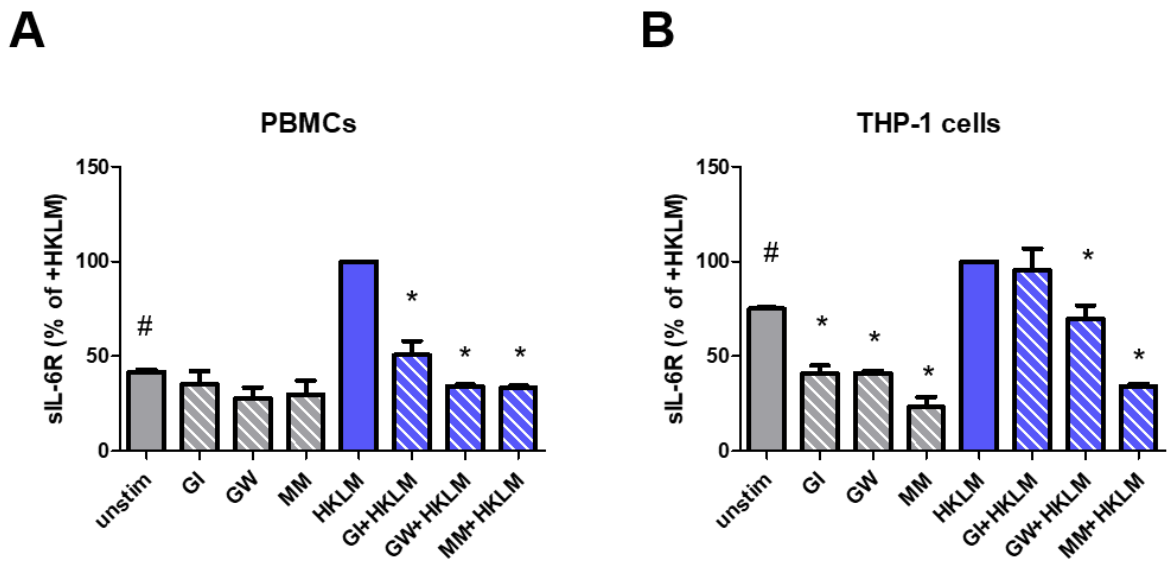

Figure 4.24: sIL-6R ELISA of supernatants collected from PBMCs or THP-1 cells after stimulation with different protease inhibitors. (A) PBMCs were isolated from plasma-free blood and $5x10^5$ PBMCs in 1 ml serum-free RPMI were pre-incubated with the different metalloprotease inhibitors GI, GW or Marimastat (MM) for 30 min at 37°C. Following, cells were stimulated with HKLM (10^8 cells/ml) or left untreated for 24 h at 37°C and 5% CO_2. The supernatants were collected, centrifuged and sIL-6R levels in the supernatants were determined by ELISA. Data shown are the mean ± SD from two independent experiments (n=3). "#" indicates a statistically significant difference ($p < 0.05$, one sample t-test) between unstimulated and HKLM-treated cells and "*" a statistically significant difference ($p < 0.01$, one-way ANOVA with Dunnett's Multiple Comparison Test) between HKLM-treated cells and HKLM-treated cells additionally pre-incubated with the three different metalloprotease inhibitors. **(B)** The above experiment was repeated using THP-1 cells resuspended in serum-free DMEM. Data shown are the mean ± SD from three independent experiments. "#" indicates a statistically significant difference ($p < 0.05$, one sample t-test) between unstimulated and HKLM-treated cells and "*" a statistically significant difference ($p < 0.01$, one-way ANOVA with Dunnett's Multiple Comparison Test) between either untreated or HKLM-treated cells and the respective cells additionally pre-incubated with the three different metalloprotease inhibitors.

To verify the obtained results, the above experiment was repeated using THP-1 cells, which is a monocytic cell line. In contrast to unstimulated PBMCs, the release of sIL-6R contributing to the

basal sIL-6R levels could be reduced by addition of the inhibitors GI, GW and MM in unstimulated THP-1 cells. This confirmed the involvement of ADAM10 in the release of basal sIL-6R which was described before [96, 97]. GW and MM, but not GI, inhibited sIL-6R release after TLR2 activation by HKLM stimulation which indicates that ADAM17 is the responsible protease in THP-1 cells (Fig. 4.24 (B)). In both settings, ADAM17 was identified to be involved in the generation of sIL-6R upon HKLM-treatment. The role of ADAM10, however, was inconsistent in both cell types which might be a result of the origin of both cell-types. Whereas PBMCs were freshly isolated and contain primary cells, THP-1 cells are an established, immortalized cell-line. This might contribute to the different findings regarding ADAM10 in PBMCs and THP-1 cells. The same might account for the generation of the constitutively released sIL-6R.

To verify that proteolysis and not differential splicing is the major mechanism in sIL-6R generation after HKLM-treatment, a flow-cytometry based approach using THP-1 cells was conducted. The cells were pre-incubated for 30 min at 37°C with GI, GW, MM or DMSO as control in serum-free DMEM before cell-surface IL-6R was stained for 1 h at 4°C. Following, the cells were resuspended in serum-free DMEM and GI, GW, MM and DMSO were added again. Additionally, the cells were stimulated with HKLM (10^8 cells/ml) or not. After incubation for 24 h at 37°C, the cells were washed and remaining cell-surface IL-6R was stained with an APC-conjugated α-mouse-antibody for 1 h at 4°C in the dark. Finally, the cells were analyzed by flow cytometry.

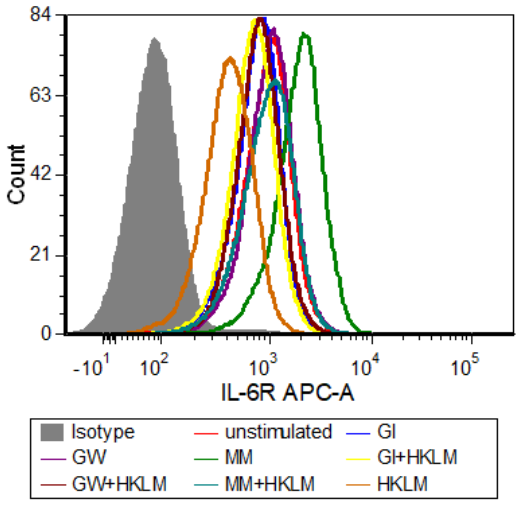

Figure 4.25: Flow cytometry analysis of THP-1 cells after incubation with different metalloprotease inhibitors and stimulation with the TLR2 agonist. THP-1 cells were pre-incubated for 30 min at 37°C with GI, GW, MM or DMSO as control in serum-free DMEM. The cells were stained for 1 h at 4°C using the IL-6R specific 4-11 antibody before being incubated in serum-free DMEM together with GI, GW, MM or DMSO. Additionally, HKLM (10^8 cells/ml) was added or not. After incubation for 24 h at 37°C, the cells were washed and stained with an APC-conjugated α-mouse-antibody for 1 h at 4°C in the dark. Finally, the cells were analyzed by flow cytometry.

In comparison to the unstimulated cells, stimulation of THP-1 cells with HKLM led to a reduction of surface IL-6R indicating that treatment with HKLM led to release of sIL-6R from the cell-surface. This release could be reduced by treatment with the metalloprotease inhibitors together with HKLM as seen by increased APC-fluorescence compared to the HKLM-treated sample. This leads

to the conclusion that, indeed, sIL-6R is generated by proteolytic cleavage by ADAM10 and ADAM17 and not by alternative splicing. Additionally, treatment with MM alone showed the highest amount of surface IL-6R confirming that the basal sIL-6R levels are caused by a metalloprotease that can be inhibited by MM and also not by alternative splicing (Fig. 4.25).

4.2.5 The Extracellular-signal Regulated Kinase (ERK) cascade differentially regulates IL-6 and sIL-6R release from PBMCs and monocytes

Stimulation of TLR2 leads to the activation of different downstream signaling pathways, especially NF-κB [239], p38/MAPK [261] and ERK [262]. It was of further interest whether one of these pathways is also involved in ADAM17-induced sIL-6R generation and IL-6 release from PBMCs and monocytes upon HKLM-stimulation. Therefore, PBMCs were isolated from serum-free blood, resuspended in serum-free RPMI and starved for 2 h at 37°C and 5% CO_2 before HKLM was added to the cells for different time points (0, 15, 30, 60 min). Finally, the cells were harvested and analyzed by immunoblotting using antibodies specific for phosphorylated ERK, phosphorylated p38 or phosphorylated p65, a subunit of NF-κB. As loading controls, antibodies directed against pan-ERK, pan-p38, pan-p65, Actinin and GAPDH were used. Analysis of ERK activation revealed an increase in phosphorylation at 15 min of incubation which declined over time again. As the loading controls showed equal loading for all samples this increase in ERK phosphorylation seems to be a result of the activation of TLR2 (Fig. 4.26 (A)). In contrast, no phosphorylation of p38 could be detected although the loading controls revealed that protein was loaded onto the gel (Fig. 4.26 (B)). Therefore, it was concluded that p38 is not activated upon TLR2 stimulation. Analysis of p65 activation showed a small increase in phosphorylation after 60 min, although it should be noticed that also in the GAPDH loading control a little more protein was detected at 60 min, which indicates that the increase in p65 phosphorylation might be due to unequal loading. (Fig. 4.26 (C)).

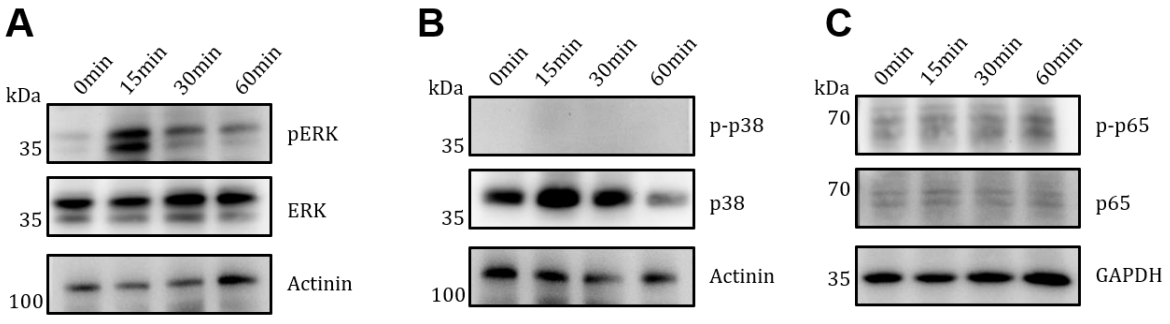

Figure 4.26: Western Blot analysis of PBMCs after stimulation with the TLR2 agonist. PBMCs were isolated from plasma-free blood, resuspended in serum-free RPMI and were starved for 2 h. The cells were stimulated with the TLR2 agonist HKLM (10^8 cells/ml) for 0, 15, 30 and 60 min and lysed afterwards. The indicated proteins were analyzed after incubation with specific antibodies. One experiment of three independently performed experiments is shown.

From this it was concluded that ERK signaling upon TLR2 activation could play a role in sIL-6R and IL-6 release whereas the p38/MAPK and NF-κB pathways seem not to be involved.

Another approach was used to verify the involvement of intracellular signaling cascades in sIL-6R and IL-6 release. PBMCs were isolated from plasma-free blood, resuspended in serum-free RPMI and pre-incubated with different signaling cascade inhibitors including Src-I (targeting the kinase Src: 10 µM), Ly294 (PI3K; 4 µM), tofacitinib (Jak1/2; 3 µM), U0126 (ERK; 10 µM), rapamycin (mTOR; 500 ng/ml), SB203580 (p38/MAPK; 10 µM) and BisI (targeting PKC; 500 nM) for 90 min at 37°C. Following, HKLM (10^8 cells/ml) was added and the cells were stimulated for 24 hours at 37°C and 5% CO_2. The supernatants were collected, centrifuged and sIL-6R and IL-6 amounts were determined by ELISA. Addition of HKLM led to an increase in sIL-6R as compared to unstimulated cells but this increase was not influenced by most of the inhibitors. As before, p38/MAPK and also PKC signaling are not involved in the sIL-6R release upon HKLM-treatment although PKC and p38/MAPK are two well-described pathways for ADAM17 activation [11, 12]. Inhibition of the ERK signaling cascade by application of U0126, in contrast, even increased sIL-6R generation from PBMCs (Fig. 4.27 (A)) confirming the involvement of ERK signaling in the release of sIL-6R after TLR2 activation.

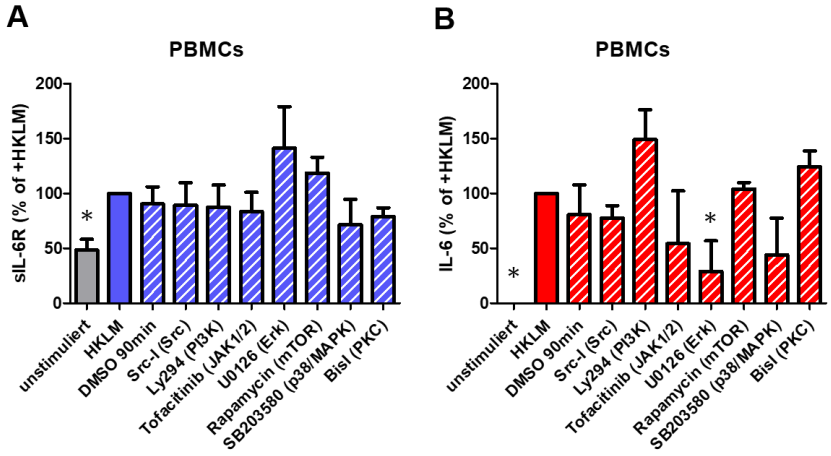

Figure 4.27: sIL-6R and IL-6 ELISA of supernatants from PBMCs after stimulation with different signaling pathway inhibitors. PBMCs were isolated from plasma-free blood and were pre-incubated with the signaling pathway inhibitors Src-I (targeting the kinase Src; 10 µM), Ly294 (PI3K; 4 µM), tofacitinib (Jak1/2; 3 µM), U0126 (ERK; 10 µM), rapamycin (mTOR; 500 ng/ml), SB203580 (p38/MAPK; 10 µM) and BisI (targeting PKC; 500 nM) for 90 min. Afterwards, TLR2 agonist HKLM (10^8 cells/ml) was added and the cells were incubated for further 24 h. The supernatants were collected and the amounts of sIL-6R **(A)** and IL-6 **(B)** were determined via ELISA. Data shown are the mean ± SEM from four independent experiments (n=8). Data were analyzed by one-way ANOVA followed by Dunnett's Multiple Comparison test. Statistical significance compared to the HKLM-treated cells is indicated.

IL-6 secretion was also analyzed using the same supernatants as above. As before, no IL-6 could be detected in the supernatant collected from unstimulated cells, while treatment with HKLM lead to the secretion of IL-6 from PBMCs. Addition of inhibitors for Src, mTOR and PKC signaling cascades did not influence IL-6 secretion whereas PI3K inhibition rather enhanced IL-6 secretion. Incubation with inhibitors for JAK1/2, p38/MAPK and ERK, in contrast, lead to a reduction of IL-6 secretion but only ERK inhibition showed statistically significant decreased IL-6 levels (Fig. 4.27 (B)) again hinting for an involvement of ERK signaling in sIL-6R and IL-6 release following TLR2 activation.

To confirm our results obtained from PBMCs, we performed the same experiment with isolated primary human monocytes. For the sIL-6R generation, the same results were seen in monocytes as for PBMCs, including the increase in sIL-6R levels upon ERK inhibition (Fig. 4.28 (A)). The influence of the different inhibitors on IL-6 secretion differed a little in both cell types. While Src and PKC inhibition did not influence IL-6 secretion from PBMCs, Src inhibition rather decreased secretion from monocytes and PKC inhibition increased IL-6 levels. As before in PBMCs, mTOR inhibition did not alter IL-6 release whereas PI3K inhibition lead to an increase in IL-6 levels in monocytes. Additionally, the decrease in IL-6 secretion resulting from JAK1/2, p38/MAPK and ERK inhibition were the same for PBMCs and monocytes (Fig. 4.28 (B)).

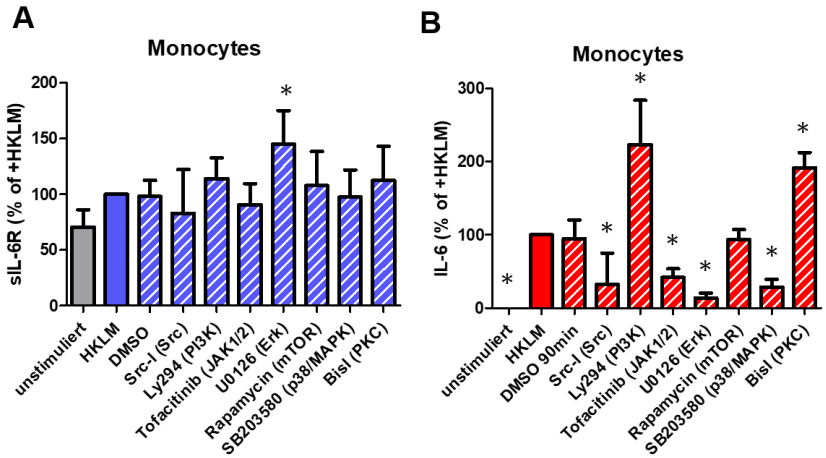

Figure 4.28: sIL-6R and IL-6 ELISA of supernatants from monocytes after stimulation with different signaling pathway inhibitors. Monocytes were isolated from PBMCs and were pre incubated with the signaling pathway inhibitors Src-I (targeting the kinase Src; 10 µM), Ly294 (PI3K; 4 µM), tofacitinib (Jak1/2; 3 µM), U0126 (ERK; 10 µM), rapamycin (mTOR; 500 ng/ml), SB203580 (p38/MAPK; 10 µM) and BisI (targeting PKC; 500 nM) for 90 min. Afterwards, TLR2 agonist HKLM (10^8 cells/ml) was added and the cells were incubated for further 24 h. The supernatants were collected and the amounts of sIL-6R **(A)** and IL-6 **(B)** were determined via ELISA. Data shown are the mean ± SEM from four independent experiments (n=8). Data were analyzed by one-way ANOVA followed by Dunnett's Multiple Comparison test. Statistical significance compared to the HKLM-treated cells is indicated.

These results confirm the involvement of the ERK signaling cascade in ADAM17-induced sIL-6R release and IL-6 secretion after TLR2 activation upon HKLM stimulation. It was shown, though, that ERK differentially regulates both processes as inhibition of the ERK signaling cascade resulted in a decrease of IL-6 secretion whereas sIL-6R generation was increased.

Analysis of endogenous stimuli for sIL-6R in humans and the involvement of TLR4 or other TLRs revealed that TLR4 does not contribute to the release of sIL-6R from PBMCs but rather activation of TLR2 is involved. Furthermore, it was revealed that monocytes, which simultaneously express the IL-6R and TLR2 at the cell-surface, are the major source of sIL-6R upon TLR2 activation. The sIL-6R generation upon HKLM stimulation was induced by the metalloproteases ADAM10 and ADAM17 and not by alternative splicing. Finally, analysis of down-stream signaling cascades activated upon TLR2-activation revealed phosphorylation of ERK and to a lesser extent p65 but not p38. Incubation of monocytes with different pathway inhibitors revealed again an

involvement of the ERK signaling cascade which seems to regulate the release of IL-6 and sIL-6R differentially.

4.3 Identification of Cathepsin S as a novel protease capable of cleaving the membrane-bound Interleukin-6 receptor

In the above described project, we focused on the identification of bacterial or viral stimuli leading to the release of ADAM17 in humans, the therein involved Toll-like receptor and the proteases leading to the generation of sIL-6R. In the following, we will not focus on the release of sIL-6R upon bacterial or viral stimuli, but we try to identify a protease involved in the generation of basal sIL-6R levels.

Previous work showed that the majority of sIL-6R in the human circulation is released via proteolysis, and only about 15% are generated by differential splicing [93]. The cleavage site leading to the generation of sIL-6R was identified to lie between proline355 and valine356, a cleavage site at which ADAM17 preferentially cleaves [102], leading to the conclusion that ADAM17 must be the main protease involved in sIL-6R generation in humans. Analysis of samples taken from an ADAM17-deficient patient demonstrated that this was only partially true. Isolated PBMCs from the patient, his unaffected mother and healthy controls were treated with PMA and ionomycin, which activates ADAM17-mediated shedding, and sIL-6R was measured. As expected, an increase in sIL-6R could be seen for the mother´s sample and the healthy control samples after PMA stimulation, but no sIL-6R generation was induced in the patient sample. This confirms a major role of ADAM17 in induced IL-6R shedding. Surprisingly, however, analysis of the sIL-6R levels in the serum of the ADAM17-deficient person revealed no difference in comparison to the healthy controls (unpublished data). sIL-6R levels were also unaffected in ADAM17-deficient mice [97, 100]. From this it was concluded that ADAM17 must play a role in the generation of sIL-6R after stimulation, but it seems not be involved in the constitutive release of sIL-6R. As also ADAM10, a protease using the same cleavage site as ADAM17, was excluded to contribute to the basal sIL-6R levels [100], a yet unidentified protease must be responsible for the constitutive release of sIL-6R.

4.3.1 Cathepsin S cleaves IL-6R peptides in an IL-6R cleavage assay

To identify the protease(s) that are responsible for the generation of the basal sIL-6R levels in humans, a MEROPS database search for proteases, known to cleave between a proline and a valine residue, was run which gave a list of 14 possible proteases, also including ADAM17 and ADAM10 (Table 1).

Table 1: A list of possible candidate proteases. The MEROPS database was searched for proteases that preferentially cleave proteins between the amino-acids proline and valine. The names and the chromosomal localization are depicted in the table.

Chromosome	Gene	Start	End
1	CTSS	150730196	150765957
2	ADAM17	9488486	9555792
2	DPP4	161992241	162074542
3	MME (≙ MMP-12)	155024124	155183729
8	CPA6	67422125	67746345
11	MMP-3	102835801	102843803
11	MMP-7	102520508	102530753
11	MMP-13	102942995	102955734
11	PRCP	82823502	82970584
14	MMP-14	22836557	22849027
15	ADAM10	58588807	58749978
15	DPP8	65442463	65517704
16	MMP-2	55389700	55506691
20	MMP-9	46008908	46016561

These proteases as recombinant proteins were used in a peptide cleavage assay to determine their ability to cleave a peptide corresponding to a part of the IL-6R stalk containing the proline355/valine356 cleavage site. Three different quenched fluorogenic peptides were used that contain either the proline/valine cleavage site ([mca]-ATSLPVQDSS[K-dnp] (IL-6R_PVQD)), the proline/valine cleavage site together with the Asp358Ala SNP rs2228145 which leads to enhanced IL-6R cleavage ([mca]-ATSLPVQASS[K-dnp] (IL-6R_PVQA)) [95] or a mutated cleavage site which blocks IL-6R cleavage ([mca]-ATSLPGQDSS[K-dnp] (IL-6R_PGQD)) [253].

10 µM of the peptides were incubated together with 10 ng or 100 ng of the candidate proteases in a total volume of 100 µl in PBS. Cleavage of the peptides by the protease was determined by measurement of the fluorescence at λem = 405 nm and λex = 320 nm at 37°C with a spectrophotometer every 30 sec for 120 min. As a control, the experiment was also performed with the protease ADAM17 together with a peptide for its known substrate TNF-α.

As shown in Fig. 4.29 (A), TNF-α was efficiently cleaved by ADAM17, indicated by an increase in fluorescence. Analysis of the cleavage capacity of the IL-6R peptides by the candidate proteases revealed that only ADAM17 and cathepsin S could cleave the IL-6R_PVQD and IL-6R_PVQA peptides whereas the latter one was cleaved more efficiently. As expected, none of the proteases was able to cleave the IL-6R_PGQD peptide (Fig. 4.29 (B)). This indicates that cathepsin S could be a protease which is responsible for the generation of the basal sIL-6R levels.

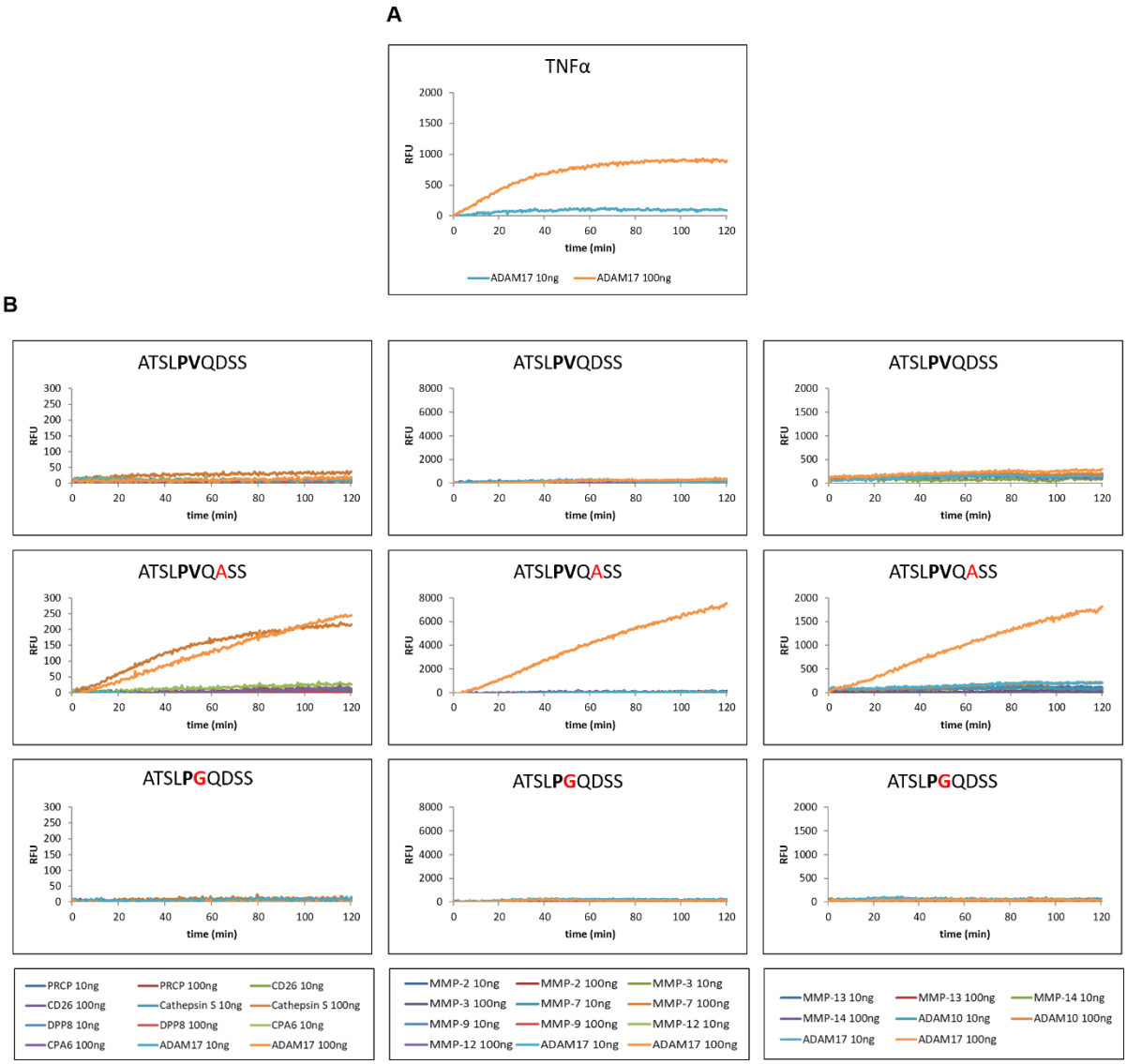

Figure 4.29: Protease cleavage assay of different peptides by the possible candidate proteases. 10 µM of the three different quenched fluorogenic peptides [mca]-ATSLPVQDSS[K-dnp], [mca]-ATSLPVQASS[K-dnp] or [mca]-ATSLPGQDSS[K-dnp] were incubated together with 10 ng or 100 ng of the different candidate proteases in a total volume of 100 µl PBS **(B).** As a control, the experiment was also performed with the protease ADAM17 together with a peptide for its known substrate TNF-α **(A).** Fluorescence was measured at λem = 405 nm and λex = 320 nm at 37°C with a spectrophotometer (Tecan) every 30 sec for 120 min. Relative fluorescence units (RFU) were calculated by subtracting the measured fluorescence from time-point 0min from the other time-points.

4.3.2 Cathepsin S cleaves the IL-6R *in vitro*

To verify the above results that cathepsin S can cleave the IL-6R, HEK293 wt cells were transfected with pN1-eGFP, pcDNA3.1-IL-6R, pcDNA3.1-IL-6R and pN1-eGFP, pcDNA3.1-mCTSS and pN1-eGFP or pcDNA3.1-IL-6R and pcDNA3.1-mCTSS. Two days after transfection the medium was replaced by fresh serum-free DMEM and the cells were incubated for 24 h at 37°C. The sample transfected with pcDNA3.1-IL-6R only was used as positive control and was therefore treated with PMA (2 µM) for 2 h at 37°C to induce ADAM17-mediated shedding of the IL-6R. The collected supernatants were centrifuged and 1 ml per sample was used for protein precipitation by trichloroacetic acid (TCA). Additionally, the cells were collected and lysed. The precipitated

proteins and the cell lysates were loaded onto SDS gels and analyzed by immunoblotting using an anti-IL-6R antibody and anti-GAPDH antibody as loading control. In all the samples where the cells were transfected with IL-6R, IL-6R could be detected in the lysates. In contrast, sIL-6R could only be detected in the supernatant of the PMA-treated positive control and in the lane where cells transfected with pcDNA3.1-IL-6R together with pcDNA3.1-mCTSS was loaded. Surprisingly, the sIL-6R generated by CTSS showed a reduced molecular weight (about 55 kDa) when compared to the PMA-induced sIL-6R (about 70 kDa) (Fig. 4.30 lanes 1-5) indicating that a different cleavage site is used by cathepsin S.

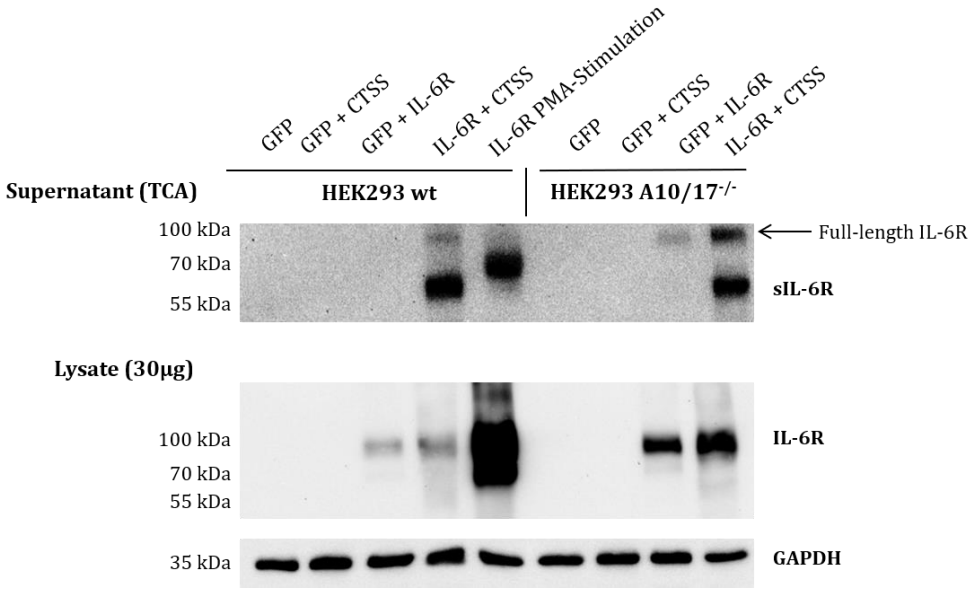

Figure 4.30: Western Blot analysis of lysates and TCA-precipitated supernatants from HEK293 wt and HEK293 A10/17$^{-/-}$ cells. HEK293 wt and HEK293 A10/17$^{-/-}$ cells were transfected with plasmids coding for GFP, GFP and CTSS, GFP and IL-6R or IL-6R and CTSS. Two days after the transfection, the medium was exchanged with 5 ml fresh serum-free DMEM and the cells were incubated for 24 h at 37°C before supernatants and cells were collected. The supernatants were used for protein precipitation by TCA and the cells were lysed. Additionally, HEK wt cells were transfected with IL-6R alone and stimulated with PMA (2 µM) for 2 h at 37°C. Cells and supernatants were treated as above. Precipitated supernatants and lysates were analyzed by immunoblotting using antibodies against (s)IL-6R (4-11) or GAPDH.

As the HEK293 wt cells express ADAM10 and ADAM17 endogenously it was possible that the sIL-6R present in the supernatants arose by ADAM-mediated cleavage and not by CTSS-mediated cleavage. To rule out this possibility, HEK293 cells were used where ADAM10 and ADAM17 have been knocked-out by CRISPR/Cas (HEK293 A10/17$^{-/-}$) [253]. The experiment was performed as described above. Analysis of the samples collected from HEK293 A10/17$^{-/-}$ cells revealed the same results as with the HEK293 wt cells (Fig. 4.30 lanes 6-9). This demonstrated that the sIL-6R found in the samples collected from cells overexpressing the IL-6R and CTSS was generated by CTSS-mediated cleavage and not by ADAM10 or ADAM17.This indicates that the IL-6R can be cleaved by cathepsin S. As the sIL-6R generated by CTSS is smaller than the one generated by ADAM17 it is quite unlikely, though, that CTSS is the searched protease which cleaves the IL-6R between proline355 and valine356 and thereby contributes to the basal sIL-6R levels.

In both experiments an additional band of about 100 kDa could be observed in the precipitates generated from supernatants of HEK293 cells transfected with IL-6R which might resemble full-length IL-6R possibly located on microvesicles that have been released into the supernatant. To confirm this, HEK293 A10/17$^{-/-}$ cells were co-transfected with either pcDNA3.1-IL-6R and pN1-eGFP or pcDNA3.1-IL-6R and pcDNA3.1-mCTSS. Two days after transfection, the medium was replaced by serum-free DMEM and the cells were incubated for an additional period of 24 h at 37°C. The supernatant was collected and 1 ml from each transfection was ultra-centrifuged for 1 h at 300,000 g and 4°C to remove possible microvesicles from the supernatant. Following, proteins from the ultra-centrifuged and not ultra-centrifuged samples were precipitated by TCA and analyzed by immunoblotting. Detection of the IL-6R in the not ultra-centrifuged supernatant from eGFP and IL-6R co-transfected cells revealed a band at about 100 kDa possibly resembling full-length IL-6R on microvesicles. The same band plus an additional band at about 55 kDa (sIL-6R) were detected in the not ultra-centrifuged supernatant from IL-6R and CTSS overexpressing cells. Lanes that were loaded with precipitated supernatants that have been ultra-centrifuged showed a loss of the 100 kDa band (Fig. 4.31) indicating that this band, indeed, resulted from full-length IL-6R possibly located on microvesicles and can be removed by ultra-centrifugation.

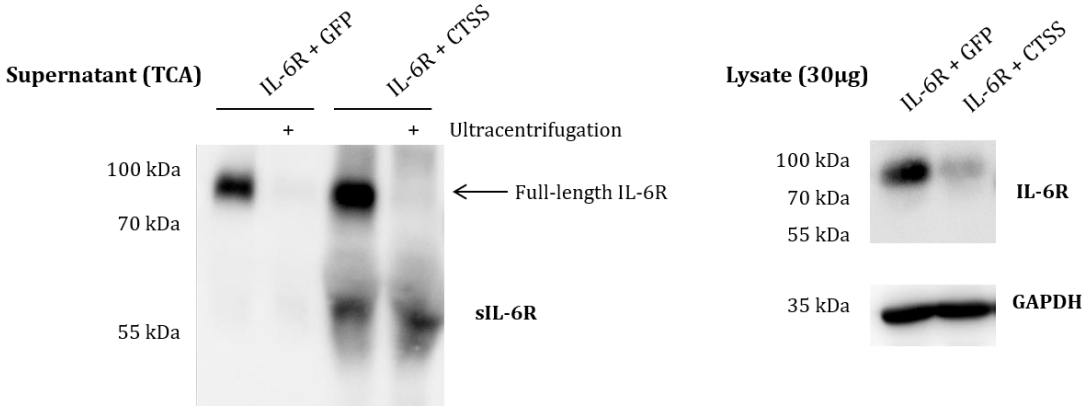

Figure 4.31: Western blot analysis of lysates and TCA-precipitated supernatants of HEK293 A10/17$^{-/-}$ cells. HEK293 A10/17$^{-/-}$ cells were transfected with IL-6R and GFP or IL-6R and CTSS. Two days after the transfection, the medium was exchanged with 5 ml fresh serum-free DMEM and the cells were incubated for another 24 h at 37°C before supernatants and cells were collected. One supernatant sample of each transfection was ultra-centrifuged for 1 h at 300,000 g and 4°C. The supernatants were used for protein precipitation by TCA and the cells were lysed. Cells and supernatants were treated as above. Precipitated supernatants and lysates were analyzed by Western blotting using antibodies against (s)IL-6R (4-11) or GAPDH.

To avoid any influence on the following experiments that may be caused by the IL-6R located on microvesicles, collected supernatants were always ultra-centrifuged prior to TCA precipitation, ELISA analysis or proliferation assays if not declared otherwise.

4.3.3 The sIL-6R generated by cathepsin S is biologically active

Following the identification of cathepsin S as a protease capable of cleaving the IL-6R, the biological activity of the generated sIL-6R was assessed. Therefore, HEK293 wt cells were transfected with pN1-eGFP or pcDNA3.1-IL-6R and HEK293 A10/17$^{-/-}$ cells were transfected as

before. Two days after transfection the medium was replaced by fresh serum-free DMEM and the cells were incubated for 24 h at 37°C. One sample of IL-6R transfected HEK293 wt cells was incubated with PMA for 2 h at 37°C to induce ADAM17-mediated IL-6R cleavage. For each transfection supernatants were collected and ultra-centrifuged for 1 h at 4°C and 300,000 g to remove microvesicles. The presence of sIL-6R in the supernatants was analyzed by ELISA (Fig. 4.32 (A)).

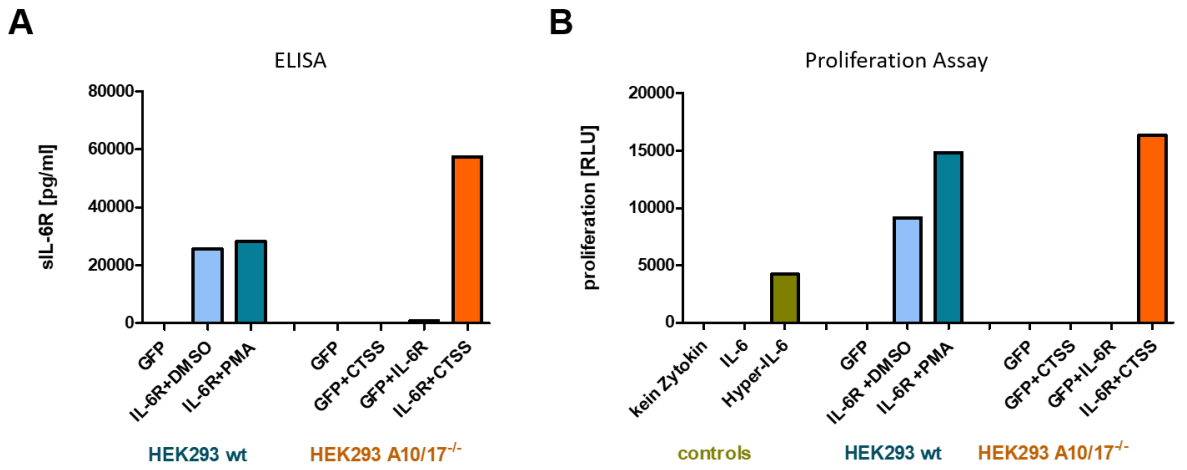

Figure 4.32: sIL-6R ELISA and proliferation assay using supernatants collected from HEK293 wt or HEK293 A10/17$^{-/-}$ cells. (A) (B) HEK293 wt cells were transfected with plasmids encoding GFP or IL-6R whereas HEK293 A10/17$^{-/-}$ cells were transfected with plasmids coding for GFP, GFP and CTSS, GFP and IL-6R or IL-6R and CTSS. Two days after the transfection, the medium was replaced by 5 ml fresh serum-free DMEM and the cells were incubated for 24 h at 37°C before supernatants were collected. Additionally, HEK293 wt cells were transfected with IL-6R alone and stimulated with PMA (2 µM) for 2 h at 37°C and supernatants were also collected. **(A)** sIL-6R levels in the supernatants were determined by ELISA. **(B)** A cell viability assay (proliferation assay) was performed using Ba/F3-gp130 cells and the collected supernatants. 5000 Ba/F3-gp130 cells were stimulated with 50 µl conditioned medium from the transfected HEK293 wt and HEK293 A10/17$^{-/-}$ cells together with IL-6 (25 ng/ml) or Hyper-IL-6 (10 ng/ml). DMEM+/+ was added to a total volume of 100 µl and the cells were incubated for 48 h at 37°C. 20 µl of Cell Titer Blue Viability Assay solution was added and fluorescence was measured at λem = 590 nm for one hour every 20 min.
One experiment from three independently performed experiments is shown.

As expected, sIL-6R could be detected in HEK293 wt cells transfected with the IL-6R and treated with PMA which induces ADAM17-mediated cleavage. sIL-6R could also be detected in the DMSO-treated sample which was probably generated by ADAM10-mediated constitutive shedding as this protease was identified to be involved in constitutive sIL-6R release before [96, 97]. DMSO-treated samples and PMA-treated samples did not differ much in their amount of sIL-6R found in the supernatant, which might be due to the 24 h incubation of the DMSO-treated cells. During this time constitutive shedding mediated by ADAM10 seems to be as efficient as PMA-induced shedding for two hours. Additionally to the sIL-6R detected in the supernatants collected from the HEK293 wt cells, sIL-6R could also be observed in HEK293 A10/17$^{-/-}$ cells that were transfected with IL-6R and CTSS but not in the supernatants collected from HEK293 A10/17$^{-/-}$ cells transfected with GFP and CTSS and only little amounts were detected when the cells were transfected with GFP and IL-6R which was probably released by constitutive shedding induced by a protease different than ADAM10 or ADAM17 as these are knocked-out in the used cells, or the

sIL-6R was generated by alternative splicing. These findings in the HEK293 A10/17$^{-/-}$ cells verified the ability of cathepsin S to cleave the IL-6R.

In order to analyze whether the sIL-6R generated by cathepsin S was biologically active the same supernatants as above were used in a cell viability assay which was performed using Ba/F3-gp130 cells. These cells overexpress the gp130 receptor and can only proliferate via trans-signaling meaning in the presence of sIL-6R and IL-6. 5000 Ba/F3-gp130 cells in 50 µl DMEM were stimulated with 50 µl conditioned medium from the transfected HEK293 wt and HEK293 A10/17$^{-/-}$ cells together with IL-6 (25 ng/ml) in a total volume of 100 µl. As controls, Ba/F3-gp130 cells in 100 µl DMEM were incubated either with IL-6 (25 ng/ml) or Hyper-IL-6 (10 ng/ml), a designer protein consisting of sIL-6R linked to IL-6 via a flexible linker [251], or were left unstimulated. The cells were incubated for 48 h at 37°C and proliferation of the Ba/F3-gp130 cells was determined by addition of 20 µl of Cell Titer Blue Viability Assay solution and fluorescence measurement at λem = 590 nm for one hour every 20 min. An increase in fluorescence indicated cell proliferation mediated by sIL-6R present in the supernatant. As shown in Fig. 4.32 (B), Ba/F3-gp130 cells were able to proliferate when stimulated with Hyper-IL-6 as this designer protein can induce trans-signaling via gp130. In contrast, cells that were incubated only with IL-6 did not proliferate as the cytokine needs to bind either the membrane-bound IL-6R or the sIL-6R to induce proliferation via binding to gp130 but in this setting neither the membrane-bound IL-6R nor sIL-6R was present. As expected, also incubation with supernatants from PMA-stimulated HEK293 wt cells induced proliferation. sIL-6R present in these samples is generated by ADAM17 and is known to induce proliferation of Ba/F3-gp130 cells by binding IL-6 and inducing homodimerization of gp130. As sIL-6R could also be detected via ELISA in the supernatants from DMSO-treated HEK293 wt cells, Ba/F3-gp130 cells incubated with these supernatants were also able to proliferate. Analysis of the supernatants collected from HEK293 A10/17$^{-/-}$ cells revealed proliferation of Ba/F3-gp130 cells only when the cells have been transfected with IL-6R and CTSS as only in these supernatants sIL-6R was present. This demonstrates that the sIL-6R generated by CTSS-mediated cleavage is indeed biologically active indicating that it must be able to bind IL-6 and together induce homodimerization of gp130 and subsequent activation of different signaling cascades leading to proliferation of the Ba/F3-gp130 cells.

4.3.4 Cleavage of the IL-6R by Cathepsin S *in vitro* occurs upstream of the previously identified proline/valine cleavage site in humans

We found that cathepsin S can cleave the IL-6R and that the generated sIL-6R is also biologically active. However, the sIL-6R generated by cathepsin S was observed to be smaller than the sIL-6R generated by ADAM17 indicating that cathepsin S might use a different cleavage site which lies

upstream of the N350 glycosylation site. In the following, we aim to identify the region in which cathepsin S cleaves the IL-6R.

In a previous work, sera from different healthy individuals was collected, sIL-6R was isolated and the cleavage site was determined via mass spectrometry. This approach revealed that the IL-6R is cleaved between proline355 and valine356 [93], which was further analyzed by using plasmids with different deletions in the IL-6R stalk region [263]. The candidate protease(s) involved in the generation of the basal sIL-6R levels should, therefore, also cleave the IL-6R between proline355 and valine356. As we already observed that cathepsin S very likely uses a different cleavage site we used the IL-6R deletion variants to identify the region that contains the cleavage site used by cathepsin S. Figure 4.33 gives an overview of the IL-6R stalk deletion variants used in the following experiment.

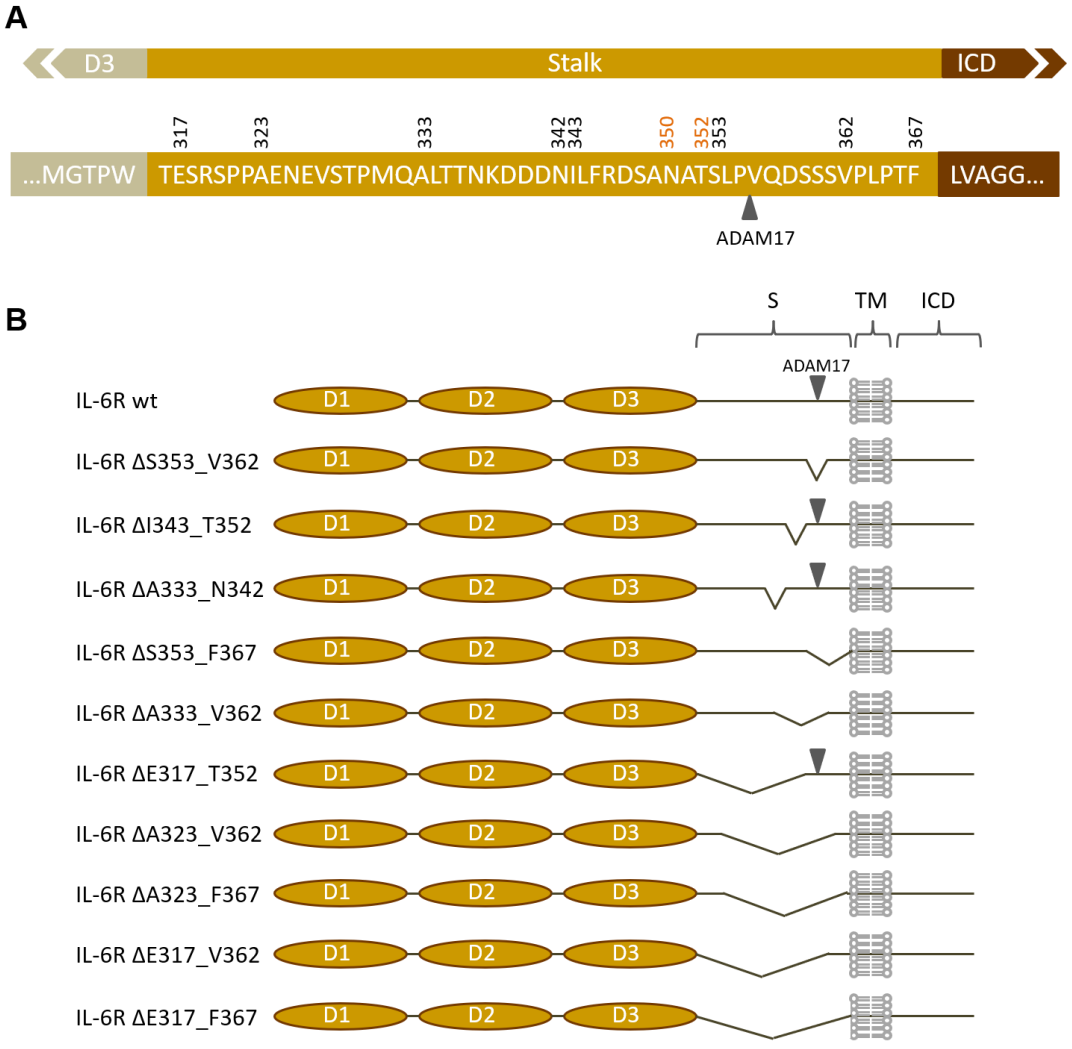

Figure 4.33: Schematic overview of the IL-6R stalk deletion variants. (A) Depicted is the IL-6R stalk region showing the amino-acid sequence from T316 to F367. Additionally, the last amino-acid residues belonging to the D3 domain and the first amino-acid residues belonging to the transmembrane domain (TM) are shown. Numbers above the stalk region indicate amino-acids where deletions start or end. Numbers in read highlight glycosylation sites. The ADAM17 cleavage site between P355/V356 is marked by an arrow. **(B)** The three extracellular domains D1, D2 and D3, the stalk region, the transmembrane domain (TM) and the intracellular domain (ICD) are shown. The arrow marks the ADAM17 cleavage site. Kinks highlight the deletions introduced into the IL-6R stalk. Written in front of each deletion variant is the range of the deleted amino-acid residues. This figure is adapted from Baran et al., JBC, 2013.

In order to determine the cleavage site of the IL-6R used by cathepsin S, HEK293 A10/17$^{-/-}$ cells were co-transfected with cathepsin S or GFP together with the different IL-6R variants containing deletions in the stalk region. The cells were incubated for 24 h at 37°C, two 1 ml aliquots of supernatant were collected from each transfection and one sample was ultra-centrifuged. Following, both samples were TCA precipitated and analyzed by immunoblotting using an α-IL-6R antibody to detect sIL-6R, and an antibody against GAPDH which was used as loading control.

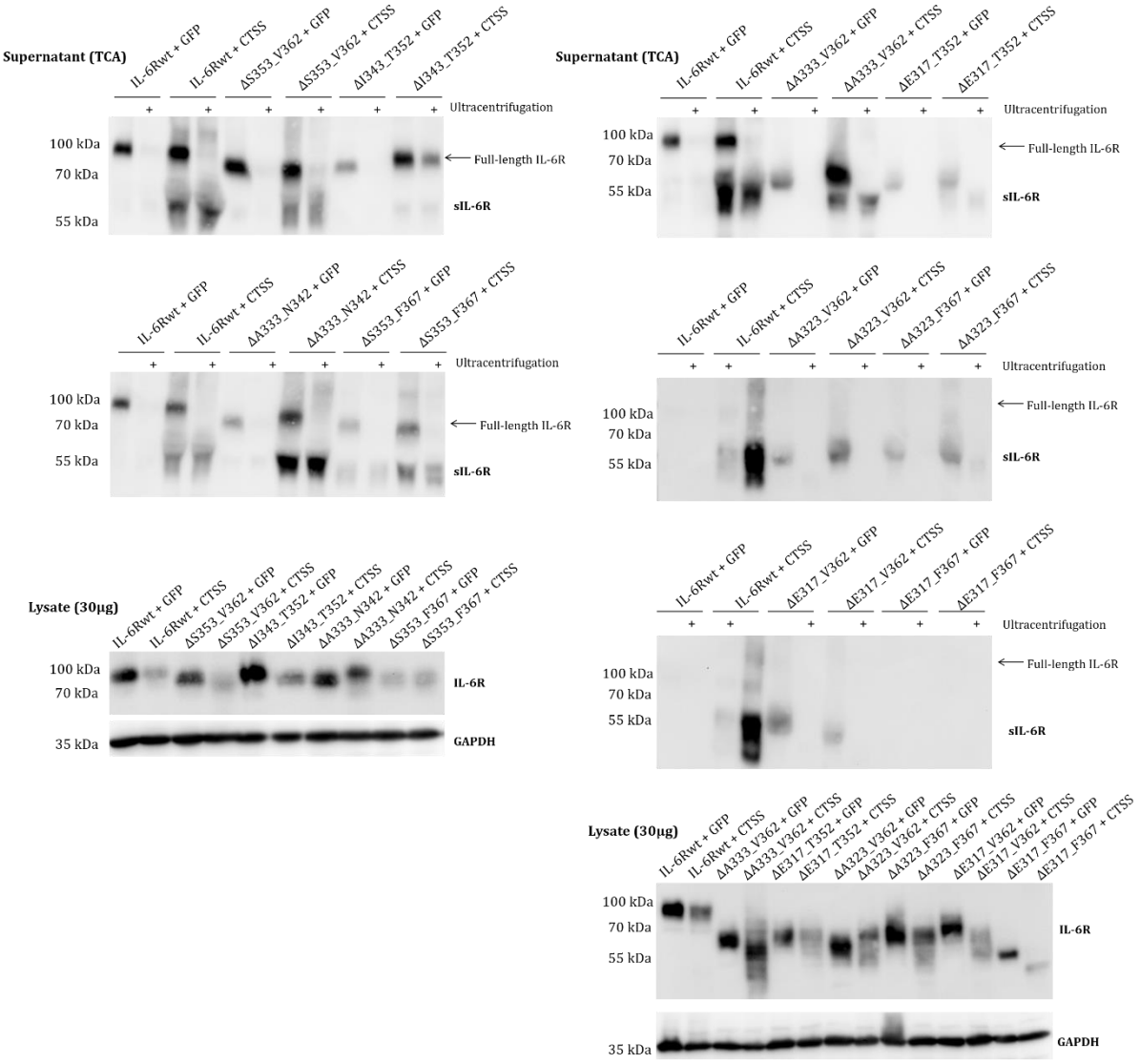

Figure 4.34: Western Blot analysis of lysates and TCA-precipitated supernatants from HEK293 A10/17$^{-/-}$ cells transfected with IL-6R deletion variants. HEK293 A10/17$^{-/-}$ cells were co-transfected with cathepsin S or GFP together with the different IL-6R deletion variants depicted above. Two days after transfection the medium was exchanged with fresh serum-free DMEM and the cells were incubated for 24 h at 37°C. Two 1 ml aliquots were collected from each transfection and one sample was ultra-centrifuged. Following, both supernatant samples were used for TCA protein precipitation before immunoblotting of lysates and precipitates using IL-6R- and GAPDH-specific antibodies. One experiment from three individually performed experiments is shown.

As shown in Fig. 4.34, transfection with IL-6Rwt and cathepsin S led to the generation of sIL-6R as indicated by the band at around 55 kDa. This band did not appear when CTSS was co-transfected with GFP which verified our previous finding that cathepsin S is able to clave the IL-6R. Additionally, the band at around 100 kDa appeared again in the samples where the cells were

transfected with IL-6R or its deletion mutants and disappeared after ultra-centrifugation. The same results were obtained when the cells were transfected with CTSS or GFP together with IL-6RΔS353_V362, IL-6RΔA333_N342, IL-6RΔS353_F367 or IL-6RΔA333_V362, indicating that these regions do not contain the cleavage site used by cathepsin S. Surprisingly, deletion of the amino acid residues between S353_V362 did not alter the generation of sIL-6R although this deletion does not contain the proline/valine cleavage site that was identified to be used to generate sIL-6R in humans again hinting to another cleavage site used by cathepsin S to generate sIL-6R. In contrast, the IL-6R deletion mutants IL-6RΔI343_T352, IL-6RΔE317_T352, IL-6RΔA323_V362, IL-6RΔA323_F367, IL-6RΔE317_V362 and IL-6RΔE317_F367 abrogated cleavage by cathepsin S leading to the conclusion that the cleavage site used by cathepsin S is located in the region I343_T352 which is upstream of the determined proline355/valine356 cleavage site in the IL-6R stalk as all the deletion variants that were not cleaved showed a loss of at least the I343_T352 region. As the size of the sIL-6R generated by cathepsin S is smaller than the sIL-6R generated by ADAM17, the cleavage site used by cathepsin S must lie upstream of the N350 glycosylation sites. From this we can narrow down the region containing the cathepsin S cleavage site to I343_A349. The actual cleavage site in the IL-6R stalk used by cathepsin S must, of course, be determined by further experiments like mass-spectrometry or additional deletion or substitution variants.

The above results regarding the identification of the region in which cathepsin S cleaves the IL-6R were verified by ELISA (Fig. 4.35 (A)) and a Ba/F3-gp130 cell viability assay (Fig. 4.35 (B)) using the same supernatants as in the above experiment. sIL-6R could be measured by ELISA in the samples obtained from the cells transfected with cathepsin S and IL-6R wt or IL-6R deletion variants IL-6RΔS353_V362, IL-6RΔA333_N342, IL-6RΔS353_F367 or IL-6RΔA333_V362. These samples also led to cell proliferation of Ba/F3-gp130 cells when incubated together with IL-6. In contrast, samples from cells transfected with CTSS and the IL-6R deletion mutants IL-6RΔI343_T352, IL-6RΔE317_T352, IL-6RΔA323_V362, IL-6RΔA323_F367, IL-6RΔE317_V362 and IL-6RΔE317_F367 did only contain low levels or even no sIL-6R as determined by ELISA. Incubation of Ba/F3-gp130 cells together with IL-6 and conditioned supernatant from these cells showed reduced or even abrogated Ba/F3-gp130 cell proliferation.

These data indicate that cathepsin S uses a cleavage site that is different from the proline355/valine356 cleavage site that was identified to be used for the generation of sIL-6R in humans. It is most likely that cathepsin S cleaves the IL-6R in the stalk region I343_A349 but the actual cleavage site needs to be determined by mass spectrometry. Taken together, these results indicate that cathepsin S is not the protease involved in the generation of basal sIL-6R levels.

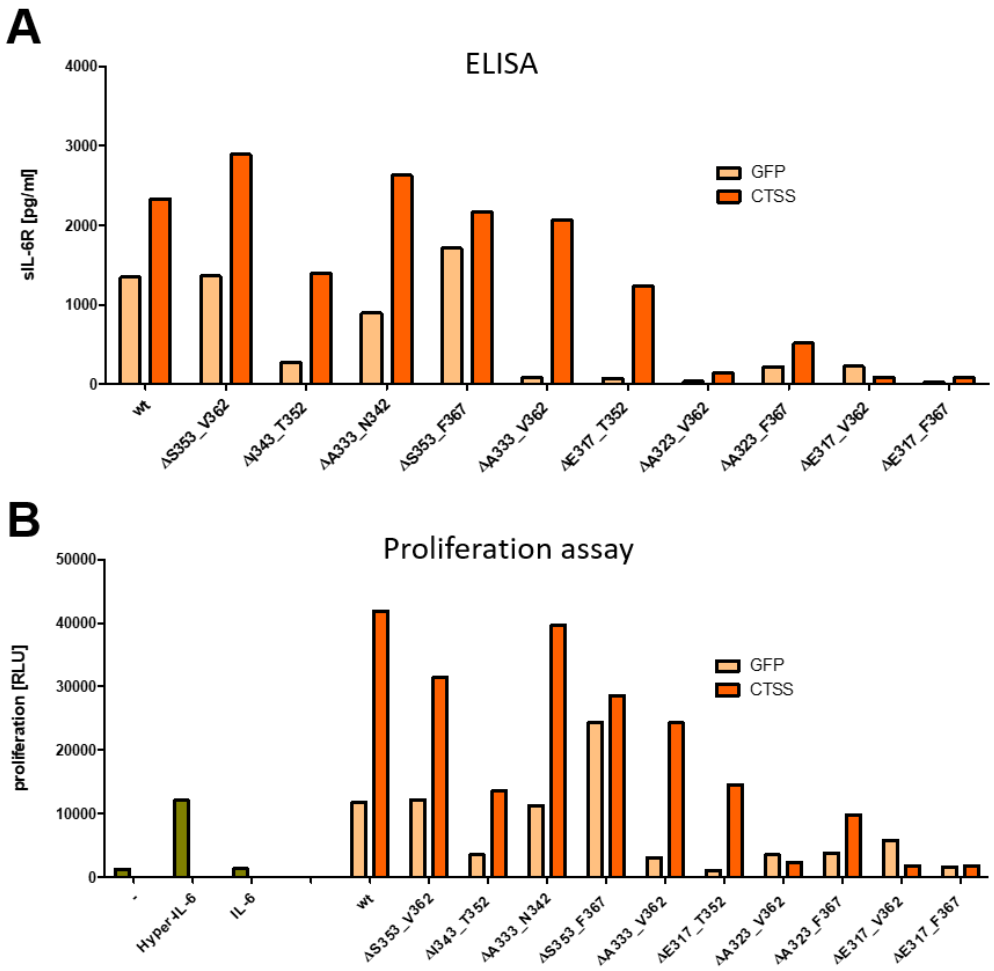

Figure 4.35: sIL-6R ELISA and proliferation assay using supernatants collected from HEK293 A10/17$^{-/-}$ cells transfected with IL-6R deletion variants. Supernatants collected from the above experiment were used to determine sIL-6R levels by ELISA **(A).** Additionally, a cell viability assay (proliferation assay) was performed using Ba/F3-gp130 cells that were incubated with these supernatants and stimulated with IL-6 (10 ng/ml). As a control, Ba/F3-gp130 cells were incubated without cytokine, with IL-6 alone or with Hyper-IL-6 (10 ng/ml) **(B).** One experiment from three individually performed experiments is shown.

4.3.5 Cathepsin S does not contribute to the constitutively generated sIL-6R in mice

The above experiments indicate that cathepsin S is most likely not involved in the generation of the basal sIL-6R levels. To verify this finding in a more *in vivo* setting, blood sera from cathepsin S knockout mice (*Ctss-/-)* and control wildtype mice were used and the sIL-6R levels were determined by ELISA (Fig. 4.36). The cathepsin S knockout did not significantly alter the generation of basal sIL-6R when compared to wt mice, supporting the conclusion from the above experiments that cathepsin S most likely does not contribute to the constitutively released sIL-6R. However, it could well be that loss of cathepsin S is compensated for by another protease leading to unchanged sIL-6R levels in mice sera.

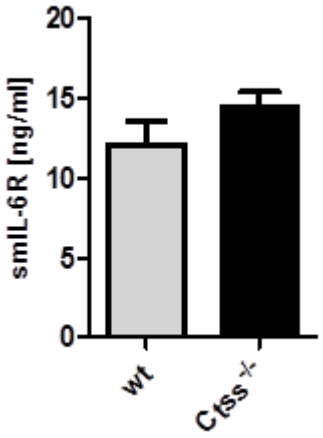

Figure 4.36: Determination of sIL-6R levels in serum collected from wt mice or *Ctss* knockout mice. Blood was collected from wt and *Ctss*-knockout mice and sera were isolated. The sIL-6R levels in these sera were analyzed by a murine (s)IL-6R ELISA. Blood sera were kindly provided by Dr. Bernd Schröder.

Taken together, we could show that cathepsin S can cleave the membrane-bound IL-6R leading to the generation of sIL-6R which was found to be biologically active. However, the size of the released sIL-6R was smaller than the sIL-6R released by ADAM17 indicating that cathepsin S cleaves the IL-6R at a site different from the identified proline355/valine356 cleavage site. Analysis of the region containing the cleavage site used by cathepsin S revealed that it must lie in the region between I343-A349. Therefore, cathepsin S is most likely not involved in the generation of the basal sIL-6R levels.

5 Discussion

5.1 Cell-surface levels of the IL-6R and gp130 are controlled by proteolysis, internalization and recycling

Different mechanisms are known that can contribute to the regulation of cell-surface levels of receptors. Cell-surface levels are reduced upon internalization of the receptors which can then be further sorted to recycling endosomes leading to recycling of the receptors back to the cell-surface, or the receptors can be sorted to lysosomes where they are degraded. Furthermore, the extracellular part of receptors can be released from the cell-surface by proteolysis which also leads to the down-regulation of cell-surface levels. To maintain receptor levels at the cell-surface constant, new receptors are synthesized which are then transported to the plasma membrane. How exactly gp130 and IL-6R cell-surface levels are regulated is still unclear, especially regarding the influence of their ligand IL-6. Elucidating the regulation of both receptors, however, would be important as IL-6-mediated signaling is involved in many different inflammatory conditions like e.g. rheumatoid arthritis [59] which is e.g. treated by tocilizumab, a monoclonal antibody against the IL-6R [65]. Knowing more about the regulatory mechanisms involved in maintaining the receptors' cell-surface levels would help to determine the necessary amount of antibody for the treatment of inflammatory diseases.

IL-6R and gp130 cell-surface levels were shown to be regulated by internalization and proteolysis but whether its ligand IL-6 influences both processes is still unclear [149-152]. Furthermore, the fate of the internalized receptors and the influence of IL-6 is still under debate.

Here, we show that gp130 and IL-6R are internalized independently of their ligand IL-6 and stimulation with IL-6 does not influence the rate of internalization. We further analyzed the pathway by which both receptors are internalized and found that clathrin and dynamin regulate internalization of both, gp130 and the IL-6R. A complete block of internalization could, however, not be reached, indicating that either another pathway is involved, or that another mechanism can compensate for the loss of clathrin and dynamin, or inhibition with both inhibitors was not efficient enough to completely block internalization. The involvement of other pathways like the caveolin-mediated pathway should, therefore, be also analyzed in the future.

As cell-surface protein levels are regulated by different mechanisms, it was no surprise that Basagiannis et al. found that the loss of VEGFR internalization and therefore the loss of a regulatory mechanism in cell-surface levels of VEGFR could be compensated for by shedding [256]. They observed that once internalization was blocked higher amounts of soluble VEGFR could be detected. We, therefore, also investigated whether proteolytic cleavage could compensate for the loss of IL-6R internalization and observed an increase in proteolytic cleavage

of the IL-6R when internalization could not take place. Additionally, we analyzed whether internalization could compensate for the loss of proteolytic cleavage and we could, indeed, detect such compensatory effect. It seems that cell-surface levels of the IL-6R are strictly regulated by proteolysis and internalization and that both mechanisms can compensate for one another to maintain normal IL-6R cell-surface levels.

For the internalization of cell-surface proteins via clathrin and dynamin different internalization motifs have been identified which are necessary for clathrin- and dynamin-dependent internalization. Such motifs were also identified in the cytoplasmic region of the IL-6R, namely 408-YSLG and 427-LI [152]. Although these motifs were identified to be similar to motifs that are associated to clathrin-dependent endocytosis, the involvement of both motifs in IL-6R internalization is still under debate. Dittrich et al. [264] showed that the motifs are dispensable for IL-6R internalization whereas Fujimoto et al. [152] described that both motifs are necessary for IL-6R internalization and furthermore for targeting of the IL-6R to the lysosome. Therefore, we also analyzed the involvement of the YSLG and the LI motif in IL-6R endocytosis. We generated cell lines that express the IL-6R with mutated internalization motifs or an IL-6R with a complete deletion of the ICD. These cells were used in a flow-cytometry based internalization assay and compared internalization of the mutated IL-6R variants with internalization of wild-type IL-6R. We could observe no difference in IL-6R internalization, indicating that the YSLG and the LI motifs in the IL-6R-ICD are dispensable for internalization when gp130 is present which is in line with studies by Dittrich et al. [264]. The contradictory results published by Fujimoto et al. [152] might be due to differences in their experimental setting. They analyzed internalization of the IL-6R in an indirect approach by analyzing internalization of the antibody tocilizumab bound to IL-6R using immunofluorescence (IF) microscopy. Additionally, we observed reduced cell-surface levels of the mutated IL-6R variants which might be the case also in the cells used by Fujimoto et al.. This would lead to reduced binding sites for tocilizumab resulting in diminished intracellular tocilizumab levels.

However, we favored the conclusion that IL-6R internalization must be regulated otherwise, maybe by complex formation with gp130 and internalization of both receptors in complex which was also suggested by Dittrich et al. [153, 264]. They identified a di-leucine motif 145LL in the gp130-ICD and showed that this motif is important for IL-6R internalization. To verify the involvement of gp130 in IL-6R internalization, we used cells that are devoid of gp130 and again performed the flow-cytometry based internalization assay with these cells. Interestingly, we could observe reduced internalization of the IL-6R in the absence of gp130, indicating that gp130 is indeed important for IL-6R internalization maybe by forming a complex with the IL-6R which is then internalized in a clathrin- and dynamin-dependent manner. However, the IL-6R was also internalized in the absence of gp130, indicating that IL-6R internalization also occurs

independently of gp130. The mechanism involved in the gp130-independent internalization of the IL-6R is so far unclear and should be addressed in future experiments.

Receptors present at the cell-surface are important for the activation of different signaling pathways upon binding of their respective ligand. Activated receptors are often internalized and degraded, a mechanism that is important for signaling termination. Internalization was long believed to be solely important for signaling termination, but studies nowadays indicate that internalization can also be a prerequisite for signaling initiation. A study focusing on IL-13 and its receptor revealed that endocytosis of the IL-13/IL-13R complex was important for the induction of STAT6 signaling, a connection that has been also suggested for IL-6-mediated signaling [154-157, 265]. After we found that cell-surface gp130 and IL-6R levels are regulated by internalization, we were therefore also interested whether this is important for signal initiation and transduction upon IL-6 binding. Our analysis revealed that inhibition of IL-6R/gp130 internalization leads to reduced STAT3 activation, supporting the notion that internalization is not important for signaling termination but rather for STAT3 activation at endosomal structures. We therefore concluded that signal transduction is initiated by binding of the ligand IL-6 to its α-receptor, which leads to homodimerization of gp130. This complex is internalized which leads to signal transduction at endosomal structures. Following, signaling is terminated by e.g. SOCS3, and the receptors are sorted to lysosomes where they are degraded by lysosomal proteases.

IL-6R was initially thought to be exclusively degraded in the lysosome but further analysis additionally suggested recycling of the IL-6R. However, this was only analyzed using an indirect approach by following recycling of the cytokine IL-6 which might also occur independently of the IL-6R [1, 2]. Recycling of gp130 was not demonstrated so far, and in which compartment gp130 is degraded is still under debate [3, 4]. We therefore sought to analyze the fate of both receptors and demonstrated for the first time that the IL-6R is, indeed, recycled back to the cell-surface via Rab11-positive recycling endosomes. Additionally, we found that the IL-6R is sorted to lysosomes where it is degraded. The same results were obtained regarding the fate of gp130. We showed for the first time that also gp130 is recycled via Rab11-positive recycling endosomes back to the cell-surface but is also sorted to lysosomes for degradation. We further analyzed whether IL-6 influenced the sorting of the receptors and observed an increase in recycling of both receptors upon IL-6 stimulation. In humans, the presence of IL-6 is a sign for inflammation which leads to the activation of different pro- and anti-inflammatory functions. To execute these effects, IL-6R and gp130 are necessary to bind IL-6 which leads e.g. to the activation of different immune cells. Thus, IL-6 might lead to an increase in the recycling of both receptors so that more receptor is present at the cell-surface to react most efficiently to the circulating IL-6.

As stated above, we also observed that both receptors are transported to lysosomes for degradation. We also analyzed the influence of IL-6 on the sorting of both receptors to lysosomes and could demonstrate an increase in lysosomal sorting of gp130 whereas the IL-6R levels in

lysosomes was not influenced by IL-6. As signal transduction is initiated at the intracellular domain of gp130, degradation of gp130 is maybe needed to stop signaling and therefore lysosomal degradation of gp130 is increased upon IL-6 stimulation. In contrast, IL-6R degradation is not increased although IL-6, IL-6R and gp130 form a complex to induce signal transduction and are internalized together. We expected that also IL-6R degradation in the lysosome would be increased. As this is not the case one could speculate that the IL-6/IL-6R/gp130 complex falls apart after arriving at endosomal structures, however this has not been demonstrated so far and warrants further investigation. A possibility to analyze complex formation and decay of the complex could be done by using the proximity ligation assay and additional staining of different cellular compartments. Thereby, one could detect when the IL-6R/gp130 complex is formed and in which compartment the complex disassembles again. Following transport to endosomal structures, the IL-6R is recycled to the cell-surface whereas gp130 is transported to the lysosome and degraded there. Whether the ligand IL-6 is recycled to the cell-surface or is also degraded still needs to be investigated.

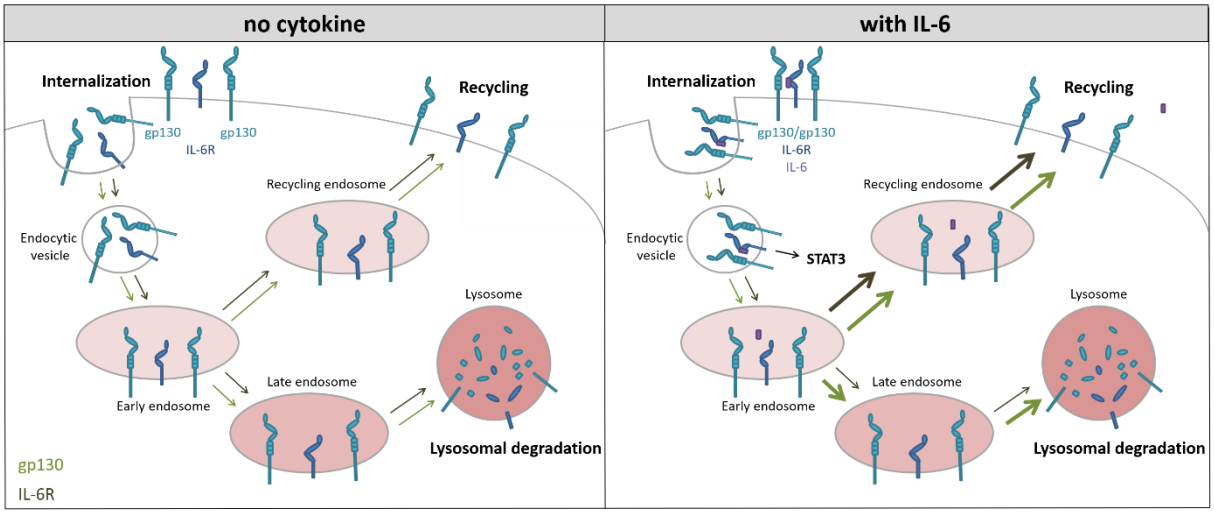

Figure 5.1: Interleukin-6 influences the intracellular fate of gp130 and IL-6R but not their internalization. In the absence of IL-6 both receptors are internalized constitutively, are transported to the early endosome and are sorted from there to lysosomes or recycling endosomes. In the presence of IL-6, gp130 and IL-6R are internalized but the rate of internalization is not changed. Following internalization, both receptors are transported to early endosomes from where STAT3 signaling is activated. Upon IL-6 stimulation, gp130 and IL-6R recycling is increased and, additionally, more gp130 is transported to the lysosome whereas lysosomal transport of the IL-6R is unaffected.

In summary, we could show that both, gp130 and IL-6R are internalized constitutively in a clathrin- and dynamin-dependent manner, and, following, are recycled to the cell-surface or are degraded in the lysosome. We could also demonstrate that the ligand IL-6 does not influence internalization of both receptors but rather influences the fate of both receptors. Upon IL-6 stimulation both receptors are recycled to the cell-surface in higher amounts and, additionally, more gp130 is transported to lysosomes (Fig. 5.1). Therefore, IL-6 bound to the IL-6R and gp130 could maybe serve as a sorting signal for gp130 and IL-6R.

5.2 Activation of Toll-like receptor 2 (TLR2) induces Interleukin-6 trans-signaling

IL-6 can not only induce signaling via the membrane-bound surface IL-6R and gp130 but also by using a soluble form of the IL-6R (sIL-6R) which is generated mainly by proteolytic cleavage by the metalloproteases ADAM17 and ADAM10 [96, 97, 253]. Signaling via the sIL-6R is termed trans-signaling and was attributed to the pro-inflammatory properties of IL-6 including the recruitment of mononuclear cells, inhibition of T cell apoptosis or inhibition of Treg differentiation [68, 112, 266]. Although a lot is known about the function of the sIL-6R only a little is known about endogenous stimuli that lead to the release of sIL-6R in humans. Studies in mice revealed that sIL-6R was released upon injection with LPS by activating TLR4 which in turn leads to the activation of ADAM17 [223]. As ADAM17 was identified to cleave the IL-6R also *in vivo*, an involvement of LPS and TLR4 activation in the release of sIL-6R could be imagined in humans, too. To analyze a possible involvement of TLR4 in the release of sIL-6R in humans, PBMCs were isolated and stimulated with LPS, a ligand of TLR4. We used PBMCs as the IL-6R is not only expressed on the cell-surface of hepatocytes but also on monocytes, T cells, B cells and dendritic cells, cell types that are present in the isolated PBMCs and are involved in fighting pathogens. We determined sIL-6R levels in the supernatants and observed no increase in sIL-6R release upon LPS-treatment when compared to healthy controls. In contrast, IL-6 levels were increased, indicating that the LPS was functional and the cells reactive to the used LPS. These results suggest, that activation of TLR4 is not so much involved in the release of sIL-6R in humans as it is in mice. To verify our findings, we furthermore, analyzed sIL-6R serum levels in sepsis patients. Sepsis is a severe inflammatory condition which is characterized by a massive increase in IL-6 often caused by infection with LPS-bearing bacteria and therefore activation of TLR4. We would expect to observe an increase in sIL-6R levels in the sepsis samples if activation of TLR4 would be involved in the release of sIL-6R. However, sIL-6R levels were not significantly elevated in the sepsis samples compared to healthy control samples although IL-6 levels were increased. This supported our above findings that activation of TLR4 does not contribute to the release of sIL-6R in humans. As innate immune responses and therefore the release of sIL-6R depend on the recognition of pathogen-associated microbial peptides (PAMPs) by pattern-recognitions receptors (PRRs) like the Toll-like receptors (TLRs), the possible involvement of another TLR in the release of sIL-6R in humans seemed to be likely. To analyze this further, we isolated PBMCs and stimulated these cells with different TLR agonists. Only incubation with TLR2 agonists led to an increase in sIL-6R levels although this did not reach statistical significance. However, we could still observe a three-fold increase in sIL-6R levels upon TLR2 activation. That the increase in sIL-6R levels did not show statistical significance might be due to the fact, that PBMCs were isolated from different donors and the differing total IL-6R levels between human individuals. It could also well be that some cell

samples were more reactive to TLR2 activation than others. From this we concluded that TLR2 activation is involved in the release of sIL-6R in humans and not TLR4, a connection not described so far.

The above experiments were conducted with PBMCs which consist of different cell types, namely monocytes, T cells, B cells, NK cells and immature dendritic cells. We were therefore interested from which cellular subset sIL-6R was released upon TLR2 activation. To analyze this, we stained the different cell-types with specific antibodies and additionally with antibodies directed against TLR2 and IL-6R. Cells that co-express TLR2 and IL-6R at the cell-surface are most likely to be the source of sIL-6R. Flow-cytometry analysis revealed such co-expression only on monocytes and dendritic cells suggesting that these cells are involved in the release of sIL-6R. To further investigate their potential in releasing sIL-6R upon TLR2 activation, we isolated dendritic cells and monocytes, incubated them with and without the TLR2 agonist and examined sIL-6R levels. Only stimulation of monocytes resulted in an increase of sIL-6R compared to the unstimulated samples although both cell-types released sIL-6R constitutively, indicating that monocytes are the source of sIL-6R upon TLR2 activation. The reason why dendritic cells express both receptors but do not release sIL-6R upon TLR2 activation is not clear and needs to be further investigated. Surprisingly, T cells did not express TLR2 at the cell-surface in our experimental setting although they were described to express TLR2 at the cell-surface. Furthermore, T cells were described to release sIL-6R by ADAM17 [267, 268]. Therefore, T cells were a quite good candidate for the release of sIL-6R upon TLR2 activation. However, in our experimental setting, T cells were negative for TLR2 cell-surface expression and therefore unlikely to be involved in TLR2-mediated sIL-6R release. It must be noted, however, that in the above-mentioned publication activated T cells were analyzed but, in this approach, T cells were not activated which might be the reason for the absence of surface TLR2.

In mice, it was shown that activation of TLR4 lead to activation of ADAM17 which resulted in the cleavage of the membrane-bound IL-6R and subsequent release of sIL-6R [223]. Additionally, it was described before in humans that the membrane-bound IL-6R is proteolytically cleaved by ADAM10 and ADAM17 leading to the release of sIL-6R [96, 97, 253]. Whether metalloproteases, especially ADAM10 and ADAM17, are also involved in the release of sIL-6R upon TLR2 activation in humans was of further interest. We, therefore, isolated PBMCs and incubated them with the broad-spectrum metalloprotease inhibitor Marimastat, or with the ADAM10- and ADAM17-specific inhibitors, GI and GW, in the presence or absence of the TLR2 agonist. Determination of sIL-6R levels in the supernatants revealed that, indeed, ADAM10 and ADAM17 are involved in the release of sIL-6R upon TLR2 activation, as inhibition of both proteases led to reduced sIL-6R levels.

Stimulation of TLR2 was shown to activate different downstream signaling pathways, especially NF-κB [239], p38/MAPK [261] and ERK [262]. It was of further interest which of these pathways

is involved in ADAM17-induced sIL-6R generation upon TLR2 activation. To analyze this, we isolated PBMCs, stimulated them with the TLR2 agonist for different time-points and analyzed phosphorylation of NF-κB, p38 and ERK by Western Blot. We thereby revealed that only ERK signaling was activated upon stimulation with the TLR2 agonist whereas NF-κB and p38/MAPK signaling pathways were not activated. This indicates that TLR2 stimulation leads to the activation of ERK signaling but whether and how this in turn regulates sIL-6R release was of further interest. To answer this question, we isolated PBMCs and incubated these with different signaling pathway inhibitors in the presence of the TLR2 agonist. Determination of sIL-6R levels upon signaling inhibition revealed that inhibition of ERK signaling led to an increase in sIL-6R release. This was quite surprising, as a study demonstrated that ERK signaling leads to the activation of ADAM17 [269]. Thus, inhibition of ERK would rather result in a decrease of sIL-6R levels. The reason for this difference and the underlying mechanism need to be investigated further in the future. In contrast to the increase in sIL-6R levels upon ERK inhibition, inhibition resulted in a decrease in IL-6 release. ERK signaling, therefore, seems to differentially regulate the production of both proteins upon TLR2 activation.

In summary, it was found that TLR2 activation of monocytes leads to the release of IL-6 and the generation of sIL-6R by ADAM10 and ADAM17. HKLM-induced TLR2 activation results in ERK phosphorylation which seems to differentially regulate IL-6 and sIL-6R release.

5.3 Identification of Cathepsin S as a novel protease capable of cleaving the membrane-bound Interleukin-6 receptor

In healthy humans sIL-6R is present in the blood at concentrations ranging from 30-80 ng/ml [94, 95]. Analysis of sIL-6R levels in the sera from healthy humans revealed that about 85% of the sIL-6R is generated by proteolytic cleavage whereas the remaining 15% come from differential splicing [93]. Furthermore, MS analysis of the sIL-6R isolated from human sera revealed that it is cleaved between P355 and V356, amino-acid residues preferentially cleaved by ADAM17 and also ADAM10, suggesting that the human IL-6R is proteolytically cleaved by ADAM17 and/or ADAM10 [93, 102]. It was of interest whether the IL-6R can be still cleaved from the cell-surface when ADAM17 is not present and so PBMCs and sera isolated from an ADAM17-deficient patient were analyzed. The PBMCs from this patient were stimulated with PMA and ionomycin to induce ADAM17-mediated cleavage, but this did not lead to an increase in sIL-6R levels as compared to healthy controls. The basal sIL-6R level in the serum of this patient, however, was unaffected by the absence of ADAM17 and showed same levels as compared to the healthy controls (unpublished results). These effects could also be observed in ADAM17-deficient mice [97, 100]. From this it was concluded that ADAM17 indeed plays a role in the generation of sIL-6R during inflammation in humans but its involvement in the release of constitutively cleaved IL-6R is unclear. Two theories arose that might explain these unexpected results in the ADAM17-deficient

patient and also in mice: 1) different proteases are responsible for the generation of basal sIL-6R levels and sIL-6R released during inflammatory conditions or 2) ADAM17 is responsible for the basal sIL-6R levels but, once ADAM17 is lost, other proteases can compensate for the loss and induce constitutive sIL-6R release.

We therefore tried to identify novel proteases capable of cleaving the IL-6R and which would contribute to the generation of basal sIL-6R levels. For this, a MEROPS database search was conducted to find possible candidate proteases that can cleave proteins between a proline and a valine residue, the cleavage site identified to be used for the generation of sIL-6R in humans. This search revealed a total of 14 candidate proteases, also including ADAM10 and ADAM17. In a peptide cleavage assay, these recombinant proteases were tested for their capability of cleaving IL-6R peptides that contain the proline/valine cleavage site. Along with ADAM17 only cathepsin S was able to cleave the IL-6R peptides and was therefore analyzed further. Although no other tested protease was able to cleave the IL-6R peptide, it can, however, not be excluded that one of the other proteases is also able to cleave the IL-6R peptides.

Cathepsin S is a lysosomal protease and is involved in the degradation of proteins that have been directed to the lysosome. In contrast to the other lysosomal proteases that are only active at acidic pH, cathepsin S was found to be also active at neutral or even basic pH [203, 204]. Furthermore, it can not only cleave proteases present in the lysosome but was also identified to cleave proteins belonging to the extracellular matrix as it is not only located in lysosomes but also in the extracellular space [205, 206]. These special features of cathepsin S further support the possible involvement of this protease in the generation of sIL-6R. Western blot analysis of supernatants collected from ADAM10/ADAM17-deficient HEK293 cells (HEK293 A10/A17$^{-/-}$) that were co-transfected with IL-6R- and cathepsin S-encoding plasmids revealed a band at about 55 kDa after incubation with an anti-IL-6R antibody. This indicates that cathepsin S is able to cleave the IL-6R *in vitro*. However, the sIL-6R generated by cathepsin S was smaller compared to the sIL-6R released upon PMA-stimulation. In a recently published paper glycosylation of the IL-6R was analyzed and five N-linked glycosylation sites and one O-linked glycosylation site were identified in the extracellular part of the IL-6R [93]. The sIL-6R cleaved by ADAM17 contains all the glycosylation sites. As the sIL-6R generated by cathepsin S is smaller than the ADAM17-induced sIL-6R it is therefore likely that cathepsin S cleaves the IL-6R at a different position than ADAM17, probably upstream of the N350 glycosylation site. From this it was concluded that cathepsin S might not be involved in the generation of the basal sIL-6R levels as the responsible protease has to cleave the IL-6R between P355 and V356.

Although cathepsin S could cleave the IL-6R peptide which contained the P355/V356 cleavage site in the cleavage assay, it was quite surprising that it seems to use a different cleavage site when the whole IL-6R protein is present. Cathepsin S was found to be able to cleave proteins between

proline and valine, which it also did in the cleavage assay, but it maybe prefers a different cleavage site when the total IL-6R protein is present.

To further determine the cleavage site of cathepsin S in the IL-6R protein HEK293 A10/17$^{-/-}$ cells were transfected with plasmids encoding the IL-6R with different deletions in the stalk region ranging from 10 amino-acid deletions to a complete deletion of the stalk region. Analysis of the supernatants by Western blot revealed that the cleavage site used by cathepsin S is situated in the region I343-T352 as no sIL-6R could be detected in the supernatants when cells were transfected with the IL-6R constructs where this region was deleted. Due to the reduced size of the cathepsin S-generated sIL-6R compared to the sIL-6R generated by ADAM17, cathepsin S cleavage must occur upstream of the P355/V356 cleavage site, most likely even upstream of the N350 glycosylation site. Therefore, cathepsin S probably cleaves the IL-6R in the region I343-A349. Closer analysis of this region and comparison with cleavage sites identified for other proteins cleaved by cathepsin S using the MEROPS database revealed three potential cleavage sites in the IL-6R that could be used by cathepsin S: 1) R346/D347, 2) D347/S348 or 3) S348/A349. Whether one of these sites is really cleaved by cathepsin S needs to be evaluated by MS analysis or further deletion or substitution variants.

As cathepsin S cleaves the IL-6R in the region I343-T352 which does not contain the P355/V356 cleavage site identified by MS analysis, this is a further hint that cathepsin S might not be the protease involved in the constitutive release of sIL-6R. However, all experiments regarding the identification of the cleavage site and the molecular weight of the generated sIL-6R were performed with serum isolated from healthy ADAM17-expressing donors and not with serum isolated from the ADAM17-deficient patient [253]. It could well be that analysis of the sIL-6R isolated from the patient's serum would reveal a different cleavage site and therefore also a shift in the molecular weight of the generated sIL-6R.

To further evaluate a compensatory effect of cathepsin S in the generation of sIL-6R a mouse strain could be generated that is not only deficient for ADAM17 but also for cathepsin S. A decrease in basal sIL-6R levels in these mice compared to cathepsin S knockout mice or ADAM17-deficient mice would hint to a compensatory effect of cathepsin S. That the loss of ADAM17 is compensated for by other proteases is not very unlikely as sIL-6R and sgp130 are proposed to form a buffer system to neutralize IL-6 and prevent systemic effects that might be induced by IL-6. Missing sIL-6R would disrupt this protective buffer system and IL-6, which can be found even in healthy humans at concentrations of 2-6 pg/ml, could induce classic signaling via IL-6R and gp130 although no inflammation is present [266]. It would be therefore important that the loss of ADAM17 is compensated for by other proteases to sustain this buffer.

In contrast to the ADAM17- or ADAM10-knockout mice, that showed no alterations in the release of sIL-6R, knockout of TIMP3 (tissue inhibitor of metalloproteinases 3), an inhibitor of different matrix-metalloproteases (MMPs), ADAM and ADAMTS proteases [270], led to an increase of sIL-

6R generation [271], indicating that the candidate protease involved in the constitutive release of sIL-6R must be inhibited by TIMP3. Therefore, proteases regulated by TIMP3 should be tested for their potential of cleaving the membrane-bound IL-6R by performing the cleavage assay used in this work, and the candidate protease(s) should be analyzed further.

In summary, we could show that in addition to ADAM17, cathepsin S is able to cleave the IL-6R *in vitro*. However, the generated sIL-6R was smaller in size indicating that cathepsin S cleaves the IL-6R at a different site than ADAM17. Western blot analysis of different IL-6R variants revealed that cathepsin S cleaves the IL-6R most likely in the region I343-T352 and, therefore, might not contribute to the generation of basal sIL-6R levels in humans. However, one should keep in mind that the cleavage site localization and size determination of sIL-6R were only done with material from healthy humans and not with material from the ADAM17-deficient patient.

6 References

1. Takeda, K. and Akira, S., *TLR signaling pathways.* Semin Immunol, 2004. **16**(1): p. 3-9.

2. Takei, K. and Haucke, V., *Clathrin-mediated endocytosis: membrane factors pull the trigger.* Trends Cell Biol, 2001. **11**(9): p. 385-391.

3. Guichard, A., Nizet, V., and Bier, E., *RAB11-mediated trafficking in host–pathogen interactions.* Nat Rev Microbiol, 2014. **12**(9): p. 624-634.

4. Parkin, J. and Cohen, B., *An overview of the immune system.* Lancet, 2001. **357**(9270): p. 1777-1789.

5. Romo, M., Martínez, D., and Ferrer, C., *Innate immunity in vertebrates: an overview.* Immunology, 2016. **148**(2): p. 125-139.

6. Bonilla, F.A. and Oettgen, H.C., *Adaptive immunity.* J Allergy Clin Immunol, 2010. **125**(2 Suppl 2): p. S33-40.

7. Rose-John, S., *Interleukin-6 Family Cytokines.* Cold Spring Harb Perspect Biol, 2018. **10**(2).

8. Bazan, J.F., *Haemopoietic receptors and helical cytokines.* Immunol Today, 1990. **11**(10): p. 350-354.

9. Taga, T., Hibi, M., Hirata, Y., Yamasaki, K., Yasukawa, K., Matsuda, T., Hirano, T., and Kishimoto, T., *Interleukin-6 triggers the association of its receptor with a possible signal transducer, gp130.* Cell, 1989. **58**(3): p. 573-581.

10. Yin, T., Taga, T., Tsang, M.L., Yasukawa, K., Kishimoto, T., and Yang, Y.C., *Involvement of IL-6 signal transducer gp130 in IL-11-mediated signal transduction.* J Immunol, 1993. **151**(5): p. 2555-2561.

11. Plun-Favreau, H., Elson, G., Chabbert, M., Froger, J., deLapeyriere, O., Lelievre, E., Guillet, C., Hermann, J., Gauchat, J.-F., Gascan, H., and Chevalier, S., *The ciliary neurotrophic factor receptor α component induces the secretion of and is required for functional responses to cardiotrophin-like cytokine.* EMBO J, 2001. **20**(7): p. 1692-1703.

12. Plun-Favreau, H., Perret, D., Diveu, C., Froger, J., Chevalier, S., Lelievre, E., Gascan, H., and Chabbert, M., *Leukemia inhibitory factor (LIF), cardiotrophin-1, and oncostatin M share structural binding determinants in the immunoglobulin-like domain of LIF receptor.* J Biol Chem, 2003. **278**(29): p. 27169-27179.

13. Liu, J., Modrell, B., Aruffo, A., Marken, J.S., Taga, T., Kiyoshi, Y., Murakami, M., Kishimoto, T., and Shoyab, M., *Interleukin-6 signal transducer gp130 mediates oncostatin M signaling.* J Biol Chem, 1992. **267**(24): p. 16763-16766.

14. Mosley, B., Imus, D.C., Friend, D., Boiani, N., Thoma, B., Park, L.S., and Cosman, D., *Dual oncostatin M (OSM) receptors cloning and characterization of an alternative signaling subunit conferring OSM-specific receptor activation.* J Biol Chem, 1996. **271**(50): p. 32635-32643.

15. Pflanz, S., Hibbert, L., Mattson, J., Rosales, R., Vaisberg, E., Bazan, J.F., Philips, J.H., McClanahan, T.K., de Waal Malefyt, R., and Kastelein, R.A., *WSX-1 and glycoprotein 130 constitute a signal-transducing receptor for IL-27.* J Immunol, 2004. **172**(4): p. 2225-2231.

16. Diveu, C., Lagrue Lak-Hal, A.H., Froger, J., Ravon, E., Grimaud, L., Barbier, F., Hermann, J., Gascan, H., and Chevalier, S., *Predominant expression of the long isoform of GP130-like (GPL) receptor is required for interleukin-31 signaling.* Eur Cytokine Netw, 2004. **15**(4): p. 291-302.

17. Dreuw, A., Radtke, S., Pflanz, S., Lippok, B.E., Heinrich, P.C., and Hermanns, H.M., *Characterization of the signaling capacities of the novel gp130-like cytokine receptor.* J Biol Chem, 2004. **279**(34): p. 36112-36120.

18. Dienz, O. and Rincon, M., *The effects of IL-6 on CD4 T cell responses.* Clin Immunol, 2009. **130**(1): p. 27-33.

19. Diehl, S. and Rincón, M., *The two faces of IL-6 on Th1/Th2 differentiation.* Mol Immunol, 2002. **39**(9): p. 531-536.

20. Schneider, R., Yaneva, T., Beauseigle, D., El-Khoury, L., and Arbour, N., *IL-27 increases the proliferation and effector functions of human naive CD8+ T lymphocytes and promotes their development into Tc1 cells.* Eur J Immunol, 2011. **41**(1): p. 47-59.

21. Takeuchi, Y., Watanabe, S., Ishii, G., Takeda, S., Nakayama, K., Fukumoto, S., Kaneta, Y., Inoue, D., Matsumoto, T., Harigaya, K., and Fujita, T., *Interleukin-11 as a stimulatory factor for bone formation prevents bone loss with advancing age in mice.* J Biol Chem, 2002. **277**(50): p. 49011-49018.

22. Agthe, M., Garbers, Y., Putoczki, T., and Garbers, C., *Interleukin-11 classic but not trans-signaling is essential for fertility in mice.* Placenta, 2017. **57**: p. 13-16.

23. Peters, M., Müller, A.M., and Rose-John, S., *Interleukin-6 and Soluble Interleukin-6 Receptor: Direct Stimulation of gp130 and Hematopoiesis.* Blood, 1998. **92**(10): p. 3495-3504.

24. Ogawa, M., *Differentiation and proliferation of hematopoietic stem cells.* Blood, 1993. **81**(11): p. 2844-2853.

25. Streetz, K.L., Luedde, T., Manns, M.P., and Trautwein, C., *Interleukin 6 and liver regeneration.* Gut, 2000. **47**(2): p. 309-312.

26. Masu, Y., Wolf, E., Holtmann, B., Sendtner, M., Brem, G., and Thoenen, H., *Disruption of the CNTF gene results in motor neuron degeneration.* Nature, 1993. **365**(6441): p. 27-32.

27. Chucair-Elliott, A.J., Elliott, M.H., Wang, J., Moiseyev, G.P., Ma, J.-X., Politi, L.E., Rotstein, N.P., Akira, S., Uematsu, S., and Ash, J.D., *Leukemia inhibitory factor coordinates the down-regulation of the visual cycle in the retina and retinal-pigmented epithelium.* J Biol Chem, 2012. **287**(29): p. 24092-24102.

28. Gauldie, J., Richards, C., Harnish, D., Lansdorf, P., and Baumann, H., *Interferon beta 2/B-cell stimulatory factor type 2 shares identity with monocyte-derived hepatocyte-stimulating factor and regulates the major acute phase protein response in liver cells.* Proc Natl Acad Sci U S A, 1987. **84**(20): p. 7251-7255.

29. Ganter, U., Arcone, R., Toniatti, C., Morrone, G., and Ciliberto, G., *Dual control of C-reactive protein gene expression by interleukin-1 and interleukin-6.* EMBO J, 1989. **8**(12): p. 3773-3779.

30. Muraguchi, A., Hirano, T., Tang, B., Matsuda, T., Horii, Y., Nakajima, K., and Kishimoto, T., *The essential role of B cell stimulatory factor 2 (BSF-2/IL-6) for the terminal differentiation of B cells.* J Exp Med, 1988. **167**(2): p. 332-344.

31. Tosato, G. and Pike, S.E., *Interferon-beta 2/interleukin 6 is a co-stimulant for human T lymphocytes.* J Immunol, 1988. **141**(5): p. 1556-1562.

32. Habetswallner, D., Pelosi, E., Bulgarini, D., Camagna, A., Samoggia, P., Montesoro, E., Gianella, G., Lazzaro, D., Isacchi, G., Testa, U., and Peschle, C., *Activation and proliferation of normal resting human T lymphocytes in serum-free culture: role of IL-4 and IL-6.* Immunology, 1988. **65**(3): p. 357-364.

33. Hirano, T., Yasukawa, K., Harada, H., Taga, T., Watanabe, Y., Matsuda, T., Kashiwamura, S.-I., Nakajima, K., Koyama, K., Iwamatsu, A., Tsunasawa, S., Sakiyama, F., Matsui, H., Takahara, Y., Taniguchi, T., and Kishimoto, T., *Complementary DNA for a novel human interleukin (BSF-2) that induces B lymphocytes to produce immunoglobulin.* Nature, 1986. **324**(6092): p. 73-76.

34. Kharazmi, A., Nielsen, H., Rechnitzer, C., and Bendtzen, K., *Interleukin 6 primes human neutrophil and monocyte oxidative burst response.* Immunol Lett, 1989. **21**(2): p. 177-184.

35. Lotz, M., Jirik, F., Kabouridis, P., Tsoukas, C., Hirano, T., Kishimoto, T., and Carson, D.A., *B cell stimulating factor 2/interleukin 6 is a costimulant for human thymocytes and T lymphocytes.* J Exp Med, 1988. **167**(3): p. 1253-1258.

36. Elias, J.A., Trinchieri, G., Beck, J.M., Simon, P.L., Sehgal, P.B., May, L.T., and Kern, J.A., *A synergistic interaction of IL-6 and IL-1 mediates the thymocyte-stimulating activity produced by recombinant IL-1-stimulated fibroblasts.* J Immunol, 1989. **142**(2): p. 509-514.

37. Ikebuchi, K., Wong, G.G., Clark, S.C., Ihle, J.N., Hirai, Y., and Ogawa, M., *Interleukin 6 enhancement of interleukin 3-dependent proliferation of multipotential hemopoietic progenitors.* Proc Natl Acad Sci U S A, 1987. **84**(24): p. 9035-9039.

38. Baumann, H. and Kushner, I., *Production of interleukin-6 by synovial fibroblasts in rheumatoid arthritis.* Am J Pathol, 1998. **152**(3): p. 641-644.

39. Navarro, S., Debili, N., Bernaudin, J.F., Vainchenker, W., and Doly, J., *Regulation of the expression of IL-6 in human monocytes.* J Immunol, 1989. **142**(12): p. 4339-4345.

40. Podor, T.J., Jirik, F.R., Loskutoff, D.J., Carson, D.A., and Lotz, M., *Human Endothelial Cells Produce IL-6.* Ann N Y Acad Sci, 1989. **557**(1): p. 374-387.

41. Libermann, T.A. and Baltimore, D., *Activation of interleukin-6 gene expression through the NF-kappa B transcription factor.* Mol Cell Biol, 1990. **10**(5): p. 2327-2334.

42. Fong, Y., Moldawer, L.L., Marano, M., Wei, H., Tatter, S.B., Clarick, R.H., Santhanam, U., Sherris, D., May, L.T., and Sehgal, P.B., *Endotoxemia elicits increased circulating beta 2-IFN/IL-6 in man.* J Immunol, 1989. **142**(7): p. 2321-2324.

43. Calandra, T., Gerain, J., Heumann, D., Baumgartner, J.-D., and Glauser, M.P., *High circulating levels of interleukin-6 in patients with septic shock: Evolution during sepsis, prognostic value, and interplay with other cytokines.* Am J Med, 1991. **91**(1): p. 23-29.

44. Bowcock, A.M., Kidd, J.R., Lathrop, G.M., Daneshvar, L., May, L.T., Ray, A., Sehgal, P.B., Kidd, K.K., and Cavalli-Sforza, L.L., *The human "interferon-β2/hepatocyte stimulating*

factor/interleukin-6" gene: DNA polymorphism studies and localization to chromosome 7p21. Genomics, 1988. **3**(1): p. 8-16.

45. Gross, V., Andus, T., Castell, J., Vom Berg, D., Heinrich, P.C., and Gerok, W., *O- and N-glycosylation lead to different molecular mass forms of human monocyte interleukin-6.* FEBS Lett, 1989. **247**(2): p. 323-326.

46. Santhanam, U., Ghrayeb, J., Sehgal, P.B., and May, L.T., *Post-translational modifications of human interleukin-6.* Arch Biochem Biophys, 1989. **274**(1): p. 161-170.

47. Yasukawa, K., Hirano, T., Watanabe, Y., Muratani, K., Matsuda, T., Nakai, S., and Kishimoto, T., *Structure and expression of human B cell stimulatory factor-2 (BSF-2/IL-6) gene.* EMBO J, 1987. **6**(10): p. 2939-2945.

48. Shimizu, H., Mitomo, K., Watanabe, T., Okamoto, S., and Yamamoto, K.-I., *Involvement of a NF-kappa B-like transcription factor in the activation of the interleukin-6 gene by inflammatory lymphokines.* Mol Cell Biol, 1990. **10**(2): p. 561-568.

49. Hershko, D.D., Robb, B.W., Luo, G., and Hasselgren, P.-O., *Multiple transcription factors regulating the IL-6 gene are activated by cAMP in cultured Caco-2 cells.* Am J Physiol Regul Integr Comp Physiol, 2002. **283**(5): p. R1140-R1148.

50. Iwasaki, H., Takeuchi, O., Teraguchi, S., Matsushita, K., Uehata, T., Kuniyoshi, K., Satoh, T., Saitoh, T., Matsushita, M., Standley, D.M., and Akira, S., *The IκB kinase complex regulates the stability of cytokine-encoding mRNA induced by TLR–IL-1R by controlling degradation of regnase-1.* Nat Immunol, 2011. **12**(12): p. 1167-1175.

51. Masuda, K., Ripley, B., Nishimura, R., Mino, T., Takeuchi, O., Shio, G., Kiyonari, H., and Kishimoto, T., *Arid5a controls IL-6 mRNA stability, which contributes to elevation of IL-6 level in vivo.* Proc Natl Acad Sci U S A, 2013. **110**(23): p. 9409-9414.

52. Mudter, J. and Neurath, M.F., *IL-6 signaling in inflammatory bowel disease: Pathophysiological role and clinical relevance.* Inflamm Bowel Dis, 2007. **13**(8): p. 1016-1023.

53. Krei, K., Fredrikson, S., Fontana, A., and Link, H., *Interleukin-6 is elevated in plasma in multiple sclerosis.* J Neuroimmunol, 1991. **31**(2): p. 147-153.

54. Scalzo, P., Kümmer, A., Cardoso, F., and Teixeira, A.L., *Serum levels of interleukin-6 are elevated in patients with Parkinson's disease and correlate with physical performance.* Neurosci Lett, 2010. **468**(1): p. 56-58.

55. Dufek, M., Rektorova, I., Thon, V., Lokaj, J., and Rektor, I., *Interleukin-6 May Contribute to Mortality in Parkinson's Disease Patients: A 4-Year Prospective Study.* Parkinsons Dis, 2015. **2015**(898192): p. 1-5.

56. Hüll, M., Fiebich, B.L., Lieb, K., Strauss, S., Berger, M., Volk, B., and Bauer, J., *Interleukin-6-associated inflammatory processes in Alzheimer's disease: New therapeutic options.* Neurobiol Aging, 1996. **17**(5): p. 795-800.

57. Yoshizaki, K., Matsuda, T., Nishimoto, N., Kuritani, T., Taeho, L., Aozasa, K., Nakahata, T., Kawai, H., Tagoh, H., Komori, T., Kishimoto, S., Hirano, T., and Kishimoto, T., *Pathogenic significance of interleukin-6 (IL-6/BSF-2) in Castleman's disease.* Blood, 1989. **74**(4): p. 1360-1367.

58. Brandt, S.J., Bodine, D.M., Dunbar, C.E., and Nienhuis, A.W., *Dysregulated interleukin 6 expression produces a syndrome resembling Castleman's disease in mice.* J Clin Invest, 1990. **86**(2): p. 592-599.

59. Houssiau, F.A., Devogelaer, J.-P., Van Damme, J., Nagant de Deuxchaisnes, C., and Van Snick, J., *Interleukin-6 in synovial fluid and serum of patients with rheumatoid arthritis and other inflammatory arthritides.* Arthritis Rheum, 1988. **31**(6): p. 784-788.

60. Wipke, B.T. and Allen, P.M., *Essential Role of Neutrophils in the Initiation and Progression of a Murine Model of Rheumatoid Arthritis.* J Immunol, 2001. **167**(3): p. 1601-1608.

61. Kotake, S., Sato, K., Kim, K.J., Takahashi, N., Udagawa, N., Nakamura, I., Yamaguchi, A., Kishimoto, T., Suda, T., and Kashiwazaki, S., *Interleukin-6 and soluble interleukin-6 receptors in the synovial fluids from rheumatoid arthritis patients are responsible for osteoclast-like cell formation.* J Bone Miner Res, 1996. **11**(1): p. 88-95.

62. Okada, Y., Shinmei, M., Tanaka, O., Naka, K., Kimura, A., Nakanishi, I., Bayliss, M.T., Iwata, K., and Nagase, H., *Localization of matrix metalloproteinase 3 (stromelysin) in osteoarthritic cartilage and synovium.* Lab Invest, 1992. **66**(6): p. 680-690.

63. Takizawa, M., Ohuchi, E., Yamanaka, H., Nakamura, H., Ikeda, E., Ghosh, P., and Okada, Y., *Production of tissue inhibitor of metalloproteinases 3 is selectively enhanced by calcium pentosan polysulfate in human rheumatoid synovial fibroblasts.* Arthritis Rheum, 2000. **43**(4): p. 812-820.

64. Roux-Lombard, P., Eberhardt, K., Saxne, T., Dayer, J.M., and Wollheim, F.A., *Cytokines, metalloproteinases, their inhibitors and cartilage oligomeric matrix protein: relationship to radiological progression and inflammation in early rheumatoid arthritis. A prospective 5-year study.* Rheumatology, 2001. **40**(5): p. 544-551.

65. Garbers, C., Aparicio-Siegmund, S., and Rose-John, S., *The IL-6/gp130/STAT3 signaling axis: recent advances towards specific inhibition.* Curr Opin Immunol, 2015. **34**: p. 75-82.

66. Lamb, Y.N. and Deeks, E.D., *Sarilumab: A Review in Moderate to Severe Rheumatoid Arthritis.* Drugs, 2018. **78**(9): p. 929-940.

67. Jostock, T., Müllberg, J., Ozbek, S., Atreya, R., Blinn, G., Voltz, N., Fischer, M., Neurath, M.F., and Rose-John, S., *Soluble gp130 is the natural inhibitor of soluble interleukin-6 receptor transsignaling responses.* Eur J Biochem, 2001. **268**(1): p. 160-167.

68. Scheller, J., Chalaris, A., Schmidt-Arras, D., and Rose-John, S., *The pro- and anti-inflammatory properties of the cytokine interleukin-6.* Biochim Biophys Acta 2011. **1813**(5): p. 878-888.

69. Rose-John, S., *The Soluble Interleukin 6 Receptor: Advanced Therapeutic Options in Inflammation.* Clin Pharmacol Ther, 2017. **102**(4): p. 591-598.

70. Hibi, M., Murakami, M., Saito, M., Hirano, T., Taga, T., and Kishimoto, T., *Molecular cloning and expression of an IL-6 signal transducer, gp130.* Cell, 1990. **63**(6): p. 1149-1157.

71. Moritz, R.L., Hall, N.E., Connolly, L.M., and Simpson, R.J., *Determination of the Disulfide Structure and N-Glycosylation Sites of the Extracellular Domain of the Human Signal Transducer gp130.* J Biol Chem, 2001. **276**(11): p. 8244-8253.

72. Waetzig, G.H., Chalaris, A., Rosenstiel, P., Suthaus, J., Holland, C., Karl, N., Valles Uriarte, L., Till, A., Scheller, J., Grötzinger, J., Schreiber, S., Rose-John, S., and Seegert, D., *N-linked*

glycosylation is essential for the stability but not the signaling function of the interleukin-6 signal transducer glycoprotein 130. J Biol Chem, 2010. **285**(3): p. 1781-1789.

73. Gibson, R.M., Schiemann, W.P., Prichard, L.B., Reno, J.M., Ericsson, L.H., and Nathanson, N.M., *Phosphorylation of Human gp130 at Ser-782 Adjacent to the Di-leucine Internalization Motif: Effect on expression and signaling.* J Biol Chem, 2000. **275**(29): p. 22574-22582.

74. Kernebeck, T., Pflanz, S., Müller-Newen, G., Kurapkat, G., Scheek, R.M., Dijkstra, K., Heinrich, P.C., Wollmer, A., Grzesiek, S., and Grötzinger, J., *The signal transducer gp130: Solution structure of the carboxy-terminal domain of the cytokine receptor homology region.* Protein Sci, 1999. **8**(1): p. 5-12.

75. Murakami, M., Narazaki, M., Hibi, M., Yawata, H., Yasukawa, K., Hamaguchi, M., Taga, T., and Kishimoto, T., *Critical cytoplasmic region of the interleukin 6 signal transducer gp130 is conserved in the cytokine receptor family.* Proc Natl Acad Sci U S A, 1991. **88**(24): p. 11349-11353.

76. Tanner, J.W., Chen, W., Young, R.L., Longmore, G.D., and Shaw, A.S., *The conserved box 1 motif of cytokine receptors is required for association with JAK kinases.* J Biol Chem, 1995. **270**(12): p. 6523-6530.

77. Zhang, J.G., Zhang, Y., Owczarek, C.M., Ward, L.D., Moritz, R.L., Simpson, R.J., Yasukawa, K., and Nicola, N.A., *Identification and characterization of two distinct truncated forms of gp130 and a soluble form of leukemia inhibitory factor receptor α-chain in normal human urine and plasma.* J Biol Chem, 1998. **273**(17): p. 10798-10805.

78. Narazaki, M., Yasukawa, K., Saito, T., Ohsugi, Y., Fukui, H., Koishihara, Y., Yancopoulos, G.D., Taga, T., and Kishimoto, T., *Soluble forms of the interleukin-6 signal-transducing receptor component gp130 in human serum possessing a potential to inhibit signals through membrane-anchored gp130.* Blood, 1993. **82**(4): p. 1120-1126.

79. Tanaka, M., Kishimura, M., Ozaki, S., Osakada, F., Hashimoto, H., Okubo, M., Murakami, M., and Nakao, K., *Cloning of novel soluble gp130 and detection of its neutralizing autoantibodies in rheumatoid arthritis.* J Clin Invest, 2000. **106**(1): p. 137-144.

80. Wolf, J., Waetzig, G.H., Chalaris, A., Reinheimer, T.M., Wegen, H., Rose-John, S., and Garbers, C., *Different soluble forms of the interleukin-6 family signal transducer gp130 fine-tune the blockade of interleukin-6 trans-signaling.* J Biol Chem, 2016. **291**(31): p. 16186-16196.

81. Garbers, C., Thaiss, W., Jones, G.W., Waetzig, G.H., Lorenzen, I., Guilhot, F., Lissilaa, R., Ferlin, W.G., Grötzinger, J., Jones, S.A., Rose-John, S., and Scheller, J., *Inhibition of classic signaling is a novel function of soluble glycoprotein 130 (sgp130), which is controlled by the ratio of interleukin 6 and soluble interleukin 6 receptor.* J Biol Chem, 2011. **286**(50): p. 42959-42970.

82. Taga, T. and Kishimoto, T., *Gp130 and the Interleukin-6 family of cytokines.* Annu Rev Immunol, 1997. **15**(1): p. 797-819.

83. Bauer, J., Lengyel, G., Bauer, T.M., Acs, G., and letters, G.-W., *Regulation of interleukin-6 receptor expression in human monocytes and hepatocytes.* FEBS Lett, 1989. **249**(1): p. 27-30.

84. Zhang, F., Yao, S., Yuan, J., Zhang, M., He, Q., Yang, G., Gao, Z., Liu, H., Chen, X., and Zhou, B., *Elevated IL-6 receptor expression on CD4+ T cells contributes to the increased Th17 responses in patients with chronic hepatitis B.* Virol J, 2011. **8**(270): p. 1-10.

85. Farahi, N., Paige, E., Balla, J., Prudence, E., Ferreira, R.C., Southwood, M., Appleby, S.L., Bakke, P., Gulsvik, A., Litonjua, A.A., Sparrow, D., Silverman, E.K., Cho, M.H., Danesh, J., Paul, D.S., Freitag, D.F., and Chilvers, E.R., *Neutrophil-mediated IL-6 receptor trans-signaling and the risk of chronic obstructive pulmonary disease and asthma.* Hum Mol Genet, 2017. **26**(8): p. 1584-1596.

86. Yamasaki, K., Taga, T., Hirata, Y., Yawata, H., Kawanishi, Y., Seed, B., Taniguchi, T., Hirano, T., and Kishimoto, T., *Cloning and expression of the human interleukin-6 (BSF-2/IFN beta 2) receptor.* Science, 1988. **241**(4867): p. 825-828.

87. Yamasaki, K., Taga, T., Hirata, Y., Yawata, H., Kawanishi, Y., Seed, B., Taniguchi, T., Hirano, T., and Kishimoto, T., *Molecular structure of interleukin 6 receptor.* Proc Japan Acad, 1988. **64**(7): p. 209-211.

88. John, S., Schooltink, H., Lenz, D., Hipp, E., Dufhues, G., Schmitz, H., Schiel, X., Hirano, T., Kishimoto, T., and Heinrich, P.C., *Studies on the structure and regulation of the human hepatic interleukin 6 receptor.* Eur J Biochem, 1990. **190**(1): p. 79-83.

89. Snyers, L., De Wit, L., and Content, J., *Glucocorticoid up-regulation of high-affinity interleukin 6 receptors on human epithelial cells.* Proc Natl Acad Sci U S A, 1990. **87**(7): p. 2838-2842.

90. Garbers, C., Kuck, F., Aparicio-Siegmund, S., Konzak, K., Kessenbrock, M., Sommerfeld, A., Häussinger, D., Lang, P., Brenner, D., Mak, T.W., Rose-John, S., Essmann, F., Schulze-Osthoff, K., Piekorz, R., and Scheller, J., *Cellular senescence or EGFR signaling induces Interleukin 6 (IL-6) receptor expression controlled by mammalian target of rapamycin (mTOR).* Cell Cycle, 2013. **12**(21): p. 3421-3432.

91. Hirata, Y., Taga, T., Hibi, M., Nakano, N., Hirano, T., and Kishimoto, T., *Characterization of IL-6 receptor expression by monoclonal and polyclonal antibodies.* J Immunol, 1989. **143**(9): p. 2900-2906.

92. Cole, A.R., Hall, N.E., Treutlein, H.R., Eddes, J.S., Reid, G.E., Moritz, R.L., and Simpson, R.J., *Disulfide bond structure and N-glycosylation sites of the extracellular domain of the human interleukin-6 receptor.* J Biol Chem, 1999. **274**(11): p. 7207-7215.

93. Riethmueller, S., Somasundaram, P., Ehlers, J.C., Hung, C.-W., Flynn, C.M., Lokau, J., Agthe, M., Düsterhöft, S., Zhu, Y., Grötzinger, J., Lorenzen, I., Koudelka, T., Yamamoto, K., Pickhinke, U., Wichert, R., Becker-Pauly, C., Rädisch, M., Albrecht, A., Hessefort, M., Stahnke, D., Unverzagt, C., Rose-John, S., Tholey, A., and Garbers, C., *Proteolytic Origin of the Soluble Human IL-6R In Vivo and a Decisive Role of N-Glycosylation.* PLoS Biol 2017. **15**(1): p. 1-31.

94. Novick, D., Engelmann, H., Wallach, D., and Rubinstein, M., *Soluble cytokine receptors are present in normal human urine.* J Exp Med, 1989. **170**(4): p. 1409-1414.

95. Garbers, C., Monhasery, N., Aparicio-Siegmund, S., Lokau, J., Baran, P., Nowell, M.A., Jones, S.A., Rose-John, S., and Scheller, J., *The interleukin-6 receptor Asp358Ala single nucleotide polymorphism rs2228145 confers increased proteolytic conversion rates by ADAM proteases.* Biochim Biophys Acta 2014. **1842**(9): p. 1485-1494.

96. Matthews, V., Schuster, B., Schütze, S., Bussmeyer, I., Ludwig, A., Hundhausen, C., Sadowski, T., Saftig, P., Hartmann, D., Kallen, K.-J., and Rose-John, S., *Cellular cholesterol depletion triggers shedding of the human interleukin-6 receptor by ADAM10 and ADAM17 (TACE).* J Biol Chem, 2003. **278**(40): p. 38829-38839.

97. Garbers, C., Jänner, N., Chalaris, A., Moss, M.L., Meyer, D., Koch-Nolte, F., Rose-John, S., and Scheller, J., *Species specificity of ADAM10 and ADAM17 proteins in interleukin-6 (IL-6) trans-signaling and novel role of ADAM10 in inducible IL-6 receptor shedding.* J Biol Chem, 2011. **286**(17): p. 14804-14811.

98. Chalaris, A., Adam, N., Sina, C., Rosenstiel, P., Lehmann-Koch, J., Schirmacher, P., Hartmann, D., Cichy, J., Gavrilova, O., Schreiber, S., Jostock, T., Matthews, V., Häsler, R., Becker, C., Neurath, M.F., Reiß, K., Saftig, P., Scheller, J., and Rose-John, S., *Critical role of the disintegrin metalloprotease ADAM17 for intestinal inflammation and regeneration in mice.* J Exp Med, 2010. **207**(8): p. 1617-1624.

99. Bank, U., Reinhold, D., Schneemilch, C., Kunz, D., Synowitz, H.-J., and Ansorge, S., *Selective Proteolytic Cleavage of IL-2 Receptor and IL-6 Receptor Ligand Binding Chains by Neutrophil-Derived Serine Proteases at Foci of Inflammation.* J Interferon Cytokine Res, 1999. **19**(11): p. 1277-1287.

100. Schumacher, N., Meyer, D., Mauermann, A., von der Heyde, J., Wolf, J., Schwarz, J., Knittler, K., Murphy, G., Michalek, M., Garbers, C., Bartsch, J.W., Guo, S., Schacher, B., Eickholz, P., Chalaris, A., Rose-John, S., and Rabe, B., *Shedding of Endogenous Interleukin-6 Receptor (IL-6R) Is Governed by A Disintegrin and Metalloproteinase (ADAM) Proteases while a Full-length IL-6R Isoform Localizes to Circulating Microvesicles.* J Biol Chem, 2015. **290**(43): p. 26059-26071.

101. Müllberg, J., Oberthür, W., Lottspeich, F., Mehl, E., Dittrich, E., Graeve, L., Heinrich, P.C., and Rose-John, S., *The soluble human IL-6 receptor. Mutational characterization of the proteolytic cleavage site.* J Immunol, 1994. **152**(10): p. 4958-4968.

102. Tucher, J., Linke, D., Koudelka, T., Cassidy, L., Tredup, C., Wichert, R., Pietrzik, C., Becker-Pauly, C., and Tholey, A., *LC–MS Based Cleavage Site Profiling of the Proteases ADAM10 and ADAM17 Using Proteome-Derived Peptide Libraries.* J Proteome Res, 2014. **13**(4): p. 2205-2214.

103. Horiuchi, S., Koyanagiu, Y., Zhouu, Y., Miyamotou, H., Tanakau, Y., Waki, M., Matsumoto, A., Yamamotou, M., and Yamamoto, N., *Soluble interleukin-6 receptors released from T cell or granulocyte/macrophage cell lines and human peripheral blood mononuclear cells are generated through an alternative splicing mechanism.* Eur J Immunol, 1994. **24**(8): p. 1945-1948.

104. Paonessa, G., Graziani, R., De Serio, A., Savino, R., Ciapponi, L., Lahm, A., Salvati, A.L., Tioniatti, C., and Ciliberto, G., *Two distinct and independent sites on IL-6 trigger gp130 dimer formation and signalling.* EMBO J, 1995. **14**(9): p. 1942-1951.

105. Yawata, H., Yasukawa, K., Natsuka, S., Murakami, M., Yamasaki, K., Hibi, M., Taga, T., and Kishimoto, T., *Structure-function analysis of human IL-6 receptor: dissociation of amino acid residues required for IL-6-binding and for IL-6 signal transduction through gp130.* EMBO J, 1993. **12**(4): p. 1705-1712.

106. Kurth, I., Horsten, U., Pflanz, S., Dahmen, H., Küster, A., Grötzinger, J., Heinrich, P.C., and Müller-Newen, G., *Activation of the signal transducer glycoprotein 130 by both IL-6 and IL-11 requires two distinct binding epitopes.* J Immunol, 1999. **162**(3): p. 1480-1487.

107. Pflanz, S., Kurth, I., Grötzinger, J., Heinrich, P.C., and Müller-Newen, G., *Two different epitopes of the signal transducer gp130 sequentially cooperate on IL-6-induced receptor activation.* J Immunol, 2000. **165**(12): p. 7042-7049.

108. Grötzinger, J., Kernebeck, T., Kallen, K.J., and Rose-John, S., *IL-6 Type Cytokine Receptor Complexes: Hexamer, Tetramer or Both?* Biol Chem, 1999. **380**(7-8): p. 803-813.

109. Somers, W., Stahl, M., and Seehra, J.S., *1.9 Å crystal structure of interleukin 6: implications for a novel mode of receptor dimerization and signaling.* EMBO J, 1997. **16**(5): p. 989-997.

110. Boulanger, M.J., Chow, D.-C., Brevnova, E.E., and Garcia, K.C., *Hexameric structure and assembly of the interleukin-6/IL-6 alpha-receptor/gp130 complex.* Science 2003. **300**(5628): p. 2101-2104.

111. Chow, D.-C., Ho, J., Nguyen Pham, T.L., Rose-John, S., and Garcia, K.C., *In Vitro Reconstitution of Recognition and Activation Complexes between Interleukin-6 and gp130.* Biochemistry, 2001. **40**(25): p. 7593-7603.

112. Garbers, C. and Rose-John, S., *Dissecting Interleukin-6 Classic- and Trans-Signaling in Inflammation and Cancer*, in *Methods Mol Biol*, B.J. Jenkins, Editor. 2018, Humana Press, New York, NY. p. 127-140.

113. Stahl, N., Boulton, T., Farruggella, T., Ip, N., Davis, S., Witthuhn, B., Quelle, F., Silvennoinen, O., Barbieri, G., and Pellegrini, S., *Association and activation of Jak-Tyk kinases by CNTF-LIF-OSM-IL-6 beta receptor components.* Science, 1994. **263**(5143): p. 92-95.

114. Rodig, S.J., Meraz, M.A., White, J.M., Lampe, P.A., Riley, J.K., Arthur, C.D., King, K.L., Sheehan, K.C.F., Yin, l., Pennica, D., Johnson Jr., E.M., and Schreiber, R.D., *Disruption of the Jak1 gene demonstrates obligatory and nonredundant roles of the Jaks in cytokine-induced biologic responses.* Cell, 1998. **93**(3): p. 373-383.

115. Stahl, N., Farruggella, T.J., Boulton, T.G., Zhong, Z., Darnell, J.E., and Yancopoulos, G.D., *Choice of STATs and other substrates specified by modular tyrosine-based motifs in cytokine receptors.* Science, 1995. **267**(5202): p. 1349-1353.

116. Gerhartz, C., Heesel, B., Sasse, J., Hemmann, U., Landgraf, C., Schneider-Mergener, J., Horn, F., Heinrich, P.C., and Graeve, L., *Differential activation of acute phase response factor/STAT3 and STAT1 via the cytoplasmic domain of the interleukin 6 signal transducer gp130 I. Definition of a novel phosphotyrosine motif mediating STAT1 activation.* J Biol Chem, 1996. **271**(22): p. 12991-12998.

117. Wegenka, U.M., Buschmann, J., Lütticken, C., Heinrich, P.C., and Horn, F., *Acute-phase response factor, a nuclear factor binding to acute-phase response elements, is rapidly activated by interleukin-6 at the posttranslational level.* Mol Cell Biol, 1993. **13**(1): p. 276-288.

118. Zhong, Z., Wen, Z., and Darnell, J.E., *Stat3: a STAT family member activated by tyrosine phosphorylation in response to epidermal growth factor and interleukin-6.* Science, 1994. **264**(5155): p. 95-98.

119. Tormo, A.J., Letellier, M.-C., Sharma, M., Elson, G., Crabé, S., and Gauchat, J.-F., *IL-6 activates STAT5 in T cells.* Cytokine, 2012. **60**(2): p. 575-582.

120. Schaper, F., Gendo, C., Eck, M., Schmitz, J., Grimm, C., Anhuf, D., Kerr, I.M., and Heinrich, P.C., *Activation of the protein tyrosine phosphatase SHP2 via the interleukin-6 signal transducing receptor protein gp130 requires tyrosine kinase Jak1 and limits acute-phase protein expression.* Biochem J, 1998. **335**(Pt 3): p. 557-565.

121. Takahashi-Tezuka, M., Yoshida, Y., Fukada, T., Ohtani, T., Yamanaka, Y., Nishida, K., Nakajima, K., Hibi, M., and Hirano, T., *Gab1 acts as an adapter molecule linking the cytokine*

receptor gp130 to ERK mitogen-activated protein kinase. Mol Cell Biol, 1998. **18**(7): p. 4109-4117.

122. Taniguchi, K., Wu, L.-W., Grivennikov, S.I., de Jong, P.R., Lian, I., Yu, F.-X., Wang, K., Ho, S.B., Boland, B.S., Chang, J.T., Sandborn, W.J., Hardiman, G., Raz, E., Maehara, Y., Yoshimura, A., Zucman-Rossi, J., Guan, K.-L., and Karin, M., *A gp130–Src–YAP module links inflammation to epithelial regeneration.* Nature, 2015. **519**(7541): p. 57-62.

123. Croker, B.A., Krebs, D.L., Zhang, J.G., Wormald, S., Willson, T.A., Stanley, E.G., Robb, L., Greenhalgh, C.J., Förster, I., Clausen, B.E., Nicola, N.A., Metcalf, D., Hilton, D.J., Roberts, A.W., and Alexander, W.S., *SOCS3 negatively regulates IL-6 signaling in vivo.* Nat Immunol, 2003. **4**(6): p. 540-545.

124. Nicholson, S.E., Souza, D.D., Fabri, L.J., Corbin, J., Wilson, T.A., Zhang, J.-G., Silva, A., Asimakis, M., Farley, A., Nash, A.D., Metcalf, D., Hilton, D.J., Nicola, N.A., and Baca, M., *Suppressor of cytokine signaling-3 preferentially binds to the SHP-2-binding site on the shared cytokine receptor subunit gp130.* Proc Natl Acad Sci U S A, 2000. **97**(12): p. 6493-6498.

125. Schmitz, J., Weissenbach, M., Haan, S., Heinrich, P.C., and Schaper, F., *SOCS3 exerts its inhibitory function on interleukin-6 signal transduction through the SHP2 recruitment site of gp130.* J Biol Chem, 2000. **275**(17): p. 12848-12856.

126. Sasaki, A., Yasukawa, H., Suzuki, A., Kamizono, S., Syoda, T., Kinjyo, I., Sasaki, M., Johnston, J.A., and Yoshimura, A., *Cytokine-inducible SH2 protein-3 (CIS3/SOCS3) inhibits Janus tyrosine kinase by binding through the N-terminal kinase inhibitory region as well as SH2 domain.* Genes Cells, 1999. **4**(6): p. 339-351.

127. Kershaw, N.J., Laktyushin, A., Nicola, N.A., and Babon, J.J., *Reconstruction of an active SOCS3-based E3 ubiquitin ligase complex in vitro: identification of the active components and JAK2 and gp130 as substrates.* Growth Factors, 2014. **32**(1): p. 1-10.

128. Liu, B., Liao, J., Rao, X., Kushner, S.A., Chung, C.D., Chang, D.D., and Shuai, K., *Inhibition of Stat1-mediated gene activation by PIAS1.* Proc Natl Acad Sci U S A, 1998. **95**(18): p. 10626-10631.

129. Chung, C.D., Liao, J., Liu, B., Rao, X., Jay, P., Berta, P., and Shuai, K., *Specific Inhibition of Stat3 Signal Transduction by PIAS3.* Science, 1997. **278**(5344): p. 1803-1805.

130. Heinrich, P.C., Bode, J., Decker, M., Graeve, L., Martens, A., Müller-Newen, G., Pflanz, S., Schaper, F., and Schmitz, J., *Termination and modulation of IL-6-type cytokine signaling*, in *Progress in Basic and Clinical Immunology*, A. Mackiewicz, M. Kurpisz, and J. Żeromski, Editors. 2001, Springer US: Boston, MA. p. 153-160.

131. Blouin, C.M. and Lamaze, C., *Interferon Gamma Receptor: The Beginning of the Journey.* Front Immunol, 2013. **4**(267): p. 1-10.

132. Roth, T.F. and Porter, K.R., *Yolk protein uptake in the oocyte of the mosquito Aedes aegypti l.* J Cell Biol, 1964. **20**: p. 313-332.

133. Pearse, B.M., *Clathrin: a unique protein associated with intracellular transfer of membrane by coated vesicles.* Proc Natl Acad Sci U S A, 1976. **73**(4): p. 1255-1259.

134. Henne, W.M., Boucrot, E., Meinecke, M., Evergren, E., Vallis, Y., Mittal, R., and McMahon, H.T., *FCHo proteins are nucleators of clathrin-mediated endocytosis.* Science 2010. **328**(5983): p. 1281-1284.

135. Collins, B.M., McCoy, A.J., Kent, H.M., Evans, P.R., and Owen, D.J., *Molecular architecture and functional model of the endocytic AP2 complex.* Cell, 2002. **109**(4): p. 523-535.

136. Shih, W., Gallusser, A., and Kirchhausen, T., *A clathrin-binding site in the hinge of the 2 chain of mammalian AP-2 complexes.* J Biol Chem, 1995. **270**(52): p. 31083-31090.

137. Conner, S.D. and Schmid, S.L., *Identification of an adaptor-associated kinase, AAK1, as a regulator of clathrin-mediated endocytosis.* J Cell Biol, 2002. **156**(5): p. 921-929.

138. Jackson, A.P., Flett, A., Smythe, C., Hufton, L., Wettey, F.R.J., and Smythe, E., *Clathrin promotes incorporation of cargo into coated pits by activation of the AP2 adaptor μ2 kinase.* J Cell Biol, 2003. **163**(2): p. 231-236.

139. Ohno, H., Fournier, M.C., Poy, G., and Bonifacino, J.S., *Structural determinants of interaction of tyrosine-based sorting signals with the adaptor medium chains.* J Biol Chem, 1996. **271**(46): p. 29009-29015.

140. Kelly, B.T., McCoy, A.J., Späte, K., Miller, S.E., Evans, P.R., Höning, S., and Owen, D.J., *A structural explanation for the binding of endocytic dileucine motifs by the AP2 complex.* Nature, 2008. **456**(7224): p. 976-979.

141. Meyerholz, A., Hinrichsen, L., Groos, S., Esk, P.C., Brandes, G., and Ungewickell, E.J., *Effect of clathrin assembly lymphoid myeloid leukemia protein depletion on clathrin coat formation.* Traffic, 2005. **6**(12): p. 1225-1234.

142. Wigge, P., Köhler, K., Vallis, Y., Doyle, C.A., Owen, D., Hunt, S.P., and McMahon, H.T., *Amphiphysin heterodimers: potential role in clathrin-mediated endocytosis.* Mol Biol Cell, 1997. **8**(10): p. 2003-2015.

143. Sundborger, A., Soderblom, C., Vorontsova, O., Evergren, E., Hinshaw, J.E., and Shupliakov, O., *An endophilin–dynamin complex promotes budding of clathrin-coated vesicles during synaptic vesicle recycling.* J Cell Sci, 2011. **124**(1): p. 133-143.

144. Kosaka, T. and Ikeda, K., *Possible temperature-dependent blockage of synaptic vesicle recycling induced by a single gene mutation in Drosophila.* J Neurobiol, 1983. **14**(3): p. 207-225.

145. Baba, T., *Role of Dynamin in Clathrin-coated Vesicle Formation.* Cold Spring Harb Symp Quant Biol, 1995. **LX**(60): p. 235-242.

146. Sweitzer, S.M. and Hinshaw, J.E., *Dynamin undergoes a GTP-dependent conformational change causing vesiculation.* Cell, 1998. **93**(6): p. 1021-1029.

147. Schlossman, D.M., Schmid, S.L., Braell, W.A., and Rothman, J.E., *An enzyme that removes clathrin coats: purification of an uncoating ATPase.* J Cell Biol, 1984. **99**(2): p. 723-733.

148. Ungewickell, E., Ungewickell, H., Holstein, S., Lindner, R., Prasad, K., Barouch, W., Martini, B., Greene, L.E., and Eisenberg, E., *Role of auxilin in uncoating clathrin-coated vesicles.* Nature, 1995. **378**(6557): p. 632-635.

149. Gerhartz, C., Dittrich, E., Stoyan, T., Rose-John, S., Yasukawa, K., Heinrich, P.C., and Graeve, L., *Biosynthesis and half-life of the interleukin-6 receptor and its signal transducer gp130.* Eur J Biochem, 1994. **223**(1): p. 265-274.

150. Thiel, S., Dahmen, H., Martens, A., Müller-Newen, G., Schaper, F., Heinrich, P.C., and Graeve, L., *Constitutive internalization and association with adaptor protein-2 of the interleukin-6 signal transducer gp130.* FEBS Lett, 1998. **441**(2): p. 231-234.

151. Zohlnhöfer, D., Graeve, L., Rose-John, S., Schooltink, H., Dittrich, E., and Heinrich, P.C., *The hepatic interleukin-6 receptor. Down-regulation of the interleukin-6 binding subunit (gp80) by its ligand.* FEBS Lett, 1992. **306**(2-3): p. 219-222.

152. Fujimoto, K., Ida, H., Hirota, Y., Ishigai, M., Amano, J., and Tanaka, Y., *Intracellular Dynamics and Fate of a Humanized Anti-Interleukin-6 Receptor Monoclonal Antibody, Tocilizumab.* Mol Pharmacol, 2015. **88**(4): p. 660-675.

153. Dittrich, E., Haft, C.R., Muys, L., Heinrich, P.C., and Graeve, L., *A di-leucine motif and an upstream serine in the interleukin-6 (IL-6) signal transducer gp130 mediate ligand-induced endocytosis and down-regulation of the IL-6 receptor.* J Biol Chem, 1996. **271**(10): p. 5487-5494.

154. Sorkin, A. and von Zastrow, M., *Endocytosis and signalling: intertwining molecular networks.* Nat Rev Mol Cell Biol, 2009. **10**(9): p. 609-622.

155. Chen, Y.-G.G., *Endocytic regulation of TGF-beta signaling.* Cell Res, 2009. **19**(1): p. 58-70.

156. German, C.L., Sauer, B.M., and Howe, C.L., *The STAT3 beacon: IL-6 recurrently activates STAT3 from endosomal structures.* Exp Cell Res, 2011. **317**(14): p. 1955-1969.

157. Schmidt-Arras, D., Müller, M., Stevanovic, M., Horn, S., Schütt, A., Bergmann, J., Wilkens, R., Lickert, A., and Rose-John, S., *Oncogenic deletion mutants of gp130 signal from intracellular compartments.* J Cell Sci, 2014. **127**(2): p. 341-353.

158. Thiel, S., Sommer, U., Kortylewski, M., Haan, C., Behrmann, I., Heinrich, P.C., and Graeve, L., *Termination of IL-6-induced STAT activation is independent of receptor internalization but requires de novo protein synthesis.* FEBS Lett, 2000. **470**(1): p. 15-19.

159. Heinrich, P.C., Behrmann, I., Haan, S., Hermanns, H.M., Müller-Newen, G., and Schaper, F., *Principles of interleukin (IL)-6-type cytokine signalling and its regulation.* Biochem J, 2003. **374**(Pt 1): p. 1-20.

160. Wang, Y. and Fuller, G.M., *Phosphorylation and internalization of gp130 occur after IL-6 activation of Jak2 kinase in hepatocytes.* Mol Biol Cell, 1994. **5**(7): p. 819-828.

161. Tanaka, Y., Tanaka, N., Saeki, Y., Tanaka, K., Murakami, M., Hirano, T., Ishii, N., and Sugamura, K., *c-Cbl-Dependent Monoubiquitination and Lysosomal Degradation of gp130.* Mol Cell Biol, 2008. **28**(15): p. 4805-4818.

162. Harding, C., Heuser, J., and Stahl, P., *Receptor-mediated endocytosis of transferrin and recycling of the transferrin receptor in rat reticulocytes.* J Cell Biol, 1983. **97**(2): p. 329-339.

163. Hopkins, C.R. and Trowbridge, I.S., *Internalization and processing of transferrin and the transferrin receptor in human carcinoma A431 cells.* J Cell Biol, 1983. **97**(2): p. 508-521.

164. van der Sluijs, P., Hull, M., Webster, P., Mâle, P., and Cell, G.B., *The small GTP-binding protein rab4 controls an early sorting event on the endocytic pathway.* Cell, 1992. **70**(5): p. 729-740.

165. Ullrich, O., Reinsch, S., Urbé, S., Zerial, M., and Parton, R.G., *Rab11 regulates recycling through the pericentriolar recycling endosome.* J Cell Biol, 1996. **135**(4): p. 913-924.

166. Sönnichsen, B., Renzis, D.S., Nielsen, E., Rietdorf, J., and Zerial, M., *Distinct membrane domains on endosomes in the recycling pathway visualized by multicolor imaging of Rab4, Rab5, and Rab11.* J Cell Biol, 2000. **149**(4): p. 901-913.

167. Pagano, A., Crottet, P., Prescianotto-Baschong, C., and Spiess, M., *In vitro formation of recycling vesicles from endosomes requires adaptor protein-1/clathrin and is regulated by rab4 and the connector rabaptin-5.* Mol Biol Cell, 2004. **15**(11): p. 4990-5000.

168. Deneka, M., Neeft, M., Popa, I., van Oort, M., Sprong, H., Oorschot, V., Klumperman, J., Schu, P., and Van der Sluijs, P., *Rabaptin-5α/rabaptin-4 serves as a linker between rab4 and γ1-adaptin in membrane recycling from endosomes.* EMBO J, 2003. **22**(11): p. 2645-2657.

169. D'Souza, R.S., Semus, R., Billings, E.A., Meyer, C., Conger, K., and Casanova, J.E., *Rab4 orchestrates a small GTPase cascade for recruitment of adaptor proteins to early endosomes.* Curr Biol, 2014. **24**(11): p. 1187-1198.

170. Kouranti, I., Sachse, M., Arouche, N., Goud, B., and Echard, A., *Rab35 regulates an endocytic recycling pathway essential for the terminal steps of cytokinesis.* Curr Biol, 2006. **16**(17): p. 1719-1725.

171. Pant, S., Sharma, M., Patel, K., Caplan, S., Carr, C.M., and Grant, B.D., *AMPH-1/Amphiphysin/Bin1 functions with RME-1/Ehd1 in endocytic recycling.* Nat Cell Biol, 2009. **11**(12): p. 1399-1410.

172. Hales, C.M., Vaerman, J.-P.P., and Goldenring, J.R., *Rab11 family interacting protein 2 associates with Myosin Vb and regulates plasma membrane recycling.* J Biol Chem, 2002. **277**(52): p. 50415-50421.

173. Lapierre, L.A., Kumar, R., Hales, C.M., Navarre, J., Bhartur, S.G., Burnette, J.O., Provance, D.W., Mercer, J.A., Bähler, M., and Goldenring, J.R., *Myosin vb is associated with plasma membrane recycling systems.* Mol Biol Cell, 2001. **12**(6): p. 1843-1857.

174. Takahashi, S., Kubo, K., Waguri, S., Yabashi, A., Shin, H.-W., Katoh, Y., and Nakayama, K., *Rab11 regulates exocytosis of recycling vesicles at the plasma membrane.* J Cell Sci, 2012. **125**(17): p. 4049-4057.

175. Johnson, J.L., He, J., Ramadass, M., Pestonjamasp, K., Kiosses, W.B., Zhang, J., and Catz, S.D., *Munc13-4 Is a Rab11-binding Protein That Regulates Rab11-positive Vesicle Trafficking and Docking at the Plasma Membrane.* J Biol Chem, 2016. **291**(7): p. 3423-3438.

176. Duve, D.C., Pressman, B.C., Gianetto, R., Wattiaux, R., and Applemans, F., *Tissue fractionation studies. 6. Intracellular distribution patterns of enzymes in rat-liver tissue.* Biochem J, 1955. **60**(4): p. 604-617.

177. Novikoff, A.B., Beaufay, H., and de Duve, C., *Electron microscopy of lysosome-rich fractions from rat liver.* J Biophys Biochem Cytol, 1956. **2**(4): p. 179-184.

178. Dell´Angelica, E.C., Mullins, C., Caplan, S., and Bonifacino, J.S., *Lysosome-related organelles.* FASEB J, 2000. **14**(10): p. 1265-1278.

179. Lefrancois, S., Zeng, J., Hassan, A.J., Canuel, M., and Morales, C.R., *The lysosomal trafficking of sphingolipid activator proteins (SAPs) is mediated by sortilin.* EMBO J, 2003. **22**(24): p. 6430-6437.

180. Reczek, D., Schwake, M., Schröder, J., Hughes, H., Blanz, J., Jin, X., Brondyk, W., Van Patten, S., Edmunds, T., and Saftig, P., *LIMP-2 is a receptor for lysosomal mannose-6-phosphate-independent targeting of β-glucocerebrosidase.* Cell, 2007. **131**(4): p. 770-783.

181. Graves, A.R., Curran, P.K., Smith, C.L., and Mindell, J.A., *The Cl-/H+ antiporter ClC-7 is the primary chloride permeation pathway in lysosomes.* Nature, 2008. **453**(7196): p. 788-792.

182. Cuppoletti, J., Aures-Fischer, D., and Sachs, G., *The lysosomal H+ pump: 8-azido-ATP inhibition and the role of chloride in H+ transport.* Biochim Biophys Acta 1987. **899**(2): p. 276-284.

183. Carlsson, S.R., Roth, J., Piller, F., and Fukuda, M., *Isolation and characterization of human lysosomal membrane glycoproteins, h-lamp-1 and h-lamp-2. Major sialoglycoproteins carrying polylactosaminoglycan.* J Biol Chem, 1988. **263**(35): p. 18911-18919.

184. Peters, C. and von Figura, K., *Biogenesis of lysosomal membranes.* FEBS Lett, 1994. **346**(1): p. 108-114.

185. Turk, V., Stoka, V., Vasiljeva, O., Renko, M., Sun, T., Turk, B., and Turk, D., *Cysteine cathepsins: from structure, function and regulation to new frontiers.* Biochim Biophys Acta, 2012. **1824**(1): p. 68-88.

186. Drenth, J., Jansonius, J.N., Koekoek, R., Swen, H.M., and Wolthers, B.G., *Structure of Papain.* Nature, 1968. **218**(5145): p. 929-932.

187. Reiser, J., Adair, B., and Reinheckel, T., *Specialized roles for cysteine cathepsins in health and disease.* J Clin Invest, 2010. **120**(10): p. 3421-3431.

188. Kaulmann, G., Palm, G.J., Schilling, K., Hilgenfeld, R., and Wiederanders, B., *The crystal structure of a Cys25→ Ala mutant of human procathepsin S elucidates enzyme–prosequence interactions.* Protein Sci, 2006. **15**(11): p. 2619-2629.

189. Turk, B., Turk, D., and Salvesen, G.S., *Regulating cysteine protease activity: essential role of protease inhibitors as guardians and regulators.* Curr Pharm Des, 2002. **8**(18): p. 1623-1637.

190. Yamaza, T., Tsuji, Y., Goto, T., Kido, M.A., Nishijima, K., Moroi, R., Akamine, A., and Tanaka, T., *Comparison in localization between cystatin C and cathepsin K in osteoclasts and other cells in mouse tibia epiphysis by immunolight and immunoelectron microscopy.* Bone, 2001. **29**(1): p. 42-53.

191. Jenko, S., Dolenc, I., Gunčar, G., Doberšek, A., Podobnik, M., and Turk, D., *Crystal structure of Stefin A in complex with cathepsin H: N-terminal residues of inhibitors can adapt to the active sites of endo-and exopeptidases.* J Mol Biol, 2003. **326**(3): p. 875-885.

192. Haves-Zburof, D., Paperna, T., Gour-Lavie, A., Mandel, I., Glass-Marmor, L., and Miller, A., *Cathepsins and their endogenous inhibitors cystatins: expression and modulation in multiple sclerosis.* J Cell Mol Med, 2011. **15**(11): p. 2421-2429.

193. Goto, T., Yamaza, T., and Tanaka, T., *Cathepsins in the osteoclast.* J Electron Microsc, 2003. **52**(6): p. 551-558.

194. Turnšek, T., Kregar, I., and Lebez, D., *Acid sulphydryl protease from calf lymph nodes.* Biochim Biophys Acta 1975. **403**(2): p. 514-520.

195. Shi, G.P., Webb, A.C., Foster, K.E., Knoll, J.H., Lemere, C.A., Munger, J.S., and Chapman, H.A., *Human cathepsin S: chromosomal localization, gene structure, and tissue distribution.* J Biol Chem, 1994. **269**(15): p. 11530-11536.

196. Nakagawa, T.Y., Brissette, W.H., Lira, P.D., Griffiths, R.J., Petrushova, N., Stock, J., McNeish, J.D., Eastman, S.E., Howard, E.D., Clarke, S.R., Rosloniec, E.F., Elliott, E.A., and Rudensky, A.Y., *Impaired invariant chain degradation and antigen presentation and diminished collagen-induced arthritis in cathepsin S null mice.* Immunity, 1999. **10**(2): p. 207-217.

197. Morton, P.A., Zacheis, M.L., S., G.K., Manning, J.A., and Schwartz, B.D., *Delivery of nascent MHC class II-invariant chain complexes to lysosomal compartments and proteolysis of invariant chain by cysteine proteases precedes peptide binding in B-lymphoblastoid cells.* J Immunol, 1995. **154**(1): p. 137-150.

198. Shi, G.P., Munger, J.S., Meara, J.P., Rich, D.H., and Chapman, H.A., *Molecular cloning and expression of human alveolar macrophage cathepsin S, an elastinolytic cysteine protease.* J Biol Chem, 1992. **267**(11): p. 7258-7262.

199. Turkenburg, J.P., Lamers, M.B., Brzozowski, A.M., Wright, L.M., Hubbard, R.E., Sturt, S.L., and Williams, D.H., *Structure of a Cys25-->Ser mutant of human cathepsin S.* Acta Crystallogr D Biol Crystallogr 2002. **58**(Pt 3): p. 451-455.

200. McGrath, M.E., Palmer, J.T., Brömme, D., and Somoza, J.R., *Crystal structure of human cathepsin S.* Protein Sci, 1998. **7**(6): p. 1294-1302.

201. Rückrich, T., Brandenburg, J., Cansier, A., M., M., Stevanovic, S., Schilling, K., Wiederanders, B., Beck, A., Melms, A., Reich, M., Driessen, C., and Kalbacher, H., *Specificity of human cathepsin S determined by processing of peptide substrates and MHC class II-associated invariant chain.* Biol Chem, 2006. **387**(10-11): p. 1503-1511.

202. Brömme, D., Bonneau, P.R., Lachance, P., Wiederanders, B., Kirschke, H., Peters, C., Thomas, D.Y., Storer, A.C., and Vernet, T., *Functional expression of human cathepsin S in Saccharomyces cerevisiae. Purification and characterization of the recombinant enzyme.* J Biol Chem, 1993. **268**(7): p. 4832-4838.

203. Kirschke, H., Wiederanders, B., Brömme, D., and Rinne, A., *Cathepsin S from bovine spleen. Purification, distribution, intracellular localization and action on proteins.* Biochem J, 1989. **264**(2): p. 467-473.

204. Jordans, S., Jenko-Kokalj, S., Kühl, N.M., Tedelind, S., Sendt, W., Brömme, D., Turk, D., and Brix, K., *Monitoring compartment-specific substrate cleavage by cathepsins B, K, L, and S at physiological pH and redox conditions.* BMC Biochem, 2009. **10**(23): p. 1-15.

205. Wang, B., Sun, J., Kitamoto, S., Yang, M., Grubb, A., Chapman, H.A., Kalluri, R., and Shi, G.P., *Cathepsin S controls angiogenesis and tumor growth via matrix-derived angiogenic factors.* J Biol Chem, 2006. **281**(9): p. 6020-6029.

206. Burden, R.E., Gormley, J.A., Jaquin, T.J., Small, D.M., Quinn, D.J., Hegarty, S.M., Ward, C., Walker, B., Johnston, J.A., Olwill, S.A., and Scott, C.J., *Antibody-mediated inhibition of cathepsin S blocks colorectal tumor invasion and angiogenesis.* Clin Cancer Res, 2009. **15**(19): p. 6042-6051.

207. Petanceska, S., Canoll, P., and Devi, L.A., *Expression of rat cathepsin S in phagocytic cells.* J Biol Chem, 1996. **271**(8): p. 4403-4409.

208. Riese, R.J., Wolf, P.R., Brömme, D., Natkin, L.R., Villadangos, J.A., Ploegh, H.L., and Chapman, H.A., *Essential role for cathepsin S in MHC class II-associated invariant chain processing and peptide loading.* Immunity, 1996. **4**(4): p. 357-366.

209. Schurigt, U., *Role of cysteine cathepsins in joint inflammation and destruction in human rheumatoid arthritis and associated animal models*. Innovative Rheumatology. 2013: InTech.

210. Beck, H., Schwarz, G., Schröter, C.J., Deeg, M., Baier, D., Stevanovic, S., Weber, E., Driessen, C., and Kalbacher, H., *Cathepsin S and an asparagine-specific endoprotease dominate the proteolytic processing of human myelin basic protein in vitro.* Eur J Immunol, 2001. **31**(12): p. 3726-3736.

211. Gocheva, V., Zeng, W., Ke, D., Klimstra, D., Reinheckel, T., Peters, C., Hanahan, D., and Joyce, J.A., *Distinct roles for cysteine cathepsin genes in multistage tumorigenesis.* Genes Dev, 2006. **20**(5): p. 543-556.

212. Fan, Q., Wang, X., Zhang, H., Li, C., Fan, J., and Xu, J., *Silencing cathepsin S gene expression inhibits growth, invasion and angiogenesis of human hepatocellular carcinoma in vitro.* Biochem Biophys Res Commun, 2012. **425**(4): p. 703-710.

213. Watson, J. and Riblet, R., *Genetic control of responses to bacterial lipopolysaccharides in mice I. Evidence for a Single Gene that Influences Mitogenic and Immunogenic Respones to Lipopolysaccharides.* J Exp Med, 1974. **140**(5): p. 1147-1161.

214. Watson, J., Riblet, R., and Taylor, B.A., *The response of recombinant inbred strains of mice to bacterial lipopolysaccharides.* J Immunol, 1977. **118**(6): p. 2088-2093.

215. Watson, J., Kelly, K., Largen, M., and Taylor, B.A., *The genetic mapping of a defective LPS response gene in C3H/HeJ mice.* J Immunol, 1978. **120**(2): p. 422-424.

216. Poltorak, A., Smirnova, I., He, X., Liu, M.Y., Huffel, V.C., McNally, O., Birdwell, D., Alejos, E., Silva, M., Du, X., Thompson, P., Chan, E.K., Ledesma, J., Roe, B., Clifton, S., Vogel, S.N., and Beutler, B., *Genetic and physical mapping of the Lps locus: identification of the toll-4 receptor as a candidate gene in the critical region.* Blood Cells Mol Dis, 1998. **24**(3): p. 340-355.

217. Rock, F.L., Hardiman, G., Timans, J.C., Kastelein, R.A., and Bazan, F.J., *A family of human receptors structurally related to Drosophila Toll.* Proc Natl Acad Sci U S A, 1998. **95**(2): p. 588-593.

218. Moresco, E.Y., LaVine, D., and Beutler, B., *Toll-like receptors.* Curr Biol, 2011. **21**(13): p. R488-R493.

219. Leifer, C.A. and Medvedev, A.E., *Molecular mechanisms of regulation of Toll-like receptor signaling.* J Leukoc Biol, 2016. **100**(5): p. 927-941.

220. Botos, I., Segal, D.M., and Davies, D.R., *The structural biology of Toll-like receptors.* Structure, 2011. **19**(4): p. 447-459.

221. Kawai, T. and Akira, S., *The role of pattern-recognition receptors in innate immunity: update on Toll-like receptors.* Nat Immunol, 2010. **11**(5): p. 373-384.

222. Lee, C.C., Avalos, A.M., and L., P.H., *Accessory molecules for Toll-like receptors and their function.* Nat Rev Immunol, 2012. **12**(3): p. 168-179.

223. Yan, I., Schwarz, J., Lücke, K., Schumacher, N., Schumacher, V., Schmidt, S., Rabe, B., Saftig, P., Donners, M., Rose-John, S., Mittrücker, H.-W.W., and Chalaris, A., *ADAM17 controls IL-6 signaling by cleavage of the murine IL-6Rα from the cell surface of leukocytes during inflammatory responses.* J Leukoc Biol, 2016. **99**(5): p. 749-760.

224. Flo, T.H., Halaas, O., Torp, S., Ryan, L., Lien, E., Dybdahl, B., Sundan, A., and Espevik, T., *Differential expression of Toll-like receptor 2 in human cells.* J Leukoc Biol, 2001. **69**(3): p. 474-481.

225. Komai-Koma, M., Jones, L., Ogg, G.S., Xu, D., and Liew, F.Y., *TLR2 is expressed on activated T cells as a costimulatory receptor.* Proc Natl Acad Sci U S A, 2004. **101**(9): p. 3029-3034.

226. Alexopoulou, L., Thomas, V., Schnare, M., Lobet, Y., Anguita, J., Schoen, R.T., Medzhitov, R., Fikrig, E., and Flavell, R.A., *Hyporesponsiveness to vaccination with Borrelia burgdorferi OspA in humans and in TLR1- and TLR2-deficient mice.* Nat Med, 2002. **8**(8): p. 878-884.

227. Takeuchi, O., Kawai, T., Mühlradt, P.F., Morr, M., Radolf, J.D., Zychlinsky, A., Takeda, K., and Akira, S., *Discrimination of bacterial lipoproteins by Toll-like receptor 6.* Int Immunol, 2001. **13**(7): p. 933-940.

228. Takeuchi, O., Sato, S., Horiuchi, T., Hioshino, K., Takeda, K., Dong, Z., Modlin, R.L., and Akira, S., *Cutting edge: role of Toll-like receptor 1 in mediating immune response to microbial lipoproteins.* J Immunol, 2002. **169**(1): p. 10-14.

229. Buwitt-Beckmann, U., Heine, H., Wiesmüller, K.-H., Jung, G., Brock, R., Akira, S., and Ulmer, A.J., *TLR1-and TLR6-independent recognition of bacterial lipopeptides.* J Biol Chem, 2006. **281**(14): p. 9049-9057.

230. Schaefer, L., Babelova, A., Kiss, E., Hausser, H.-J.J., Baliova, M., Krzyzankova, M., Marsche, G., Young, M.F., Mihalik, D., Götte, M., Malle, E., Schaefer, R.M., and Gröne, H.-J.J., *The matrix component biglycan is proinflammatory and signals through Toll-like receptors 4 and 2 in macrophages.* J Clin Invest, 2005. **115**(8): p. 2223-2233.

231. Jiang, D., Liang, J., Fan, J., Yu, S., Chen, S., Luo, Y., Prestwich, G.D., Mascarenhas, M.M., Garg, H.G., Quinn, D.A., Homer, R.J., Goldstein, D.R., Bucala, R., Lee, P.J., Medzhitov, R., and Noble, P.W., *Regulation of lung injury and repair by Toll-like receptors and hyaluronan.* Nat Med, 2005. **11**(11): p. 1173-1179.

232. Kim, S., Takahashi, H., Lin, W.-W., Descargues, P., Grivennikov, S., Kim, Y., Luo, J.-L., and Karin, M., *Carcinoma-produced factors activate myeloid cells through TLR2 to stimulate metastasis.* Nature, 2009. **457**(7225): p. 102-106.

233. Hoebe, K., Georgel, P., Rutschmann, S., Du, X., Mudd, S., Crozat, K., Sovath, S., Shamel, L., Hartung, T., Zähringer, U., and Beutler, B., *CD36 is a sensor of diacylglycerides.* Nature, 2005. **433**(7025): p. 523-527.

234. Triantafilou, M., Gamper, F.G.J., Haston, R.M., Mouratis, M.A., Morath, S., Hartung, T., and Triantafilou, K., *Membrane sorting of toll-like receptor (TLR)-2/6 and TLR2/1 heterodimers at the cell surface determines heterotypic associations with CD36 and intracellular targeting.* J Biol Chem, 2006. **281**(41): p. 31002-31011.

235. Jimenez-Dalmaroni, M.J., Xiao, N., Corper, A.L., Verdino, P., Ainge, G.D., Larsen, D.S., Painter, G.F., Rudd, P.M., Dwek, R.A., Hoebe, K., Beutler, B., and Wilson, I.A., *Soluble CD36 ectodomain binds negatively charged diacylglycerol ligands and acts as a co-receptor for TLR2.* PloS One, 2009. **4**(10): p. 1-12.

236. Manukyan, M., Triantafilou, K., Triantafilou, M., Mackie, A., Nilsen, N., Espevik, T., Wiesmüller, K.-H.H., Ulmer, A.J., and Heine, H., *Binding of lipopeptide to CD14 induces physical proximity of CD14, TLR2 and TLR1.* Eur J Immunol, 2005. **35**(3): p. 911-921.

237. Gerold, G., Abu Ajaj, K., Bienert, M., Laws, H.-J., Zychlinsky, A., and de Diego, J.L., *A Toll-like receptor 2–integrin β3 complex senses bacterial lipopeptides via vitronectin.* Nat Immunol, 2008. **9**(7): p. 761-768.

238. Shin, D.-M.M., Yang, C.-S.S., Yuk, J.-M.M., Lee, J.-Y.Y., Kim, K.H., Shin, S.J., Takahara, K., Lee, S.J., and Jo, E.-K.K., *Mycobacterium abscessus activates the macrophage innate immune response via a physical and functional interaction between TLR2 and dectin-1.* Cell Microbiol, 2008. **10**(8): p. 1608-1621.

239. Arbibe, L., Mira, J.P., Teusch, N., Kline, L., Guha, M., Mackman, N., Godowski, P.J., Ulevitch, R.J., and Knaus, U.G., *Toll-like receptor 2-mediated NF-kappa B activation requires a Rac1-dependent pathway.* Nat Immunol, 2000. **1**(6): p. 533-40.

240. Lin, S.-C., Lo, Y.-C., and Wu, H., *Helical assembly in the MyD88–IRAK4–IRAK2 complex in TLR/IL-1R signalling.* Nature, 2010. **465**(7300): p. 885-890.

241. Gray, P., Dunne, A., Brikos, C., Jefferies, C.A., Doyle, S.L., and O'Neill, L.A.J., *MyD88 adapter-like (Mal) is phosphorylated by Bruton's tyrosine kinase during TLR2 and TLR4 signal transduction.* J Biol Chem, 2006. **281**(15): p. 10489-10495.

242. Fearns, C., Pan, Q., Mathison, J.C., and Chuang, T.H., *Triad3A regulates ubiquitination and proteasomal degradation of RIP1 following disruption of Hsp90 binding.* J Biol Chem, 2006. **281**(45): p. 34592-34600.

243. Mansell, A., Smith, R., Doyle, S.L., Gray, P., Fenner, J.E., Crack, P.J., Nicholson, S.E., Hilton, D.J., O'Neill, L.A.J., and Hertzog, P.J., *Suppressor of cytokine signaling 1 negatively regulates Toll-like receptor signaling by mediating Mal degradation.* Nat Immunol, 2006. **7**(2): p. 148-155.

244. Langjahr, P., Díaz-Jiménez, D., De la Fuente, M., Rubio, E., Golenbock, D., Bronfman, F.C., Quera, R., González, M.-J.J., and Hermoso, M.A., *Metalloproteinase-dependent TLR2 ectodomain shedding is involved in soluble toll-like receptor 2 (sTLR2) production.* PloS One, 2014. **9**(12): p. 1-20.

245. Kuroishi, T., Tanaka, Y., Sakai, A., Sugawara, Y., Komine, K.-I., and Sugawara, S., *Human parotid saliva contains soluble toll-like receptor (TLR) 2 and modulates TLR2-mediated interleukin-8 production by monocytic cells.* Mol Immunol, 2007. **44**(8): p. 1969-1976.

246. LeBouder, E., Rey-Nores, J.E., Rushmere, N.K., Grigorov, M., Lawn, S.D., Affolter, M., Griffin, G.E., Ferrara, P., Schiffrin, E.J., Morgan, B.P., and Labéta, M.O., *Soluble forms of Toll-like receptor (TLR)2 capable of modulating TLR2 signaling are present in human plasma and breast milk.* J Immunol, 2003. **171**(12): p. 6680-6689.

247. Dulay, A.T., Buhimschi, C.S., Zhao, G., Oliver, E.A., Mbele, A., Jing, S., and Buhimschi, I.A., *Soluble TLR2 is present in human amniotic fluid and modulates the intraamniotic inflammatory response to infection.* J Immunol, 2009. **182**(11): p. 7244-7253.

248. Chalaris, A., *Apoptosis is a natural stimulus of IL-6R shedding and contributes to the proinflammatory trans-signalling function of neutrophils*. 2007. Dissertation at the CAU Kiel

249. Ketteler, R., Glaser, S., Sandra, O., Martens, U.M., and Klingmüller, U., *Enhanced transgene expression in primitive hematopoietic progenitor cells and embryonic stem cells efficiently transduced by optimized retroviral hybrid vectors.* Gene Ther, 2002. **9**(8): p. 477-487.

250. van Dam, M., Müllberg, J., Schooltink, H., Stoyan, T., Brakenhoff, J.P.J., Graeve, L., Heinrich, P.C., and Rose-John, S., *Structure-function analysis of interleukin-6 utilizing human/murine chimeric molecules. Involvement of two separate domains in receptor binding.* J Biol Chem, 1993. **268**(20): p. 15285-15290.

251. Fischer, M., Goldschmitt, J., Peschel, C., Brakenhoff, J.P., Kallen, K.J., Wollmer, A., Grötzinger, J., and Rose-John, S., *I. A bioactive designer cytokine for human hematopoietic progenitor cell expansion.* Nat Biotechnol, 1997. **15**(2): p. 142-145.

252. Schroers, A., Hecht, O., Kallen, K.J., Pachta, M., Rose-John, S., and Grötzinger, J., *Dynamics of the gp130 cytokine complex: a model for assembly on the cellular membrane.* Protein Sci, 2005. **14**(3): p. 783-790.

253. Riethmueller, S., Ehlers, J.C., Lokau, J., Düsterhöft, S., Knittler, K., Dombrowsky, G., Grötzinger, J., Rabe, B., Rose-John, S., and Garbers, C., *Cleavage Site Localization Differentially Controls Interleukin-6 Receptor Proteolysis by ADAM10 and ADAM17.* Sci Rep, 2016. **6**(25550): p. 1-14.

254. Vollmer, P., Oppmann, B., Voltz, N., Fischer, M., and Rose-John, S., *A role for the immunoglobulin-like domain of the human IL-6 receptor: intracellular protein transport and shedding.* Eur J Biochem, 1999. **263**(2): p. 438-446.

255. Stautz, D., Leyme, A., Grandal, M.V., Albrechtsen, R., van Deurs, B., Wewer, U., and Kveiborg, M., *Cell-surface metalloprotease ADAM12 is internalized by a clathrin- and Grb2-dependent mechanism.* Traffic, 2012. **13**(11): p. 1532-1546.

256. Basagiannis, D. and Christoforidis, S., *Constitutive Endocytosis of VEGFR2 Protects the Receptor against Shedding.* J Biol Chem, 2016. **291**(32): p. 16892-16903.

257. von Kleist, L., Stahlschmidt, W., Bulut, H., Gromova, K., Puchkov, D., Robertson, M.J., MacGregor, K.A., Tomilin, N., Pechstein, A., Chau, N., Chircop, M., Sakoff, J., von Kries, J.P., Saenger, W., Kräusslich, H.-G.G., Shupliakov, O., Robinson, P.J., McCluskey, A., and Haucke, V., *Role of the clathrin terminal domain in regulating coated pit dynamics revealed by small molecule inhibition.* Cell, 2011. **146**(3): p. 471-484.

258. McCluskey, A., Daniel, J.A., Hadzic, G., Chau, N., Clayton, E.L., Mariana, A., Whiting, A., Gorgani, N.N., Lloyd, J., Quan, A., Moshkanbaryans, L., Krishnan, S., Perera, S., Chircop, M., von Kleist, L., McGeachie, A.B., Howes, M.T., Parton, R.G., Campbell, M., Sakoff, J.A., Wang, X., Sun, J.-Y.Y., Robertson, M.J., Deane, F.M., Nguyen, T.H., Meunier, F.A., Cousin, M.A., and Robinson, P.J., *Building a better dynasore: the dyngo compounds potently inhibit dynamin and endocytosis.* Traffic 2013. **14**(12): p. 1272-1289.

259. Boucrot, E., Ferreira, A.P.A., Almeida-Souza, L., Debard, S., Vallis, Y., Howard, G., Bertot, L., Sauvonnet, N., and McMahon, H.T., *Endophilin marks and controls a clathrin-independent endocytic pathway.* Nature, 2015. **517**: p. 460-488.

260. Ullah, M., Revez, J.A., Loh, Z., Simpson, J., Zhang, V., Bain, L., Varelias, A., Rose-John, S., Blumenthal, A., and Smyth, M.J., *Allergen-induced IL-6 trans-signaling activates T cells to promote type 2 and type 17 airway inflammation.* J Allergy Clin Immunol, 2015. **136**(4): p. 1065-1073.

261. Chen, X., Meng, X., Foley, N.M., Shi, X., Liu, M., Chai, Y., Li, Y., Redmond, H.P., Wang, J., and Wang, J.H., *Activation of the TLR2-mediated downstream signaling pathways NF-kappaB and MAPK is responsible for B7-H3-augmented inflammatory response during S. pneumoniae infection.* J Neuroimmunol, 2017. **310**: p. 82-90.

262. Lu, Z., Xie, D., Chen, Y., Tian, E., Muhammad, I., Chen, X., Miao, Y., Hu, W., Wu, Z., Ni, H., Xin, J., Li, Y., and Li, J., *TLR2 mediates autophagy through ERK signaling pathway in Mycoplasma gallisepticum-infected RAW264.7 cells.* Mol Immunol, 2017. **87**: p. 161-170.

263. Baran, P., Nitz, R., Grötzinger, J., Scheller, J., and Garbers, C., *Minimal Interleukin 6 (IL-6) Receptor Stalk Composition for IL-6 Receptor Shedding and IL-6 Classic Signaling.* J Biol Chem, 2013. **288**(21): p. 14756-14768.

264. Dittrich, E., Rose-John, S., Gerhartz, C., Müllberg, J., Stoyan, T., Yasukawa, K., Heinrich, P.C., and Graeve, L., *Identification of a region within the cytoplasmic domain of the interleukin-6 (IL-6) signal transducer gp130 important for ligand-induced endocytosis of the IL-6 receptor.* J Biol Chem, 1994. **269**(29): p. 19014-19020.

265. Moraga, I., Richter, D., Wilmes, S., Winkelmann, H., Jude, K., Thomas, C., Suhoski, M.M., Engleman, E.G., Piehler, J., and Garcia, K.C., *Instructive roles for cytokine-receptor binding parameters in determining signaling and functional potency.* Sci Signal, 2015. **8**(402): p. ra114 1-ra114 17.

266. Rose-John, S., *IL-6 trans-signaling via the soluble IL-6 receptor: importance for the pro-inflammatory activities of IL-6.* Int J Biol Sci, 2012. **8**(9): p. 1237-1247.

267. Oberg, H.-H., Ly, T.T.H., Ussat, S., Meyer, T., Kabelitz, D., and Wesch, D., *Differential but Direct Abolishment of Human Regulatory T Cell Suppressive Capacity by Various TLR2 Ligands.* J Immunol, 2010. **184**(9): p. 4733-4740.

268. Briso, E.M., Dienz, O., and Rincon, M., *Cutting Edge: Soluble IL-6R Is Produced by IL-6R Ectodomain Shedding in Activated CD4 T Cells.* J Immunol, 2008. **180**(11): p. 7102-7106.

269. Navar, L.G., Gooz, M., Bell, H.L., and Gööz, M., *ADAM-17 Is Activated by the Mitogenic Protein Kinase ERK in a Model of Kidney Fibrosis.* Am J Med Sci, 2010. **339**(2): p. 105-107.

270. Brew, K. and Nagase, H., *The tissue inhibitors of metalloproteinases (TIMPs): An ancient family with structural and functional diversity.* Biochim Biophys Acta 2010. **1803**(1): p. 55-71.

271. Mavilio, M., Marchetti, V., Fabrizi, M., Stöhr, R., Marino, A., Casagrande, V., Fiorentino, L., Cardellini, M., Kappel, B., Monteleone, I., Garret, C., Mauriello, A., Monteleone, G., Farcomeni, A., Burcelin, R., Menghini, R., and Federici, M., *A Role for Timp3 in Microbiota-Driven Hepatic Steatosis and Metabolic Dysfunction.* Cell Rep, 2016. **16**(3): p. 731-743.

7 Appendix

Abbreviations

A	ampere
aa	amino-acid
AAK1	adaptor-associated kinase 1
ADAM	a disintegrin and metalloprotease
ANTH	AP180 N-terminal homology
AP	alkaline phosphatase
AP-2	adaptor protein 2
AP180	adaptor protein 180
APC	allophycocyanin
Arf6	ADP-ribosylation factor 6
BCA	bicinchoninic acid
bp	base pair
Btk	Bruton's tyrosine kinase
BSA	bovine serum albumin
CALM	clathrin assembly lymphoid myeloid leukemia protein
CBM	cytokine binding module
CLC	cardiotrophin-1 like cytokine
CLIC/GEEC	clathrin-independent carriers/GPI-enriched endocytic compartment
CNTF	ciliary neurotrophic factor
CT-1	cardiotrophin-1
ctrl	control
CTSS	cathepsin S
DAPI	4′,6-diamidino-2-phenylindole
DC	dendritic cell
DMEM	Dulbecco's modified Eagle's Medium
DMSO	dimethyl sulfoxide
DNA	deoxyribonucleic acid
dnp	2,4-dinitrophenyl
ECD	extracellular domain
ECL	enhanced chemiluminescence
ECM	extracellular matrix
EDTA	ethylenediaminetetraacetic acid
EGF	epidermal growth factor

ELISA	enzyme-linked immunosorbent assay
em	emission
EPSIN15	EGFR pathway substrate 15
ER	endoplasmic reticulum
ERK	extracellular signal regulated kinase
FACS	fluorescence-activated cell sorting
FCHO	FCH domain only protein
FCS	fetal calf serum
g	acceleration of gravity
Gab1	Grb2-associated binding protein 1
GAK	cyclin-G associated kinase
GAPDH	glyceraldehyde 3-phosphate dehydrogenase
GFP	green fluorescent protein
GI	GI254023X (ADAM10 Inhibitor)
gp130	glycoprotein 130
GPL	gp130-like
Grb2	growth factor receptor-bound protein 2
GTP	guanosine triphosphate
GW	GW280264X (ADAM10- und ADAM17 Inhibitor)
h	hour
HGMB1	high-mobility group box 1
HKLM	heat-killed *Listeria monocytogenes*
HRP	horse-radish peroxidase
HSC70	heat shock cognate 70
ICD	intracellular domain
Ig	immunoglobulin
IL	interleukin
IL-6R	interleukin-6 receptor
IRAK	interleukin-1 receptor associated kinase
JAK	Janus kinase
kb	kilobases
kDa	kilo Dalton
LAMP-2	Lysosome-associated membrane protein 2
LB	lysogeny broth
LIF	leukemia inhibitory factor
LIMP-2	lysosomal integral membrane protein type 2
LPS	lipopolysaccharide

LRR	leucine-rich repeats
M	molar
M6P	mannose-6-phosphate
MACS	magnetic activated cell sorting
MAPK	mitogen-activated protein kinase
MBP	myelin basic protein
mca	7-methyloxycoumarin-4-yl
MFI	mean fluorescent intensity
µg	microgram
mg	milligram
MHC	major histocompatibility complex
min	minute
µl	microlitre
ml	millilitre
mm	millimeter
µM	micromolar
mM	millimolar
MM	Marimastat
MMP	matrix-metalloprotease
mRNA	messenger ribonucleic acid
MyD88	Myeloid differentiation primary response 88
Myo Vb	Myosin Vb
NF-κB	nuclear factor kappa B
ng	nanogram
NK	natural killer cell
nm	nanometer
OSM	oncostatin M
PAGE	polyacrylamide gel electrophoresis
PAMP	pathogen-associated microbial peptide
PBMC	peripheral blood mononuclear cell
PBS	phosphate buffered saline
PCR	polymerase chain reaction
PFA	paraformaldehyde
pg	picogram
PI3K	phosphoinositide-3-kinase
PIAS	protein inhibitor of activated STAT
PIP2	phosphatidylinositol-4,5-bisphosphate

PMA	phorbol-12-myristate-13-acetate
POD	peroxidase
PRR	pattern-recognition receptors
PVDF	polyvinylidene difluoride
RA	rheumatoid arthritis
Rab11-FIP2	Rab11-family interacting protein 2
Ras	rat sarcoma
RBP	RNA-binding protein
RFU	relative fluorescence unit
RLU	relative light units
rpm	rounds per minute
RPMI	Roswell Park Memorial Institute
SDS	sodium dodecylsulfate
Sec	second
SEM	standard error of means
sgp130	soluble glycoprotein 130
SHP-2	Src homology-2 domain containing phosphatase 2
sIL-6R	soluble interleukin-6 receptor
SNP	single nucleotide polymorphism
SOCS3	suppressor of cytokine signaling 3
SOE-PCR	splicing by overlap extension PCR
SOS	son of sevenless
STAT	transducer and activator of transcription
TBS	Tris-buffered saline
TCA	trichloroacetic acid
Tf	transferrin
TfR	transferrin receptor
TIR domain	Toll IL-1 receptor domain
TIRAP	TIR domain containing adaptor protein
TLR	Toll-like receptor
TM	transmembrane
TNF-α	tumor necrosis factor alpha
TRAM	TRIF-related adaptor molecule
TRIF	TIR-domain-containing adapter-inducing interferon-β
Tyk2	tyrosine kinase 2
U	unit
V	volts

wt	wild-type
YAP	yes-associated protein

Plasmids

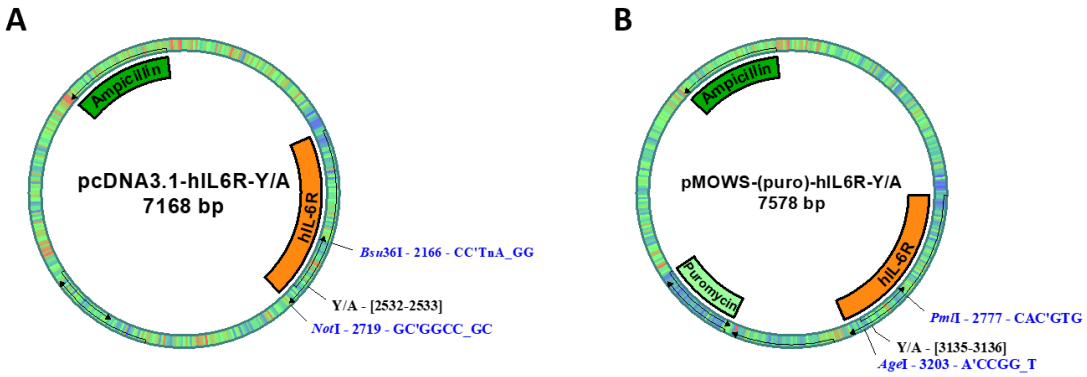

Figure 7.1: Maps of the generated plasmids pcDNA3.1-hIL-6R-Y/A and pMOWS-(puro)-hIL-6R-Y/A. Depicted are the maps of (A) the pcDNA3.1-hIL-6R-Y/A plasmid and (B) the pMOWS-(puro)-hIL-6R-Y/A plasmid. The DNA sequence coding for the hIL-6R is highlighted in orange, the DNA sequence coding for ampicillin is highlighted in green and the DNA sequence coding for puromycin is highlighted in light green. The restriction sites used for the enzymatic digestions are marked in blue, the site of the Y/A-mutation is marked in black.

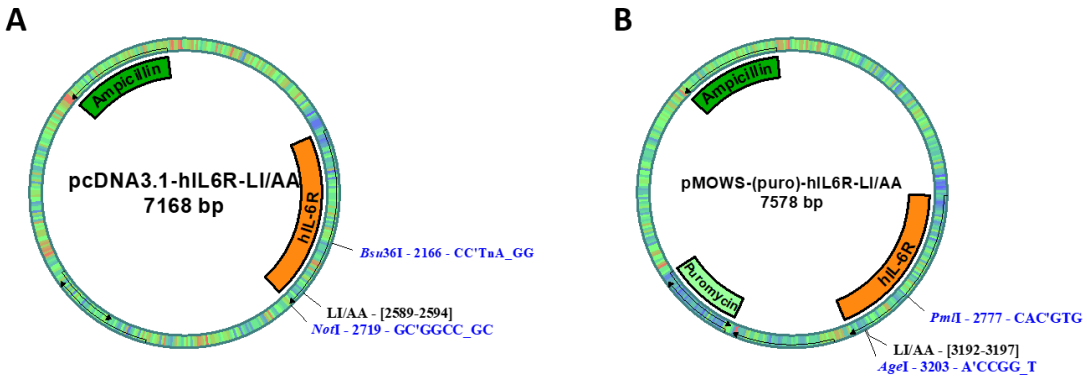

Figure 7.2: Maps of the generated plasmids pcDNA3.1-hIL-6R-LI/AA and pMOWS-(puro)-hIL-6R-LI/AA. Depicted are the maps of (A) the pcDNA3.1-hIL-6R-LI/AA plasmid and (B) the pMOWS-(puro)-hIL-6R-LI/AA plasmid. The DNA sequence coding for the hIL-6R is highlighted in orange, the DNA sequence coding for ampicillin is highlighted in green and the DNA sequence coding for puromycin is highlighted in light green. The restriction sites used for the enzymatic digestions are marked in blue, the site of the LI/AA-mutation is marked in black.

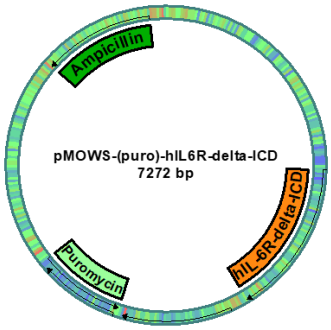

Figure 7.3: Map of the generated plasmids pMOWS-(puro)-hIL-6R-delta-ICD. Depicted is the map of the pMOWS-(puro)-hIL-6R-delta-ICD plasmid. The DNA sequence coding for the hIL-6R-delta-ICD is highlighted in orange, the DNA sequence coding for ampicillin is highlighted in green and the DNA sequence coding for puromycin is highlighted in light green.

Publications

Flynn, C.M., Wiechert, R., Lokau, J., Gerneth, A., Garbers, Y., Aparicio-Siegmund, S., Garbers, C., *Identification of Cathepsin S as a novel protease capable of cleaving membrane-bound Interleukin-6 receptor*. 2018 (in preparation)

Flynn, C.M., Kespohl, B., Daunke, T., Garbers, C., Garbers, Y., Aparicio-Siegmund, S., *Cell-surface levels of the Interleukin-6 receptor are controlled by proteolysis, internalization and recycling*. 2018 (in preparation)

Flynn, C.M., Garbers, Y., Lokau J., Wesch, D., Laudes, M., Aparicio-Siegmund, S., Garbers, C., *Activation of Toll-like Receptor 2 (TLR2) induces Interleukin-6 trans-signaling*. 2018 (submitted)

Agthe, M., Brügge, J., Garbers, Y., Wandel, M., Kespohl, B., Arnold, P., **Flynn, C.M.**, Lokau, J., Bretscher, C., Waetzig, G.H., Putoczki, T., Grötzinger, J., Garbers, C., *Mutations in craniosynostosis patients cause defective interleukin-11 receptor maturation and drive craniosynostosis-like disease in mice.* Cell Rep, 2018. 25(1):10-18.

Lokau, J., **Flynn, C.M**., Garbers, C., *Cleavage of the Interleukin-11 receptor induces processing of its C-terminal fragments by the gamma-secretase and the proteasome*. Biochemical and biophysical research communication, 2017. 491(2):296-302.

Lokau, J., Agthe, M., **Flynn, C.M.**, Garbers, C., *Proteolytic control of Interleukin-11 and Interleukin-6 biology.* Biochimica et biophysica acta, 2017. 1864(11 Pt B):2105-2117.

Riethmueller, S., Somasundaram, P., Ehler, J.C., Hung, C.W., **Flynn, C.M.**, Lokau, J., Agthe, M., Düsterhöft, S., Zhu, Y., Lorenzen, I., Koudelka, T., Yamamoto, K., Pickhinke, U., Wichert, R., Becker-Pauly, C., Rädisch, M., Albrecht, A., Hessefort, M., Stahnke, D., Unverzagt, C., Rose-John, S., Tholey, A., Garbers, C., *Proteolytic Origin of the Soluble Human IL-6R In Vivo and a Decisive Role of N-Gylcosylation*. PLoS biology, 2017. 15(1):e2000080.

Danksagungen

Zu guter Letzt möchte ich mich bei all denen bedanken, die mich während meiner Doktorandenzeit unterstützt und begleitet haben. Insbesondere möchte ich mich bei den folgenden Personen bedanken:

Prof. Dr. Stefan Rose-John, für die Möglichkeit meine Doktorarbeit am Biochemischen Institut anzufertigen und für die vielen Kommentare und Anregungen während der vielen Progress Reports.

Prof. Dr. Christoph Garbers, für die Möglichkeit in seiner Arbeitsgruppe an meiner Doktorarbeit zu arbeiten und die tolle Betreuung. Danke, dass du mein Potential erkannt und mich in deiner Gruppe aufgenommen hast. Auch wenn es mal nicht so erfolgreich lief, hast du an mich geglaubt, mich unterstützt und mich aufgebaut. Danke dafür!

Dr. Samadhi Aparicio-Siegmund, für die liebevolle Betreuung und Hilfe. Danke, dass du dir immer Zeit für mich genommen hast, mich ermutigt hast und dass ich mit allem zu dir kommen konnte. Auch während deiner Babypause hattest du immer ein offenes Ohr für mich und hast mich aus der Ferne unterstützt. Danke dafür!

Jule und Maria, für die großartige Zusammenarbeit und die wunderbare Zeit im Labor. Danke, dass ich bei Fragen immer zu euch kommen konnte, und Danke für eure Unterstützung und Hilfe in sämtlichen Lebenslagen.

Birte und Tina, für die großartige gemeinsame Zeit im Labor und für die Gesellschaft während der Laborarbeiten. Danke, dass ihr nicht nur den Laboralltag, sondern auch die Feierabende und das ein oder andere Wochenende so viel lustiger und abenteuerlicher gemacht habt. Es war mir eine Freude, euch während eurer Bachelorarbeiten zu betreuen und zu begleiten.

Alyn, Steffi und Christian, für die Hilfestellungen im Laboralltag, die großartige Zusammenarbeit und die wunderbare Zeit im Labor. Danke, dass ihr mich bei meinen Experimenten tatkräftig unterstützt habt und zum Erfolg dieser Arbeit beigetragen habt.

AG Garbers, für eine wunderbare Zeit, gemeinsame Mittagessen, viele lustige Geschichten und gesellige Abende. Es war mir eine Ehre und ich werde euch alle sehr vermissen!

Meiner Familie, für die Unterstützung und Ermutigung während meiner Zeit in Kiel. Ohne euch wäre meine Arbeit nicht möglich gewesen. Danke, dass ihr immer für mich da seid und immer an mich glaubt!

Eidesstattliche Erklärung

Hiermit versichere ich, dass die vorliegende Dissertation nach den Regeln der guten wissenschaftlichen Praxis der Forschungsgemeinschaft von mir selbstständig unter Anleitung meiner akademischen Lehrer angefertigt wurde. Des Weiteren versichere ich, dass keine anderen als die angegebenen Quellen und Hilfsmittel benutzt wurden.

Teile dieser Arbeit wurden bereits zur Veröffentlichung eingereicht. Ich versichere, dass die vorliegende Dissertation an keiner anderen Universität eingereicht wurde, ich keinen erfolglosen Promotionsversuch unternommen habe und mir kein akademischer Grad entzogen wurde.

Kiel, Oktober 2018

_____

Charlotte Flynn